OFFICE OF NAVAL RESEARCH WORKSHOP REPORT

CONVENTIONAL WEAPONS UNDERWATER EXPLOSIONS

Tower Place Hotel
Atlanta, Georgia
August 2-3, 1988

Final Report: Office of Naval Research
Contract No. N00014-88-J-1150

December 15, 1988

Prepared by

GEORGIA INSTITUTE OF TECHNOLOGY
A UNIT OF THE UNIVERSITY SYSTEM OF GEORGIA
SCHOOL OF AEROSPACE ENGINEERING
ATLANTA, GEORGIA 30332

Uncl. sified
SECURITY SSIFICATION OF THIS PAGE

REPORT DOCUMENTATION PAGE

Form Approved
OMB No. 0704-0188

1a. REPORT SECURITY CLASSIFICATION Unclassified	1b. RESTRICTIVE MARKINGS None
2a. SECURITY CLASSIFICATION AUTHORITY	3. DISTRIBUTION/AVAILABILITY OF REPORT Distribution unlimited
2b. DECLASSIFICATION/DOWNGRADING SCHEDULE	
4. PERFORMING ORGANIZATION REPORT NUMBER(S)	5. MONITORING ORGANIZATION REPORT NUMBER(S)
6a. NAME OF PERFORMING ORGANIZATION Georgia Institute of Technology 6b. OFFICE SYMBOL (If applicable)	7a. NAME OF MONITORING ORGANIZATION Office of Naval Research Power Program Office
6c. ADDRESS (City, State, and ZIP Code) School of Aerospace Engineering Georgia Institute of Technology Atlanta, GA 30332	7b. ADDRESS (City, State, and ZIP Code) 800 N. Quincy St. Arlington, VA 22217
8a. NAME OF FUNDING/SPONSORING ORGANIZATION Office of Naval Research 8b. OFFICE SYMBOL (If applicable)	9. PROCUREMENT INSTRUMENT IDENTIFICATION NUMBER N00014-88-J-1150
8c. ADDRESS (City, State, and ZIP Code)	10. SOURCE OF FUNDING NUMBERS PROGRAM ELEMENT NO. / PROJECT NO. / TASK NO. / WORK UNIT ACCESSION NO.

11. TITLE (Include Security Classification)
Conventional Weapons Underwater Explosions (U)

12. PERSONAL AUTHOR(S)
Warren C. Strahle (ed.)

13a. TYPE OF REPORT	13b. TIME COVERED	14. DATE OF REPORT (Year, Month, Day)	15. PAGE COUNT
Final	FROM 880701 TO 881215	88, Dec. 15	210

16. SUPPLEMENTARY NOTATION

17 COSATI CODES			18 SUBJECT TERMS (Continue on reverse if necessary and identify by block number)
FIELD	GROUP	SUB-GROUP	Explosions, underwater, bubbles, detonations, metal combustion, combustion

19 ABSTRACT (Continue on reverse if necessary and identify by block number)

Results are reported upon from an ONR-sponsored workshop in conventional weapons underwater explosions. The report contains background tutorial material as well as workshop results. Organized into sub-groups, individual workshop reports are presented in the areas of detonations, bubble dynamics, bubble-water interface phenomena and metal combustion behavior. It was concluded that there are many potential research areas which require attention to bring the phenomena under scientific understanding and control. The general areas of research recommended involve metal behavior, experimental diagnostics and verifiable computational methods.

20 DISTRIBUTION/AVAILABILITY OF ABSTRACT	21. ABSTRACT SECURITY CLASSIFICATION
☒ UNCLASSIFIED/UNLIMITED ☐ SAME AS RPT. ☐ DTIC USERS	Unclassified
22a NAME OF RESPONSIBLE INDIVIDUAL	22b. TELEPHONE (Include Area Code) / 22c. OFFICE SYMBOL

OFFICE OF NAVAL RESEARCH WORKSHOP REPORT

CONVENTIONAL WEAPONS UNDERWATER EXPLOSIONS

Tower Place Hotel
Atlanta, Georgia
August 2-3,1988

Final Report: Office of Naval Research
Contract No. N00014-88-J-1150

December 15,1988

Submitted by

Warren C. Strahle
Workshop Chairman
School of Aerospace Engineering
Georgia Institute of Technology
Atlanta, Georgia 30332

PREFACE

Warren C. Strahle
Georgia Institute of Technology

On September 23 and 24 1987 a preliminary, small workshop was held at the Naval Surface Weapons Center, White Oak to explore some issues related to conventional weapons underwater explosions. The purpose was to decide whether or not the unclassified research community, previously untapped for work in the area, might be able to contribute to the technical issues involved. The decision was that there is potentially much scientific work to be done in understanding many phenomena in the underwater explosion field. It was decided to hold a much larger workshop in the future to invite the 6.1 research community to become involved in the problem. Indeed, a major recommendation at an ONR research program review at the National Academy of Sciences, held in November 1987, concluded that a major research effort was needed in this field of underwater explosions by conventional weapons.

This report is a result of a workshop held in Atlanta, GA on August 2 and 3, 1988; the meeting was held in accordance with the above recommendations. Dr. Richard S. Miller was the ONR sponsor for the meeting and Dr. Warren C. Strahle of the School of Aerospace Engineering at the Georgia Institute of Technology was the workshop Chairman. Fifty-five research workers from universities, government and industry were present, and this number includes some government administrative personnel. Four western bloc countries were represented.

The specific goals of the workshop were to a) define the limits of scientific understanding in conventional weapons underwater explosions and b) deliver a prioritized set of recommendations for research in this area that could be carried out by the unclassified research community. The chairman, thanking all speakers, principals and attendees, believes the goals were accomplished.

TABLE OF CONTENTS

SUMMARY OF RECOMMENDATIONS

Warren C. Strahle
Georgia Institute of Technology

ORGANIZATION

In the first section of this report, entitled State of the Art Reviews, the audience was briefed on current knowledge and deficiencies in understanding in the field of conventional weapons underwater explosions. The participants then split into four groups, in various disciplines, to formulate a prioritized list of research items which are essential to advance scientific understanding in the field. The individual groups generally followed a procedure known as the "Nominal Group Method" which the Chairman had seen work with success at a prior NSF workshop. From the smaller sessions the Chairman, with input from the original speakers and workshop recorders, has formulated the list below of overall research items.

The listing below is given without explicit regard to funding limitations. Tacitly, however, some judgement has been applied concerning the total number of recommendations because of the large quantity resulting from the workshop.

RECOMMENDED RESEARCH

Research Crossing Discipline Lines

1. Because of their energetics, metals (Al and other promising metals) are of interest as an ingredient in conventional explosives. However, research is required in many aspects of their (and their oxides) behavior through the entire gamut of the explosion process - the detonation, bubble formation, water-bubble interface phenomena and final jetting action. Research is required in a) the kinetics and spatial distribution of the interesting species during the detonation and bubble phases, b) their interaction with steam and water and c) equation of state (EOS) data at pressures and temperatures characteristic of both detonation and bubble conditions.

2. Experimental diagnostics of new and novel nature are required for visual observation and scientific measurements of the entire explosion process. Short time transients and observation through water have hampered efforts to obtain quality data. Research is required for measurement of a) metals parameters as in (1) above, b) interface phenomena, c) interface shape and instability behavior during jetting, d) temperature, pressure and species concentration and e) jet impact loads on targets.

   It should be mentioned here that while this recommendation is given high priority, the problem is a difficult one and and an inordinate amount of resources could be expended here. The recommendation is to look at truly unique and high potential payoff methodologies without embarking on a diagnostics funding binge.

3. Development of analytical models and experiments for verification for many of the several processes involved should receive high research priority. Good, verifiable models and numerical procedures either do not exist or are incomplete which incorporate a) chemical kinetics and condensation kinetics, b) bubble dynamics for both "simple" bubbles and bubbles generated by non-ideal explosives, c) transfer of the detonation energy to the water, d) interface mass and heat transfer, e) interface instability and f) detonation and bubble turbulence effects, g) jet structure near bodies and h) superheated interface behavior.

Other Research

Two other important issues were raised which deserve research attention. These are a) the role of the explosive casing in the energy transfer to the water and b) the effect of designed spatial and temporal multiple explosions (including residual gas vaporific explosions) on blast and bubble jet strength and directionality.

CONCLUSION

The workshop has identified three general areas requiring scientific research in the field of conventional weapons underwater explosions. Broadly, the three most important areas involve aspects of metal behavior, diagnostics and computational tools. These areas cut across all elements of the explosion process - from detonation initiation to bubble dynamics. The technological impact of progress in these research fields can be large and it is recommended that a coordinated research program be implemented.

INTRODUCTION TO THE PROBLEM

Gregory S. Harris
Explosion Damage Branch, Code R14
Naval Surface Warfare Center

The purpose of this section is to present an introduction to underwater explosion phenomena and set the stage for the more in-depth presentations that will follow. In order to avoid overwhelming the audience with details, the presentation graphics were generally self-explanatory and are provided here in lieu of a formal paper. Where necessary, text has been added below each figure for further clarification.

For completeness, a summary of the phenomena associated with the detonation of an explosive charge underwater as given by Snay[1] is repeated here. The following discussion refers to the illustration contained on vugraph number five, entitled "Explosion Bubble and Pressure-Time History."

"The detonation of an explosive charge underwater converts the solid explosive material into gaseous reaction products which have an exceedingly high pressure. This pressure is transmitted into the surrounding water and propagates as a shock wave in all directions.

"The figure illustrates the pressure-time history which is observed in the water at a fixed distance from the point of explosion. Upon arrival of the shock wave the pressure rises practically instantaneously to the peak value. Subsequently, the pressure decreases steadily but at a very fast rate. The shock wave peak pressure and rate of decay depend on the charge weight and distance of the point of observation. Empirical equations for these as well as other shock wave parameters can be found in the literature[2].

"The figure shows that subsequent to the shock wave other pressure pulses occur. These pulses arise from a much slower phenomena, namely the pulsating of the gas bubble which contains the gaseous products of the explosion. The high pressure of the gas causes an initially rapid expansion of the bubble and the inertia of the outward moving water carries it far beyond the point of pressure equilibrium. The outward motion stops only after the gas pressure has fallen substantially below the ambient pressure. Now the higher surrounding pressure reverses the motion. Again the flow overshoots the equilibrium and when the bubble reaches its minimum size the gas is recompressed to a pressure up to several hundred atmospheres. At this point there is effectively a second explosion and the whole process is repeated. The bubble oscillates in this way several times.

"In the illustration, the position and size of the bubble is shown for a few specific moments which correspond to the pressure-time curve as indicated above. The pressure-time history reflects the low gas pressure during the phases where the bubble is large and it shows the pressure pulses which are emitted from the bubble near its minimum.

"The period of the first pulsation is more than one-half second for common charges. This a long time when compared with the extremely fast processes occurring with explosions. In particular, this duration is long enough for gravity to become effective. Such a bubble has great buoyancy and, therefore, migrates upward. However, it does not float up like a balloon, but shoots up in jumps.

"The dotted curve in the figure represents the position of the bubble center as a function of time. This curve shows that the rate of rise is largest when the bubble is near its minimum, but is almost zero when the bubble is large."

REFERENCES

1. Snay, H. G., Hydrodynamics of Underwater Explosions, reprinted from NAVAL HYDRODYNAMICS, Publication 515, National Academy of Sciences - National Research Council, 1957.

2. Swisdak, M. M., ed., Explosion Effects and Properties: Part II - Explosion Effects in Water, NSWC TR 76-116, 22 February 1978.

ONR - GIT WORKSHOP ON CONVENTIONAL EXPLOSIVE UNDERWATER EXPLOSIONS

Introduction to the Problem

Gregory S. Harris

Naval Surface Warfare Center
Silver Spring, Maryland

Figure 1

CONVENTIONAL EXPLOSIVE

- Heterogeneous mixture of Fuels and Oxidizers

Figure 2

EXPLOSION

Rapid energy release, caused by:

- Detonation of chemical HE
- Steam explosion

Figure 3

UNDERWATER EXPLOSION

Detonation

- Exothermic chemical reaction that converts solid explosive into:
- Shockwave
- Product gasses and solids (bubble)

Figure 4

EXPLOSION BUBBLE AND PRESSURE-TIME HISTORY

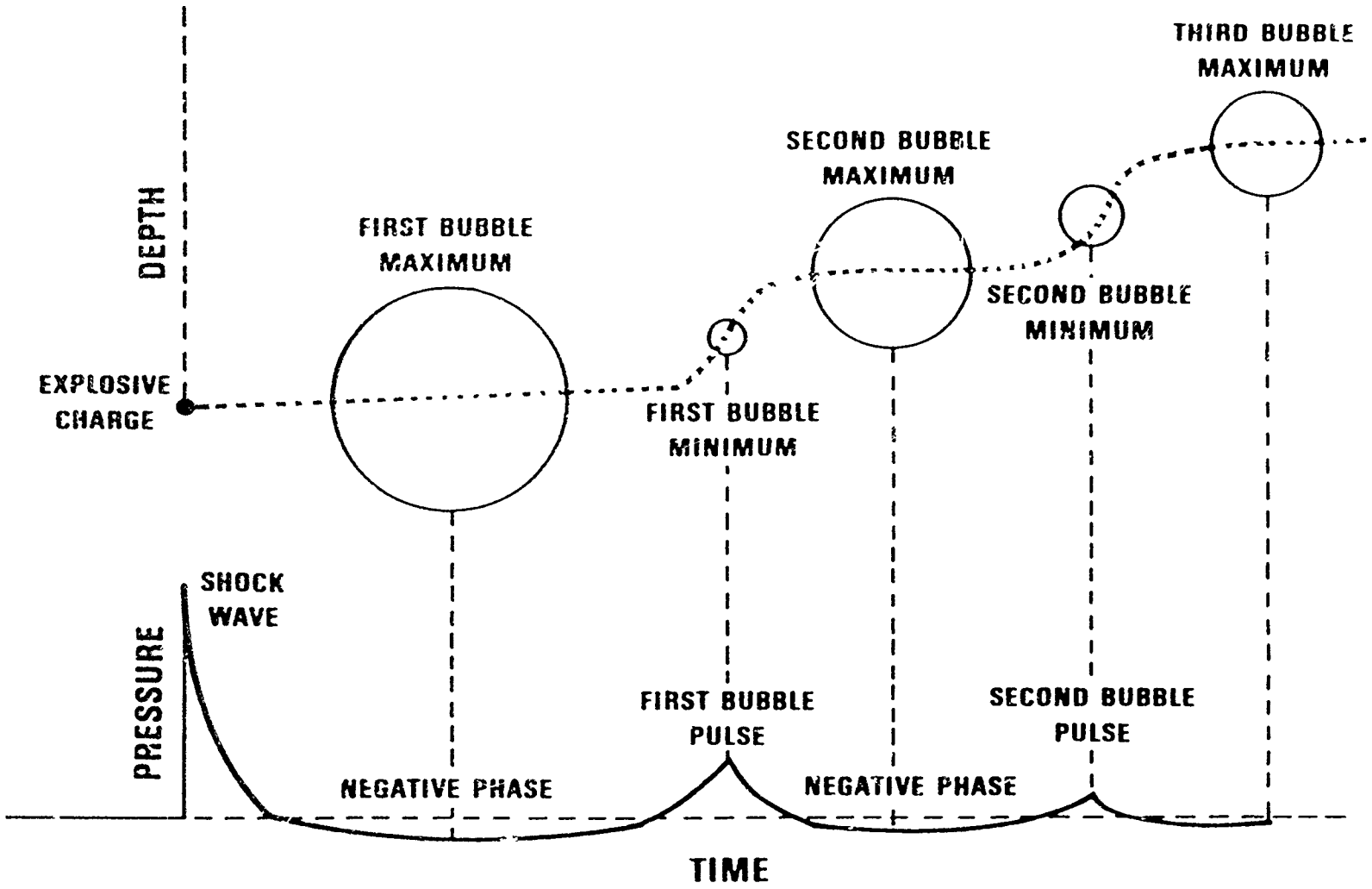

FREE FIELD BUBBLE MIGRATION

First maximum

Near first minimum

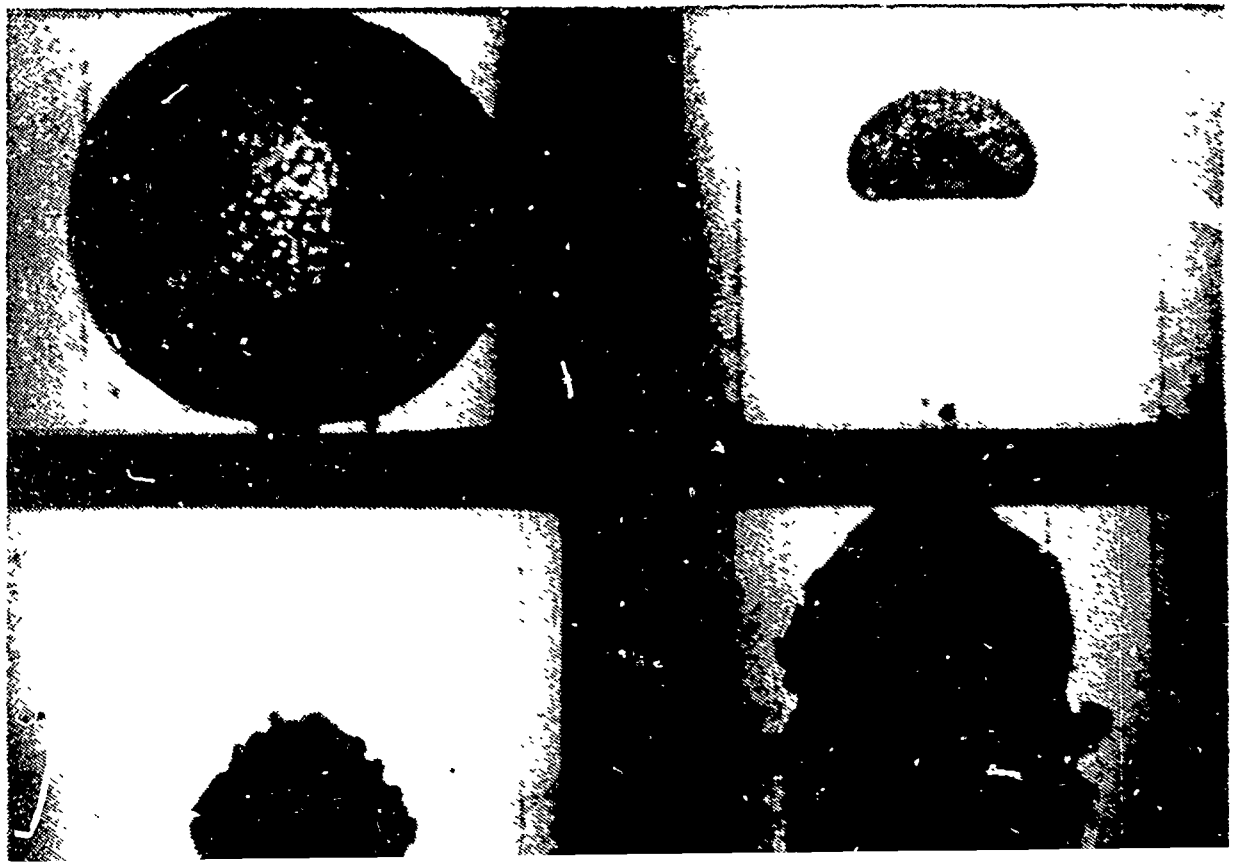

SCALED CONDITIONS:

244 LB HBX - 1
81 FT WATER DEPTH

UNDERWATER EXPLOSION EFFECTS

- Shock Wave (short duration, impulsive)
- Bubble (long duration)

Figure 7

ENERGY PARTITION OF A BULK WARHEAD FIRED UNDER WATER (U)

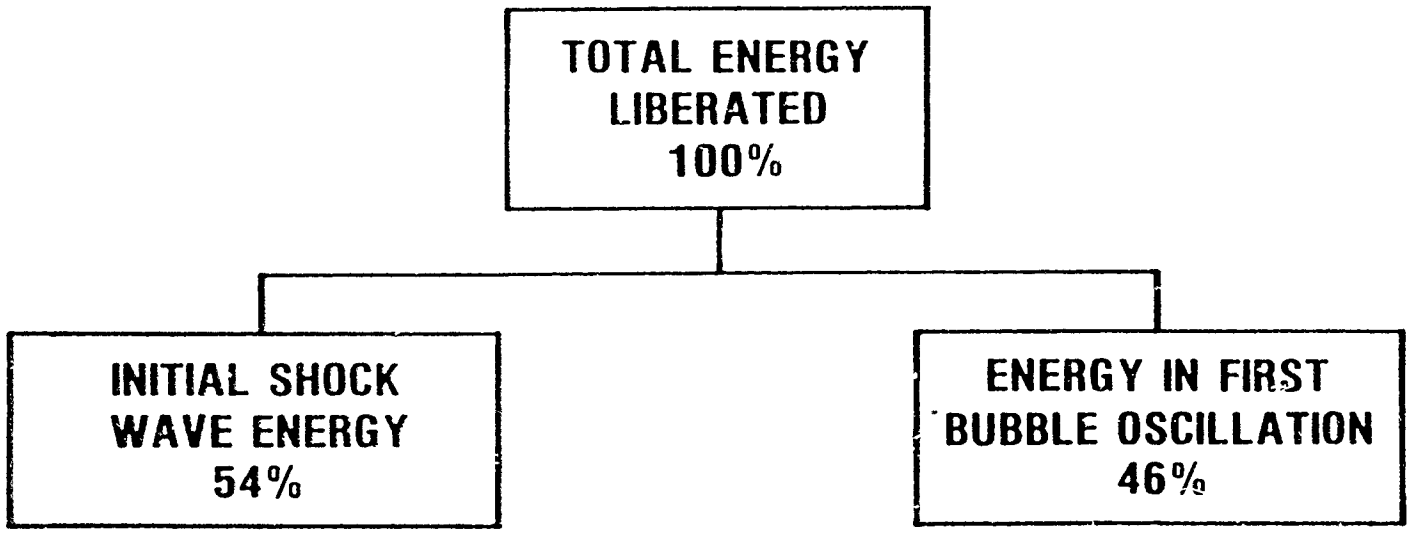

NON-ALUMINIZED, IDEAL EXPLOSIVE

The energy partition between shock and bubble can be tuned, depending on how the explosive energy is to be used.

ENERGY PARTITION

Tuning of Shock Wave and Bubble Contributions

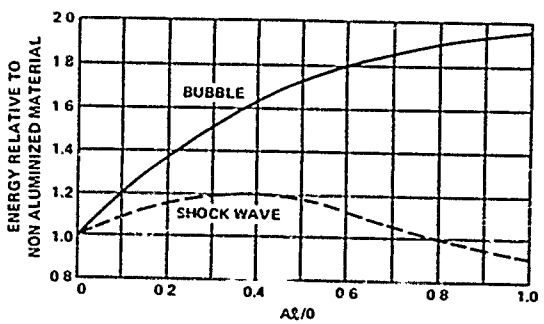

Baseline : TNT / RDX Mixture

Example:

Effect of Aluminum Content on Explosive Output Performance

Figure 9

SHOCK WAVE CHARACTERISTICS

- **Dependent on explosive composition**
- **For chemical HE, approximated by decaying exponential wave**
- **Typical experimental pressure record :**

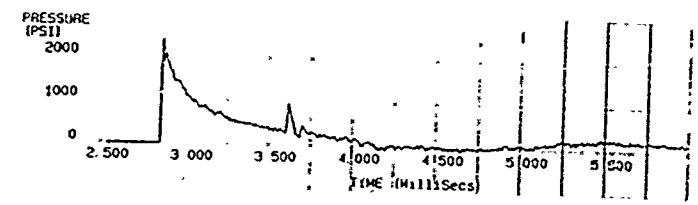

Figure 10

SHOCK WAVE CHARACTERISTICS

Current Understanding

- Empirical relations hold for P < 20ksi
- Long distance propagation well understood
  - Surface and bottom effects
- Close-in characteristics not as well known:
  - extremely difficult to measure
  - rely on hydrocode calculations (difficult to validate, EOS problems)

Figure 11

SHOCK WAVE

Some Problem Areas of Interest

- Detonation physics
- Equation of state for modern explosives
  - for detonation and reaction products
- Techniques for close-in measurements

Figure 12

UNDERWATER EXPLOSION

Typical Pressure Record

- Shock wave

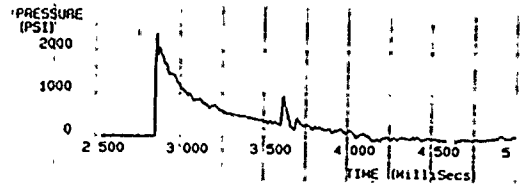

- Shock wave + three bubble pulses

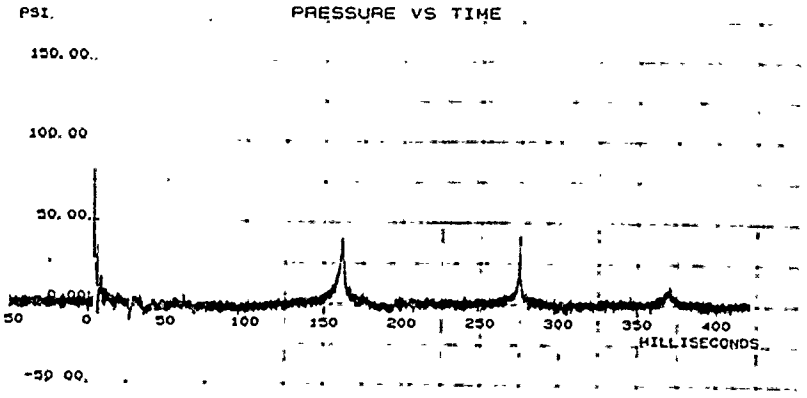

Figure 13

EXPLOSION BUBBLE CHARACTERISTICS

- Early-time bubble growth
  - dependent on energy release rate
- First cycle of oscillation
  - size, period and migration dependent on chemical composition, charge weight and depth of detonation
- Subsequent cycles
  - dependent on first cycle properties
  - rate of energy loss at each minimum:
    - radiated pressure (bubble pulse)
    - losses due to cooling
    - energy lost during migration

Figure 14

LOADINGS PRODUCED BY UNDERWATER EXPLOSIONS

- **Shock Wave**
  - **Large amplitude, short duration pressure pulse**

- **Bubble**
  - **Flow field around pulsating, migrating bubble**
  - **Water jet formed by collapsing bubble (impact loads, flow pressures)**
  - **Bubble pulse (low amplitude, long duration pressure pulse)**

Figure 15

BUBBLE SIZE EXAMPLES

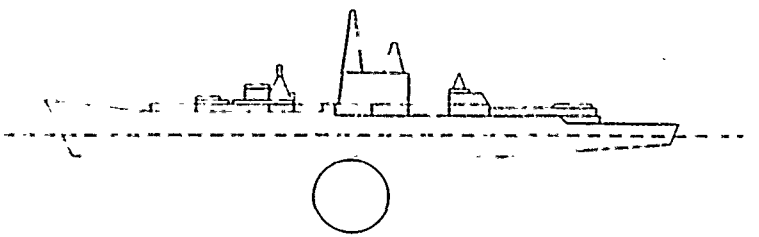

1000 POUNDS TNT AT 50 FT

Radius = 30.00 FT
Volume = 113,455 CU FT
Weight = 3630 TONS OF WATER DISPLACED
Period = 1.1 SEC

SHIP : DESTROYER
LENGTH : 500 FT
DISPLACEMENT : 7600 TONS

Figure 16

BUBBLE EFFECTS

SHIP HULL WHIPPING

- Induced by radial flow field around the pulsating bubble
  - primary loading from fluid accelerations
  - rapid early bubble growth is essential
- Induced by bubble jet impact

A pulsating explosion bubble in close proximity to a ship produces a localized flow loading on the hull, which in turn can excite low frequency, beam-like bending response of the entire ship hull.

Figure 17

BUBBLE EFFECTS

BUBBLE JETTING

- Free field effect for strongly migrating bubbles (plumes)
- Complex interaction with a solid boundary
- Generally a 3-D problem
- Prohibitive for general purpose hydrocodes due to long computer running times

Figure 18

UNDERWATER EXPLOSION BUBBLE COLLAPSE

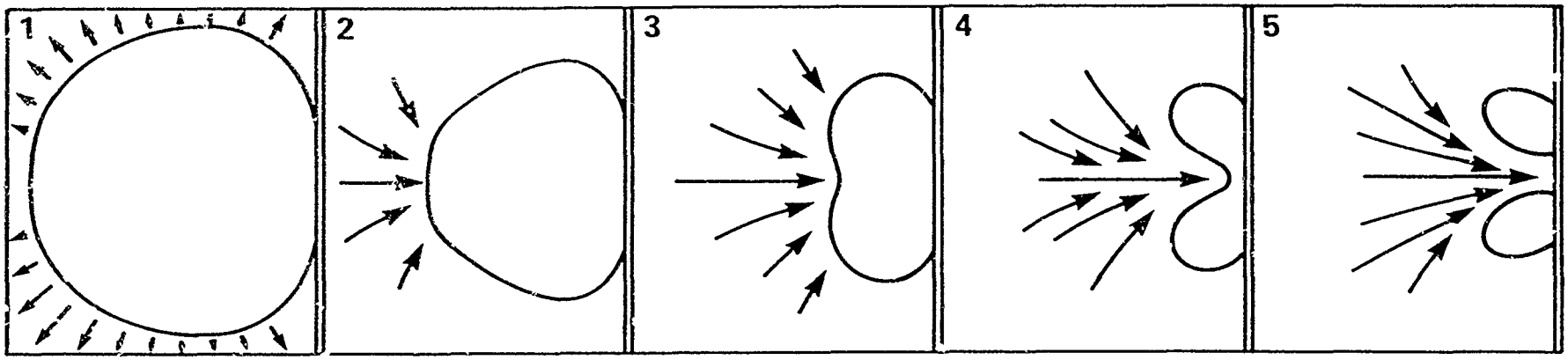

- A RESULT OF THE APPARENT "ATTRACTION" TOWARDS A RIGID SURFACE
- CAUSED BY THE DISTURBANCE OF THE FLOW OF WATER AROUND THE PULSATING EXPLOSION BUBBLE
- FACTORS AFFECTING THE COLLAPSE PROCESS INCLUDE:
  - BUBBLE SIZE
  - BUBBLE PERIOD
  - STANDOFF FROM WALL
  - INFLUENCE OF GRAVITY
  - ORIENTATION
  - RELATIVE CURVATURE OF WALL AND BUBBLE

Figure 19

EXPLOSION BUBBLE

Some Problem Areas of Interest

- True composition of reaction products
  - as a function of time
- Early bubble growth for 'non-ideal' explosives
- Interface phenomena
  - Early time
  - Near the minima
  - Sub-scale testing
- Physical properties of the bubble near the minima
- Three-dimensional bubble dynamics
  - Free field
  - Interactions with surfaces

Figure 20

REVIEW OF THE PHYSICS AND CHEMISTRY OF DETONATION AS APPLIED TO UNDERWATER EXPLOSIONS

Dr. Raymond R. McGuire
Lawrence Livermore National Laboratory

INTRODUCTION

The following should not be construed as a detailed exposure of the theory of detonation. Rather, I would like to concentrate on those aspects of detonation physics and chemistry that are peculiarly applicable to explosions under water.

To begin, we need to define some terms. When I speak of "detonation," I mean a steady state hydrodynamic conditions where a chemically driven compression wave (reactive shock wave) proceeds through a mass of material. Thus, detonation is, by definition, an equilibrium (dynamic equilibrium) condition. An "explosion," on the other hand, is an ill-defined word that describes the rapid expansion of matter into a volume it did not previously occupy. It (explosion) may or may not involve a traveling wave and may or may not imply exothermic chemistry. A unique explosion condition resulting from a simultaneous ignition at all points of the explosive-included volume is termed a "volume explosion."

With these in mind, let us look at the classic example of a detonation; i.e. a detonation wave proceeding down an unconfined cylinder of explosive. (See Fig. 1). In a condensed ideal explosive, the detonation front is relatively linear in the center of the charge but begins to "drop" as it nears the edge of the charge. This results from the rarefaction waves that "eat into" the reactive zone from the edge. At some distance behind the detonation front is a surface of a shape similar to the front surface, where the mass flow becomes sonic. The volume bounded by these two surfaces (the detonation front and the sonic surface) is termed the reaction zone. (The sonic surface is sometimes termed the C-J surface). Any chemistry that occurs within the reaction zone can affect the detonation front (detonation pressure and

detonation velocity); any reactions that proceed behind this sonic surface cannot affect the detonation front; although they can contribute to work done by the expanding detonation products. It is generally understood that, in ideal explosives, reactions behind the sonic surface are equilibrium reactions; i.e. are in thermal equilibrium and comprise a minimu free energy at the local P,V,T, condition. I have depicted a number of particle paths or "characteristics" in Figure 1. We shall return to the importance of these later.

Figures 2 and 3 show other graphical depictions of an ideal detonation in PV and Pt space, respectively. In Figure 2 we see the classical depiction of an explosive compressed to a point on the unreacted Hugoniot. The pressure relaxes along a Rayleigh line to the sonic or C-J point. (Note, the C-J state is a point on the Hugoniot of the reaction products). It is during this relaxation process that chemical reaction takes place. This is the reaction zone. The detonation products then expand and cool along an adiabatic path. This classical picture has been termed the ZND (Zeldovich, von Neuman, Doering) model for an ideal detonation. Figure 3 shows a different snapshot of this process.

For our particular interest, here, in explosives for underwater applications, we need to focus on the C-J surface. Our interest is in how we might affect the partitioning of energy between what is released in the reaction zone and what is available in the detonation products to do P-V work on the surrounding water.

Before Proceeding further, let me define an additional term, i.e. "composite explosive." I have spoken of ideal detonation in a "physics" sense: let me now speak in a "chemistry" sense. An "ideal" explosive is one where mass transport is not an important rate determining process. A dependent upon transport processes. A composite explosive is one where the "fuel" and "oxidizer" are contained in separate molecules or even separate crystalites. Composite explosives may be either ideal or non-ideal depending on the size and configuration of the experiment and the scale of intimacy of the fuel and oxidizer.

Let us now focus on the question of partitioning energy at the C-J surface.

In a series of experiments (Fig. 4) (Ref. 1) designed to recover tagged detonation products on the expansion isentrope, we have shown the following:

1) There is a finite scale length over which reactions occur.
2) In a cylindrical configuration, little if any reaction takes place during the expansion behind the C-J surface. (As I have shown in Figure 1, the particle paths are divergent; thus the probability of effective collisions becomes increasingly smaller as the expansion progresses.

In an experiment (Fig. 5) (Ref. 2,3) on a unimolecular, isotopically labeled explosive at specific positions, we found there to be a total scrambling of the tags throughout the detonation products. While this result does not establish what occurred in the reaction zone and what occurred later, additional experiments suggest that essentially all of the reaction occurs in the reaction zone.

A composite explosive of ammonium nitrate and TNT where only the nitrogens in the ammonium nitrate were labeled, gave only a small amount of isotopic scrambling. Similarly, in experiments (Fig. 6) on mixtures of explosives where each of the components was deficient in an element necessary for one of the common detonation products, we found that the expected products were not present in the equilibrium concentration (Ref. 1). Thus, there is limited mass exchanges between separate crystals of solid explosives.

This suggests that, in a cylindrical configuration, reactions which do not occur in the reaction zone do not occur later, and is consistent with known charge diameter and particle size effects on performance. I has been well documented by Campbell at LANL (Ref. 4) and many others that the detonation velocity of cylindrical charges of explosives decreases as the charge diameter decreases. These decreases can be quite large for composite explosives. Finger, et al (Ref. 5) and myself (Ref. 6) at LLNL (Fig. 7) have likewise established that the performance of composite explosives as measured by the cylinder test also scales with charge diameter. We have also shown that, for composite explosives, the cylinder test performance also decreases as charge diameter decreases (Fig. 8). The cylinder test is predominantly a measure of the energy in the expanding detonation products.

In more recent work (Fig. 9) (Ref. 1) we have found that "seeding" composite explosives with materials that will increase the detonation temperature has the effect of increasing cylinder test performance compared with unseeded material. Our experience with aluminum as a fuel in composite explosives (Fig. 10) suggests that it reacts exactly as other components.

We have recently proposed a model (Fig. 11) (Ref. 7)that is being used to enhance our understanding of how composite, non-ideal explosives work.

If we accept that we cannot obtain reaction behind the C-J surface, how can we alter the partitioning of energy at that surface (Fig. 12). The answer, I suggest, lies in composite explosives; particularly metallized composite explosives. Because of the very high negative heat of formation of most metal oxides, metal loaded composite explosives have a very high detonation temperature. This results in a lot of energy being deposited in rotational and vibrational states of the detonation product fluid. This energy becomes available for PV work as the molecules relax during the expansion. By controlling the initial composition to provide products molecules with more rotational and vibrational states, we can maximize this "late time energy release"; i.e. flatten out the expansion isentrope.

I have limited myself, until now, to cylindrical detonations. A spherical explosion is a configuration that maximizes detonation product interactions (Fig. 13). In this configuration, the particle streamlines are convergent rather than divergent. This maintains a very high pressure behind the C-J surface. If the explosive has a low detonation temperature, there is little or no configurational effect (Fig. 13) (Ref. 8). We see no difference in the equation of state for nitromethane or ANFO as measured in cylinders or centrally initiated spheres. Again, we should look to metallized composite explosives with their high detonation temperatures to maximize the energy in the detonation product fluid.

The use of metallized composite explosives for applications under water and related applications in excavation is, of course, not new. However, we would suggest that the more understanding we gain in the fundamental chemistry and physics of detonation will allow us to make better selections of composition for maximizing the desired effect.

References

1. McGuire, R. R. and Finger, M., "Composite Explosives for Metal Acceleration: The Effect of Detonation Temperature", Eighth Symposium on Detonation, NSWC-MP86-194, pp. 1018-24 (1985).

2. Ornellas, D. L., et al, Rev. Sci. Instrum. 37, p. 909 (1966).

3. McGuire, R. R. et al, "Detonation Chemistry, Diffusion Control in Non-Ideal Explosives", Propellants and Explosives, 4 No. 2, pp. 23-26 (1979).

4. Campbell, A. W. and Engelke, R., "The Diameter Effect in High Density Heterogeneous Explosives," Sixth Symposium on Detonation, ACR-221, pp. 642-652 (1976).

5. Finger, M. et al, "Characterization of Commercial, Composite Explosives," Sixth Symposium on Detonation, ACR-221, pp. 729-739 (1976).

6. McGuire, R. R., unpublished results.

7. McGuire, R. R., Reference 1 and Tarver, unpublished results.

8. Helm, F. H. et al, "Detonation Product Behavior at Large Expansion: The Underwater Detonation of Nitromethane," UCRL 52903, December 1980.

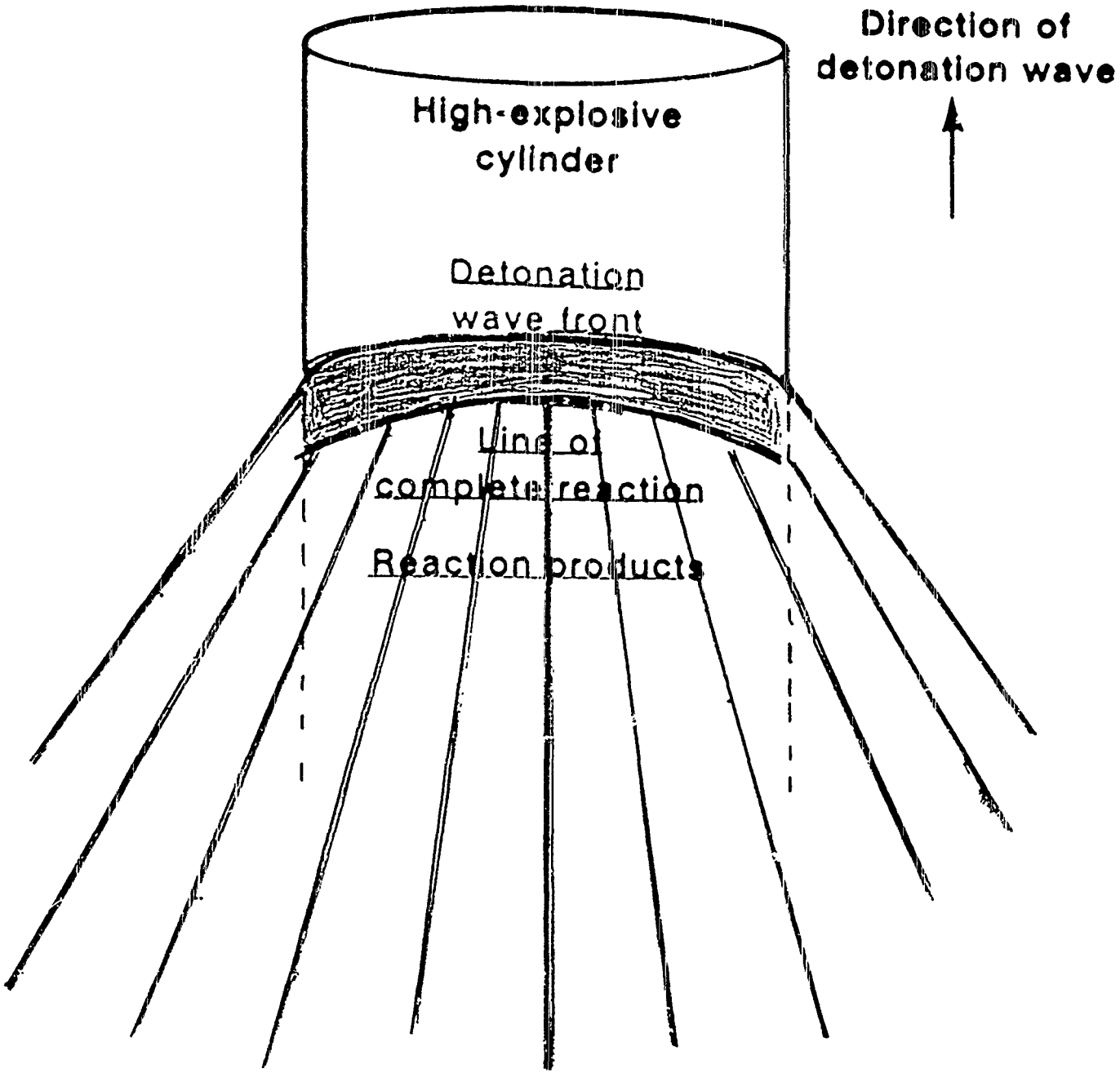
Direction of
detonation wave
High-explosive
cylinder
Detonation
wave front
Line of
complete reaction
Reaction products

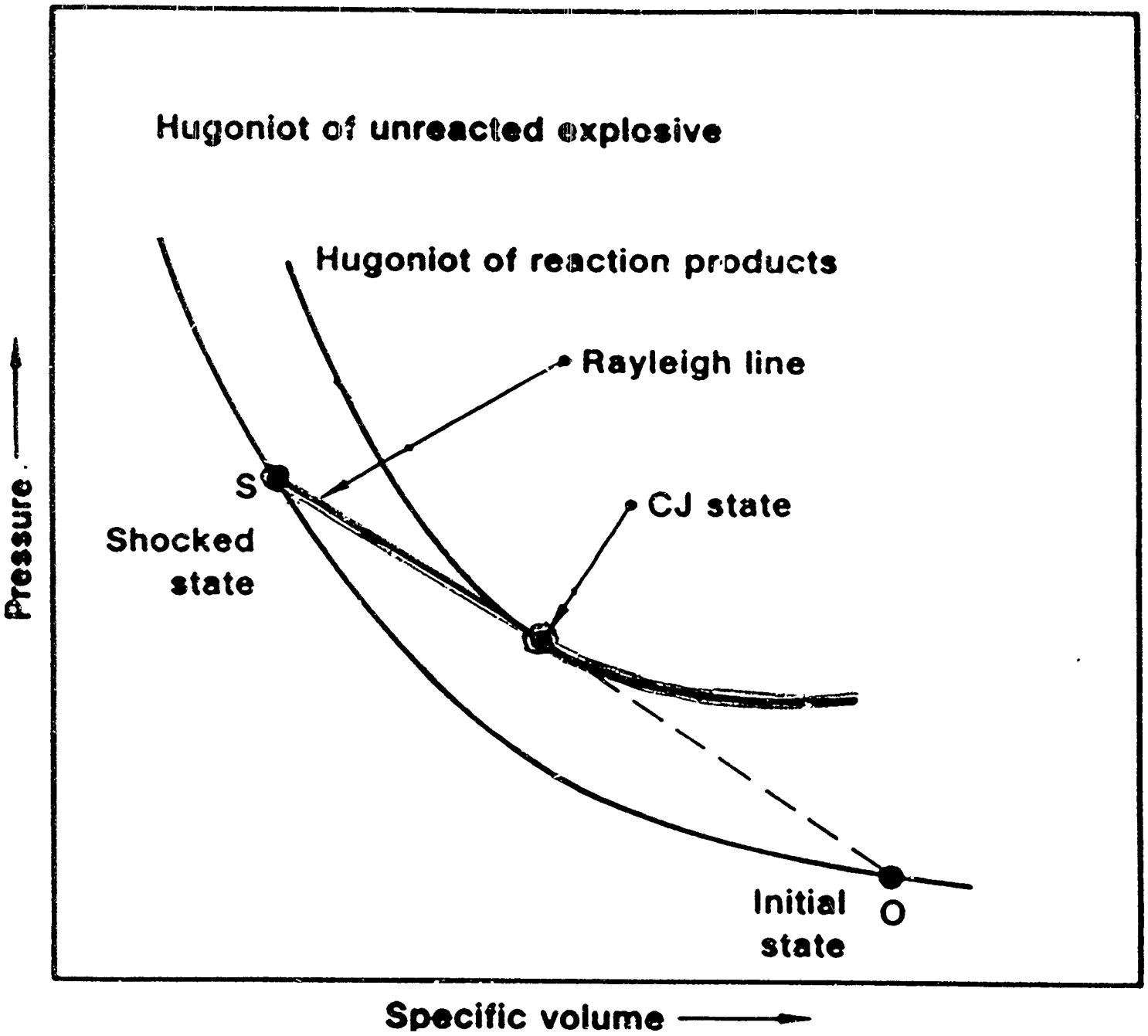
Hugoniot of unreacted explosive
Hugoniot of reaction products
Rayleigh line
S
Shocked state
CJ state
Initial state
O
Pressure
Specific volume

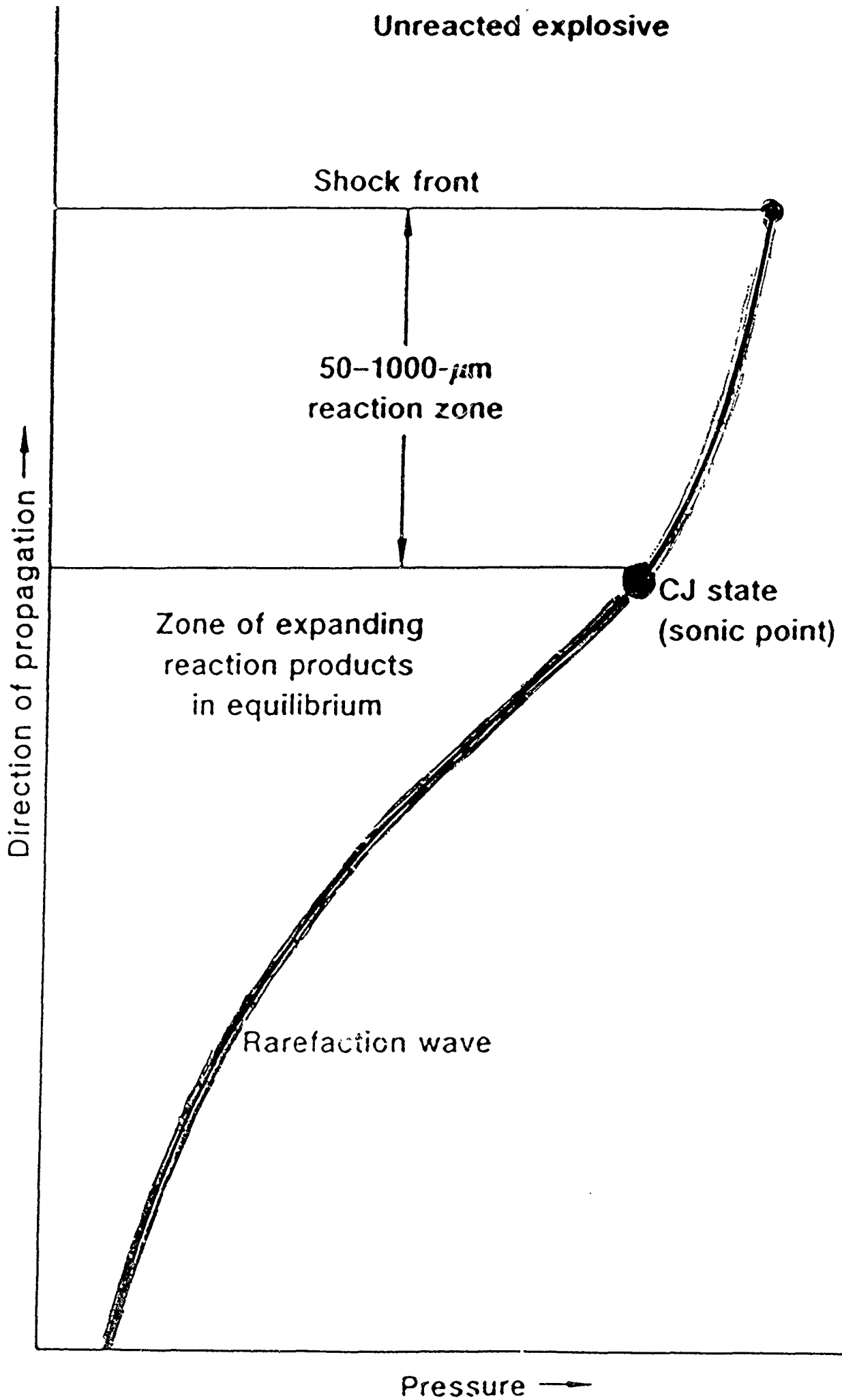
Unreacted explosive
Shock front
50–1000-μm
reaction zone
CJ state
(sonic point)
Zone of expanding
reaction products
in equilibrium
Rarefaction wave
Direction of propagation
Pressure

Detonation calorimetry measures total energy available and detonation products

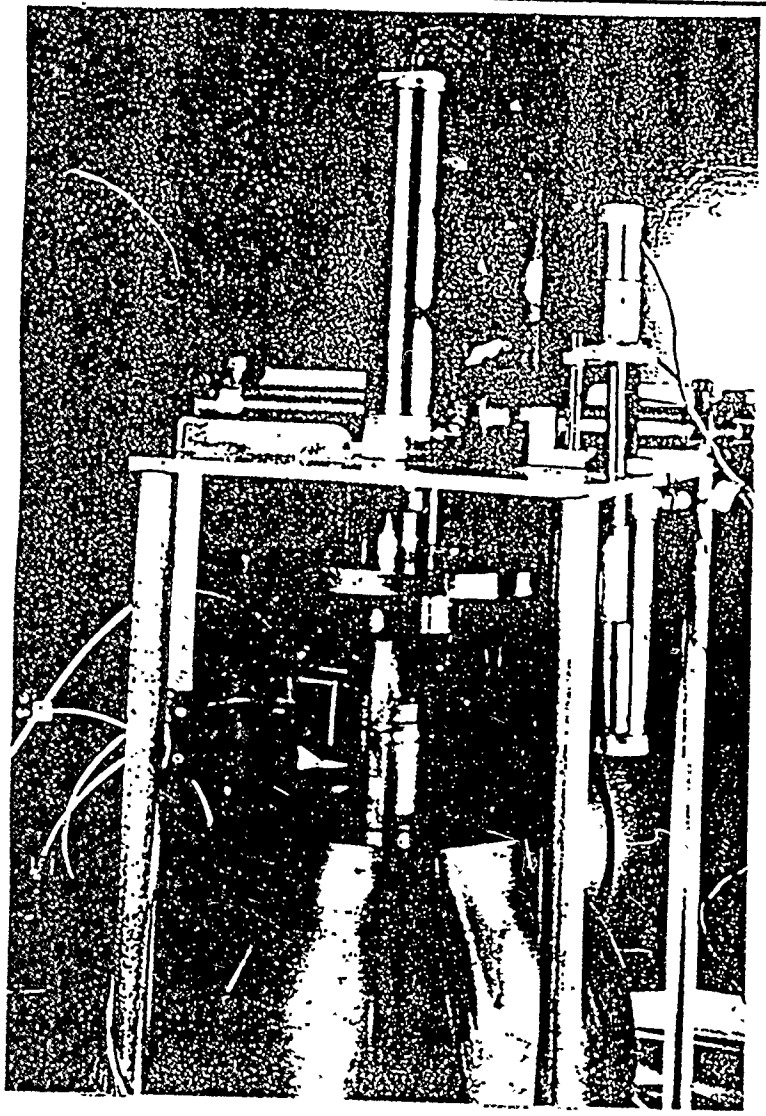

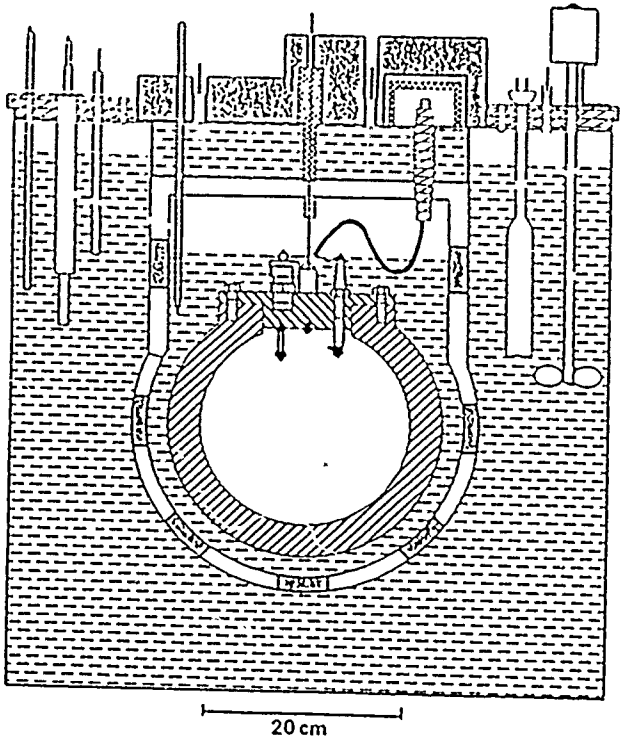

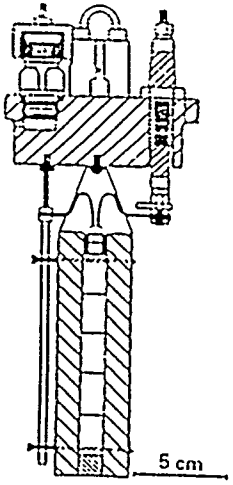

Detonation calorimetry provides data on RXN zone and early isentrope

- Ideal explosives show complete scrambling at the atomic level

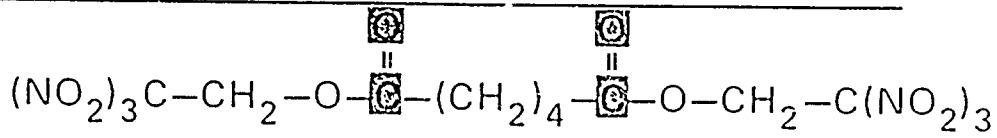

BTNEA

In BTNEA
C/O = 4.80
O/O = 11.70

→ Detonation →

In products
C/O = 4.3 —· 4.8
O/O = 11.2 —· 11.4

- Non-ideal explosives show diffusion control

Matl	ΔH_D	CO_2/CO	NO/N_2	$N^{15} \equiv N^{14}$
TNT	1,090	0.63	0.0000	
AMATOL 20/80†	1,105	1.08	0.0044	0.085†
65/35	1,100	4.59	0.084	
80/20	1,080	15.97	0.232	

†From $N^{15}H_4N^{15}O_3$ 100% mixing = 0.818 0% mixing = 0.000

Explosives used in detonation calorimetry mixing experiments

Bitetrazole
BTZ
$C_2H_2N_8$

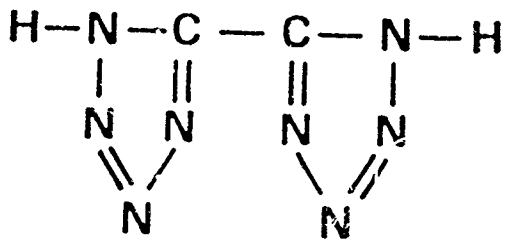

W_{50} particle diameter 19μm
ρ_{TMD} = 1.685 g/cc
ΔH_f = +151 Kcal/mole

Hydrazinium nitrate
HN
$H_5N_3O_3$

$N_2H_5^+O_3^-$

W_{50} particle diameter 15μm
ρ_{TMD} = 1.665
ΔH_f = -59 Kcal/mole

Benzotrifuroxan
BTF
$C_6N_6O_6$

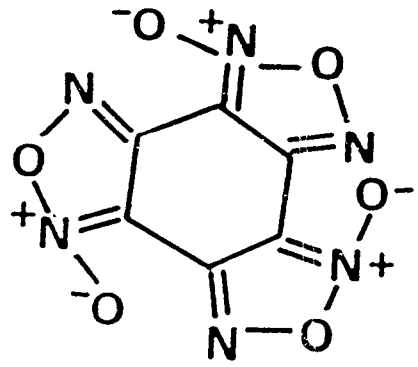

W_{50} particle diameter 4.5μm
ρ_{TMD} = 1.901 g/cc
ΔH_f = +144.5 Kcal/mole

Figure 6

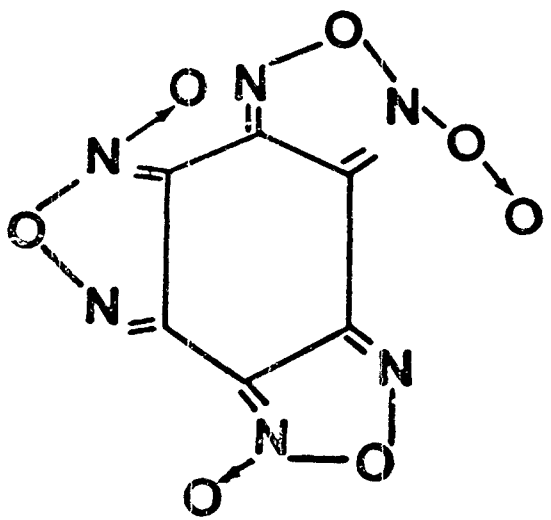

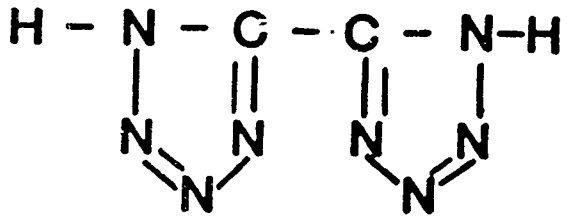

NO H_2O

NO H_2O

H_2O

"46%"

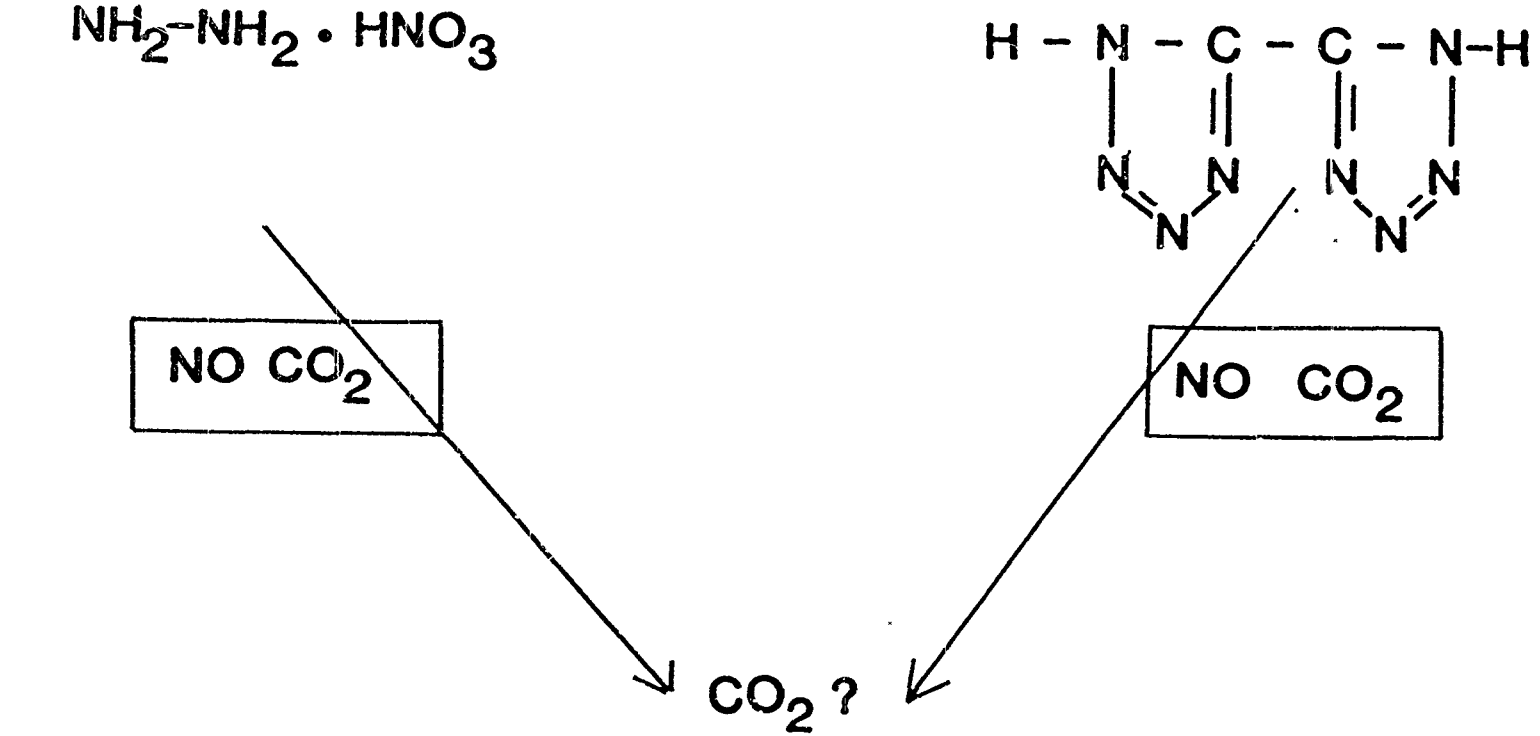

"46%"

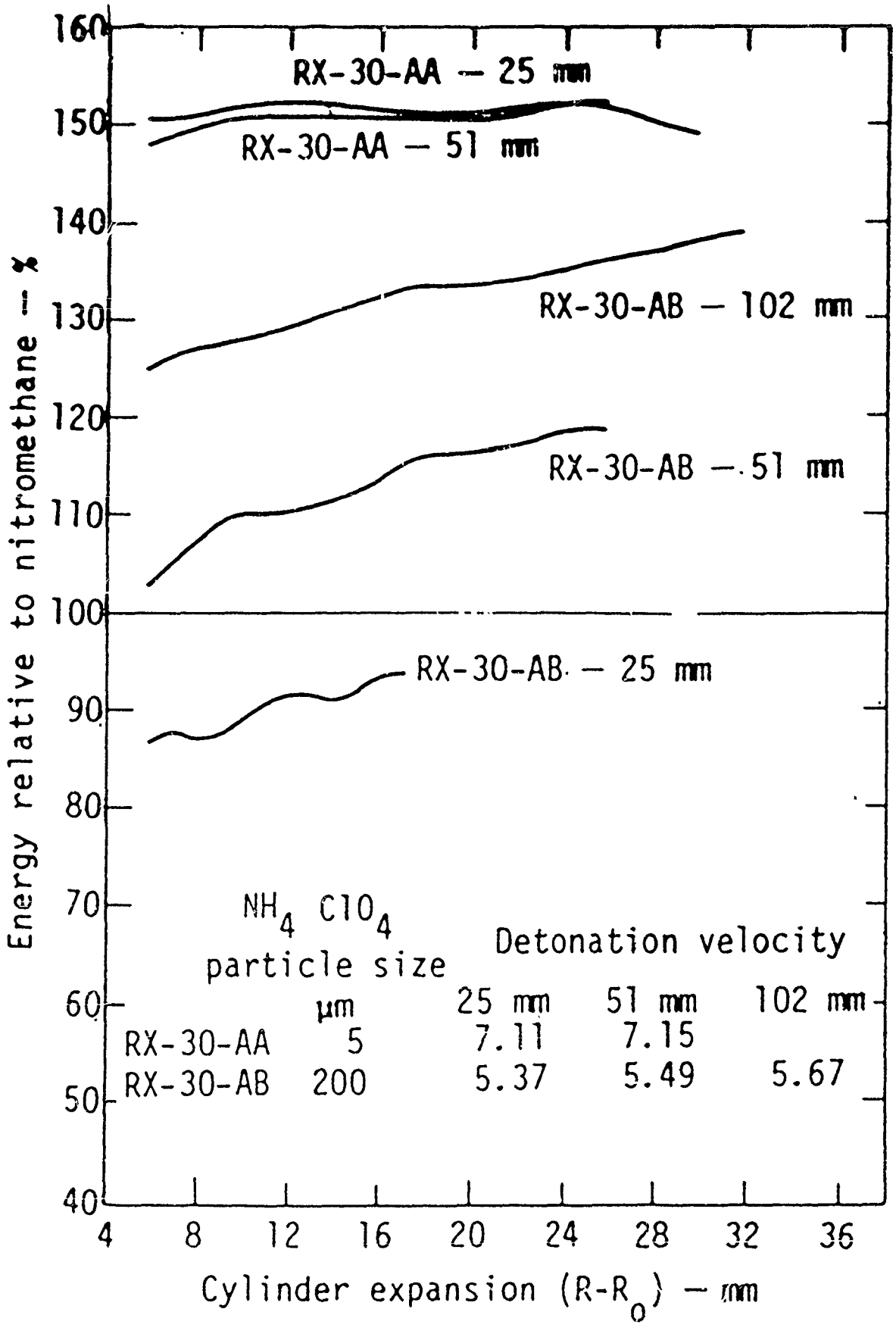

Fig. 7 - Cylinder Test of Ammonium Perchlorate in Nitromethane Shows Effects of AP Particle Size and Charge Diameter.

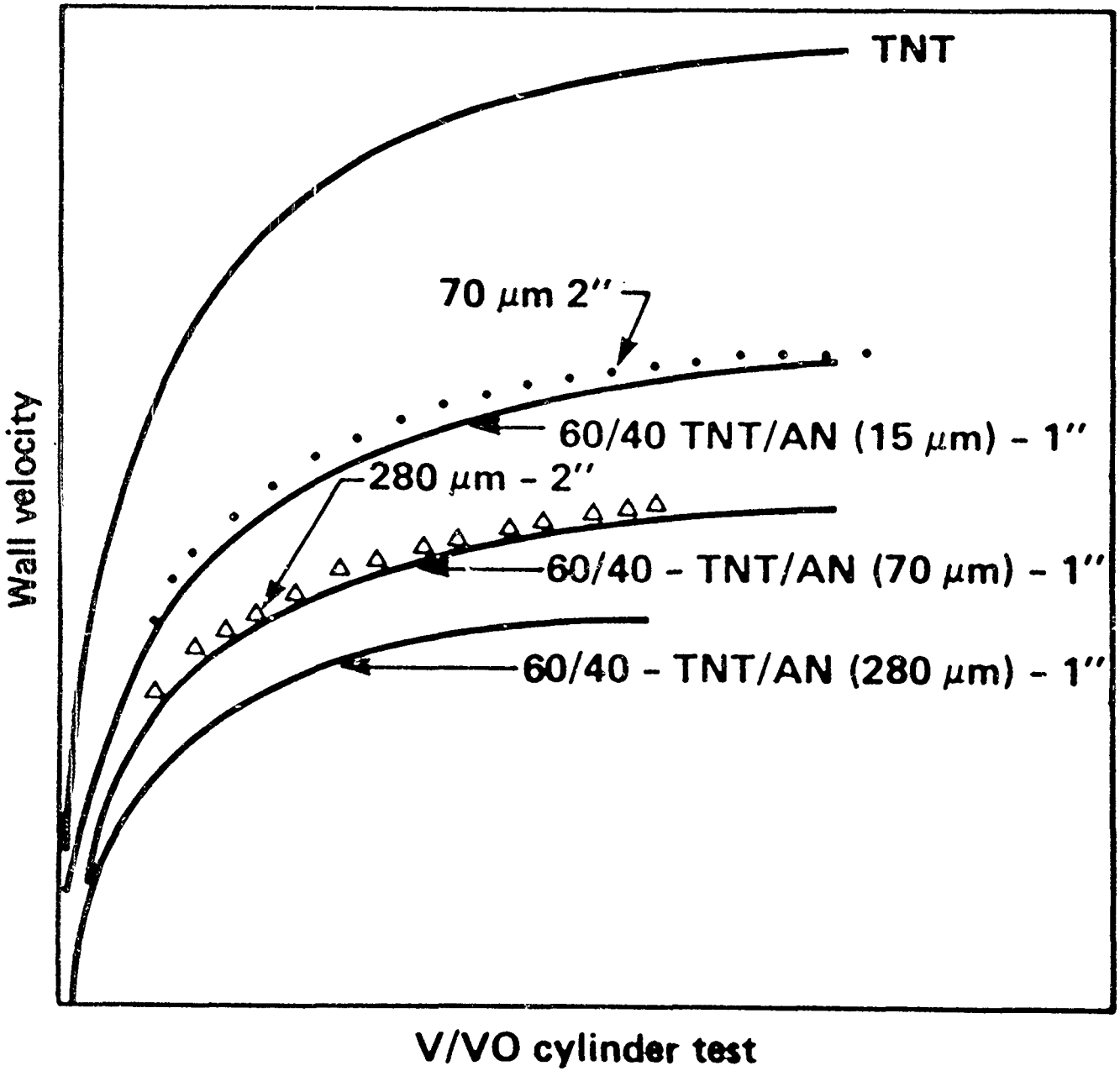

Fig. 8 - Cylinder Test of Amatols Shows Particle Size Effect and Charge Size Effect.

Raising the temperature of detonation increases the reactivity of solid carbon in a TNM-carbon system

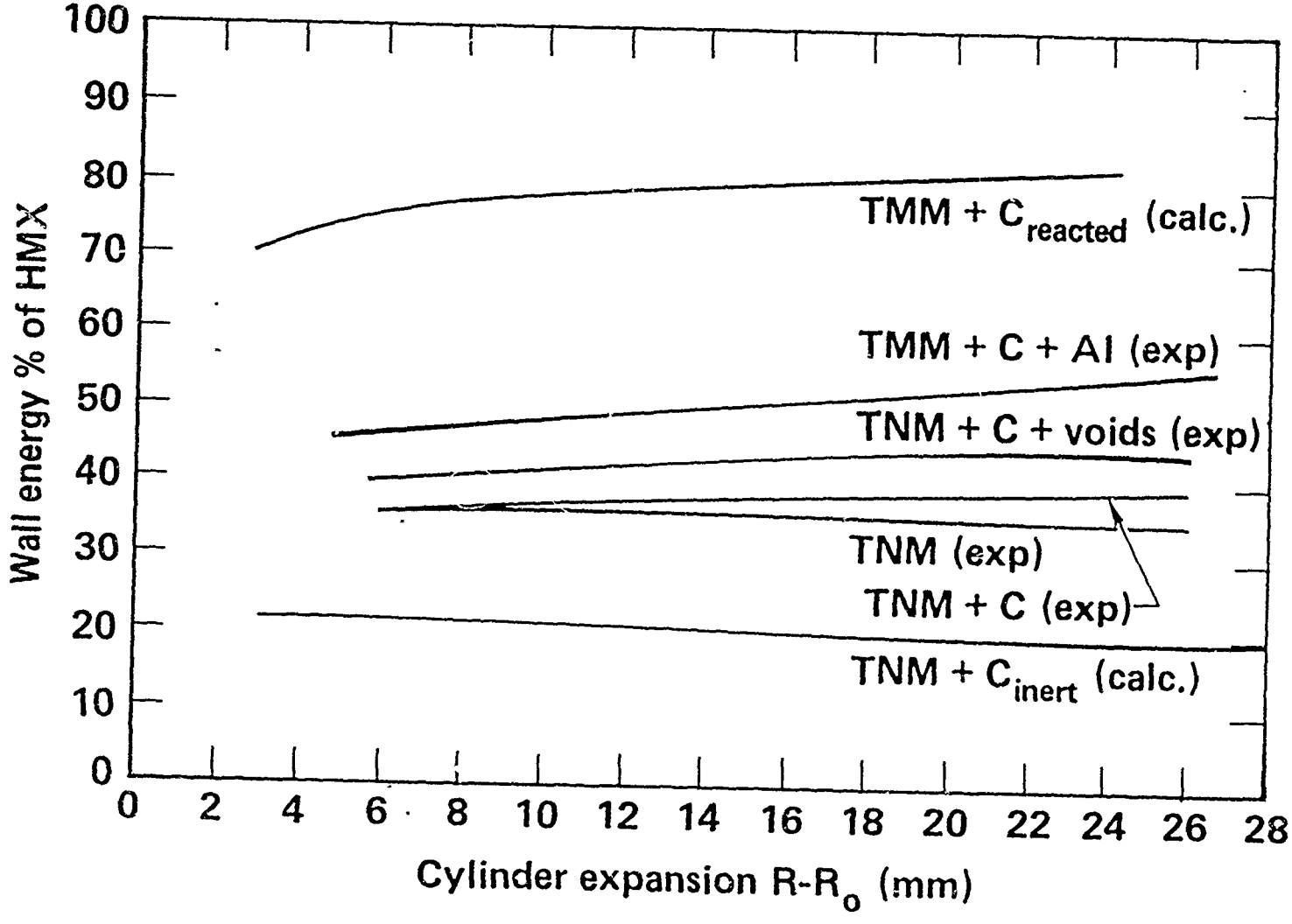

Raising the detonation temperature, increases the performance; TATB/AP at CO balance

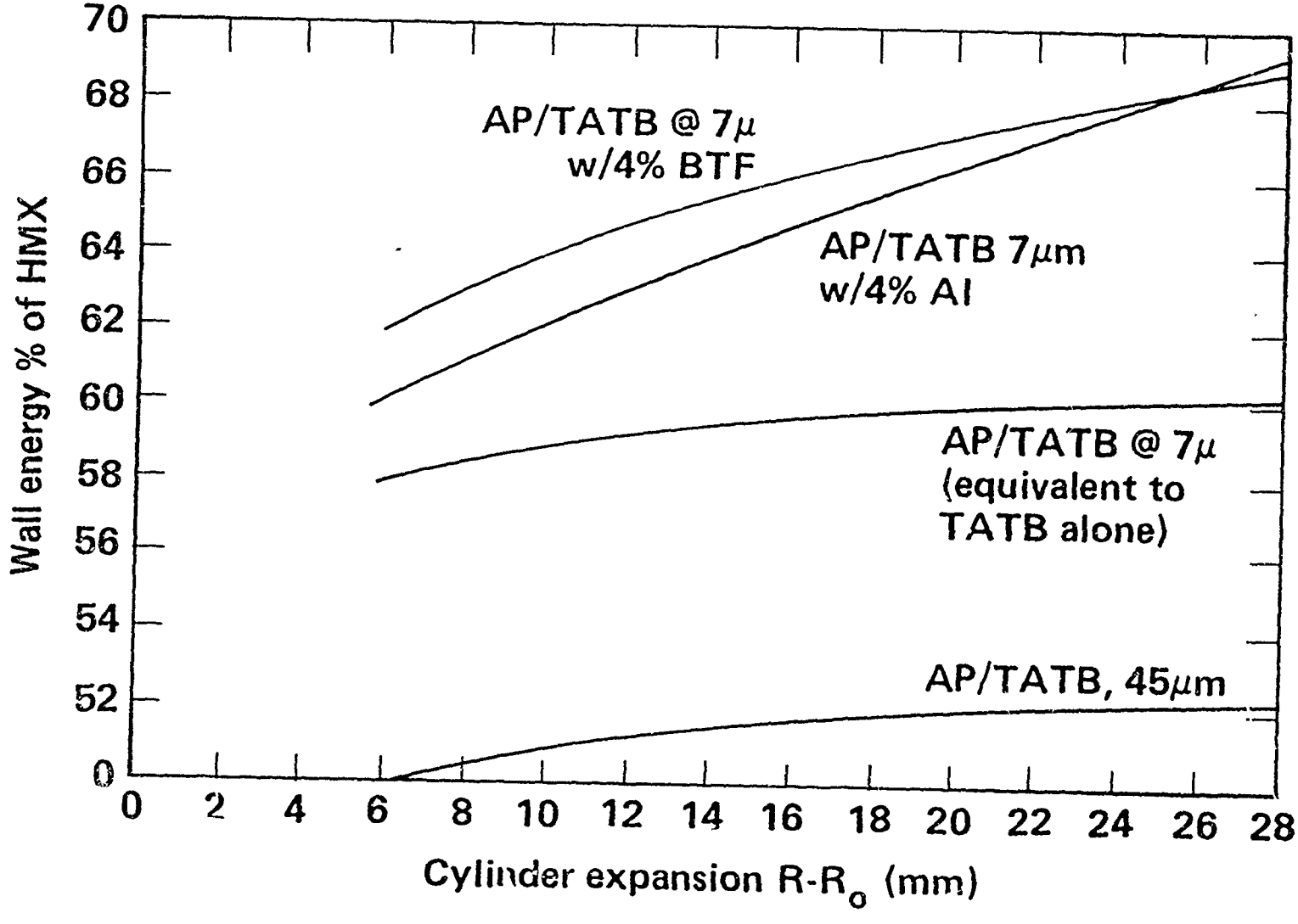

Cylinder test performance: gas volume at CJ (V) ~ constant temperature at CJ (T) increasing

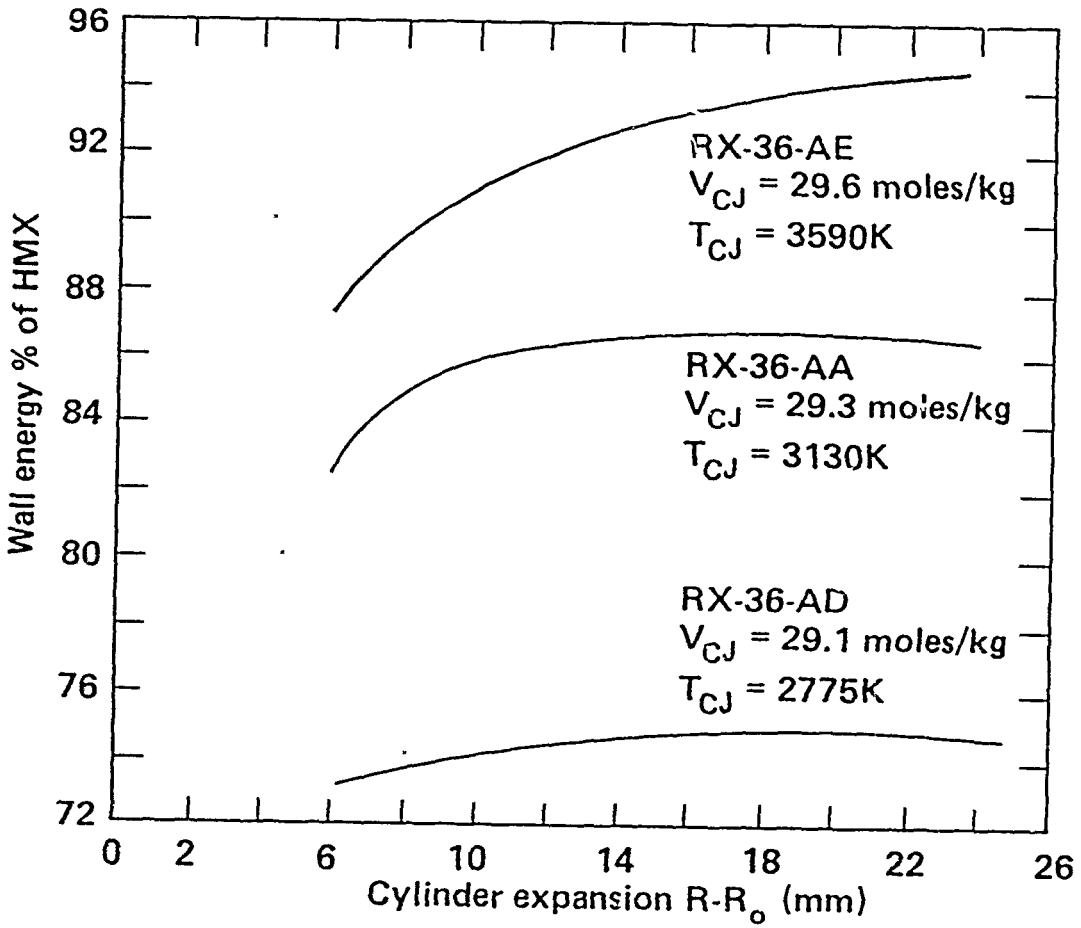

Figure 9b

Aluminum in composite explosives reacts completely independent of host explosive

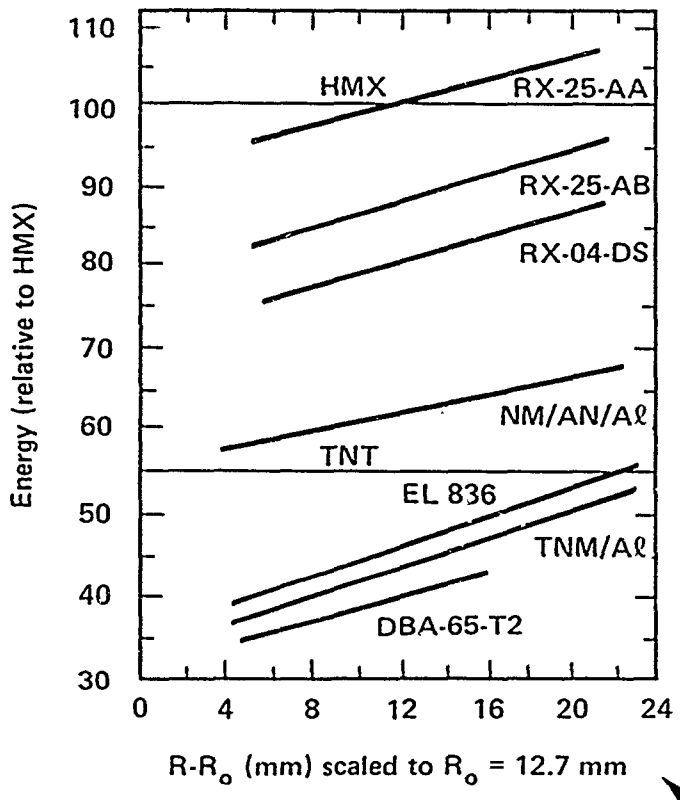

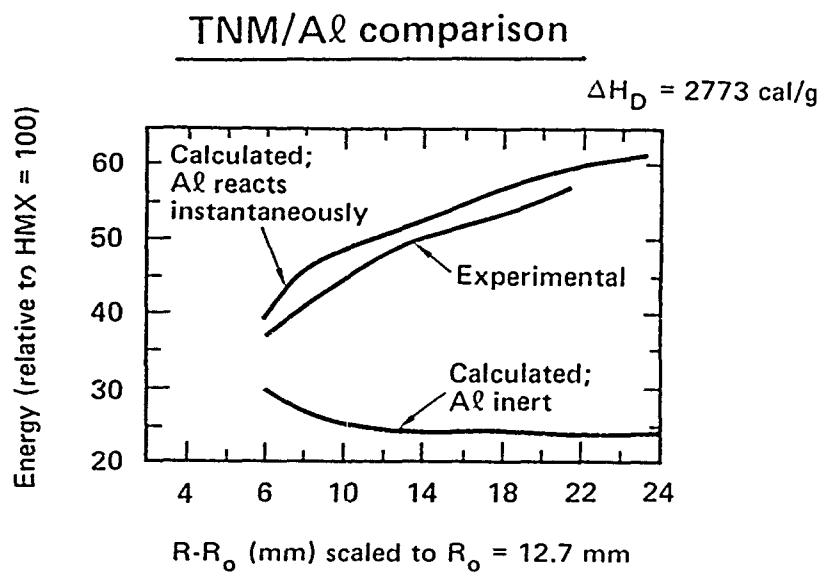

Cylinder expansion

Figure 10

Composite explosives are REDOX reactions with added complication of transport (diffusion and radiation) processes

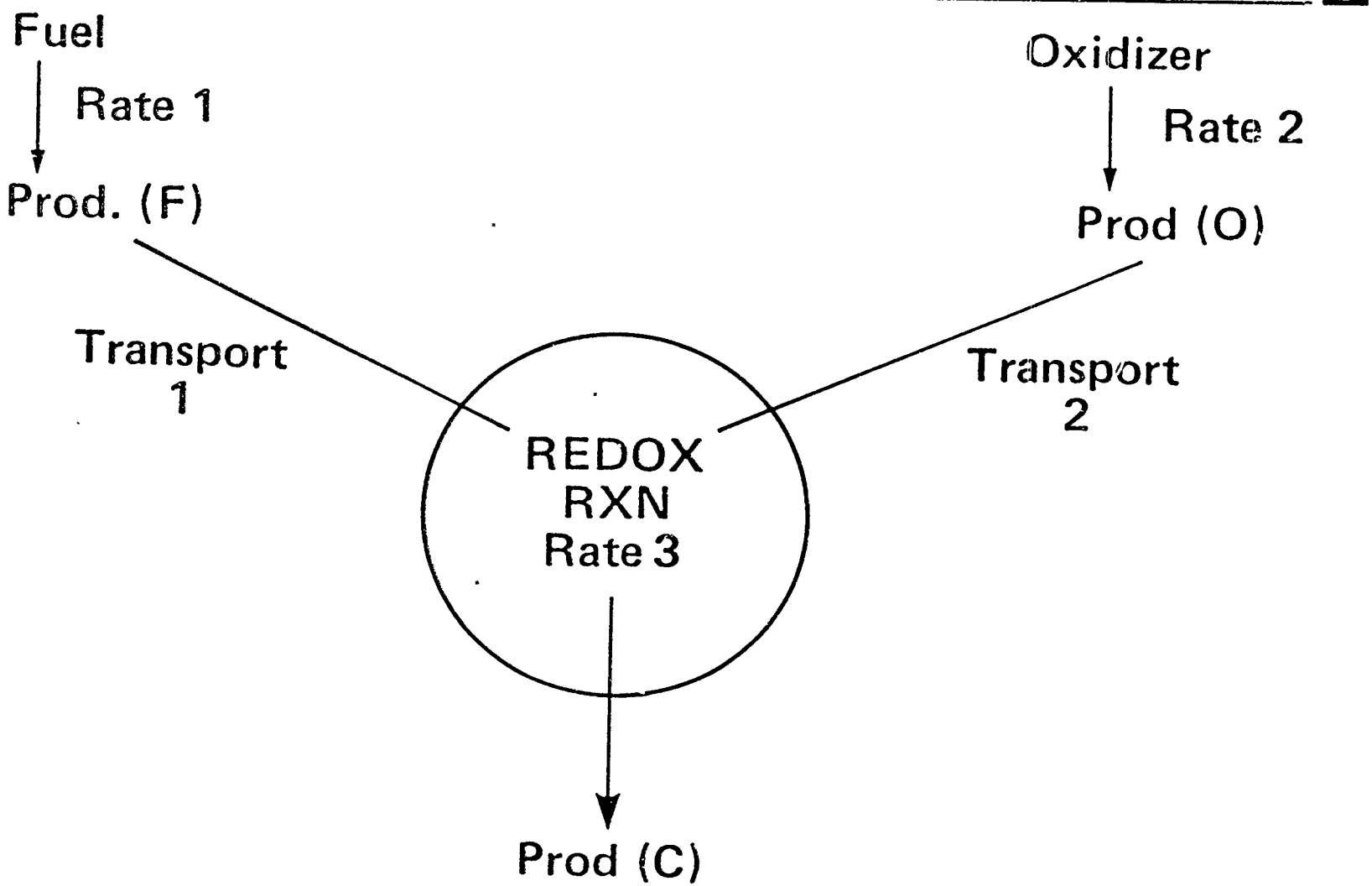

COMPOSITE EXPLOSIVE MODEL

- FIVE EQUATIONS OF STATE IN PRESSURE EQUILIBRIUM.

  JWL FORM

$$P = A\left(1 - \frac{W}{RV}\right)\bullet^{-RV} + B\left(1 - \frac{W}{R_2V}\right)\bullet^{-R_2V} + W\,E/V$$

  EASILY DIFERENTIABLE (AND INTEGRABLE) FIT TO SOUND VELOCITY, HUGONIOT, DETONATION EXPERIMENTS.

COMPOSITE EXPLOSIVE MODEL-CONT'D

- 3 CHEMICAL RATES

  IGNITION & GROWTH FORM FOR 2 RATES

$$\frac{\partial F}{\partial T} = I(1-F)^{2/3}\left(\frac{\rho}{\rho_0} - 1\right)^{A} + G(1-F)^{2/3} F^{b} P^{c}$$

  FOR EXPERIMENTAL DATA, I.E., FAILURE DIAMETER, ETC.

- THIRD RATE DIFFUSION CONTROLLED

  DEPENDS ON CONCENTRATIONS, TEMPERATURE AND DIFFUSION CONSTANTS.

  DISTANCE PARAMETER RELATED TO PARTICLE SIZE.

EXPLOSIVE - JCZ-3

$$P = P_0(v) + G(v,T)\frac{RT}{V}$$

P_0 = Lattice pressure along the "0" degree isotherm

G = Thermal contribution to pressure from intermolecular forces related to lattice vibrations at high ρ.

G = is ultimately related to Γ, $(d\ln P/d\ln v)_S$, for ideal gas C_p/C_v

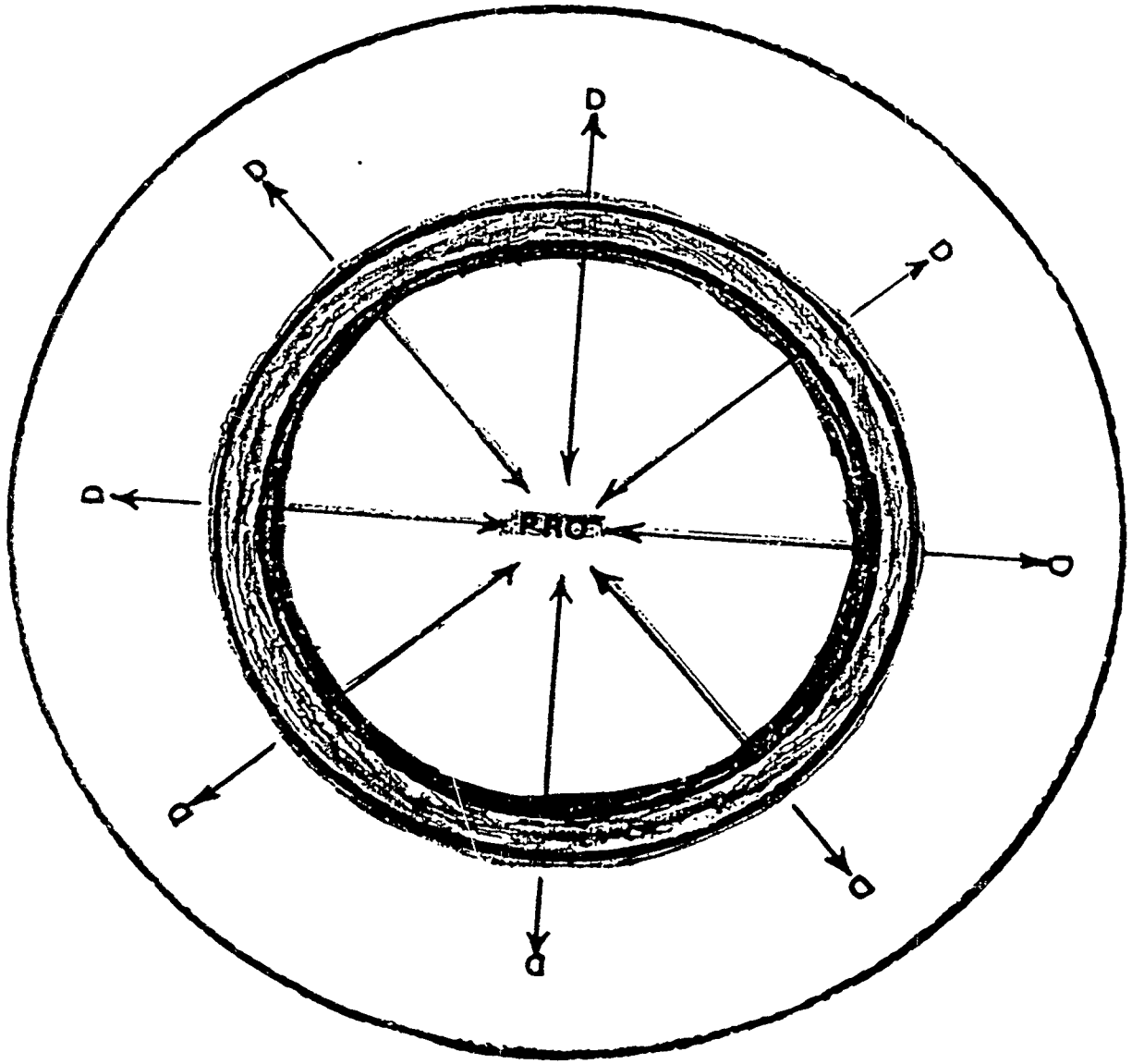

Fig. 13 - Exploding Spherical Detonation Showing Converging Product Streamlines

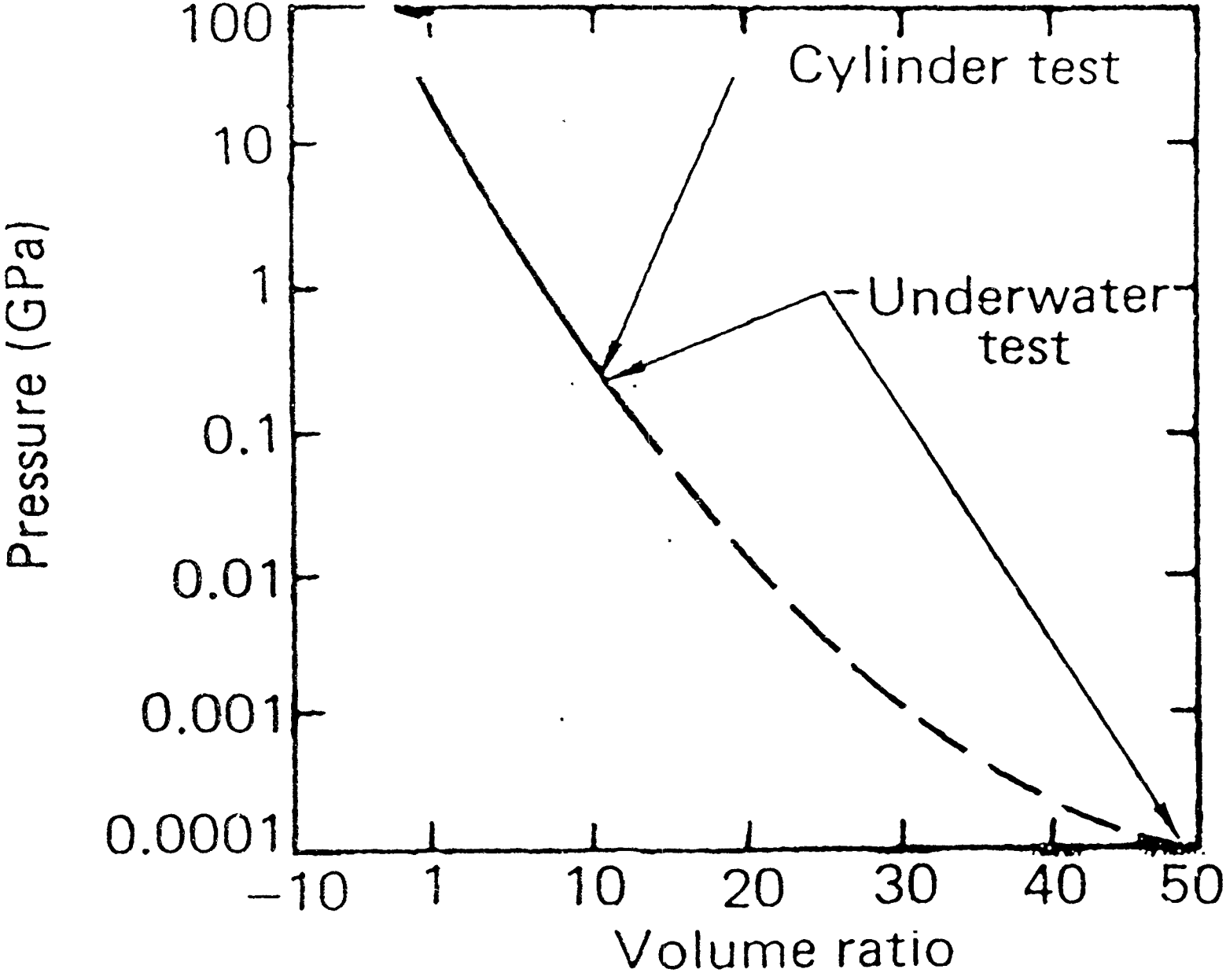

Fig. 14 - Cylinder Expansion and Underwater Spherical Explosion Match for Nitromethane.

Interface Effects in Underwater Explosions

J. E. Shepherd

Rensselaer Polytechnic Institute
Department of Mechanical Engineering,
Aeronautical Engineering and Mechanics
Troy, NY

Abstract

The interface between explosive products and the surrounding water plays an important role in underwater explosion phenomena. The effects of the energy and mass transfer processes occurring at the interface significantly influence shock wave production, bubble oscillation, migration and interaction with adjacent surfaces. Density and impedance differences across the interface are factors in determining the initial shock wave strength and the subsequent decay. Superheated water is created due to shock heating and bubble overexpansion during oscillations. Evaporation of this water alters the bubble period, oscillation amplitude and migration rate. These effects are particularly important in subscale testing. Hydrodynamic and/or diffusive instabilities of the interface are observed during some phases of the motion. Evaporative instability could be the rate-determining process that limits mass transfer. Taylor instability during the bubble collapse phase could limit the collapse velocities and the strength of the associated jets produced near boundaries. Our present understanding is summarized and future research areas are identified.

Introduction

A conventional underwater explosion creates a bubble of hot product gases (a mixture of water, carbon dioxide, carbon monoxide, nitrogen, hydrogen, and sometimes solid carbon or metal oxides) at high temperature (2000–4500 K) and pressure (150–400 kbar). The exact composition and thermodynamic state of the products depend on the type of explosive and it's elemental composition. The bubble of products rapidly expands, producing a shock wave in the surrounding water. The shock wave decays as it moves outward and the bubble oscillates and migrates upward (Fig. 1). In addition to the initial shock wave, a sequence of smaller pressure waves or "bubble pulses" are produced at the minimum radius of each bubble oscillation cycle.

The **interface** is the surface or more generally, region, between the explosive products and surrounding water. The interfacial region serves to couple the motion of the product gases to the surrounding water. In turn, the motion and thermodynamic state of the fluid adjacent to the interface determine the energy and mass transfer processes

across the interfacial region. It is this nonlinear coupling that is really being referred to when we talk of interface dynamics. The subject of the present report is the effects of interface dynamics on all the phenomena associated with underwater explosions. The phenomena affected include: shock pressure and decay rate; bubble oscillation period and amplitude; bubble pulse magnitude and shape; bubble migration rate; bubble-structure interaction, i.e., the formation of jets during the collapse phase.

The physical processes that are important to the present discussion are indicated on the idealized space–time diagram of Fig. 2. On this graph are shown the trajectories of the detonation, interface, shock wave in the water, pressure waves within the products, and also the bubble overexpansion, collapse, and rebound. The bubble oscillation period has purposely been made unrealistically small in order to show all these features on the same plot. The processes indicated are: A – detonation propagation; B – detonation-water interaction; C – gasdynamics within the bubble; D – acoustic wave interaction with the interface; E – disturbance propagation up to the shock; F – shock compression of the water; G – evaporation of the water at the interface; H – isentropic expansion of the products; I – interface instability near collapse; J – geometrical vs nonlinear effects in bubble pulse propagation. In the three sections that follow: Detonation Wave Interaction; Mass Transfer; and Instabilities, these physical processes are discussed with a particular emphasis on the relationships to the interfacial region and dynamics.

In writing the present review, three sources of information were used: the classical references[1,2] from World War II; papers published in journals and symposia; and contractor and government laboratory reports. It is clear that the most widely known reference, R. H. Cole's book **Underwater Explosions**,[1] which pays scant attention to interface issues, is completely out of date. Unfortunately, this is the only readily available comprehensive compilation of information. A new primer and reference book is sorely needed to help newcomers to this field.

Detonation Wave Interaction

The physical process which dominates the initial phase of the explosion is the propagation of the detonation wave through the explosive and the interaction with the surrounding water. Numerical computations of this process show that this interaction generates a complex system of waves propagating within the products, partially reflecting from the interface and catching up with the shock wave. The results of Sternberg and Walker[4] for a Pentolite sphere are shown in Fig. 3.

When the detonation reaches the edge of the explosive, a shock wave is propagated outward into the water and an expansion wave is usually propagated back into the explosive products. Both waves then interact with the expansion or "Taylor" wave that follows the detonation. However, near the instant of interaction the process can be idealized as the production of two simple waves at a planar surface, shown in Fig. 4. The pressure at the interface immediately following interaction can be determined

by matching pressure and velocity at the contact surface (the water-product interface); this matching process is shown graphically in Fig. 5.

To carry out this computation, we must know the Chapman-Jouguet state of the explosive, the equation of state of water and also the explosive products. The TIGER computer code[5] was used with the BKW equation of state (with the LLNL recalibrated constants[6]) and standard thermochemical parameters.[7] The hugoniot for water was taken from the experimental data and analysis reported by Rice and Walsh[8], Gurtman et al.[9], and Steinberg[10]. The explosive product isentropes were either obtained from the JWL equation of state[7] or computed using TIGER and the BKW equation of state.

The results for 5 explosives: HMX, Pentolite, H-6, TNT, and NM are given in Table 1 and Fig. 6. All these materials *except* H-6 are simple CHNO compounds that behave as ideal explosives in kilogram quantities, i.e., they have short reaction zones, small failure diameters, detonation velocities independent of size and good agreement between computed and measured properties. H-6 is a mixture of CHNO explosives and aluminum (in particulate form) and is more typical of explosives used in modern underwater applications; it exhibits nonideal behavior: a strong size dependence of measured properties. The interface pressures range from a high value of 230 kbar for HMX down to 121 kbar for NM; the CJ state for NM is so close to the water hugoniot that only a small expansion wave is reflected back into the products.

This computation illustrates one difficulty in obtaining high water shock pressures and associated high strain rates on adjacent targets. A substantial amount of the high pressure generated by detonating RDX is reflected back into the products due to the impedance mismatch with the water. Furthermore, the remaining energy in the high pressure shock is rapidly dissipated due to the irreversible nature of the shock wave propagation. The difference between isentropic compression and shock compression as represented in pressure–volume coordinates (Fig. 7) is due to the increase in entropy across the shock wave. As the shock pressure is released by the essentially isentropic wave system following behind, the water pressure returns to ambient but the temperature and specific volume (see Fig. 7) are higher due to the energy deposited by the shock wave. This shock heating has three effects: the shock wave in the water decays rapidly after leaving the interface; a layer of superheated water is created next to the bubble; and less energy remains in the water–bubble system to drive the oscillation process. The heating effect is confined to a thin layer due to the rapid attenuation by geometrical spreading, the interaction with transmitted Taylor wave, and the increase of the entropy jump with increasing shock strength.

The entropy increase across the shock wave can be computed from the experimental hugoniot and simple thermodynamic relations as described in Ref. 8. If we neglect diffusive thermal transport processes within the water , a reliable approximation in most shock propagation problems, the entropy change in a fluid element depends only on the strength of the shock wave at the time it passed through that location. This function, entropy jump vs shock pressure, is shown in Fig. 8. These entropy changes will be used, in conjunction with a temperature-entropy phase diagram of water, to

examine in the next section the issue of superheating and evaporation.

The effect of the initial shock pressure and fraction of the explosive energy dissipated by the shock has been parametrically studied by Sternberg and Hurwitz[11]. They computed energy budgets (shown in Fig. 9) as a function of shock position for 4 explosives. The highest shock pressure and largest dissipation is generated by detonating PBX9404 (the principle ingredient is HMX); over 50% of the original energy has been dissipated when the shock has reached 30 R_o, where R_o is the initial charge radius. The Pentolite has a CJ and initial interface pressure that is two–thirds that of PBX9404; 40% of the initial energy has been dissipated at 30 R_o. A constant–volume explosion of high–density (1.65 g/cm^3) Pentolite produces an interface pressure of 30 kbars and results in 30% of the original energy being dissipated at 30 R_o. The constant volume explosion of low–density (0.4125 g/cm^3) Pentolite produces an interface pressure of 6 kbars and results in less than 5% of the energy being dissipated by 30 R_o.

How does this wide range of interaction pressures and dissipation rates affect the pressure wave at some distance from the explosive? In applications and experimental measurements, it is not the interface pressure that is significant but the pressure at some distance away from the explosive. Weapon systems operate with a range of standoff distances from the target; pressure and shock trajectory measurements are performed in the water surrounding the charge. The shock pressure at a given location is the result of several factors: the initial interface pressure; decay due to the geometrical increase in shock front area; and the integrated effects of the interface motion producing acoustic signals that propagate from the interface to the shock. These signals are propagated along characteristics as shown in Fig. 10.

The net result of these processes on near and farfield pressure are shown in the pressure vs. distance diagram of Fig. 11, taken from Sternberg and Hurwitz. The four cases shown correspond to those of Fig. 9 and the size of the individual charges have been adjusted so that the total energy release is the same in all cases. In the near field (at distances of 1-4 charge radii), the interface pressure substantially influences the shock pressures; lower interface pressures result in lower shock pressures at the same scaled distance.

However, as the distance from the charge is increased, the lower interface pressure is compensated for by lower dissipation and a lower shock decay rate. This lower decay rate is due to the interface deceleration being lower in the constant–volume and low–density explosions than in the high-density detonation cases. The net result is that the three cases with similar initial explosive density yield essentially identical pressures at the same scaled distance from the charge, beyond 5–10 charge radii. This result is the basis of the standard explosive scaling rules,[3,12] which holds that for equivalent energy releases, the far field pressures are the same at equal scaled distances. This scaling appears to hold for a variety of atmospheres and explosives, including air,[11,12] there is however, an initial density effect that is imperfectly understood. Very low density explosives can show significant departures from the standard scaling rules. This has been observed[13,14] in soviet tests of underwater gaseous detonations and can be seen in

the low density Pentolite explosion results shown in Fig. 11.

Clearly, a low *brisance* (small CJ pressure) explosive is better for transferring kinetic energy to the water and obtaining large amplitude bubble oscillations. This advantage is obtained at the expense of lowering the initial shock pressure. Apparently the only manner to obtain high strain rates is through high initial shock pressure and concomitant dissipation. The optimum tradeoff between high initial shock pressure and high final bubble energy must be determined by considering damage mechanisms and the particular weapon application. The results shown in Fig. 11 suggest that the standoff distance is a key parameter in these considerations.

In addition to the simple thermodynamic and hydrodynamic factors mentioned above, there are other issues that must be considered when examining real systems. Among these are: the nonideal nature of many explosives, particularly aluminized materials used in modern underwater weapon systems; influence of an extended reaction zone structure behind the detonation front; multi-dimensional nature of charge and detonation front geometry; curvature effects on detonation propagation; the nonideal character of the interface in a cased charge; attenuation of the shock while propagating through the case. Two of these issues: the influence of adding aluminum to the explosive and the effect of a metal case, are discussed next.

The addition of powdered or flake aluminum (micron-size particles) to a conventional explosive is found to significantly improve the performance in underwater applications. The equivalent amount of energy, as determined by intermediate-field (5–10 R_o) shock pressure measurements and bubble oscillation period determinations, is an increasing function of aluminum concentration (see Fig. 12) up to an aluminum/oxygen molar ratio of 0.4. A substantial fraction of this gain is just due to the better energetics of aluminum as a fuel rather than carbon.

Computations and measurements[7] indicate that the heat of detonation (the energy available per mass of explosive) is an increasing function of the aluminum content. As shown in Table 2, the heat of detonation of RDX is 6.15 MJ/kg; addition of 30 wt % Al increases this to 10.12 – a factor of 1.64. Fig. 12 indicates a bubble energy increase of 1.9 over pure RDX and an equal strength shock wave. However, it cannot just be energetics alone since the energy distribution is shifting from the shock wave to the bubble with increasing aluminum concentration.

Some of this shift is due to the decrease in Chapman-Jouguet pressures and therefore, lower interface pressures and shock dissipation, with an increasing fraction of aluminum. Calculated interface conditions for some RDX/Al explosive mixtures are shown in Fig. 13 and given in Table 2. These are idealized computations in which the aluminum is quickly burned to Al_2O_3(s) and the free carbon rapidly coagulates into a solid graphitic form. The formation of C(s) and Al_2O_3(s) are interrelated since the product composition shifts

$$CO + CO_2 + 2Al \rightarrow 2C(s) + Al_2O_3$$

to these condensed species with increasing amounts of initial aluminum.

The ideal interaction pressures are lowered but not enough to provide the gain in bubble oscillation energy shown in Fig. 12. This implies that the nonideal nature of these explosives is responsible for the remaining shift in energy distribution. The obvious problem with the ideal theory is the assumption of the rapid formation of both Al_2O_3(s) and graphitic carbon clusters within a short reaction zone. These processes both involve heterogeneous reactions and species diffusion to and from particles of up to micron size; the slowness of diffusive processes in comparison to unimolecular or bimolecular reactions suggests a two-stage reaction zone.

In the first stage, lasting nanoseconds, molecular products such as H_2O, CO, CO_2, and H_2 are produced; in the second, lasting microseconds,[13] the Al_2O_3 and C atoms coagulate into clusters. This two-stage process and the introduction of a long reaction time scale will cause the detonation development to steady state to be delayed and the ideal conditions will be achieved only after a long buildup time in an exceedingly large charge. During the buildup period, the detonation and interface pressures will be lower than predicted by the ideal theory and the long-time-scale reactions will contribute to the bubble energy rather than the shock.

The maximum reductions in detonation and interface pressure can be estimated by performing the detonation thermochemical computations without any solid product formation. For 15 wt % Al in RDX/Al explosive, the detonation pressure is reduced from 331 to 305 kbar and the interface pressure from 200 to 187 kbar. For 30 wt % Al in RDX/Al explosive, the detonation pressure is reduced from 267 to 171 kbar, the interface pressure from 150 to 96 kbar. There is also evidence[14] that the microstructure of these heterogeneous materials can produce comparable nonideal behavior that results in substantially lower detonation front pressures at nearly ideal values of the detonation velocity.

Weapon systems and many experiments use a metal case to contain the explosive. This case will interact with the detonation wave (Fig. 14a) and produce nonideal interface conditions and an extended multiphase region instead of a sharp discontinuity. Impedance mismatches at the explosive–case and case -water interface will produce multiple reflections (Fig. 14b) and an interface pressure lower than ideal. In addition, the expansion wave following the detonation will attenuate the initial shock as it traverses the case material, this will also reduce the interface and water shock pressure as shown in Fig. 15a. The high strains and strain rates induced in the case by the explosion will cause fracture of the case and the shock heated fragments will be dispersed into the surrounding water and products. The mixing action of the dispersal process and the heat transfer from the case fragments will result in the creation of the multiphase interface region shown in Fig. 15b. Such an extended region will behave very differently than the ideal interfaces considered so far.

Mass Transfer

Mass transfer between the explosion products and surrounding liquid water can occur through several mechanisms: evaporation, condensation, dissolution of product gases into the water, explosive boiling of superheated liquids, and direct entrainment of gases into the liquid water. Two causes of mass transfer will be examined in this section; first is the rapid evaporation or explosive boiling of the shock–heated water located within the entropy layer next to the bubble surface; second is the evaporation that occurs when the overshoot in bubble size results in a reduction of the partial pressure of water in the explosion products below the equilibrium vapor pressure of the liquid on the bubble surface.

The magnitude of the effects associated with these processes depends very strongly on the ambient conditions (water temperature and pressure). Evaporation effects appear to be much more significant for scale modeling done at reduced pressure than for deep ocean testing. Parameters associated with bubble motion are most likely to be affected by evaporation. Observations of bubble oscillation period, oscillation amplitude, bubble migration rates, and bubble interaction with structures all show a pronounced effect of ambient conditions in subscale testing and can cause failures in similitude.

As discussed in the previous section, a layer of high–entropy water is created next to the bubble due to shock heating (see Fig. 16). This layer becomes superheated when the interface pressure decreases after the shock has propagated away and the bubble begins to expand. The superheated water can rapidly evaporate into the bubble, mixing with the existing products of the explosion. The amount of water that is superheated depends on several factors: the initial strength of the shock wave; the rate of decay; and the ambient pressure. The relationship between these factors can be illustrated on a temperature–entropy diagram (Fig. 17) for water.

When the shock wave overtakes a fluid element, the fluid state will jump up to a point on the indicated hugoniot of Fig. 17. Following the passage of the shock, the state of the fluid will move from the shock adiabat vertically downwards along an isentrope, examples of which are shown on Fig. 17. As the shock moves away from the bubble and the strength decays, the entropy decreases back toward ambient. When the fluid state passes through the coexistence curve (denoted σ on Fig. 17), the water becomes superheated. At a given pressure, this occurs first for the highest entropy states adjacent to the interface. The entropy jump for these states (ΔS) and the pressure (P_σ) at which the coexistence curve is encountered, is given in Tables 1 and 2 for each of the explosives discussed in the previous section.

The shocked interface coexistence pressures range from a high of 140 bars for HMX to 8 bars for NM. The actual minimum pressure achieved at the interface is determined by the ambient pressure and the bubble dynamics. The ambient pressure is usually expressed in terms of the equivalent depth of the water (taking into account reduced surface pressure for subscale modeling). For reference, a depth of 100 meters in the ocean corresponds to 11 bars ambient pressure, the critical pressure of water, 220

bars, is reached at a depth of 1.3 miles. Due to the overshoot of equilibrium during bubble oscillations, the minimum interface pressure (at maximum bubble radius) can be as much as 10-50 times below ambient. Therefore, for almost all of the explosives mentioned in Tables 1 and 2, some water near the interface will become superheated and evaporates if the explosion occurs at a depth of 100 meters or less.

How much of the water in the entropy layer will actually change phase? Numerical computations are required for each type of explosive in order to predict the entropy distribution and interface pressure histories needed to answer this question. Sternberg and Walker[4] found that the water out to a radius of $1.3R_o$ could be evaporated in a shallow (ambient pressure of 1 bar) pentolite detonation (they did not actually include this effect in their computations). This represents a volume of water that is 1.2 times the original explosive volume or a mass of water that is 0.7 of the original explosive mass. The coexistence curve is encountered by the interface fluid fairly early in the bubble expansion process, at an interface location of $3.9R_o$; for comparison, the equilibrium radius is at $20R_o$ and the maximum radius is at $32R_o$.

An increase of 70% in the mass of the bubble is very substantial but represents a change of only 20% in the equivalent bubble radius. This figure is an upper bound computed for a ideal detonation in an uncased charge. Nonideal detonation propagation and case effects will both tend to lower the shock and interface pressures, decreasing the amount of water vaporized. This example is for an explosive with a value of 40 bars for P_σ, which is in the middle of the range for the explosives examined above. The amount vaporized also decreases dramatically with increasing depth. At a depth of 100 m, only fluid that has been shocked to greater than 100 kbar will evaporate – this represents a negligible addition to the mass of the bubble. We conclude that this effect is most important for high brisance explosives at small depths.

In the discussion above, it has been assumed that any water that is superheated will evaporate. However, the evaporation process may be limited by the rate at which water molecules are ejected from the liquid and transported away from the interface. If the evaporation rate is unable to keep up with the rate at which fluid is being superheated, then a nonequilibrium situation is created at the interface. A layer of metastable (superheated) water will be created next to the surface which, if sufficiently superheated, could rapidly (explosively) evaporate. This situation is plausible because the rate of superheating and the rate of evaporation are determined by completely different mechanisms. The existence of superheated liquids and the process of explosive evaporation have also been extensively documented.[17]

The intrinsic rate at which molecules are ejected from the liquid into the vapor is controlled by the molecular dynamics of the superheated liquid[18] and the gas kinetics of the Knudsen layer[19] between vapor and the liquid, Fig. 18a. In cases where the evaporation rate is low and the liquid at the interface is close to equilibrium, these processes act to keep the partial pressure of evaporated liquid close to it's equilibrium value. The net rate of evaporation is then determined by the coupled problem of transporting vapor away from the interface and energy towards it, shown in Fig. 18b.

If diffusion is the only transport mechanism, bubbles in a uniformly superheated liquid will grow in an unsteady manner, the radius increasing with $\sqrt{t}$ and the mass flux inversely proportional to $\sqrt{t}$.[20] This is the process that controls the growth of bubbles in ordinary boiling. A similar process will control the evaporation rate of a near-equilibrium bubble surface created by a deep underwater explosion or a shallow low–brisance explosive. The thermal and mass transport processes occurring in the boundary layers adjacent to the interface will determine the evaporation rates and ultimately, the net effect of evaporation on the bubble motion.

Numerical techniques developed for unsteady laminar mass–transfer boundary–layer problems in chemical processing, heat transfer, and combustion applications could be applied to solve this problem. A number of methods exist[20] for modeling bubble growth under conditions of ordinary boiling that could be extended to treat the explosion bubble problem. Some features that are particular to the explosion bubble are: gas and liquid motion induced by the explosion; nonuniform superheating of the liquid; time dependent gas and liquid thermodynamic states; radiant heat transfer from the explosion products; and real fluid (compressibility) effects in the gas.

A much more difficult problem is to treat the case of an interface far from equilibrium. The mass flux can approach the kinetic theory limit of the one-way molecular flux $n\bar{c}/4$. The proper interface boundary conditions are poorly understood; the high mass fluxes through the phase interface can create instabilities of the interface; liquid droplets may be ejected from the surface along with vapor, creating a multiphase flow within the bubble. These effects have been observed in experiments[21,22] designed to examine the phenomenon of rapid evaporation of superheated liquids. There has been some consideration of nonequilibrium effects in modeling evaporation[23] or condensation[24] during bubble or cavity motion. However, a comprehensive model for the rapid evaporation of superheated liquids that accounts for all these observations and postulated effects is yet to be developed.

As the evaporation proceeds, a layer of evaporated vapor will build up next to the interface. This water vapor is transported away from the interface by diffusion and the convective motion of the explosion products. Deep explosions result in spherical bubbles during the initial expansion phase and only radial motion of the products occurs; diffusion is the only means of transporting vapor away from the interface in these cases. Bubbles created by shallow explosions quickly become deformed due to the large gradient in pressure and influence of the nearby boundaries (water surface and bottom). In these cases, significant product motion transverse to the interface and an overall internal circulation within the bubble may occur. If the Reynolds number is large enough, the flow will be turbulent, greatly enhancing the mixing of evaporated water vapor with the explosion products. While such effects have been considered for conditions encountered in ordinary boiling, there have been no applications to the mass transport problem for explosion bubbles.

One cause of evaporation is the superheated water originating in the entropy layer. Another cause of evaporation is the reduction in pressure within the gas bubble when

the equilibrium position is overshot during the oscillation cycle. This behavior is shown in Fig. 19 for an explosion of 250 g of tetryl at a depth of 300 ft (from Cole, Ref. 1). The experimental measurements of bubble radius vs. time were used to infer the pressure, assuming uniform conditions within the bubble and isentropic changes in state (JWL equation of state). In this case, the pressure minimum of 0.24 bar is much less than the ambient pressure of 10.4 bar but still greater than the equilibrium vapor pressure of 0.035 bar for 300 K water.

Therefore, at this depth no evaporation will occur due to the pressure undershoot. At lower depths, the minimum pressures will be even lower and evaporation will commence if the partial pressure of water in the explosive products (water is typically 20–30 mol % of the products for CHNO explosives) drops below the saturation pressure at the ambient temperature. In effect, the liquid water at the interface becomes superheated when this happens and evaporation occurs as the system attempts to restore equilibrium. Increasing the ambient temperature increases the saturation pressure and the likelihood of evaporation. This effect is particularly significant in scale model testing.

Scale model testing of underwater explosives is designed to preserve geometric and dynamic similarity of the bubble motion. Geometric scaling means preserving the ratio R_{max}/d of bubble maximum size R_{max} to depth d; the amplitude of the bubble oscillation R_{max}/R_{min}; and the ratio of structure to bubble size. Dynamic scaling means preserving the ratio of inertia to buoyancy forces, the Froude number $Fr = U^2/gL$, where U is a characteristic velocity and L a characteristic length. For a length scale, the bubble maximum radius is used $L \sim R_{max}$; the velocity scale is $U \sim R_{max}/T$ where T is the bubble oscillation period. In terms of the bubble parameters, a constant Froude number is equivalent to a scale-invariant parameter $F = T^2/R_{max}$. The parameters T and R_{max} now have to be determined as functions of initial and ambient conditions using the dynamics of the bubble–water system.

The one-dimensional dynamics of a gas bubble within an liquid is, in the simplest approximation, controlled by a nonlinear second-order differential equation[20]

$$R\frac{d^2R}{dt^2} + \frac{3}{2}\left(\frac{dR}{dt}\right)^2 = \frac{P(V) - P_\infty}{\rho_o}$$

where

$$P(V) = P_o\left(\frac{V_o}{V}\right)^\gamma, \quad \gamma \approx 1.2, \quad V = \frac{4}{3}\pi R^3$$

known as the Rayleigh or bubble equation. The oscillatory solutions to this equation and the various improved versions can be used to predict the purely radial motion of a deep explosion. The initial conditions to this equation are determined by the total amount of energy in the bubble-water system E_b, which is approximately 40% of the available energy ΔH_{det} in the explosive (for conventional CHNO materials).

From the solutions to this equation, simple scaling relations can be established for the period T, maximum radius R_{max}, and the amplitude of oscillation R_{max}/R_{min}

$$T \sim \rho_o^{1/4} \frac{E_b^{1/3}}{P_o^{5/6}}, \quad R_{max} \sim (E_b/P_o)^{1/3}, \quad R_{max}/R_{min} \sim P_o^{-1/3}$$

If the geometric scaling factor is λ between two configurations (labeled 1 and 2) , then geometric similarity requires that $\lambda = R_{max,2}/R_{max,1} = d_2/d_1$. Dynamic similarity requires that $F_1 = F_2$. These similarity conditions then reduce to the following scaling relations for pressure depth $Z = d + P_s/\rho_o g$ and bubble energy:

$$Z_2 = \lambda Z_1, \qquad E_{b,2} = \lambda^4 E_{b,1}$$

The linear reduction in pressure depth Z and physical depth d combined imply a corresponding reduction in the surface pressure P_s. This is the reason scale modeling is done in vacuum tanks at reduced surface pressures.

Scale model testing of the interaction of bubbles with structures was performed at NSWC[25,26,27] in a vacuum tank facility using very small charges (0.2 g) of lead azide located at a depth of 2 ft, the total tank depth was 6 ft. The principal observations were motion studies using movies of bubbles. The parameters varied included surface pressure (.15 - 1 bar) and ambient temperature (36 - 100 °F). After correction for a substantial effect of the nearby surfaces, significant departures from the standard scaling laws for bubble period and maximum amplitude were observed.

In terms of charge mass W and pressure depth Z, the scaling law for period (Willis formula[3]) is

$$T = K \frac{W^{1/3}}{Z^{5/6}}$$

where for deep charges, $K_\infty = 2.11$ (SI units) for TNT and the correction[3] for a free surface is

$$K = K_\infty (1 - 0.214 R_{max}/d)$$

The scaling law for maximum radius[3] is

$$R_{max} = J \frac{W^{1/3}}{Z^{1/3}}$$

where the constant is $J_\infty = 3.5$ (SI units) for TNT. The variation of the measured period and amplitude coefficients K and J from the standard values is shown in Figs. 20 and 21. Note that period constant is almost double the standard value at the smallest pressure depths and the highest ambient temperatures. Examination of photographs of the bubble surface reveals a very smooth bubble surface for the 36 °F tests and a rough appearance for 100 °F tests. Both the systematic variation in period constants and the bubble appearance indicate the occurrence of evaporation and the influence of mass transfer on the bubble motion.

Instabilities

There are two types of instabilities that are significant to the interface development and can influence bubble motion. Hydrodynamic instabilities such as Rayleigh-Taylor or Kelvin-Helmholtz mechanisms rely on feedback between the interface distortion and the induced fluid motion. Evaporative instabilities such as the Landau-Darrieus mechanism are more complex and involve feedback between vorticity production, evaporative mass flux, vapor pressure, liquid temperature distribution, and interface distortion. Hydrodynamic instabilities are most significant near the end of the first bubble oscillation cycle, when the interface velocities and accelerations are highest. Evaporative instabilities only operate when there are large evaporative mass fluxes: this is possible whenever the liquid is strongly superheated by either the entropy layer or pressure undershoot mechanisms.

The Rayleigh–Taylor mechanism produces a dramatic and permanent effect when the bubble passes through the end of the first oscillation cycle. Photographs of the bubble (see Refs. 21 and 22) after this time show a surface that is wrinkled and bulging with the disturbances characteristic of the nonlinear "bubble and spike" configuration of the developed instability. These extreme distortions in the interface shape result in the interpenetration of the water and explosion products; this is the direct entrainment mixing mechanism mentioned above. Under conditions of constant acceleration, the mixed region grows quadratically[28] with time. In the explosion bubble, accelerations are time dependent and scaling rules for the extent of the mixed region have not yet been developed. The bubbles of product gas protruding into the water eventually break off and separate from the main bubble. In this manner, the bubble is broken down into a mixed region and isolated smaller bubbles over a number of oscillation cycles.

A planar interface is Taylor–unstable if the accelerations are directed from the light fluid into the dense fluid. This occurs in an explosion bubble when the gas is being compressed and decelerates the surrounding liquid water. Therefore we expect that a detailed stability analysis for a spherical interface (bubble surface) will reach that conclusion. A rigorous criterion for instability can be obtained by analyzing the linear stability of the Rayleigh equation to three-dimensional distortions of the bubble surface. This results in a linear, second-order equation (with time-dependent coefficients) for the disturbance amplitude.

Birkhoff[29] first completely analyzed the stability conditions for the spherical surface; the application to explosion bubbles is discussed in Ref. 21. Referring to the bubble oscillation cycle shown in Fig. 22, there are three cases depending on the signs of the radial velocities and acceleration. Case A, collapsing and decelerating – potentially unstable, with algebraic growth of oscillatory disturbances; Case B: collapsing or expanding, accelerating: potentially unstable with monotonic, exponential growth; Case C: expanding and decelerating - absolutely stable. The case of greatest interest is B, a catastrophic instability that is possible whenever the radial accelerations are large and positive. This is equivalent to the Taylor instability criterion for planar interfaces.

The region of the bubble oscillation cycle in which this instability is possible is shown in Fig. 22. Note that this instability will not occur for all bubbles, but only if the oscillation amplitude is large enough.

If the bubble is unstable, there are a range of unstable wavelengths (discrete mode numbers) which have positive growth rates when the accelerations are large and positive. A maximum wavelength is fixed by the size of the bubble; a minimum wavelength is determined by the effects of surface tension. Within this range, there is a most unstable wavelength that will be preferentially amplified. This wavenumber selection process will determine the length scale for the subsequent nonlinear development of the instability. This has been demonstrated for very low energy, small-scale explosions by photographic measurements[21] of the characteristic disturbance scale immediately following the minimum radius point of the first oscillation cycle. The disturbance amplitude is usually so large after this time that the linear theory is no longer applicable and the nonlinear evolution of the interface must be considered.

What is the impact of this instability process on the overall bubble dynamics? Apparently there has been little systematic investigation of this effect. Cole[1] reports some bubble pulse pressure measurements and notes a lack of agreement with the computations available at that time. We can safely speculate that the interface instability will be a mechanism for removing energy from the bubble and should lessen the severity of the collapse process. In the case of collapse near boundaries, jet formation may be inhibited and the collapse velocities decreased. The effectiveness of the jet impingement as a damage mechanism will be diminished.

A different form of the Rayleigh-Taylor instability may be operative near the beginning of the explosion process but is not observed with conventional underwater explosives. A impulsive destabilizing acceleration is produced when the detonation wave breaks out of the explosive and the transmitted shock enters the water. This impulsive version of the Rayleigh-Taylor mechanism is known as the Richtmyer-Meshkov instability, a subject of current numerical[30] and experimental[31] investigation.

Unlike continuous acceleration, impulsive accelerations of any sign produce instability at an interface between fluids of different density and the disturbances initially grow linearly with time rather than exponentially. Apparently, the decelerating motion of the interface (which immediately follows the acceleration by the shock) stabilizes the Richtmyer-Meshkov mechanism. While no computations have been made to support this supposition, the physical mechanism is plausible. Is significant to note that experiments on extended interfaces[31], such as proposed above for cased explosives, show a dramatic slowing of the instability in comparison to sharp interfaces of the same density ratio.

Rapid evaporation instabilities are not as clearly understood as the Rayleigh-Taylor mechanism. There are numercus experimental observations of instability; particularly when the liquid is highly superheated.[21,22] These instabilities are very significant to determining the evaporation rate: unstable interfaces have effective evaporative mass fluxes that are a factor of 10^2 to 10^3 larger than predicted by the laminar diffusion-

limited theory. The observed instability onset and characteristic length scales appear to be consistent with the Landau-Darrieus mechanisms discussed in Refs. 21 and 22 but the details of the instability mechanisms remain to be clarified.

Theoretical research on evaporative instability has uncovered a variety of possible mechanisms involving the entire spectrum of transport processes and feedback mechanisms between the interface distortion and velocity, pressure, vorticity, and thermal fields in the liquid and vapor. The early studies of Miller[32] and Palmer[33] have been updated (and contradicted) by the more recent work of Prosperetti and Plesset[34] and Higuera.[35] A continuing experimental and theoretical effort will be required to unravel the complex nature of evaporative instability.

Summary

Three aspects of underwater explosions have been discussed: interaction of the detonation with the water; evaporation of water into the bubble of explosion products; and the instability of the interface between products and the surrounding water.

Upon reaching the edge of the explosive, the detonation wave produces a transmitted shock wave in the water and a reflected expansion in the explosive products. The transmitted shock provides the initial conditions for the shock propagation problem in the water. There is a tradeoff between producing a very strong shock which decays quickly and dissipates a large amount of the energy or using a lower pressure explosive with fewer losses and retaining more energy in the bubble-water system. The bubble motion generates acoustic signals which catch up to the shock and have a strong cumulative effect which is of even greater importance than the initial conditions in determining far-field shock pressures.

The optimum combination of near-field shock pressure and bubble energy needs systematic exploration. The effect of initial explosive density is not well understood. Nonideal effects in explosive propagation appear to have a significant role in shifting the energy budget from the shock to the bubble; further developments in detonation modeling are required to address this and the related issues of reaction zone structure, detonation wave instability and long-time-scale reactions.

Evaporation of water into the product bubble can be due to either the shock-generated entropy layer or pressure undershoot during the bubble oscillation cycle. Experimental observations in subscale testing verify that evaporation can significantly alter the bubble dynamics; particularly at small depths with high brisance charges. The evaporation rate will be determined by the coupled problems of mass and energy transport near the phase interface, the mass transport within the bubble by diffusion and convection, and the dynamics of superheated liquids. Existing data is difficult to interpret due to boundary effects. Numerical and analytical models of these processes need to be developed.

Instabilities of the interface are due to both hydrodynamic and evaporative mechanisms. Hydrodynamic instabilities such as the Rayleigh-Taylor mechanism are sig-

nificant near the minimum of the bubble oscillation cycle. Large deformations of the interface are produced at this point, destroying the symmetry of the collapse process and ultimately causing the fragmentation and destruction of the original bubble. Evaporative instabilities occur whenever the liquid is superheated sufficiently. These instabilities can greatly enhance the rate of mass transfer over the classical diffusion–limited values.

One of the most significant issues in modeling bubbles and predicting explosive performance is determining the composition and mass of the bubble as a function of time. What is the contribution of the entropy layer? How does the nonideal interface of real systems affect the transfer processes? What is the contribution of evaporation during pressure undershoot? Does evaporative instability play a role? It is important to develop complementary programs of analytical, numerical and experimental research to adequately answer these questions.

Acknowledgement

I would like to thank Georges Chahine (Tracor Hydronautics), Jules Enig (Enig Associates), Tom Farley, John Goertner (NSWC) and Paul Thibault (Combustion Dynamics) for their advice and references. John Goertner was particularly helpful in providing copies of his photographs and patiently explaining his experiments to me.

References

1. R. H. Cole **Underwater Explosions**, Dover, 1965.

2. **Underwater Explosion Research**, A Compendium of British and American Reports. Vol. 1 - The Shock Wave. Vol. II - The Gas Globe. Vol. III - The Damage Process. Office of Naval Research, Department of the Navy, 1950.

3. M. M. Swisdak (Editor) *Explosion Effects and Properties. Part II - Explosion Effects in Water*, NSWC/WOL TR 76-116, 1976.

4. H. M. Sternberg and W. A. Walker, "Calculated Flow and Energy Distribution Following Underwater Detonation of a Pentolite Sphere," *Phys. Fluids* 14, 1869–1878, 1971.

5. M. Cowperthwaite and W. H. Zwisler *Volume IV, TIGER User's Guide*, SRI publication Z106, 1974.

6. M. Finger, E. Lee, F. H. Helm, B. Hayes, H. Hornig, R. McGuire, and M. Kahara "The Effect of Elemental Composition on the Detonation Behavior of Explosives," *6th Symp. (Intl.) on Detonation*, Office of Naval Research - Department of the Navy, ACR–221, 710–722, 1976.

7. B. M. Dobratz *LLNL Explosives Handbook – Properties of Explosives and Explosive Simulants*, UCRL–52997, March 1981.

8. M. H. Rice and J. M. Walsh "Equation of State of Water Compressed to 250 Kilobars," *J. Chem. Phys.* **26**, 824–830, 1957.

9. G. A. Gurtman, J. W. Kirsch, and C. R. Hastings "Analytical Equation of State for Water Compressed to 300 Kbar," *J. Appl. Phys.* **42**, 851–857, 1971.

10. D. J. Steinberg *Spherical Explosions and the Equation of State of Water*, LLNL Report UCID-20974, February 1987.

11. H. M. Sternberg and H. Hurwitz "Calculated Spherical Shock Waves Produced by Condensed Explosives in Air and Water" *6th Symp. (Intl.) Detonation*, Office of Naval Research - Department of the Navy ACR–221, 528–539, 1976.

12. W. E. Baker, P. A. Cox, P. S. Westine, J. J. Kulesz, R. A. Strehlow, **Explosive Hazards and Evaluation**, Elsevier, 1983.

13. S. M. Kogarko, O. E. Popov, and A. S. Novikov "Underwater Explosion of a Gas Mixture as a Source of Pressure Waves," *Combustion, Explosion, and Shock Waves* **11**, 648–654, 1975.

14. O. E. Popov and S. M. Kogarko "Comparative Characteristic of Pressure Waves in Underwater Explosions of Gaseous and Condensed High Explosives," *Combustion, Explosion, and Shock Waves* **13**, 791–794, 1977.

15. M. S. Shaw and J. D. Johnson, "Carbon Clustering in Detonations," *J. Appl. Phys.* **62**, 2080–2085, 1987.

16. C. L. Mader **Numerical Modeling of Detonations**, Univ. California Press, 1979.

17. V. P. Skripov **Metastable Liquids**, Wiley, 1974.

18. J. A. Blink and W. G. Hoover "Fragmentation of Suddenly Heated Liquids," *Phys. Rev. A* **32**, 1027, 1985.

19. D. A. Labuntsov and A. P. Kryukov "Analysis of Intensive Evaporation and Condensation," *Int. J. Heat Mass Transfer* **22**, 989-1002, 1979.

20. M. S. Plesset and A. Prosperetti "Bubble Dynamics and Cavitation," *Ann. Rev. Fluid Mech.* **9**, 145-185, 1977.

21. J. E. Shepherd and B. Sturtevant "Rapid Evaporation at the Superheat Limit," *J. Fluid Mech.* **121**, 379-402, 1982.

22. D. Frost and B. Sturtevant "Effects of Ambient Pressure on the Instability of a Liquid Boiling Explosively at the Superheat Limit," *J. Heat Transfer* **108**, 418, 1986.

23. W. J. Bornhorst and G. N. Hatsopoulos "Bubble-Growth Calculation without Neglect of Interfacial Discontinuties," *J. Appl. Mech.* **34**, 847-853, 1967.

24. S. Fujikawa and T. Akamatsu "Effects of the non-equilibrium condensation of vapour on the pressure wave produced by the collapse of a bubble in a liquid," *J. Fluid Mech.* **97**, 481-512, 1980.

25. H. G. Snay, J. F. Goertner, and R. S. Price *Small Scale Experiments to Determine the Motion of Explosion Gas Globes Towards Submarines*, NAVORD Report 2280, 1952.

26. J. F. Goertner *Vacuum Tank Studies of Gravity Migration of Underwater Explosion Bubbles*, NAVORD Report 3902, 1956.

27. J. F. Goertner, J. R. Hendrickson, R. G. Leamon *Model Studies of the Behavior of Underwater Explosion Bubbles in Contact with a Rigid Bottom*, NOLTR 68-207, 1969.

28. K. I. Read "Experimental Investigation of Turbulent Mixing by Rayleigh–Taylor Instability," *Physica* **12 d**, 45-58, 1984.

29. G. Birkhoff "Stability of Spherical Bubbles," *Q. Appl. Math.* **13**,451, 1956.

30. D. L. Youngs "Numerical Simulation of Turbulent Mixing by Rayleigh–Taylor Instability," *Physica* **12 d**, 32-44, 1984.

31. B. Sturtevant "Rayleigh–Taylor Instability in Compressible Fluids," *16th Intl. Symp. Shock Tubes and Waves*, Ed. H. Grönig, VCH, 89–100, 1988.

32. C. A. Miller "Stability of Moving Surfaces in Fluid Systems with Heat and Mass Transport – II. Combined effects of Transport and Density Differences Between Phases," *AIChE J.* **19**, 909, 1973.

33. H. J. Palmer "The Hydrodynamic Stability of Rapidly Evaporating Liquids at Reduced Pressure," *J. Fluid Mech.* **75**, 487, 1976.

34. A. Prosperetti and M. S. Plesset "The Stability of an Evaporating Interface," *Phys. Fluids* **27**, 1590–1602, 1984.

35. F. J. Higuera "The Hydrodynamic Stability of an Evaporating Liquid," preprint, 1987.

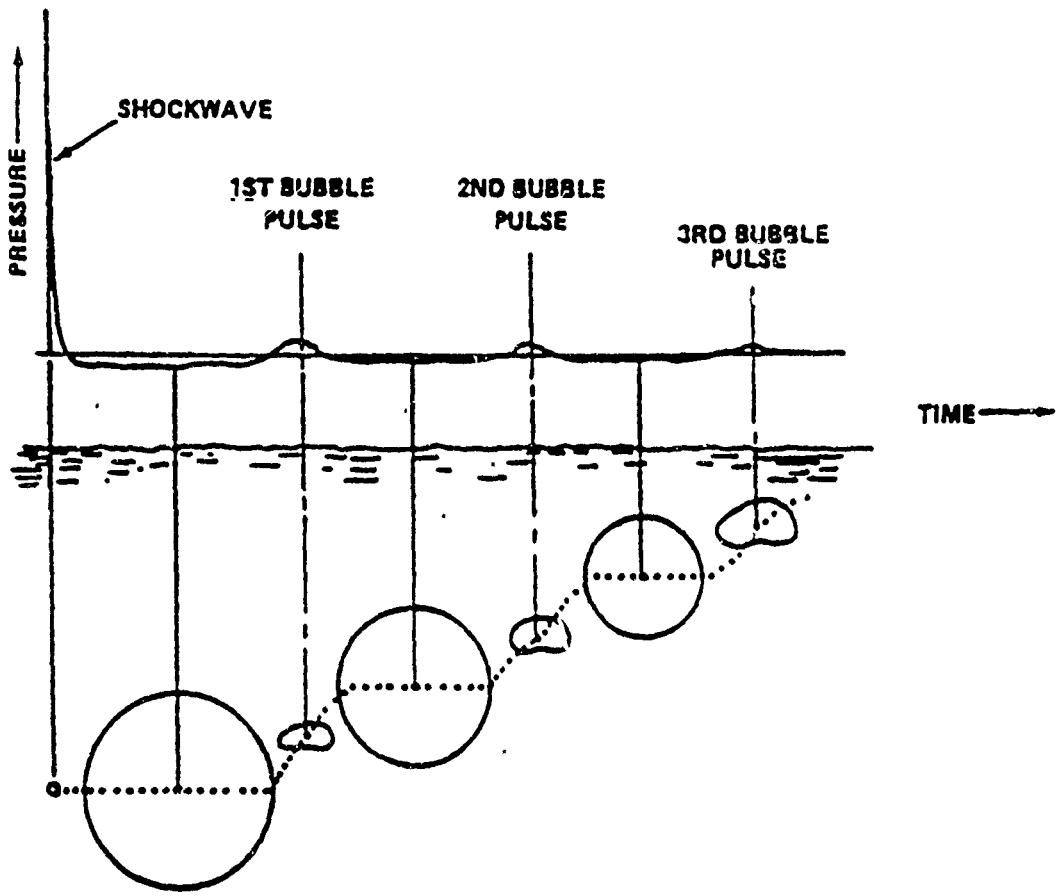

Figure 1. Schematic of an underwater explosion showing the principal phenomena. From Ref. 3.

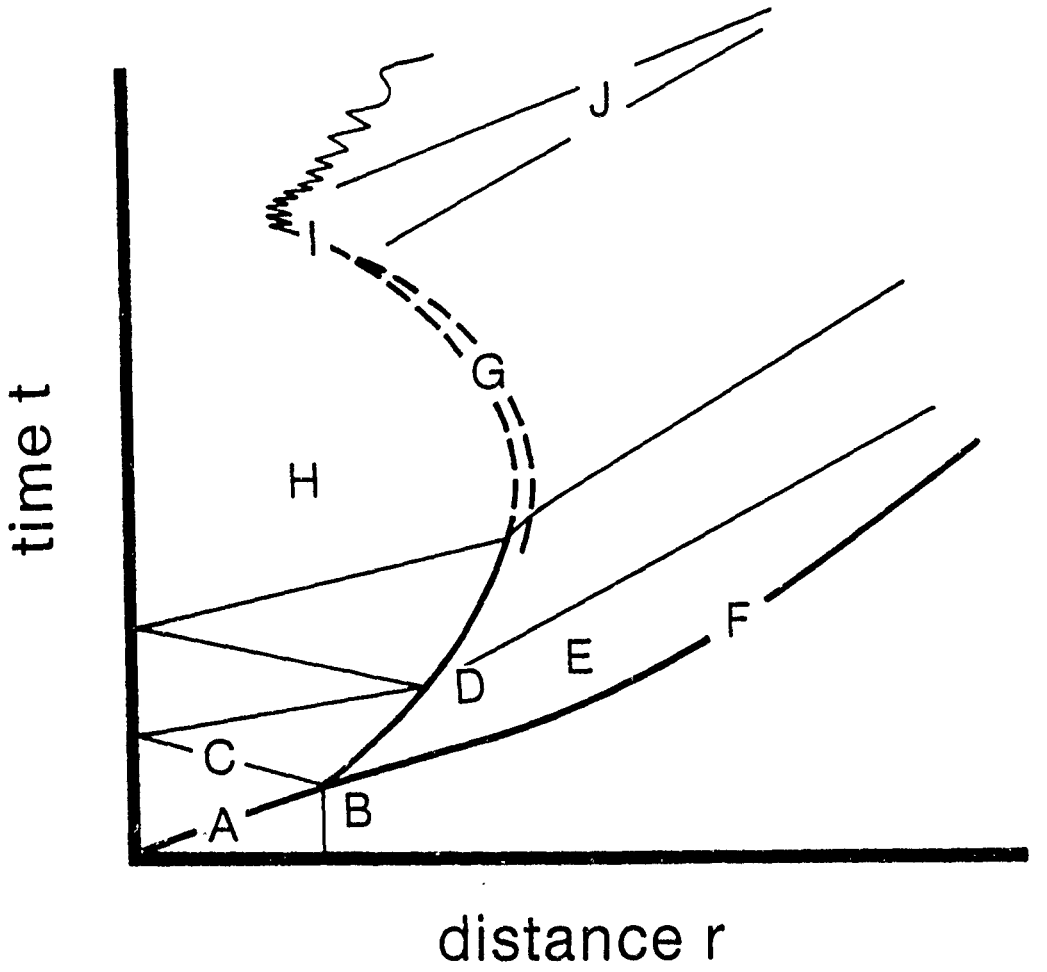

Figure 2. Schematic of interface and wave trajectories in an underwater explosion. The physical processes indicated are: A – detonation propagation; B – detonation-water interaction; C – gasdynamics within the bubble; D – acoustic wave interaction with the interface; E – disturbance propagation up to the shock: F – shock compression of the water; G – evaporation of the water at the interface; H – isentropic expansion of the products; I – interface instability near collapse; J – geometrical vs nonlinear effects in bubble pulse propagation.

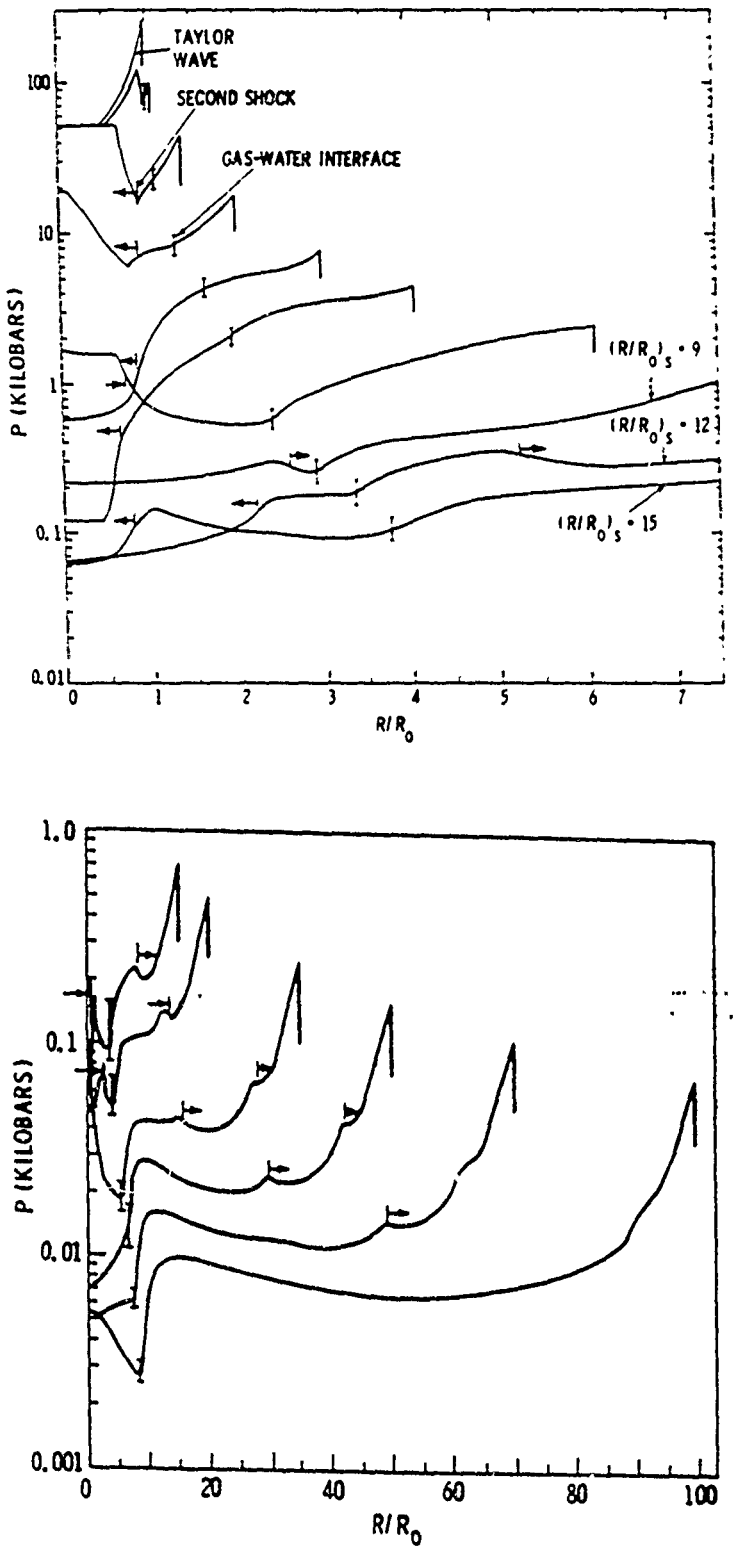

Figure 3. Pressure vs reduced distance for a spherical Pentolite detonation. From Sternberg and Walker, Ref. 4

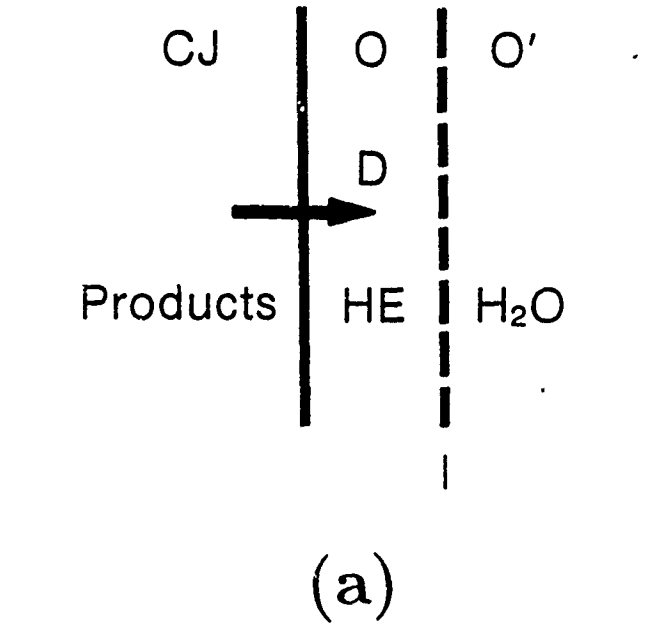

(a)

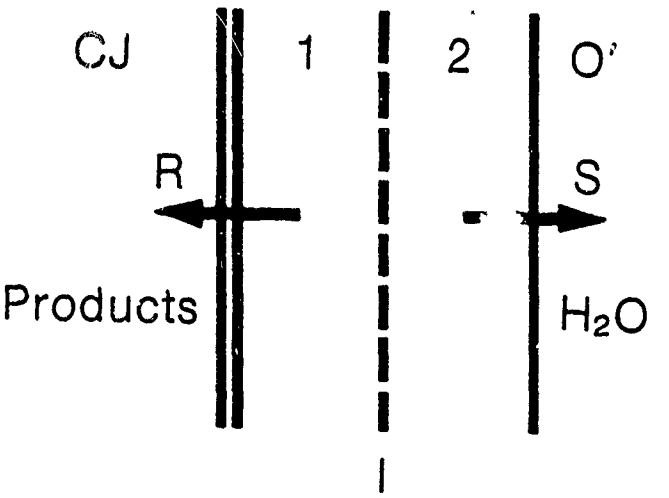

(b)

Figure 4. Idealized interaction between a detonation and the contact surface (water–explosive product interface). a) Before interaction, D – detonation, CJ - Chapman-Jouguet state. b) After interaction, S - shock in water, R – rarefaction or expansion wave in products.

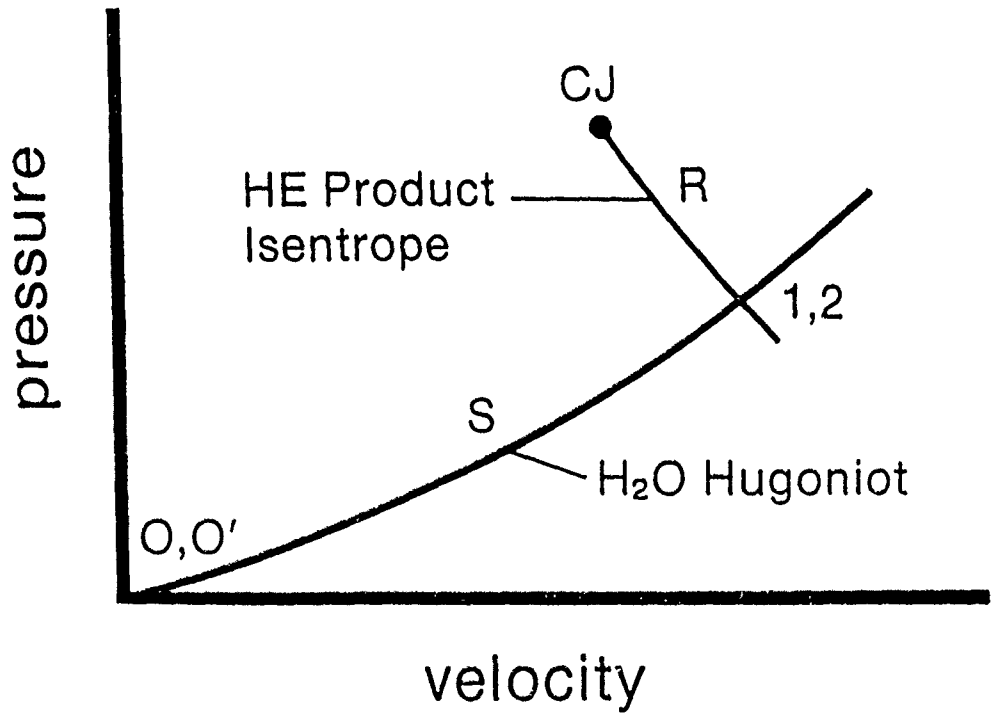

Figure 5. Pressure–velocity diagram for computing the interaction between a detonation and the contact surface (water–explosive product interface). O, Ó. initial states of explosive and water. CJ – Chapman-Jouguet state. S – shock in water. R – rarefaction or expansion wave in products.

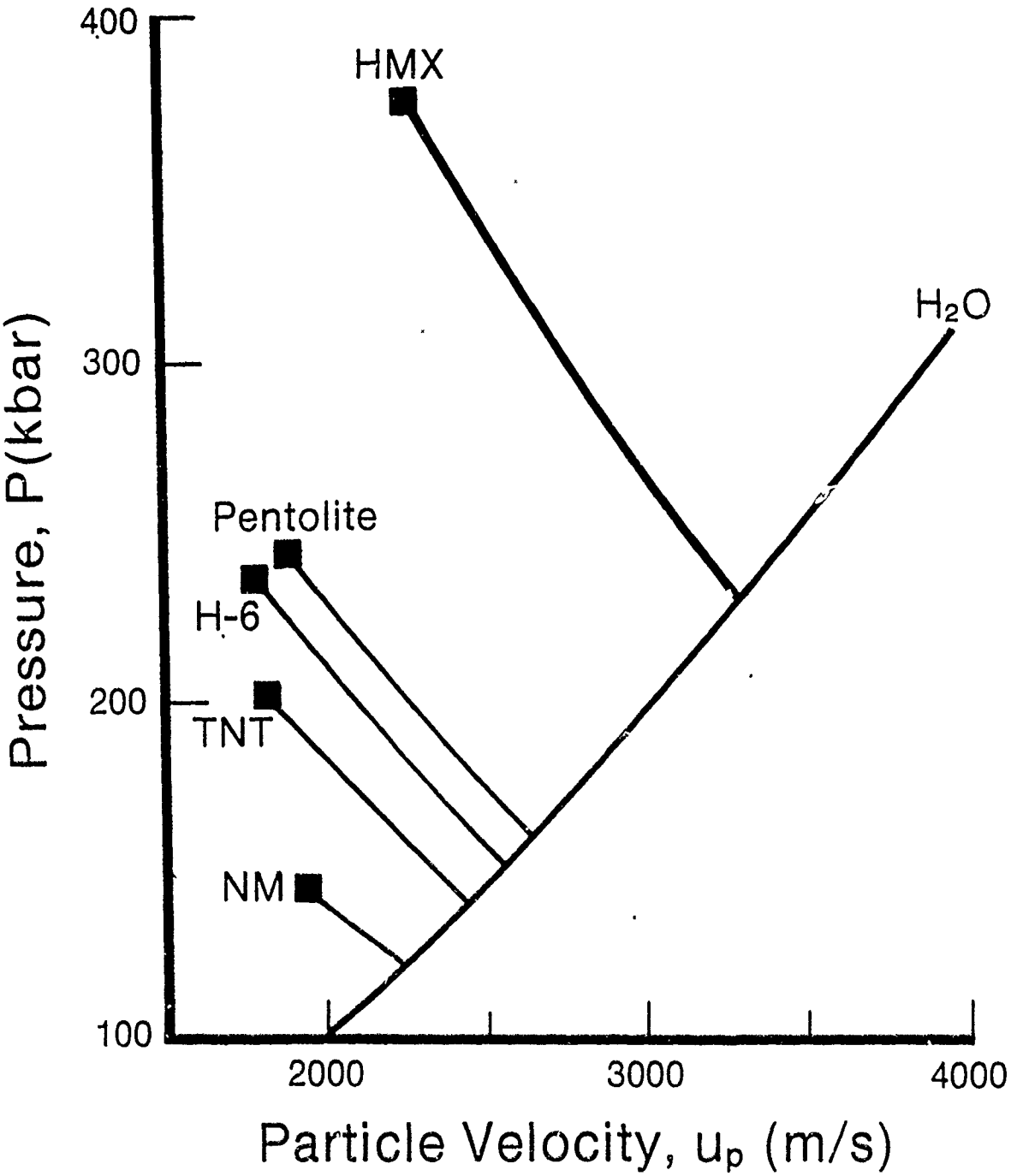

Figure 6. Pressure–velocity solutions for the detonation of 5 conventional explosives at maximum initial densities.

Table 1. CJ conditions and interface pressure for five explosives detonating in water.

HE	ρ_o (g/cm^3)	Δh_{det} (MJ/kg)	P_{CJ} (kbar)	P_I (kbar)	ΔS (kJ/kg-K)	P_σ (bar)
HMX	1.89	6.19	388	230	3.6	140
Pentolite	1.67	5.86	249	160	2.8	40
H-6	1.75	–	221	151	2.7	35
TNT	1.65	5.40	202	140	2.5	22
NM	1.13	5.69	144	121	2.0	8

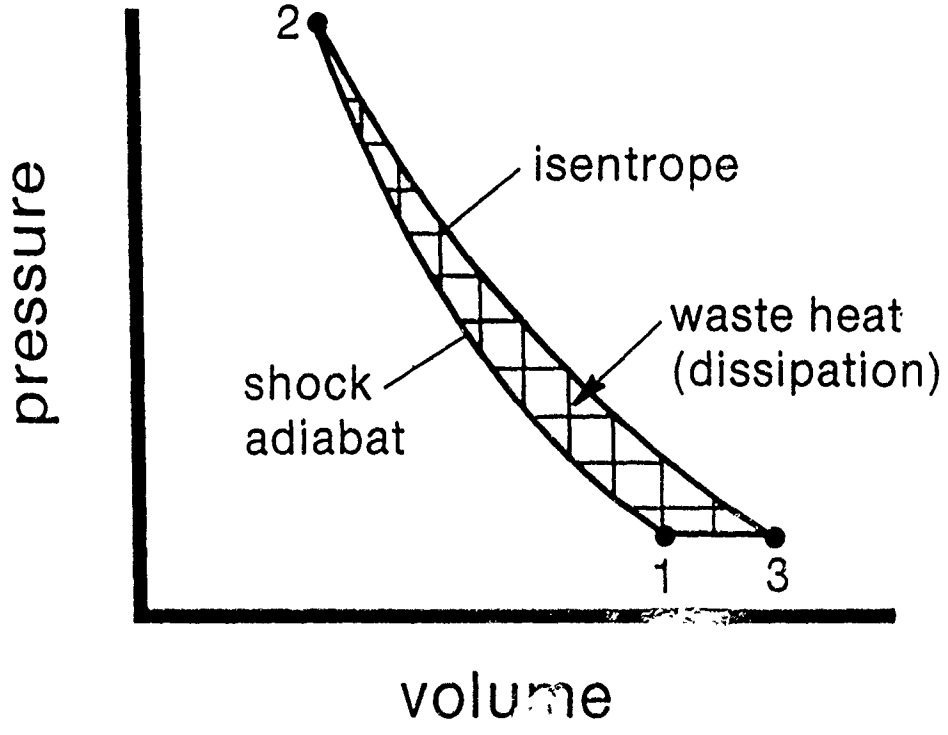

Figure 7. Shock adiabat (hugoniot) vs isentrope in pressure–volume coordinates. Shaded area is the waste heat (dissipated energy) that is not recovered when the shock pressure is released back to ambient.

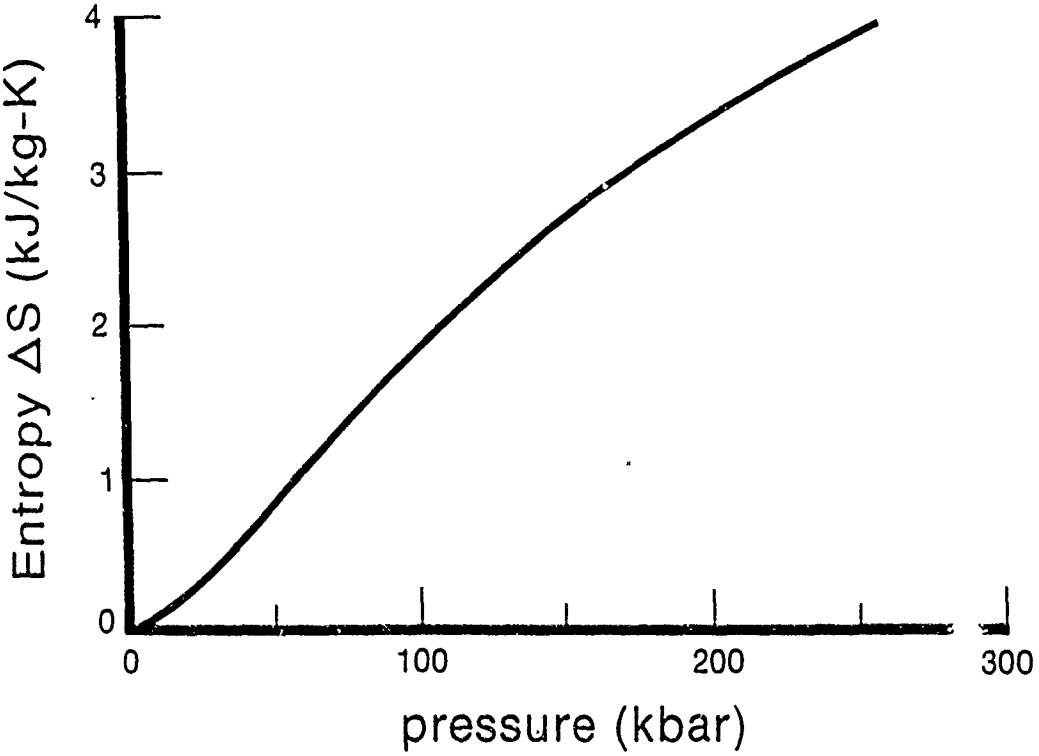

Figure 8. Entropy jump across shock wave vs shock pressure for water, initial conditions of 300 K and 1 bar.

(a). Pentolite, centrally detonated

(b). PBX 9404, centrally detonated

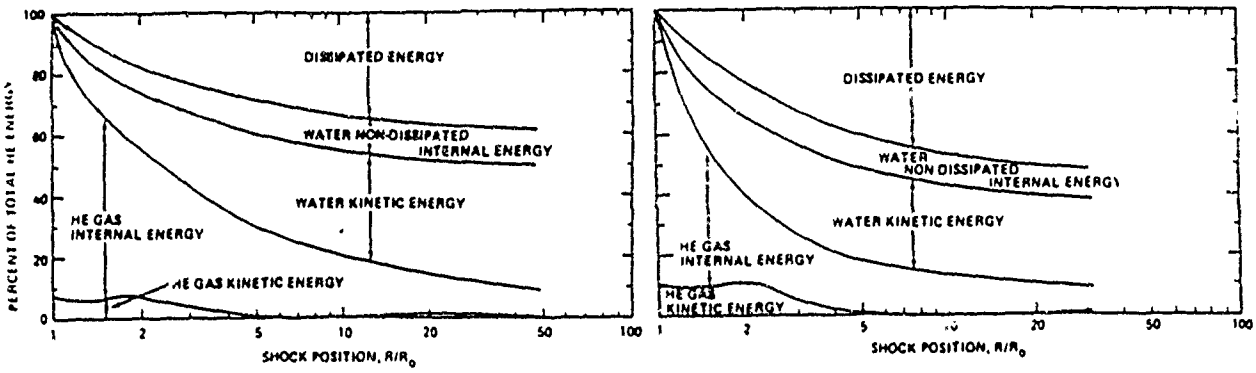

(c). Pentolite constant volume explosion, $\rho_0 = 1.65$.

(d). Pentolite constant volume explosion, $\rho_0 = 0.4125$.

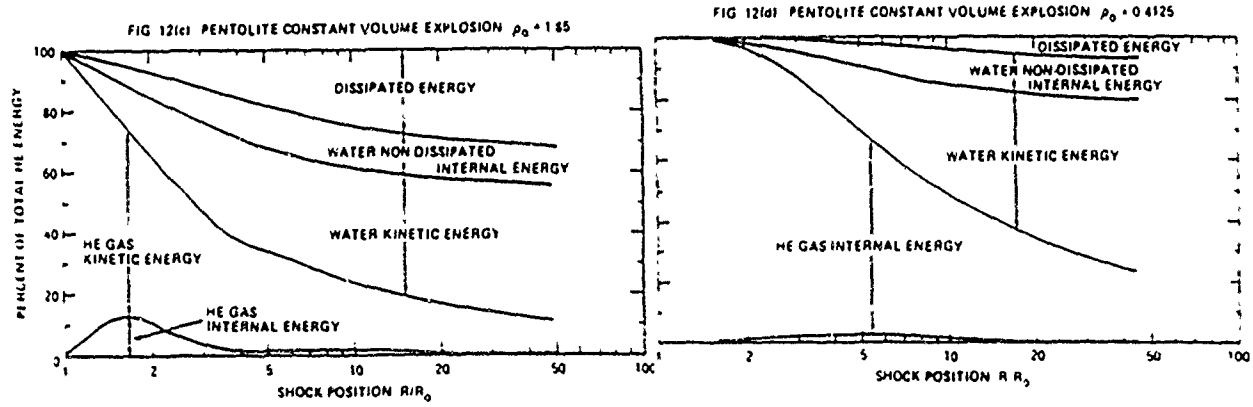

Figure 9. Energy budgets for four explosives. From Hurwitz and Sternberg.[11]

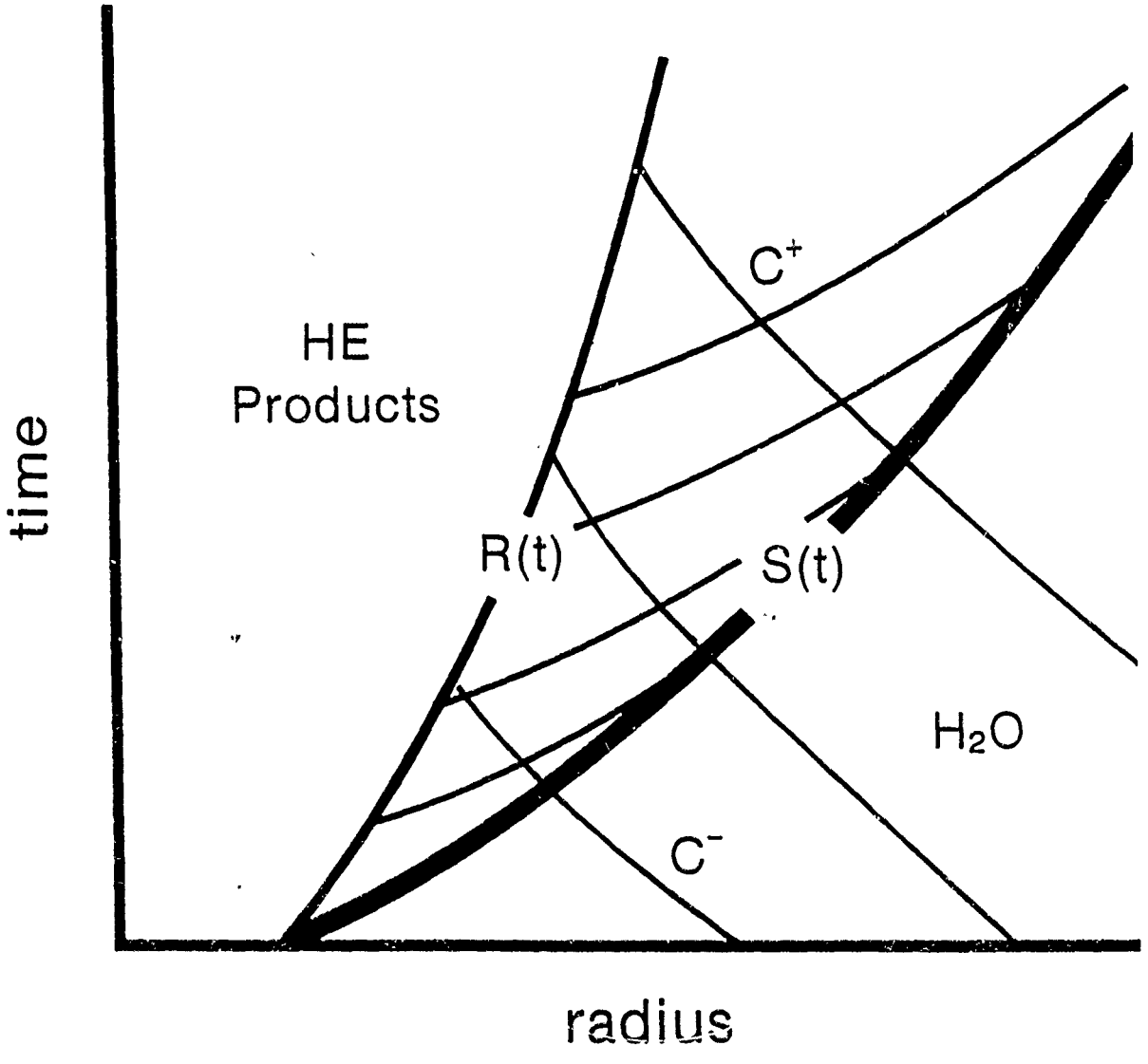

Figure 10. Interaction of acoustic waves with shock. Information about the interface motion is transmitted forward along the characteristics C^+ and the reflected waves are transmitted back along C^-.

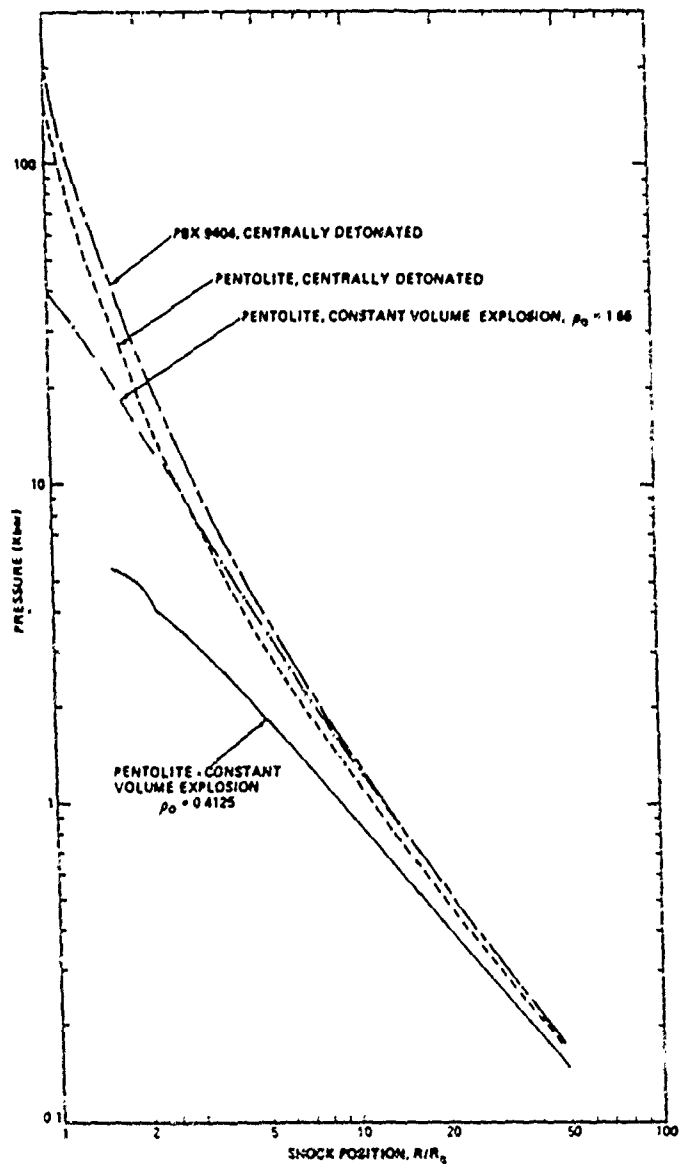

Figure 11. Decay of shock pressure with scaled distance for the four cases shown in Fig. 9. From Sternberg and Hurwitz.[12]

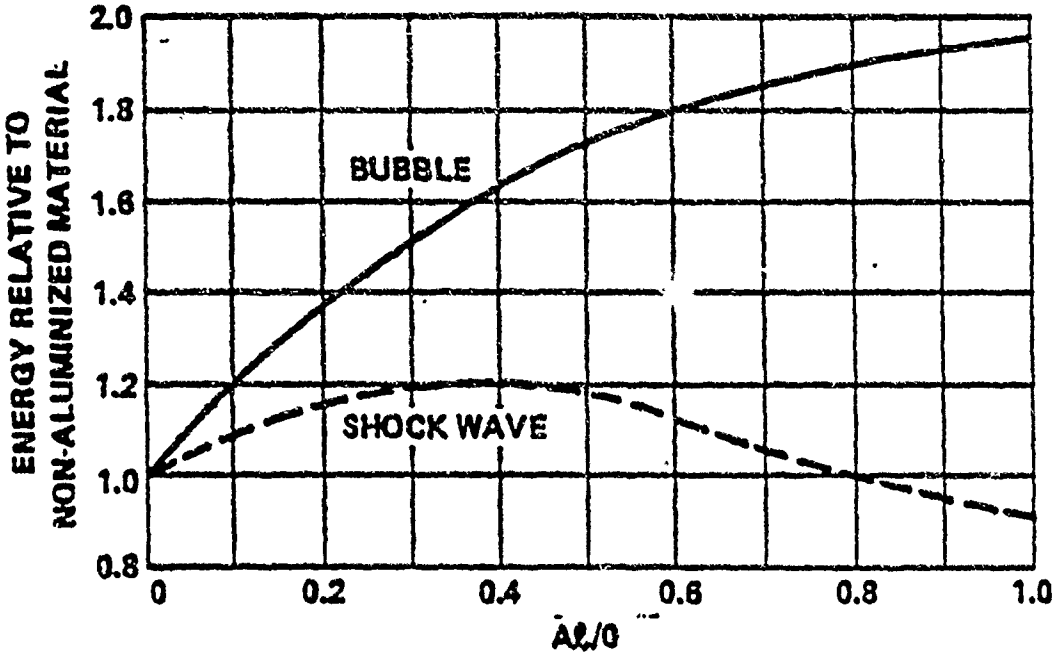

Figure 12. Effect of the addition of aluminum to conventional CHNO explosives. From Swisdak, Ref. 3. A molar Al/O ratio of 0.242 corresponds to a 15 wt % (0.59 mol %) Al in a RDX/Al mixture; a molar Al/O ratio of 0.587 corresponds to a 30 wt % (0.78 mol %) Al in a RDX/Al mixture.)

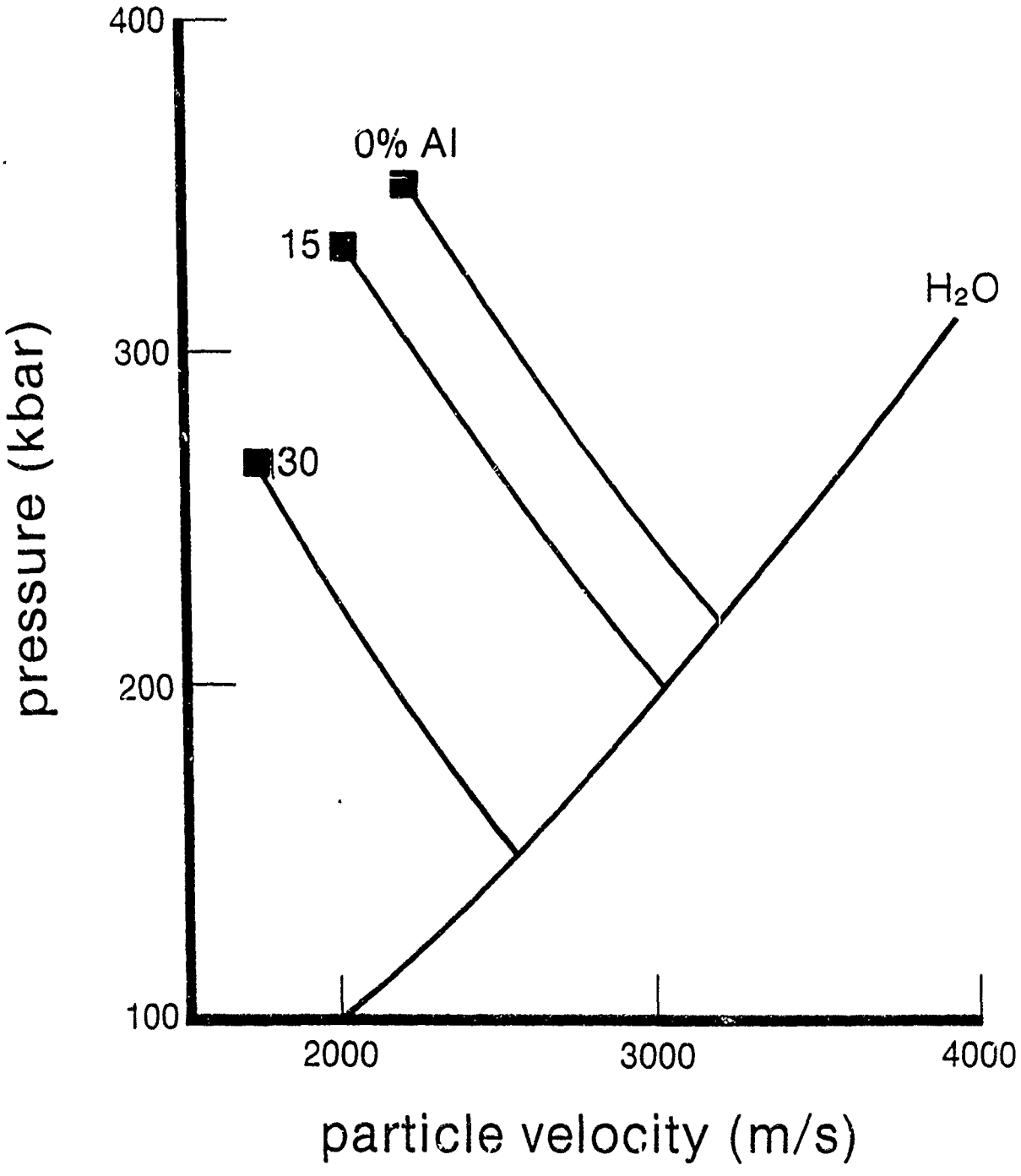

Figure 13. Detonation–water interface interaction solutions for RDX/Al explosive mixtures. Products include condensed aluminum oxide $Al_2O_3(s)$ and graphitic carbon C(s). RDX alone has CJ parameters similar to but slightly lower than HMX.

Table 2. CJ conditions and interface pressure for RDX/Al explosive mixtures detonating in water.

Al (wt %)	ρ_o (g/cm^3)	Δh_{det} (MJ/kg)	P_{CJ} (kbar)	P_I (kbar)	ΔS (kJ/kg-K)	P_σ (bar)
0	1.80	6.15	349	220	3.5	123
15	1.90	8.21	331	200	3.4	102
30	2.00	10.12	267	150	2.7	35

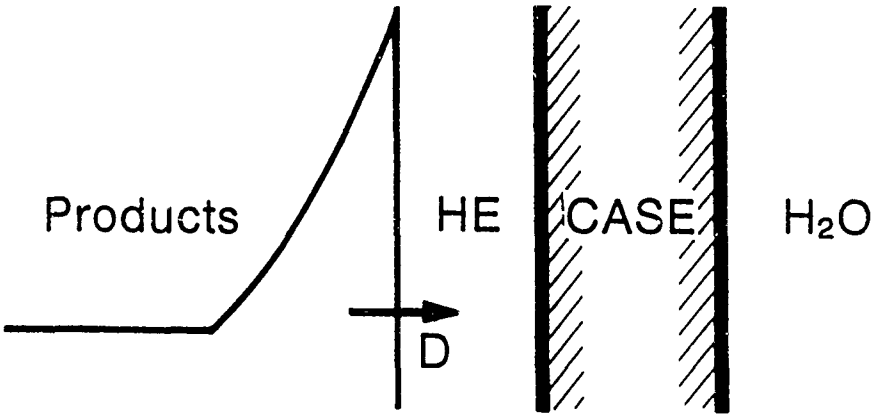

(a)

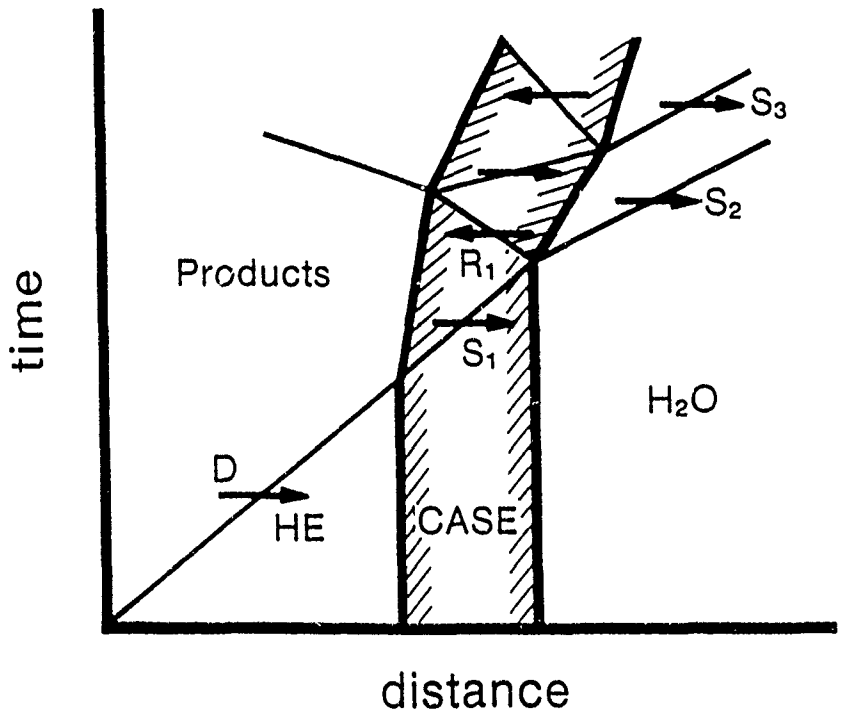

(b)

Figure 14. Detonation–case–water interaction. (a) spatial configuration. (b) distance–time diagram showing multiple reflections.

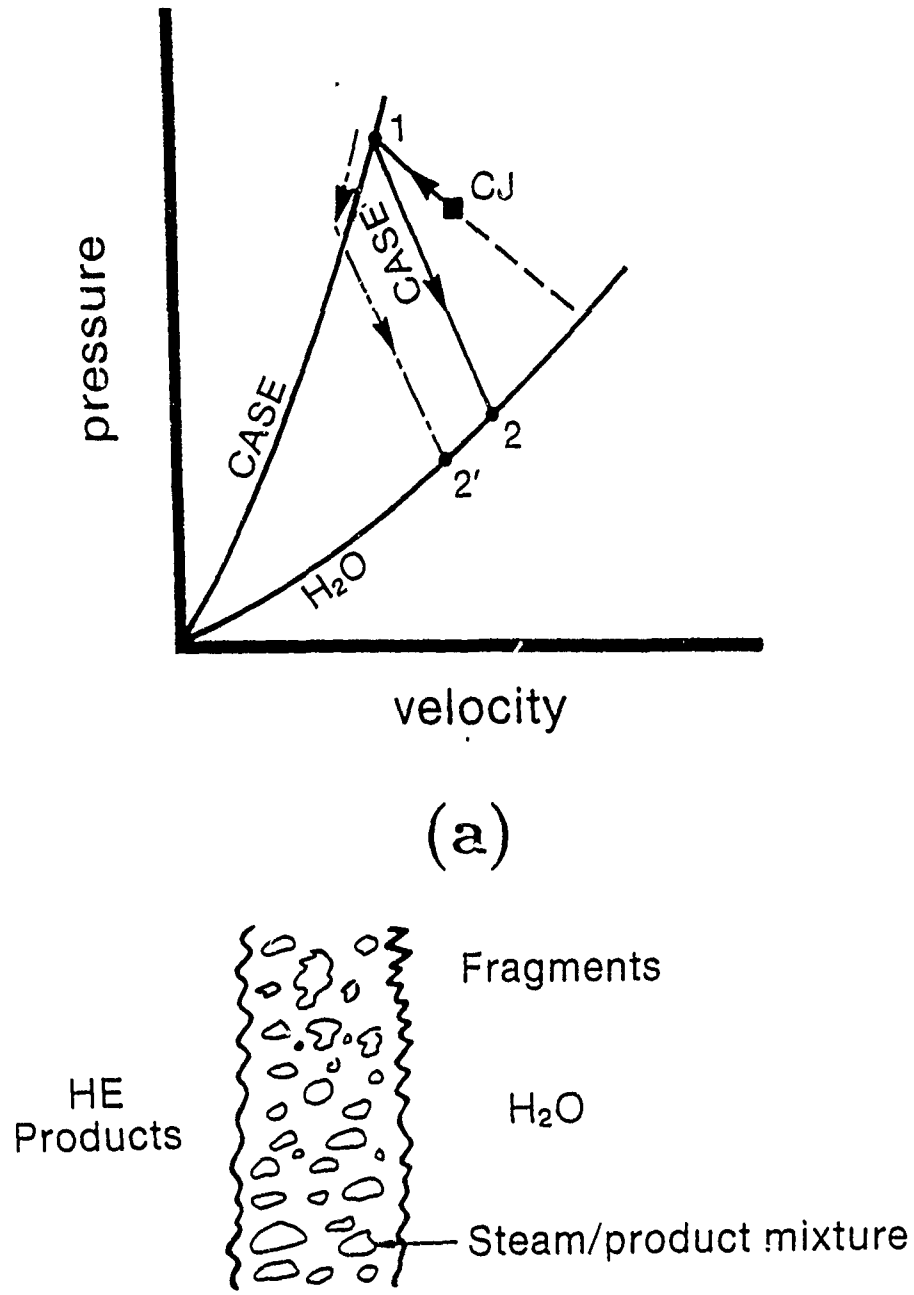

Figure 15. Detonation–case–water interaction. (a) pressure-velocity solution for interface conditions. (b) extended interface generated by case fragmentation: interface region is a mixture of fragments, steam and liquid water.

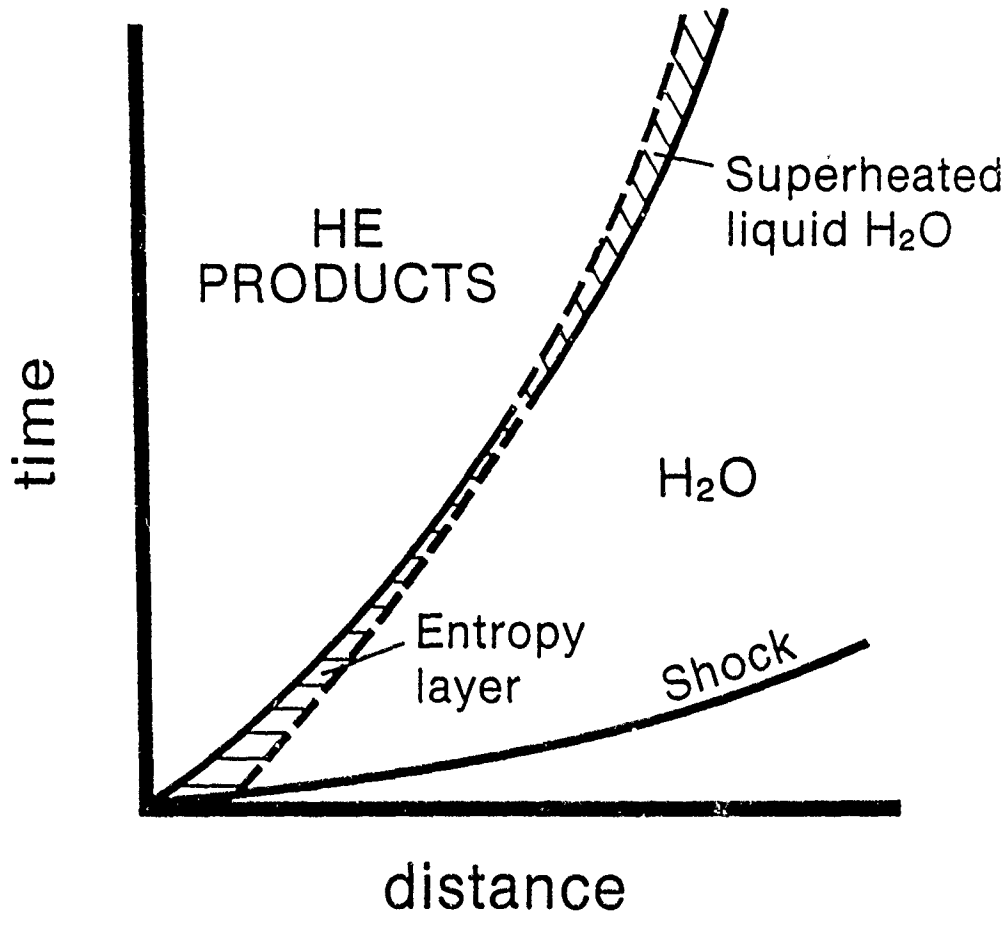

Figure 16. Distance–time diagram showing the formation of the entropy layer and the transformation into superheated water with decreasing interface pressure or increasing time.

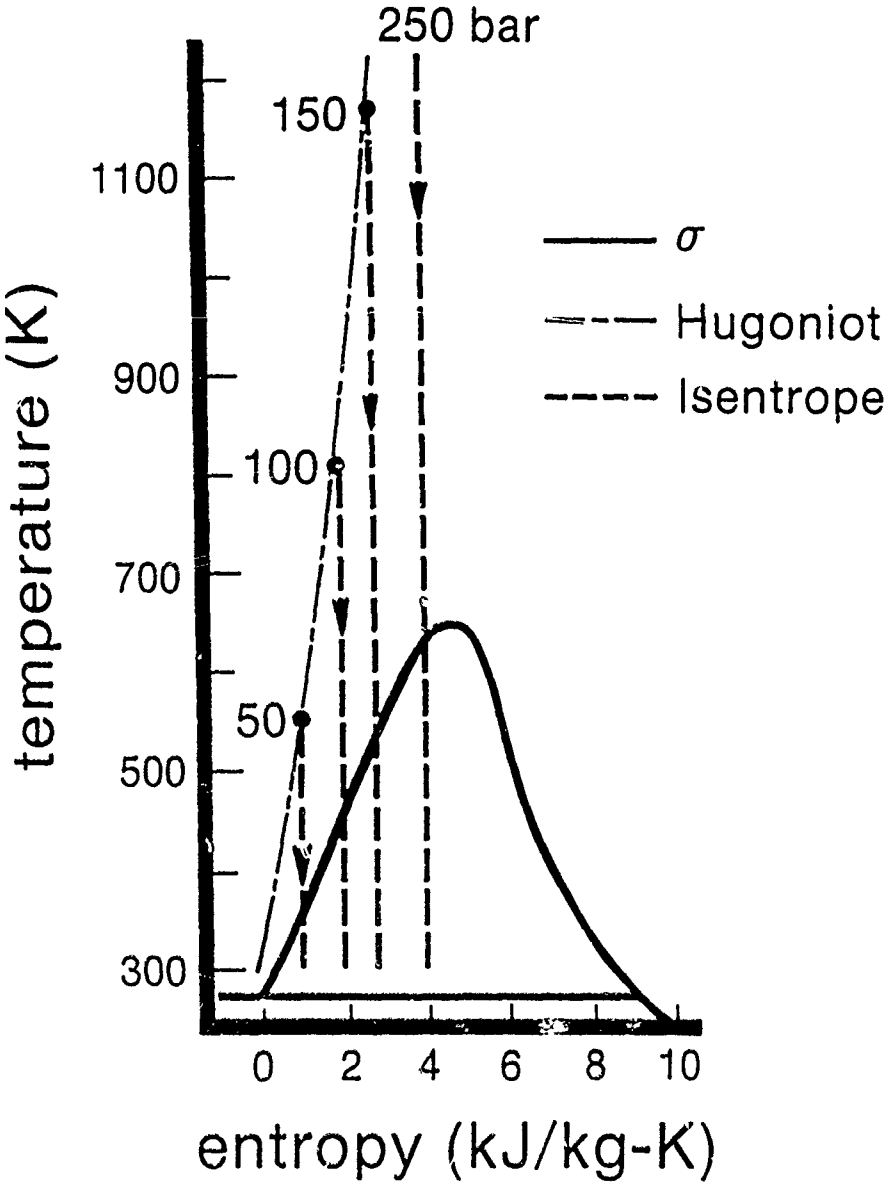

Figure 17. Temperature–entropy diagram for water. The chain-dotted line is the shock adiabat (hugoniot) with the shock pressure indicated at 50, 100, and 150 kbar (250 kbar is off scale), initial water conditions of 300 K and 1 atm. The dashed lines are the isentropes, and the heavy line is the liquid–vapor coexistence curve σ.

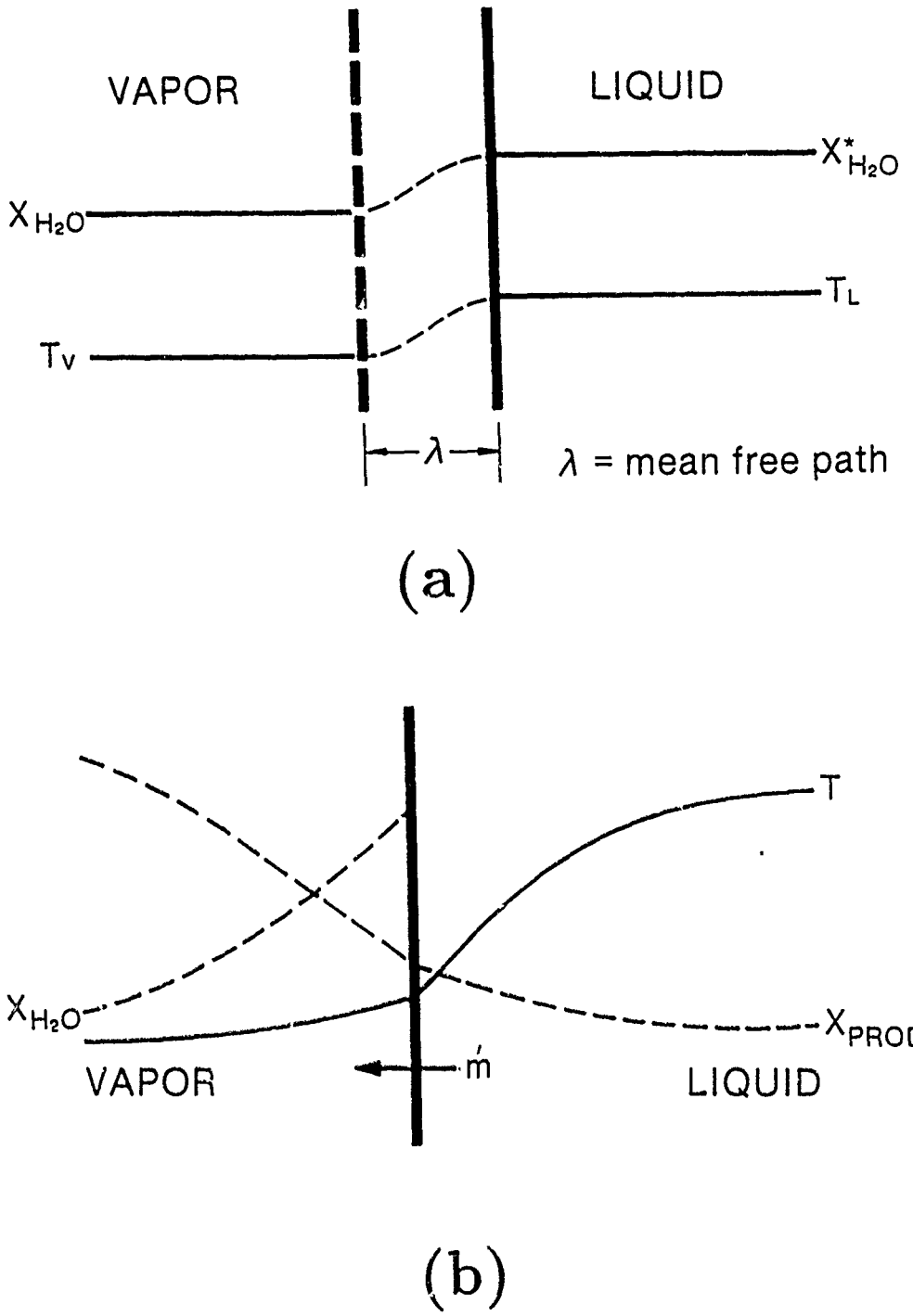

Figure 18. Evaporating interface configuration. (a) near-equilibrium situation: mass and energy boundary layers control evaporation rates. (b) nonequilibrium situation: rapid evaporation with large state variations occurring in the Knudsen layer at the interface.

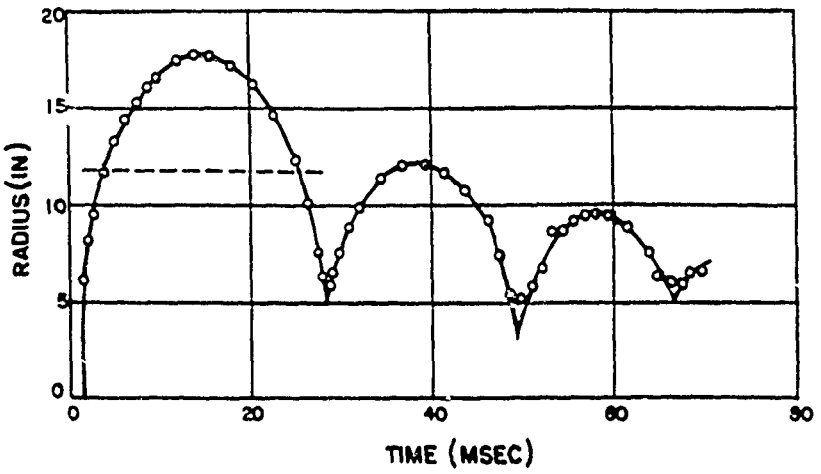

(a)

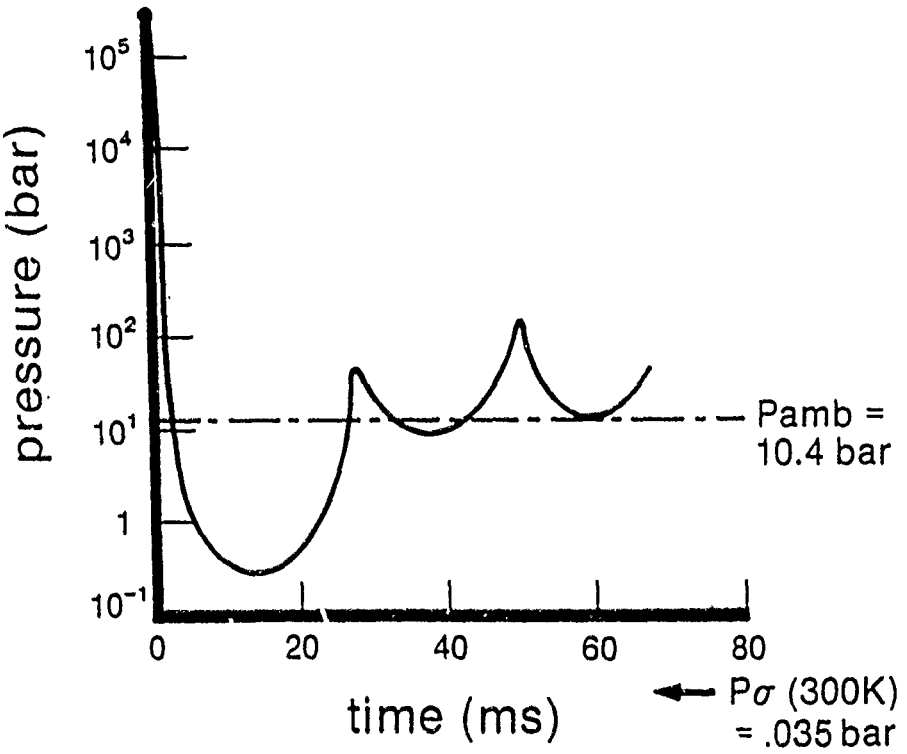

(b)

Figure 19. Explosion bubble produced by the detonation of 250 g (R_o = 1.38 in) of tetryl at a depth of 300 ft. (a) Observed radial oscillations. (b) Computed (using JWL isentrope) average pressure oscillation inside the bubble (and at the interface).

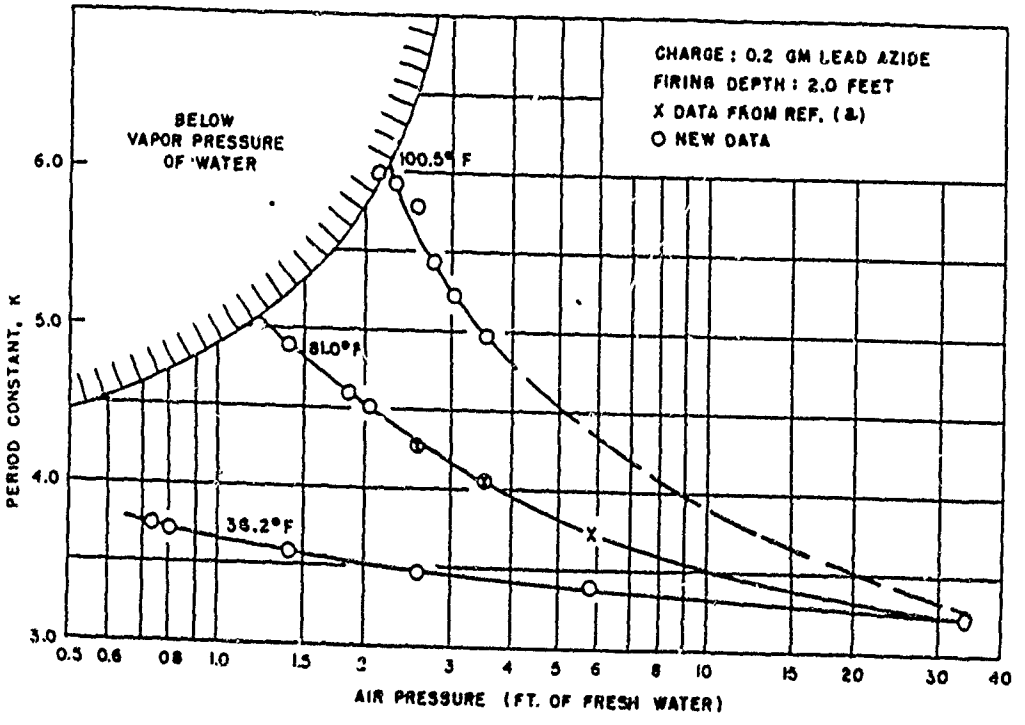

Figure 20. Effect of ambient water temperature on the bubble period constant K (English units). From Ref. 26

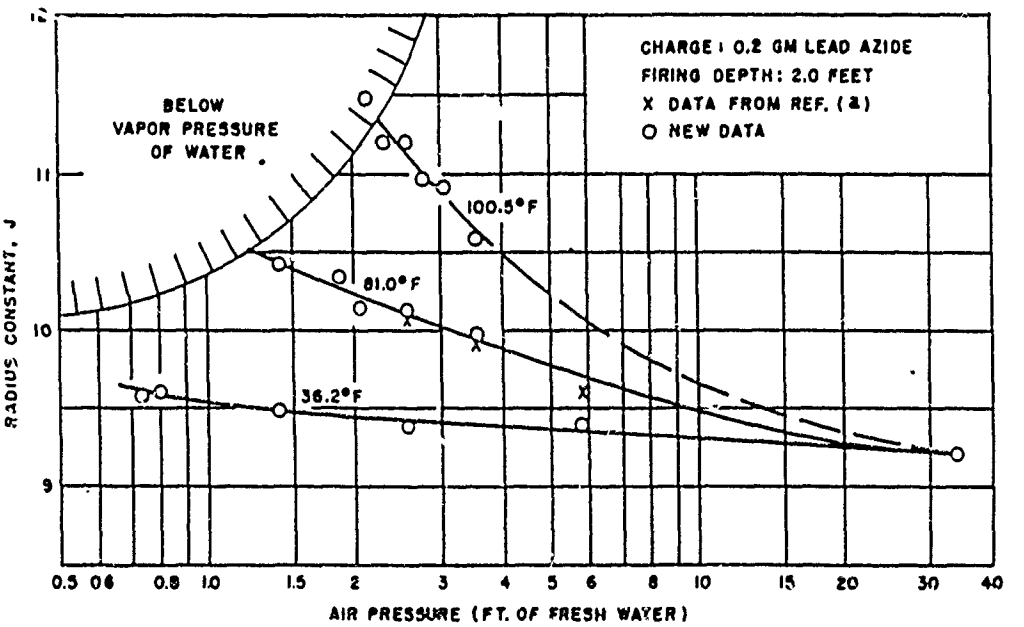

Figure 21. Effect of ambient water temperature on the bubble maximum radius constant J (English units). From Ref. 26

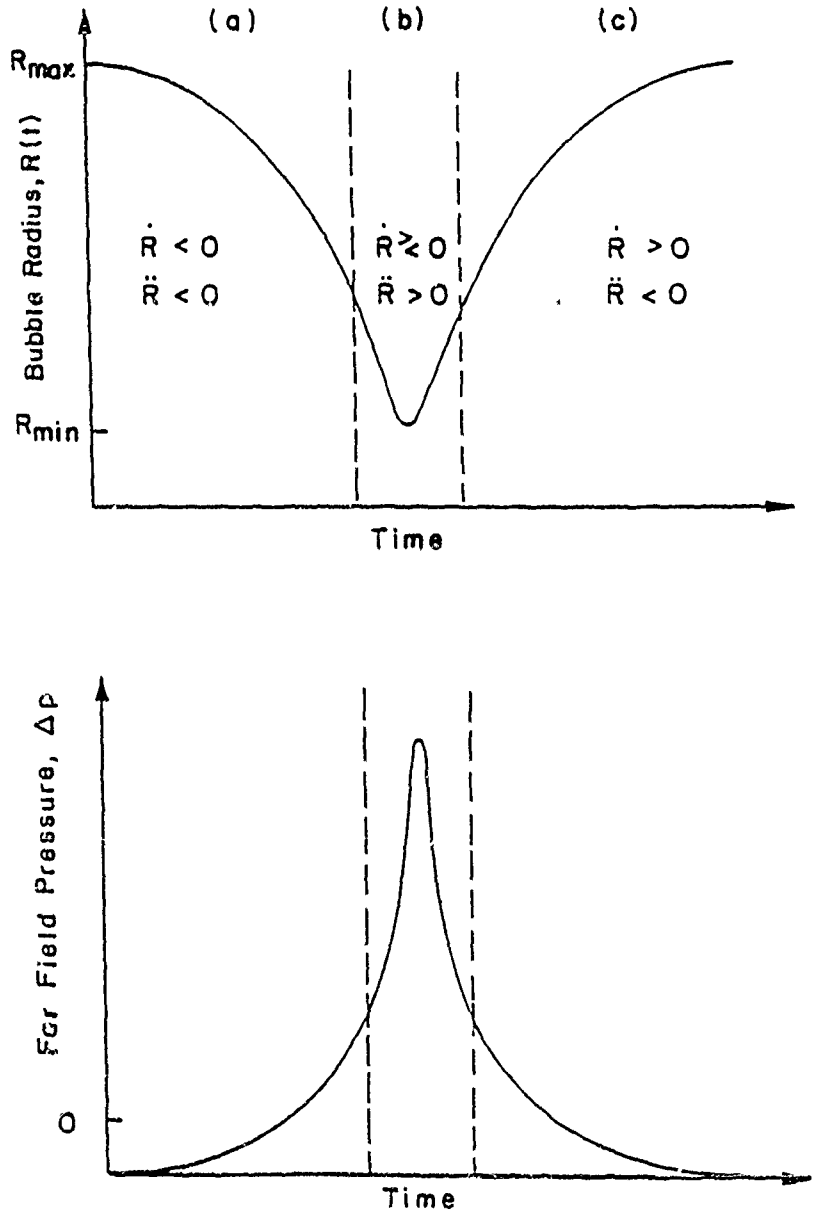

Figure 22 Bubble surface motion and resulting pressure wave. The region of potential Rayleigh–Taylor instability is near the minimum radius where the accelerations are large and positive.

UNDERWATER EXPLOSION BUBBLE DYNAMICS

Julius W. Enig
Enig Associates, Inc.,13230 Ingleside Drive, Beltsville, MD 20705

INTRODUCTION

The ability to predict the behavior of the pulsating and migrating explosion bubble is needed because the bubble-induced whipping of a surface ship or submarine can cause severe structural damage to the ship or submarine or to on-board components.

The flow arising from the underwater explosion is compressible, initially, as a shock wave propagates in the water. After a short while, as the explosion products bubble continues to expand, the pressure in the bubble and in the water behind the shock front decays to so low a value that the water can now be considered incompressible. For a much longer time, the bubble expands until it reaches its maximum radius and then starts its contraction stage. During the latter, and especcially as the bubble nears its minimum volume, it migrates in the vertical direction due to buoyancy; it also migrates because it is attracted toward rigid bodies or repulsed by free surfaces. The contraction stage is non-spherical: the bubble forms a torus under certain conditions; because of buoyancy, a jet forms at the bottom of the bubble and may strike the top of the bubble, forming a torroidal shape. In the case of attraction toward a rigid body, the jet forms on the bubble surface opposite the rigid body. The bubble continues to contract until the bubble minimum is reached. In the expansion stage that follows, the bubble may remain torroidal. Several bubble oscillations of diminishing amplitude have been observed experimentally. At each bubble minimum, energy is lost due to compressibility effects -- the jet striking the bubble surface and the shock wave that originates on bubble expansion -- cooling of the hot bubble by the instability-induced spray of water into the bubble, and turbulence at the water-bubble interface. The latter two effects are particularly difficult to model theoretically.

UNDERWATER EXPLOSION BUBBLE RESULTS

World War II was the great impetus for the development of the

ideas and concepts that describe underwater explosion phenomenology. The results of the World War II efforts by the American, British, and Canadian workers in this field has been well described by Robert Cole in his book "Underwater Explosions" published in 1948.[1] While this book is still of great use, it is unfortunate that no successor has been published, which would cover the experimental, analytical, and computational information that has been obtained since then. Nor is there any book that deals with the more limited scope: explosion bubble phenomena. A brief survey of underwater explosions published in 1977 by Holt[2] reviews the literature on the formation and early growth of underwater explosions, the migration of the product gas bubble, and the influence of ocean surface on underwater and near surface explosions, all based mainly on classical techniques of analysis.

Since World War II, many more experimental and analytical results have been obtained on the properties of underwater explosions. These to a great extent have been obtained at or through the programs of the Naval Surface Warfare Center (NSWC)/White Oak.[3-12]

The great advances in experimental techniques and computational capability has opened up new avenues for understanding the still-hidden phenomena that define the underwater explosion process and interaction with a target. In the last 20 years, computational capability has increased dramatically. One consequence has been the application of numerical methods to various underwater explosion problems, which have provided a "look into" the flow regimes that were not examined in earlier times. These calculations can be used to examine better the concepts of shockwave energy, bubble energy, available energy, and dissipated energy.

Besides the primary shock wave from an underwater explosion, it is well known that the bubble pulsation and migration causes damage to surface ship and submarine targets. "Bubble" damage is a criterion for defining the lethality of underwater weapons. Yet an accurate calculation of the long-time explosion bubble motion is still difficult for two major and independent reasons. The first concerns the inexactness of the physics involved in the explosion process: non-ideal reactions involving, e.g., aluminized explosives; thermochemical equilibria; turbulence; water spray into the detonation products; equations of state of the detonation products. The second deals with the inability to perform accurate numerical solutions in a cost effective manner over the entire time of interest, including the inability to define accurately the bubble/water interface during the contraction and subsequent reexpansion phases.

Before proceeding with any discussion of the latest state of our knowledge of explosion bubble dynamics, it is useful to describe the simple theory of the radial motion of an explosion bubble in an infinite incompressible fluid (water) neglecting gravity.[1] The conservation of mass and momentum are

$$\partial(r^2u)/\partial r = 0 \tag{1}$$

$$\partial u/\partial t + (1/2)\partial(u^2)/\partial r = -(1/\rho)\partial P/\partial r, \tag{2}$$

where t,r,P,ρ, and u are, respectively, the time, radius measured from bubble center, pressure, liquid density, and radial velocity. But Eq.(1) yields

$$r^2u = R^2\dot{R}, \tag{3}$$

where R and $\dot{R}$ are, respectively, the bubble radius and velocity. Substitution of (3) into (2) and integration between r=r and r= gives

$$(1/r)d(R^2\dot{R})/dt - (1/2)(R^2\dot{R}/r^2)^2 = -(1/\rho)[P_\infty - P(r,t)], \tag{4}$$

where P_∞ is the pressure at ∞. At the interface (r=R):

$$(1/R)d(R^2\dot{R})/dt - (1/2)\dot{R}^2 + (1/\rho)[P_\infty - P(R,t)] = 0, \tag{5}$$

Integrating with respect to t yields

$$(1/2)\rho R^3\dot{R}^2 + (1/3)P_\infty R^3 - \int_o^t P(R,t')R^2\dot{R}dt' = C, \tag{6}$$

where C is a constant of integration. The last term is just the internal energy E(R) of the bubble, which for a γ-law product gas is given by

$$E(R) = P(R)V(R)/(\gamma-1), \tag{7}$$

where V(R) is the bubble volume. The constant C represents the energy that is present at any time during the bubble motion.

The solution of Eq.(6) is a periodic motion containing a maximum and a minimum that repeat in time with unchanged amplitude. In reality, the period and amplitude of the oscillations change as can be seen in Fig.1,[1] where the radius of the gas sphere is shown as a function of time for a 0.55 pound tetryl charge detonated 300 feet below the surface. The deviation from the ideal solution is due to a number of reasons, several of which are the following: the effect of gravity (i.e., bubble bouyancy), compressibility effects, water jetting into the bubble, steam formation, and turbulence at the gas/water interface.

While attempts during WWII and in the years following have been made to account for these effects, the attempts until relatively recently have been limited by the inability to obtain accurate solutions to the partial differential equations for two-dimensional axisymmetrical, incompressible flow that include the effect of gravity. If the existences of a free surface or a rigid body in the proximity of the bubble is included, then the

situation is even more complicated.

In recent years, with the advent of ever faster computers with increasing storage capacity, progress is being made in obtaining more comprehensive solutions. Better numerical solutions will at least have the beneficial effect of more clearly isolating those areas of which we have faulty knowledge, and perhaps allow us to estimate more accurately their effects on ability to predict lethality of explosive systems.

In the remainder of the discussion on bubble dynamics, we will ignore the large number of efforts based on approximate analytical methods, which have been made since WWII to predict the bubble motion as it is affected by gravity and other bodies. This is because they do not appear to give accurate means for predicting 2- and 3-dimensional bubble motion and pressure fields on targets all by themselves; the boundary value problems are just too difficult. Powerful numerical schemes are coming to the fore and these will in the end solve the mathematical problems, if not the physical ones such as the effects of turbulence, reactions of aluminum, and the like.

While "bubble phenomena" usually implies a time long after the primary shock wave in the water, resulting from the explosive detonation, has disappeared from the scene, it is important to examine the state of the bubble early on for it contains some constraints that govern the late-time incompressible as well as compressible flows.

In a series of numerical, compressible flow calculations Sternberg and Walker[13] have calculated the flow and energy distribution following the underwater detonation of explosive spheres. Fig.2 describes the primary and secondary shocks in water resulting from a detonation of a pentolite sphere of radius R_o. The pressure distributions behind the shock front are shown in Fig.3, when the shock front in the water is at different (scaled) positions $(R/R_o)_s$. The position of the product gas (water interface is marked by a vertical bar. Figure 4 shows the energy partition in the water behind the main shock front for different values of $(R/R_o)_s$. For example, when the shock front is at 10 charge radii, only 21% of the energy is in the gas products; this drops to 7% at $(R/R_o)_s = 100$. Of great interest is the percentage of dissipated energy (i.e., internal energy <u>not</u> available to do any work). At 100 charge radii (i.e., $R/R_o)_s = 100$), this amounts to 40.5%. The dissipated energy is the difference between the internal energy in the shocked state and the work done on expanding from the shocked state to the ambient pressure, i.e., the energy dissipated in heating the water. In Fig.5 are shown the cumulative energy distributions at the times when the shock fronts are at 10 and 100 charge radii from the center. It is clear from this figure, that as expected, most of the dissipated energy is contained in those spherical shells of water that was

initially within a few charge radii of the products/water interface. When the shock front is 100 charge radii from the center, 73% of the total energy released by the detonation is contained within a 50 charge-radii sphere. These calculations by Sternberg and Walker[13] provide important information to those who need to know how much energy is actually available for use in modeling the long-time bubble motion under the assumption of incompressible flow in the water. The dissipated energy is not available.

Sternberg and Walker[13] also calculated the temperatures in the thin shells of water surrounding the interface, which contain the most dissipated energy because they had been shocked by the primary shock when the latter was at its strongest. By considering only those water isentropes that intersect the saturation line at or above 1 atmosphere, i.e., isentropes from shocked states above 54 kbars (see Fig.6), they estimated that any contribution of steam to the bubble would have increased the average bubble pressure from 3.2 bars, when $(R/R_o)_s = 100$, to 3.6 bars.

It would appear that such an increase due to steam in the bubble could have an appreciable effect on the bubble dynamics at the first minimum if there was no time to condense the steam. However, they limited themselves to the saturation line at or above 1 atmosphere, and it is well known that the pressure at the bubble maximum falls below 1 atmosphere. Therefore, it is quite possible that appreciably more water, that was shocked to pressures below 54 kbars and then expanded to (pressures below 1 atm and) temperatures below 100 C, would vaporize and affect the bubble motion during the contraction phase.

To close the discussion on purely spherical bubble phenomena, it should be noted that Mader[14] calculated the detonation of a centrally-initiated tetryl sphere in water at different depths (i.e., at different hydrostatic pressures) using a spherically-symmetric, Lagrangian, compressible flow code; the shock in the water and the bubble motion was followed through at least one complete bubble oscillation at each depth. For a hydrostatic pressure of 9.91 bars, the water shock pressure and pressure at the tetryl products/water interface are shown in Fig.7. The calculated bubble radius motion is compared to the experimental[1] (see Fig.1) in Fig. 8 and seen to be in satisfactory agreement. The calculated and experimental bubble periods as a function of water depth are compared in Fig.9 and seen to be in satisfactory agreement. These calculations performed in 1970 or earlier are apparently the first compressible flow calculations, albeit for a spherical bubble, that took the bubble motion through a minimum. The simple incompressible theory described above predicts that the maximum bubble radius is inversely proportional to the 1/3 power and the period is inversely proportional to the hydrostatic pressure to the 5/6 power; Mader's compressible flow calculations were in good agreement with the former and found an inverse 0.877 power for the latter. Inasmuch as the simple incompressible

theory also predicts that the maximum radius and the period each are proportional to the initial bubble energy (which is usually taken to be about half the total explosion energy), it is clear that the dissipated energy described by Sternberg and Walker[13] can be used to help determine what the initial bubble energy should be in any incompressible flow calculation.

In real explosion bubbles, the bubble radius is sufficiently large enough to be affected by gravity. This effect is seen in Fig.10.[15] While at the maximum, the bubble is spherical, the sphere is greatly distorted in the vicinity of the minimum (Frames 1 and 2). The lower hemispherical surface has become inverted and appears in the interior of the bubble. Snay[15] determined that the two interfaces collided forming a torus with "water all the way through the bubble near the center line." Near the minimum, the bubble migration upward (due to bouyancy) is greatest. The impinging of the lower surface on the upper near the minimum produces a "hammer effect," and presumably gives rise to compressibility effects. Frame 4 of Fig. 10 shows the bubble at its second maximum. What is not clear from the photo is whether this bubble maximum actually has the shape shown by the black, opaque products or is essentially a sphere with the black region below the bubble still opaque because of solid products in the water. At the time, Snay thought the latter.

The upward migration of the bubble under the influence of gravity is shown schematically in Fig.11.[15] The superimposed pressure-time curve reflects the existance of a low(high) pressure at the bubble maxima(minima).

Independent of the effect of gravity, a free surface is known to repel a pulsating bubble while a rigid surface attracts the bubble. In Fig.12 is shown an explosion occuring on a rigid bottom.[15,16] The bottom clearly attracts the bubble as seen in Frame 2; eventually the effect of gravity causes the bubble to rise as in Frames 3 and 4.

The pulsating bubble should be attracted to the rigid cylinder (whose axis is perpendicular to the page and) shown on the left of Fig.13. Frame 1 shows the bubble maximum and Frames 2 and 3 show bubble migration towards the cylinder and upward (due to bouyancy).

Goertner,[17] in a series of model experiments, illustrated the effect of water temperature (100°F and 36°F) on the bubble motion. While the two series of shots shown in Figs. 14 and 15 were detonated at different depths, the scaling parameters R_{max}/T^2 and R_{max}/d are roughly equal, where R_{max}, T, and d are respectively, the bubble maximum radius, bubble period, and charge depth. The higher temperature water (100°F) gives a bubble maximum with a "cratered" surface (see Fig.14). Goertner[17] notes that this "is characteristic of explosion bubbles where appreciable 'boiling'

takes place[16]"; that the much larger minimum in Fig.14 is attributable to this boiling; and that there is a more rapid change in bubble size and shape in the vicinity of the minimum for lower water temperature (see Fig.15). The bubble motions (that correspond to Figs. 14 and 15) are seen in Fig. 16 and 17, where in each figure the upper (lower) curves show the position of the upper (lower) surface of the bubble. A third bubble minimum is not discernable for 100 F water.

While for many years after WWII, Snay and coworkers at the Naval Surface Warfare Center/White Oak derived theoretical models of the explosion bubble motion based on classical analysis coupled with experimental data, it was not until 1970 that NSWC began to apply the techniques of computational fluid dynamics to describing explosion bubble phenomena in terms of unsteady, axially-symmetric, incompressible flows. VanderVorst and Van Tuyl[18] calculated the motion of an axisymmetric underwater explosion bubble in an incompressible inviscid fluid by the "marker and cell" method. The fundemental equations solved are

$$\partial u/\partial t=-(1/r)\partial(ru^2)/\partial r -\partial(uv)/\partial z-\partial p/\partial r +\nu\,[\partial u/\partial z-\partial v/\partial r]/\partial z$$

$$\partial v/\partial t=-(1/r)\partial(ruv)/\partial r- \partial(v^2)/\partial z-\partial p/\partial z-(\nu/r)\partial[r(\partial u/\partial z-\partial v/\partial r)]/\partial r+g$$

$$(1/r)\partial(r\partial p/\partial r)+\partial^2 p/\partial z^2=-Q$$

$$Q=(1/r)\partial[(1/r)\partial(ru^2)/\partial r+\partial(ru^2)/\partial r+\partial(uv)/\partial z]/\partial r$$

$$+\partial[(1/r)\partial(ruv)/\partial r+\partial(v^2)/\partial z]/\partial z,$$

where $p = P/\rho$, ν is a viscosity coefficient, g is the gravity constant, and u and v are the radical and axial velocities in the r and z directions, respectively.

These MACBUB calculations[18] describe the bubble jet and torroidal shape up to near the second minimum as seen in Fig.18; isobars corresponding to the times depicted in Fig.18 are shown in Fig.19. The calculations started from the bubble maximum shown in Fig.20; the data at the maximum, supplied by H. Snay, and the solution for a simple non-migrating, spherical bubble is shown in Fig.20 for comparison. Comparison of the computational profiles (Fig.18) with the experimental profiles (performed under scaled conditions) (see Fig.10) shows a disagreement of about 10%. The origin of their MACBUB computer code was Pritchett's MACYL code[19,20] for computing the motion of an underwater steam bubble formed by a nuclear explosion; Pritchett extended Harlow's[21] basic methodology.

Using a different technique, Van Tuyl and Collins[22] calculated the motion of axisymmetric underwater explosion bubbles by use of source distributions on free and rigid surfaces. For one problem, the bubble motion in the presence of an air-water surface

and horizontal rigid bottom, the results are shown in Figs.21-31. Cavity and torus closure is shown in Figs.26 and 28, respectively.

Dunbar, Shea, and Hancock[23] computed the underwater explosion of 450 kg of TNT at a depth of 300 meters, where the charge was located adjacent to a rigid wall at a distance approximately equal to 3/4 of the maximum free-field bubble radius. The coupled Eulerian/Lagrangian grid used in the PISCES 2DELK compressible flow code and the position of the explosive charges at time t=0 is shown in Fig.32. The growth of the bubble is shown in Fig.33. At t=40 mses the bubble touches the rigid boundary on the right. The bubble maximum is at about 70 msec (not shown); the bubble collapse until a torus is formed is shown in Fig.34. Figures 35 and 36 provide the pressure and impulse loadings at the center of the rigid wall, respectively, as a function of time. The pressure peak associated with the initial shock is 0.73 kbar, while that from the pressure loading of the water due to bubble collapse is twice as large. The impulse from bubble collapse, which is more important from the viewpoint of deforming a structure, is approximately five times greater thatn the impulse from the initial shock load.[23]

In the modeling of both the effect of gravity and the presence of a rigid body, Chan[24] has utilized a three-dimensional, compressible, two-phase flow code. In particular, numerical calculations were made and compared with NSWC experimental data[17] for the motion of an explosion bubble in the vicinity of a long solid cylinder. The relative locations are shown in Fig.37. Comparison of the calculated with the experimental bubble motions is given in Figs.38 and 39. The first maximum is reproduced reasonably well, but the minimum volume is not (see Fig.38). The same is true for three other comparisons shown in Figs.39-41. Chan speculates that the discrepancy at the first minimum is probably the result of inappropriate initial conditions. These initial conditions are obtained by working backwards from the experimental maximum radius and bubble period obtained in <u>small tank</u> experiments to find the initial conditions that would give the same values for a <u>free-field</u> explosion. It is also not clear whether there is sufficient resolution near the minimum.

Another series of calculations were made by Chan[24] to compare with a series of experiments being performed at NSWC in which a measurements are made of the loadings on a flat plate due to the collapse of an underwater explosion bubble. The steel plate, suspended in the water, is free to move under the action of the bubble. With a water temperature of 23.3 C, boiling is expected to occur at the reduced air pressure in the tank of 1.35 psia. A series of different calculations were made. In Case A, a simple boiling model

$$G = C(P_{sat}-P)$$

is used to describe the phase transition rate when boiling occurs. G is the vapor generation rate, P_{sat} the saturation vapor pressure corresponding to the water temperature, P the fluid pressure in the bubble, and C the rate coefficient. In Case B, boiling is not allowed to occur. The other cases are the same as Case B except that the standoff from the plate is different. Cases A and B are shown, respectively, in Figs.42 and 43. Boiling (Case A) helps create a slightly larger bubble.

In the code used by Chan,[24] only the convection terms have explicit differencing; the other terms have implicit differencing. Thus, the calculation of the motion is not restricted by the local sound speed restriction and larger time steps are chosen.

A series of 3-dimensional, incompressible, inviscid flow calculations with gravity present have recently been completed by Perdue and Chahine.[25] The method of solution is the boundary intergral method and integrates the potential and its derivative on triangular panels. Boiling occurs as the vapor comes off at the liquid temperature and is instantaneously diffused into a uniform bubble.

In one set of calculations,[25] comparison is made with the experimental results[16] shown in Fig. 44. The configuration of the rigid cylinder and the explosive charge is analogous to that shown in Fig. 37. The calculated results are shown in Fig. 45. The agreement is quite good. Here again, the experimental results were obtained in a cylindrical tank, and the experimental maximum bubble radius R_{max} and bubble period T were used to work backwards to the initial conditions that a non-buoyant bubble would need in an infinite medium to give the experimental R_{max} and T. As in the case of Chan's computation[24] discussed earlier, the minimum may be strongly affected by the incompatible initial conditions. Still, even at 84.1 msec the calculated bubble strongly resembles the experimental one.

Collapse of a bubble from its maximum in the presence of a plate at different orientation to the vertical was calculated for the five different orientations shown in Figs. 46-50.

A new method,[26] which will be mentioned only briefly because preliminary results were obtained just last week, employes a fixed domain algorithm based on a formulation of incompressible hydrodynamic free boundary problems by Rogers.[27] The method avoids interface tracking by employing conservation laws coupled with a variable density constrained to be no larger than the density of water. The bubble is considered as a uniform pressure region with P(V) given by the adiabatic gas law. The bubble moves in a gravitational field.

MICRO VAPOR CAVITY COLLAPSE RESULTS

While the above work dealt directly with explosion bubbles, somewhat similar calculations for different applications had been and are being performed elsewhere. It was well known experimentally that an initially spherical bubble collapsing near a solid wall develops a high-speed jet directed toward the wall. The impact of the jet is considered a primary factor responsible for cavitation damage, e.g., to propellars. The gas bubbles, or more likely vapor cavities, are minute compared to the explosion bubbles discussed earlier. In these minute bubbles, buoyancy effects are negligible unlike in explosion bubbles. Because the bubble collapse is small-scale and very rapid, it has been difficult to measure accurately the characteristics of the collapse such as the jet velocity and the pressure pulse. Thus, it was particularly necessary to turn to numerical solutions.

Plesset and Chapman,[28] using the Liebmann iterative method, solved the finite difference formulation of Laplace's equation, and calculated the collapse of a vapor bubble near a solid boundary in an inviscid incompressible liquid; they demonstrated jet formation during the early stage of collapse and found the magnitude of jet impact striking the wall. Their results were experimentally confirmed by Lauterborn and Bolle.[29] A comparison is shown in Fig.51. Mitchell and Hammitt[30] calculated vapor bubble collapse by means of a modified marker and cell technique. Nakajima and Shima[31] used a finite element technique to calculate vapor bubble collapse in a viscous incompressible liquid near a plane solid wall. An extensive review of bubble dynamics and cavitation has been written by Plesset and Prosperetti[32] describing the experimental and theoretical work to 1977. Blake and Gibson[33] used an approximate integral-equation approach to model the growth and collapse of a vapor bubble close to an initially plane surface. A boundary integral method for cavity collapse by Guerri[34] calculated the jet motion almost to impact with the opposite side of the cavity.

In a very interesting series of experimental papers Shima, *et al*[35-37] considered the collapse of a single spark-generated bubble near a solid wall and showed that there are regions where the impact wall pressure is generated mainly by a shock wave, by a liquid jet, and by interaction of both a shock wave and a liquid jet[35]; and that various kinds of impulsive pressures successively impinge on a solid boundary in the final state of bubble collapse,[36,37] namely, (i) an impulsive pressure pulse developing in the liquid near the bubble surface, (ii) an impact pressure from a liquid microjet formed inside the main bubble, (iii) impulsive pressures resulting from the interaction between the outward radial flow caused by the jet impact and the bubble surface contracting along the solid boundary, and (iv) an impact pressure from a shock wave radiated from the torus-like main

bubble at its rebound. They found that the target damage is fundamentally caused by the liquid jet impact and enhanced by impulsive pressures resulting from subsequent phenomena.

In a fascinating series of calculations, O. Voinov and V. Voinov[38] and O. Voinov[39] have shown that if at an initial time in an incompressible fluid bounded by a solid plane, there is a (non-spherical) cavity in the form of an ellipsoid of rotation whose rotation axis is perpendicular to the plane, then the process of cavity collapse may differ considerably from the process of collapse of an initially spherical cavity (see Fig.52[39]). For $k=b/a \geq 1.25$, where a and b are the initial cavity semi-axes perpendicular and parallel, respectively, to the plane, the cavity collapse is shown schematically in Fig.53.[38] At successive times, the cavity begins to neck off as shown in 53(a); the necked-off region shown expanded in 53(b); and the eventual formation of a jet as shown in 53(c). Estimates of the jet velocity into the large cavity yields extremely high values, these values increasing with increasing value of k. Obviously, the process of jet formation by the collapse of an annular region for $k \geq 1.25$ is different from the jet formation process for an initially-spherical cavity shown in Figs.51 and 52 or in Fig.53(b) for k=1.

REFERENCES

1. Cole, R.H., Underwater Explosions, Princeton University Press, 1948.

2. Holt, M., Ann. Rev. Fluid Mech., vol.9, p.187, 1977.

3. Snay, H.G., Goetner, J.F., and Price, R.S., Small Scale Experiment to Determine Migration of Explosion Gas Globes, Naval Ordnance Laboratory Report NAVORD 2280, 1952.

4. Snay, H.G., Hydrodynamics of Underwater Explosions, Naval Hydrodynamics, NAS-NRC Publication 515, pp.325-351, 1957.

5. Snay, H.G., The Hydrodynamic Background of Radiological Effects of Underwater Nuclear Explosions, US Naval Radiological Defense Laboratory Review Lecture No. 103, vol. 2, pp. 1-52, 1960.

6. Snay, H.G., The Scaling of Underwater Explosion Phenomena, Naval Ordnance Laboratory Report NOLTR 61-46, 1961.

7. Snay, H.G., Underwater Explosion Phenomena: The Parameters of Migrating Bubbles, Naval Ordnance Laboratory Report NAVORD 4185, 1962.

8. Young, G.A., The Physics of the Base Surge, Naval Ordnance Laboratory Report NOLTR 64-103, 1965.

9. Farley, T.E. and Snay, H.G., A Simplified Analysis of the Bubble Jet Pulse, Naval Ordnance Laboratory Report NOLTR 68-42, 1968.

10. Goertner, J.F., Hendrickson, J.R., and Leamon, R.G., Model Studies of the Behavior of Underwawter Explosion Bubbles in Contact With a Rigid Bottom, Naval Ordnance Laboratory Report NOLTR 68-207, 1969.

11. Young, G.A., Plume and Ejecta Hazards from Underwater Explosions, Naval Ordnance Laboratory Report NOLTR 73-111, 1973.

12. Young, G.A., Dispersion of the Chemical Products of Underwater Explosions, Naval Surface Weapons Center Report NSWC TR 82-404, 1984.

13. (a) Sternberg, H.M. and Walker, W.A., Phys.Fluids, vol.14, p.1869, 1971; (b) Walker, W.A. and Sternberg, H.M., The Chapman-Jouguet Isentrope and the Underwater Shockwave Performance of Pentolite, Fourth Symposium on Detonation, p.27, 1965.

14. Mader, C.L., Compressible Numerical Calculations of Underwater Detonations, Los Alamos Scientific Laboratory Report LA-4594, March 1971.

15. Same as reference 4.

16. Same as reference 3.

17. Goertner, J.F., Vacuum Tank Studies of Gravity Migration of Underwater Explosion Bubbles, Naval Ordnance Laboratory Report NAVORD 3902, 1956.

18. VanderVorst, M.J. and Van Tuyl, A.H., Calculation of Incompressible Underwater Bubble Phenomena by the Marker and Cell Method, Proceedings of the First International Symposium on Ship Hydrodynamics, Office of Naval Research, October 1975.

19. Pritchett, J., MACYL--A Two Dimensional Cylindrical Coordinate Incompressible Hydrodynamic Code, Naval Radiological Defense Laboratory Technical Report USNRDL-TR 67-97, October 1967.

20. Pritchett, J. and Pestaner, J., A Numerical Calculation of the Water Flow Following the WIGWAM Underwater Explosion, Naval Radiological Defense Laboratory Technical Report USNRKL-TR 69-48, May 1969.

21. Harlow, F.H. and Welch, J.E., Phys. Fluids, vol.8, p.2182 1965; Harlow, F.H. and Welch, J.E., Phys. Fluids, vol.9, p.845 1966; Welch, J.E., Harlow, F.H., Shannon, J.P., and Daly, B.J., The MAC Method - A Computing Technique for Solving Viscous, Incompressible, Transient Fluid-Flow Problems Involving Free Surfaces, Los Alamos Scientific Laboratory Report LA-3425, March 1966; Hirt, C.W. and Harlow, F.H., J. Computational Physics, vol.2, p.114, 1967.

22. Van Tuyl, A.H. and Collins, J.P., Calculation of the Motion of Axisymmetric Underwater Explosion Bubbles by Use of Source Distributions on Free and Rigid Surfaces, Naval Surface Weapons Center Report NSWC TR 84-314, July 1985.

23. Dunbar, G., Shea, J., and Hancock, S., Calculated Response of an Underwater High Explosive Bubble Adjacent to a Rigid Wall, Proc. Shock and Vibration Symposium, p.1, 1986.

24. Chan, K., Validation of the EITACC-FS Computer Code for Underwater Explosion Analysis, JAYCOR Final Report, April 1988.

25. Chahine, G., Perdue, T. and Tucker, C. Interaction Between an Underwater Explosion Bubble and a Solid Submerged Body, TRACOR Hydronautics Technical Report 86029-1 (1988).

26. Solomon, J., Szymczak, W., and Berger, A., private communication.

27. Rogers, J.C., An Algorithm for Predicting the Evolution of the Underwater Explosion Bubble, Final report for Contract No. N60921-83-M-5807, 1984; J.C. Rogers, Theoretical and Physical Analysis of the Underwater Explosion Problem, informal report, 1983.

28. Plesset, M.S. and Chapman, R.B., J. Fluid Mech., vol. 47, p.283, 1971.

29. Lauterborn, W. and Bolle, H., J. Fluid Mech., vol.72, p.391, 1975.

30. Mitchell, T.M. and Hammitt, F.G., Trans. ASME Ser I, J. Fluid Engng., vol.95, p.29, 1973.

31. Nakajima, K. and Shima, A., Ingenieur-Archiv, vol.46, p.21, 1977.

32. Plesset, M.S. and Prosperetti, A., Ann. Rev. Fluid Mech., vol.9, p.145, 1977.

33. Blake J.R. and Gibson, D.C., J. Fluid Mach., vol.111, p.123 1981.

34. Guerri, L., A numerical method for the dynamics of non-spherical cavitation bubbles, Proceedings of the Second International Colloquium on Drops and Bubbles, p. 175, 1981.

35. Shima, A., Takayama, K., and Tomita, Y., Mechanisms of the Bubble Collapse and the Induced Impact Pressure Generation, Rep. Inst. High Speed Mech., vol. 48, no. 367, pp. 77-97, 1984.

36. Shima, A., Tomita, Y., and Sugiu, T. Mechanisms of Impulsive Pressure Generation and Damage Pit Formation by Bubble-Shock Wave Interaction, International Symposium on Cavitation, Sendai, Japan, pp. 77-82, 1986.

37. Shima, A., Tomita, Y., J. Fluid Mech., vol.169, p.535, 1986.

38. Voinov, O.V. and Voinov, V.V., Dokl. Akad. Nauk SSRR, vol.227, p.63, 1976 [English translation: Sov. Phys. Dokl. vol.21, p.133, 1976].

39. Voinov, O.V., Zh. Prikladnoi Mekh. i Tekh. Fiz., no.3, p.94 1979. [1979 Plenum Publishing Corp. translation]

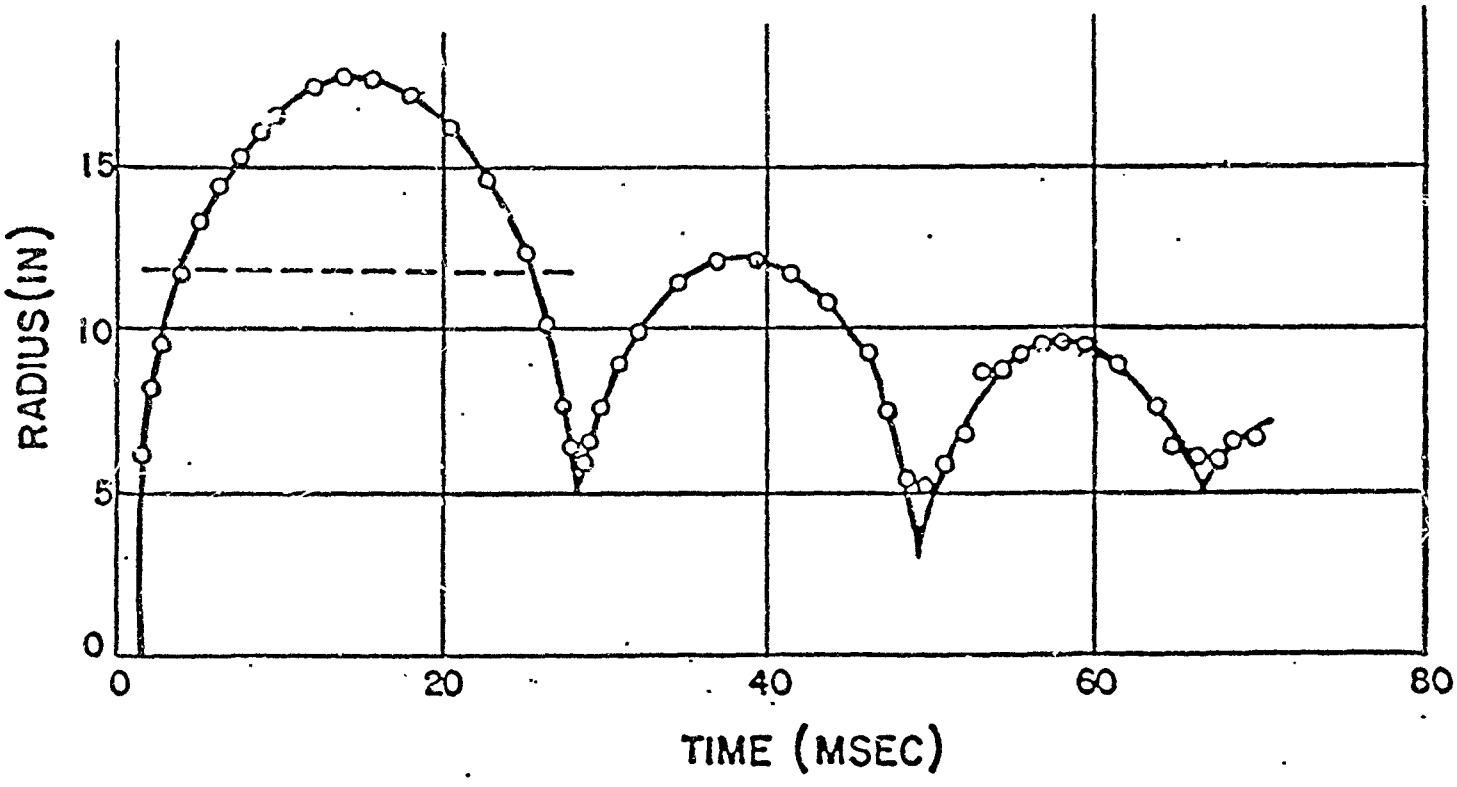

Figure 1. Radius of the gas sphere as a function of time, for a 0.55 pound tetryl charge 300 feet below the surface. (From ref.1)

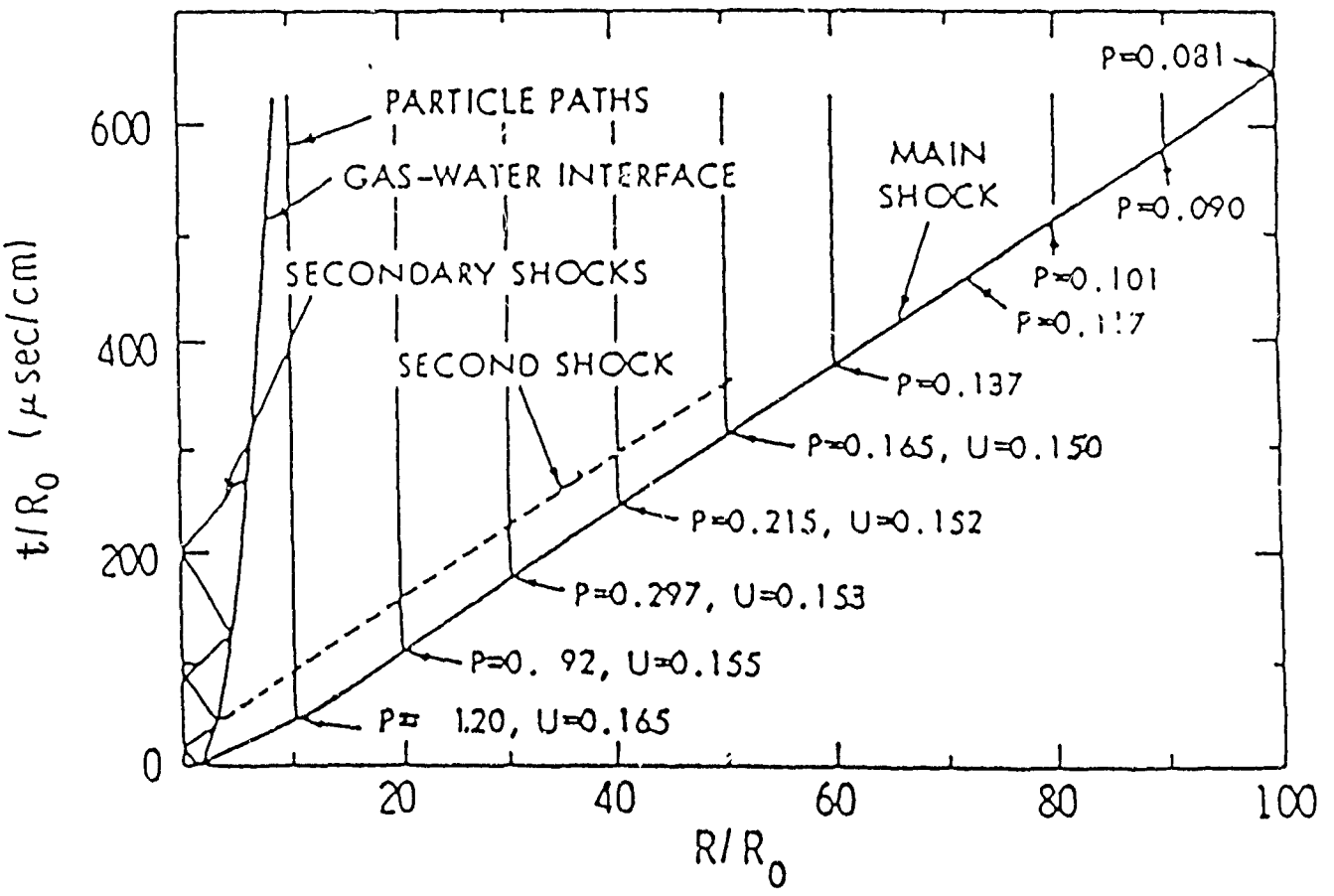

Figure 2. Space-time diagram of the spherical underwater detonation calculated by the q method. Pressures are in kilobars, shock velocities in centimeters/microsecond. (From ref.13(a))

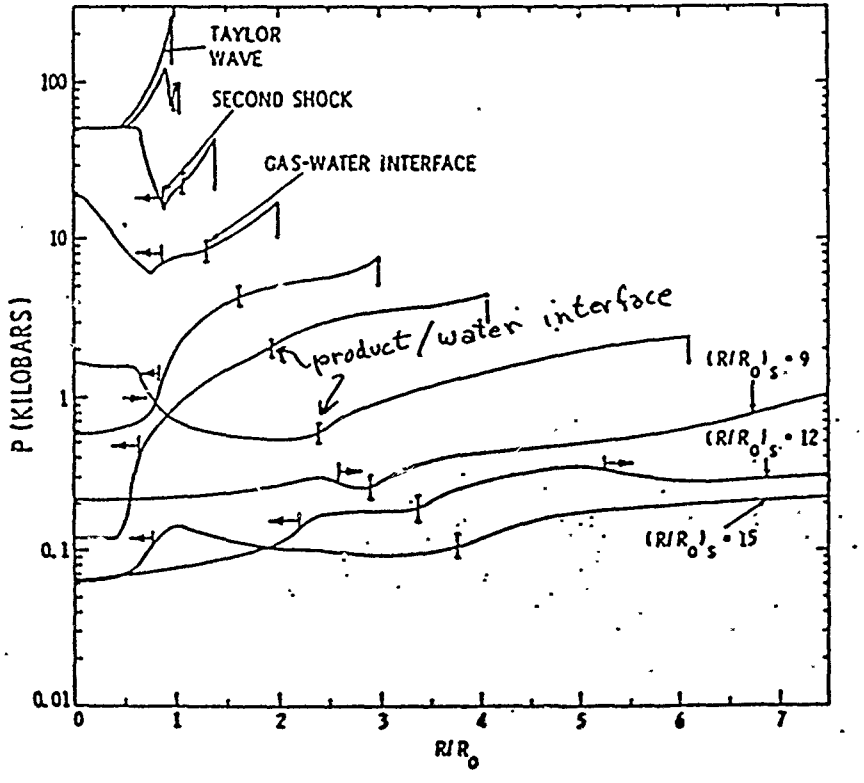

Figure 3(a). Calculated pressure versus distance at various early times, starting with the Taylor wave in the gas sphere. (From ref.13(a))

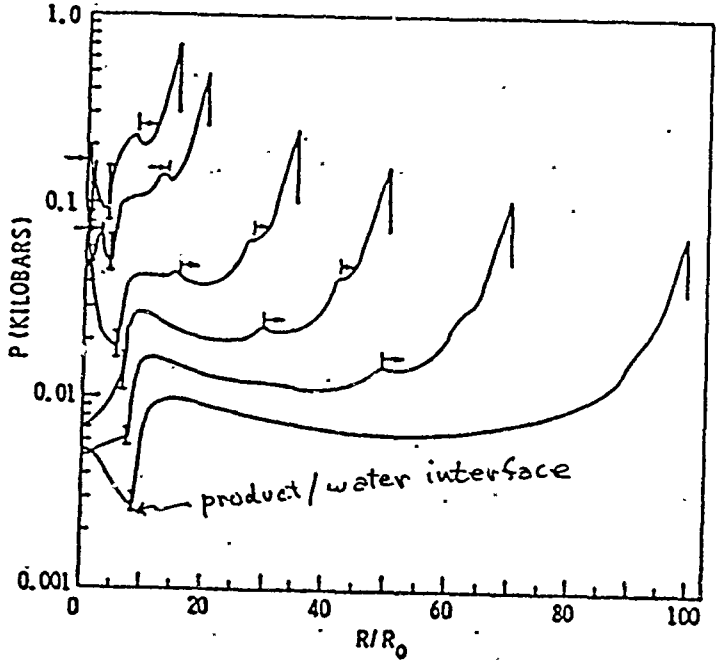

Figure 3(b). Calculated pressure versus distance at times corresponding to shock front positions of 15, 20, 35, 50, 70, and 100 charge radii.

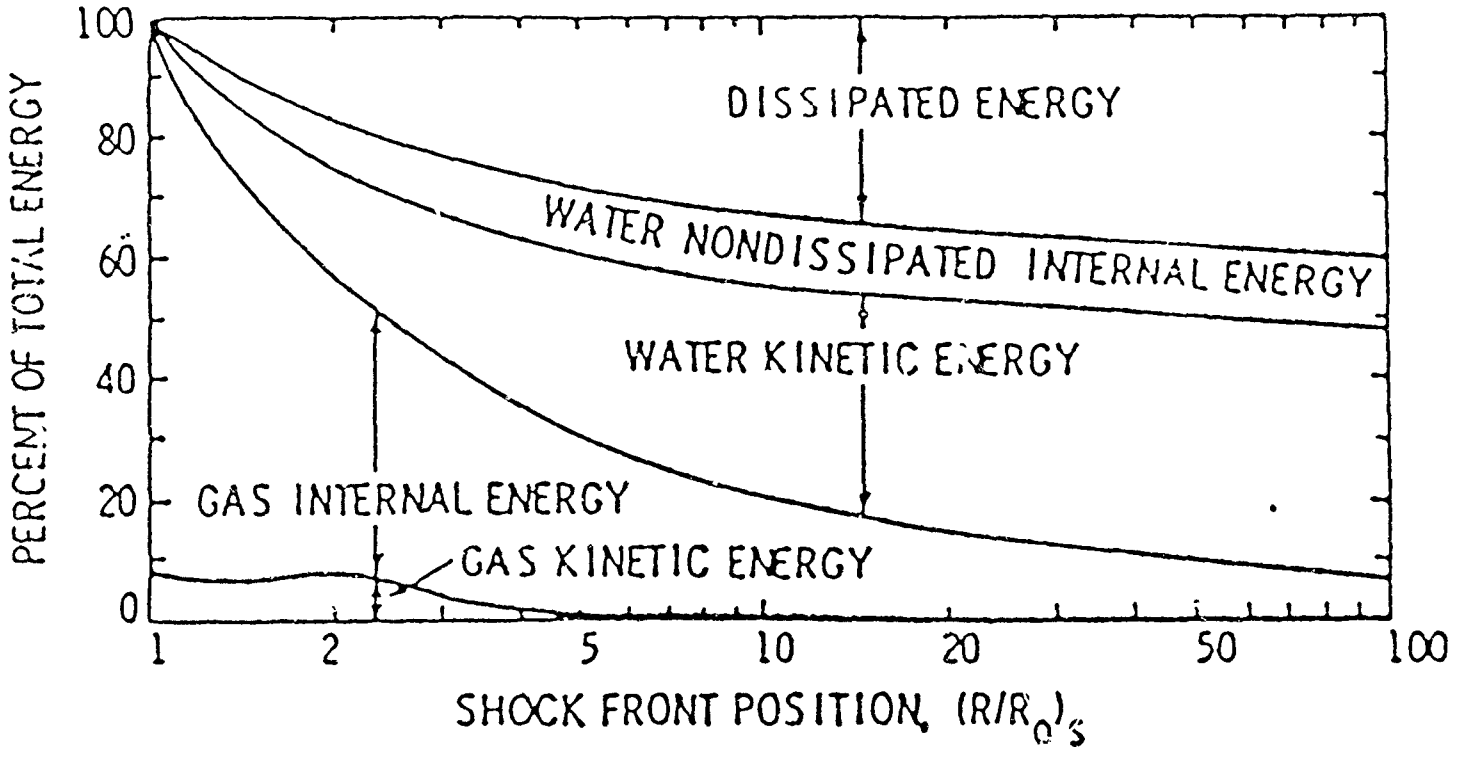

Figure 4. Calculated energy partition in the water versus position of the main shock front. (From ref.13(a))

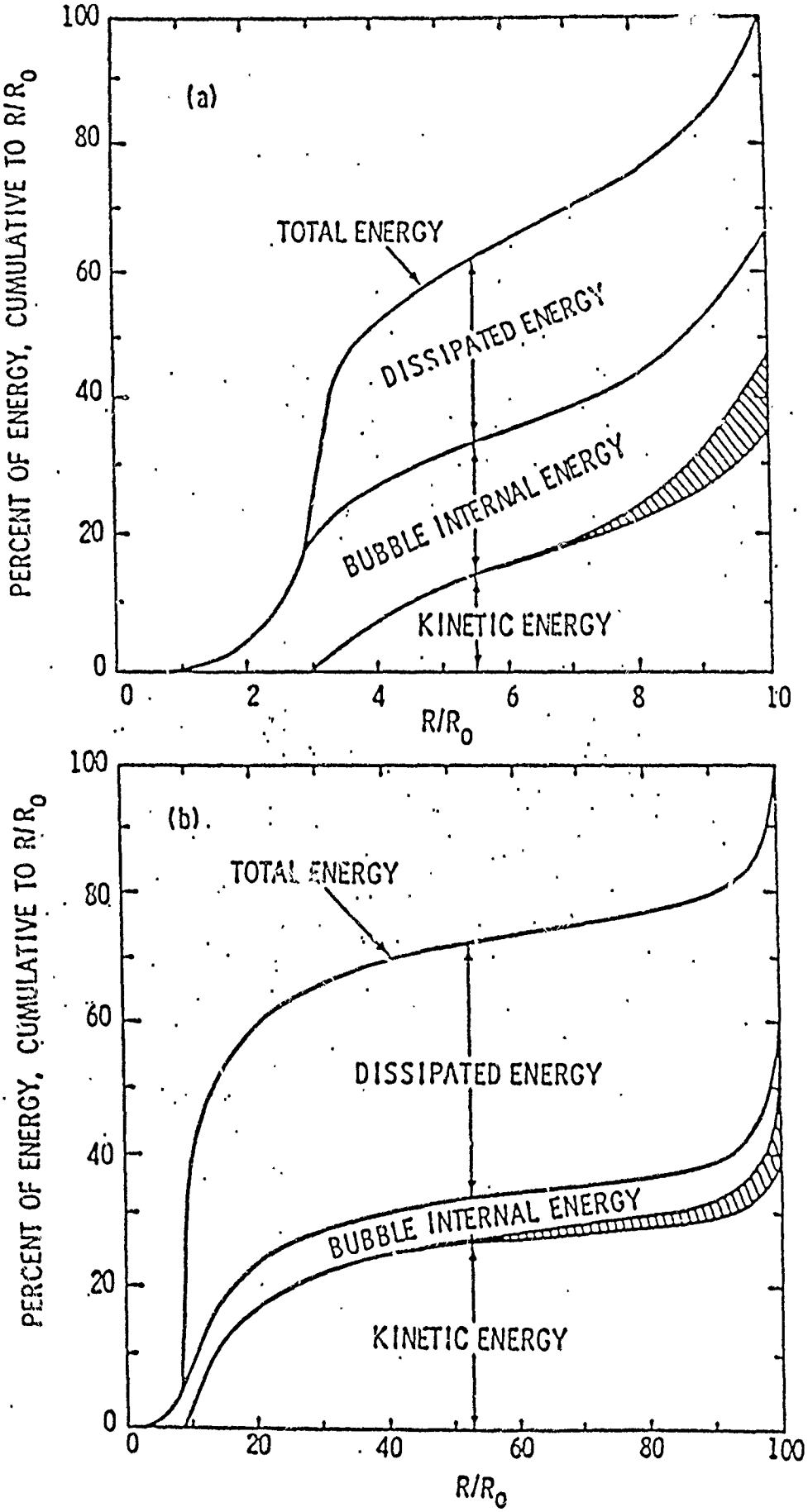

Figure 5. Energy distribution in the water at times corresponding to shock-front positions of 10 and 100 charge radii. The shaded regions denote nondissipated internal energy in the water. (From ref.13(a))

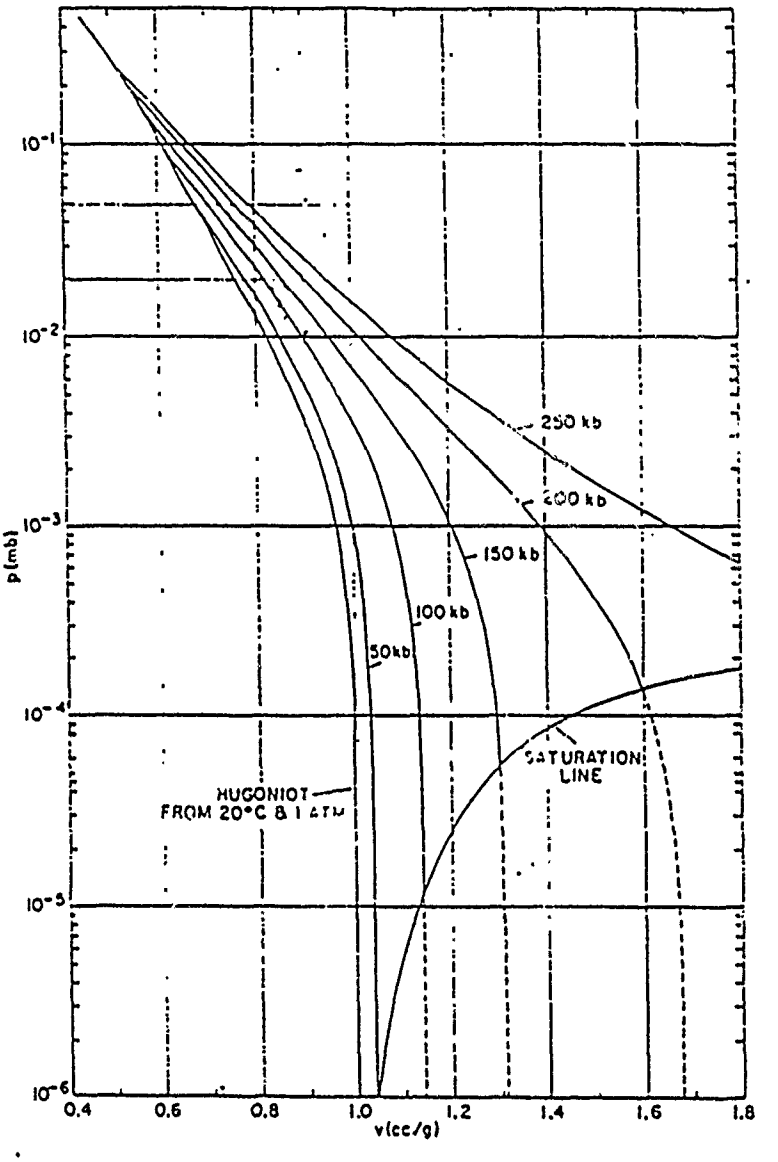

Figure 6. Water isentropes calculated with Eq.(1) (From ref.13(b))

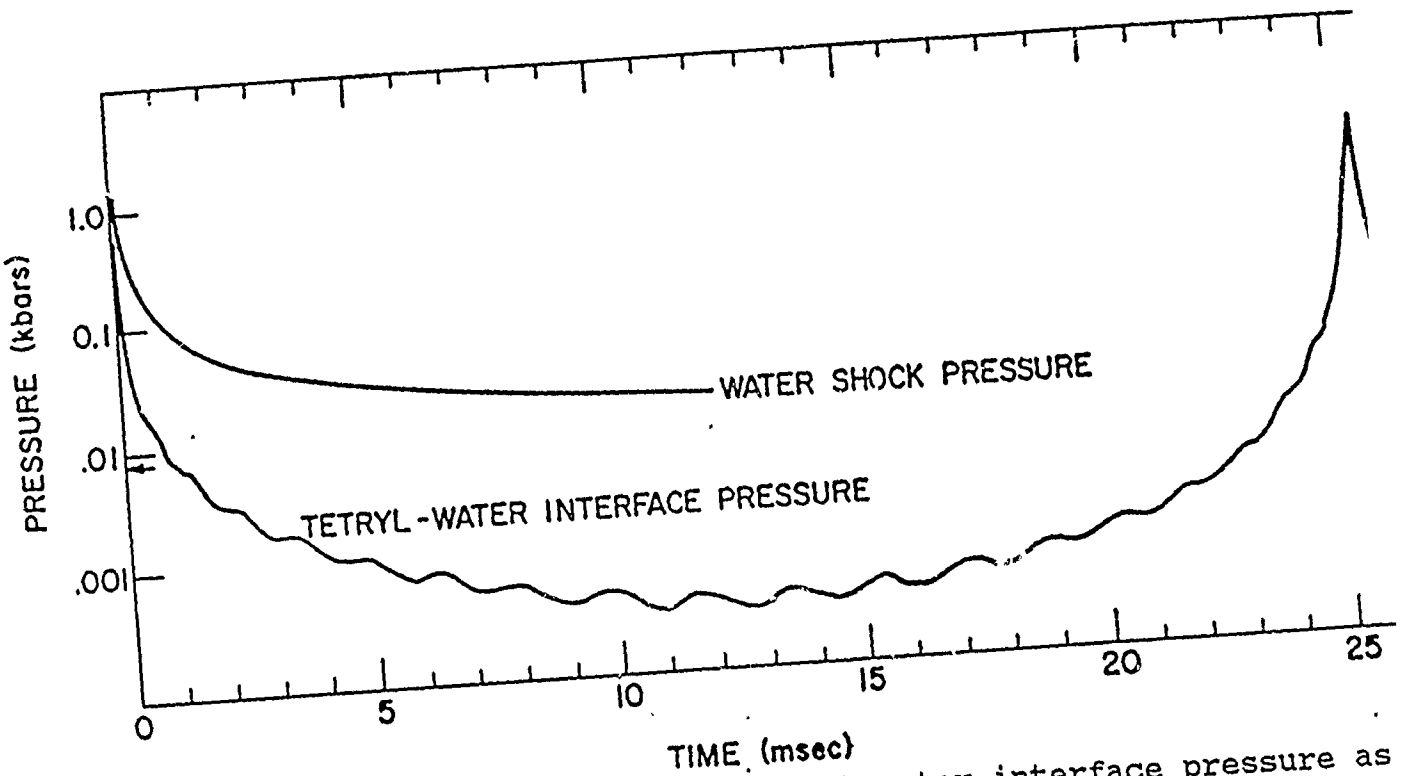

Figure 7. The water shock and tetryl-water interface pressure as a function of time for a 3.27-cm radius tetryl sphere in water at 9.91 bars. (From ref.14)

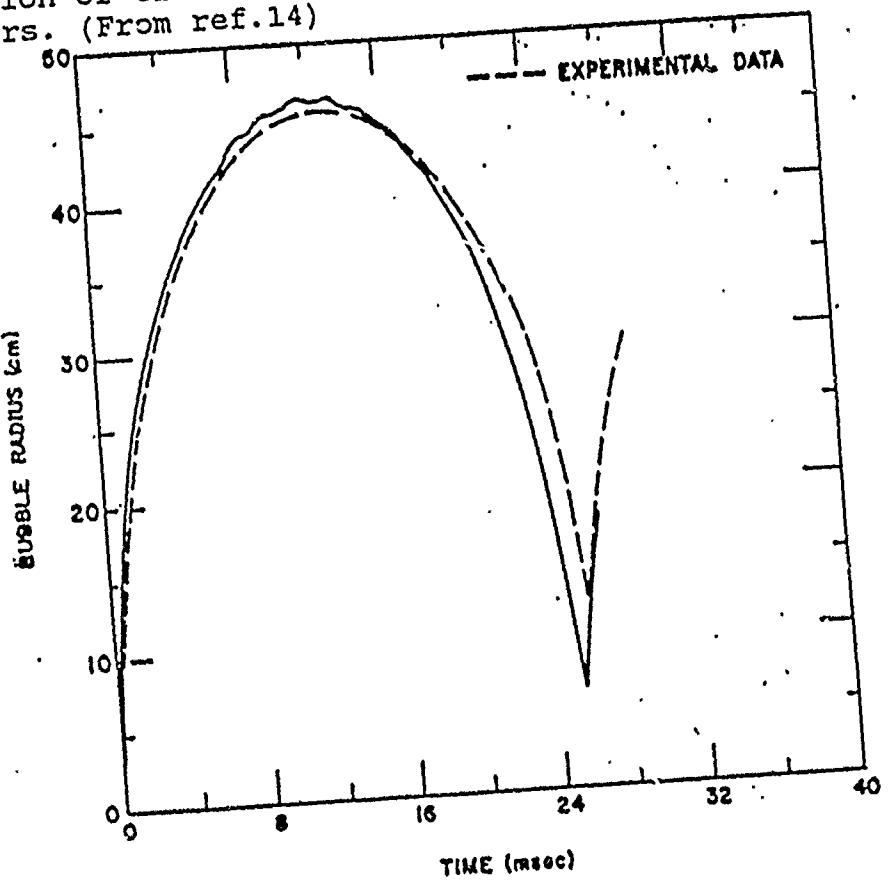

Figure 8. The bubble radius as a function of time for a 3.27-cm radius tetryl sphere in water at 9.91 bars. The experimental data are also shown. (From ref.14)

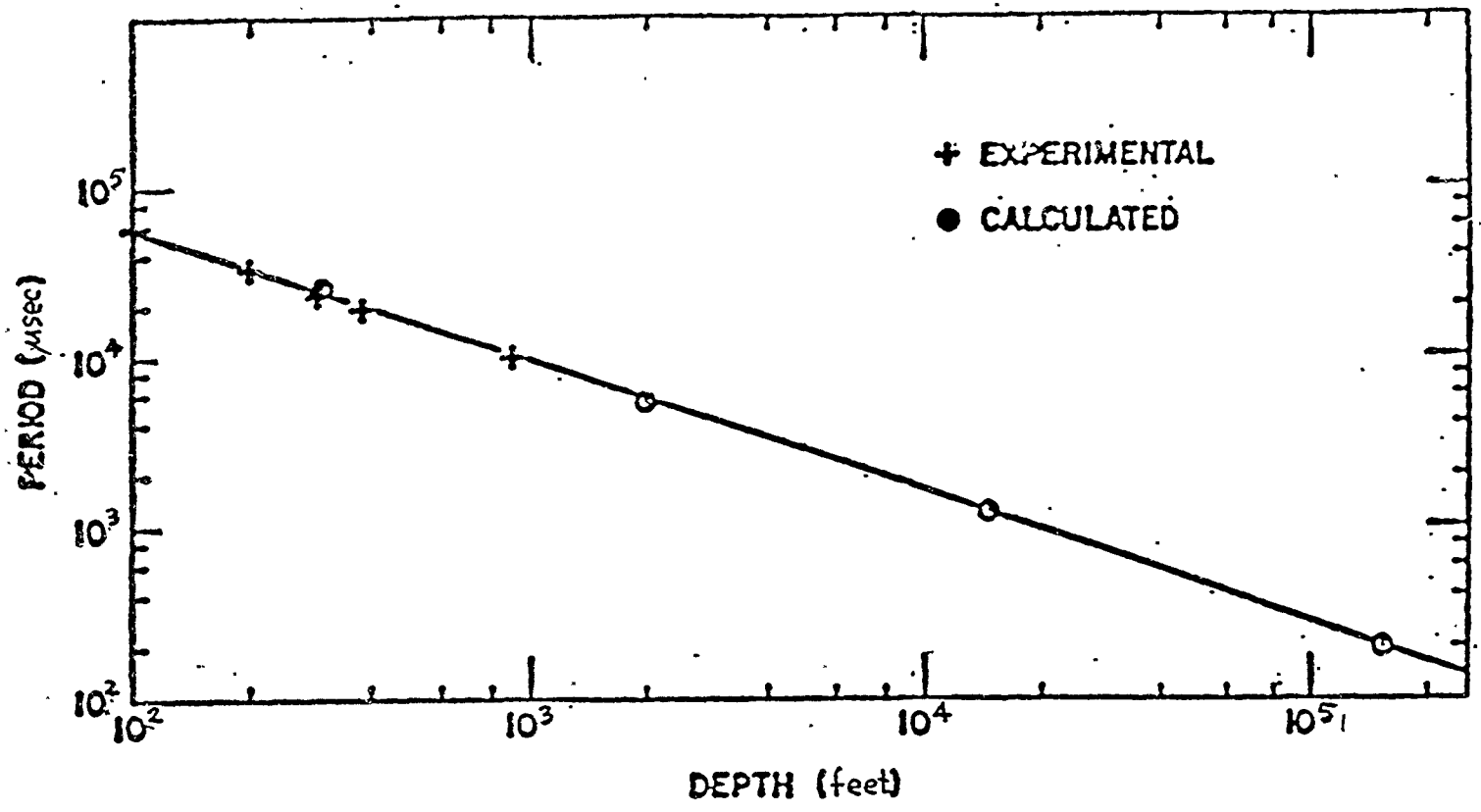

Figure 9. The calculated and experimental bubble periods as a function of water depth. (From ref.14)

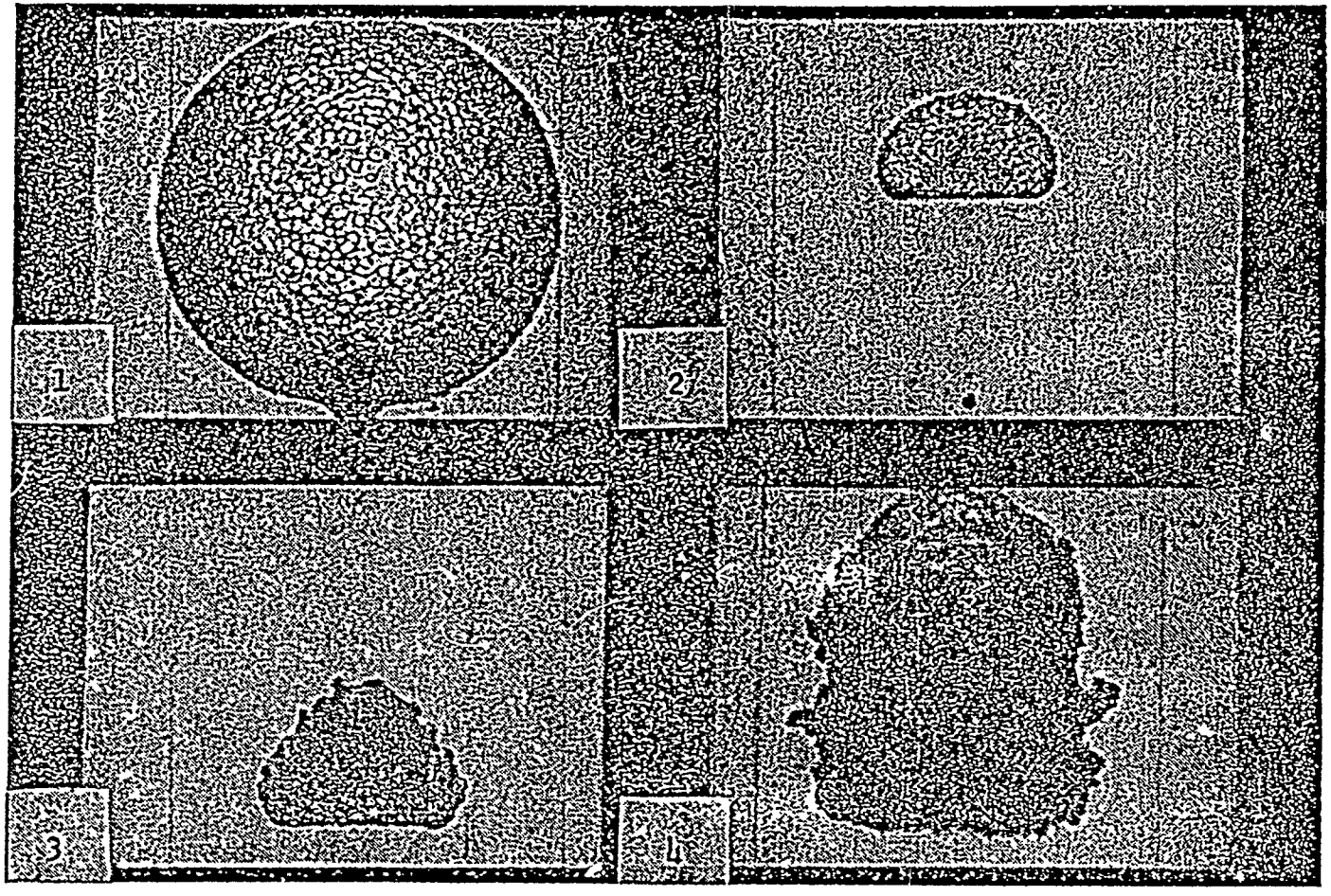

Figure 10. Gas bubble of an underwater explosion. (From ref.4)

Frame 1: Bubble maximum
Frame 2: About 6msec before bubble minimum
Frame 3: About 6msec after bubble minimum
Frame 4: Second bubble maximum

(times quoted refer to the condition scaled in this model test:
354 lbs TNT in 80.8 ft. depth)

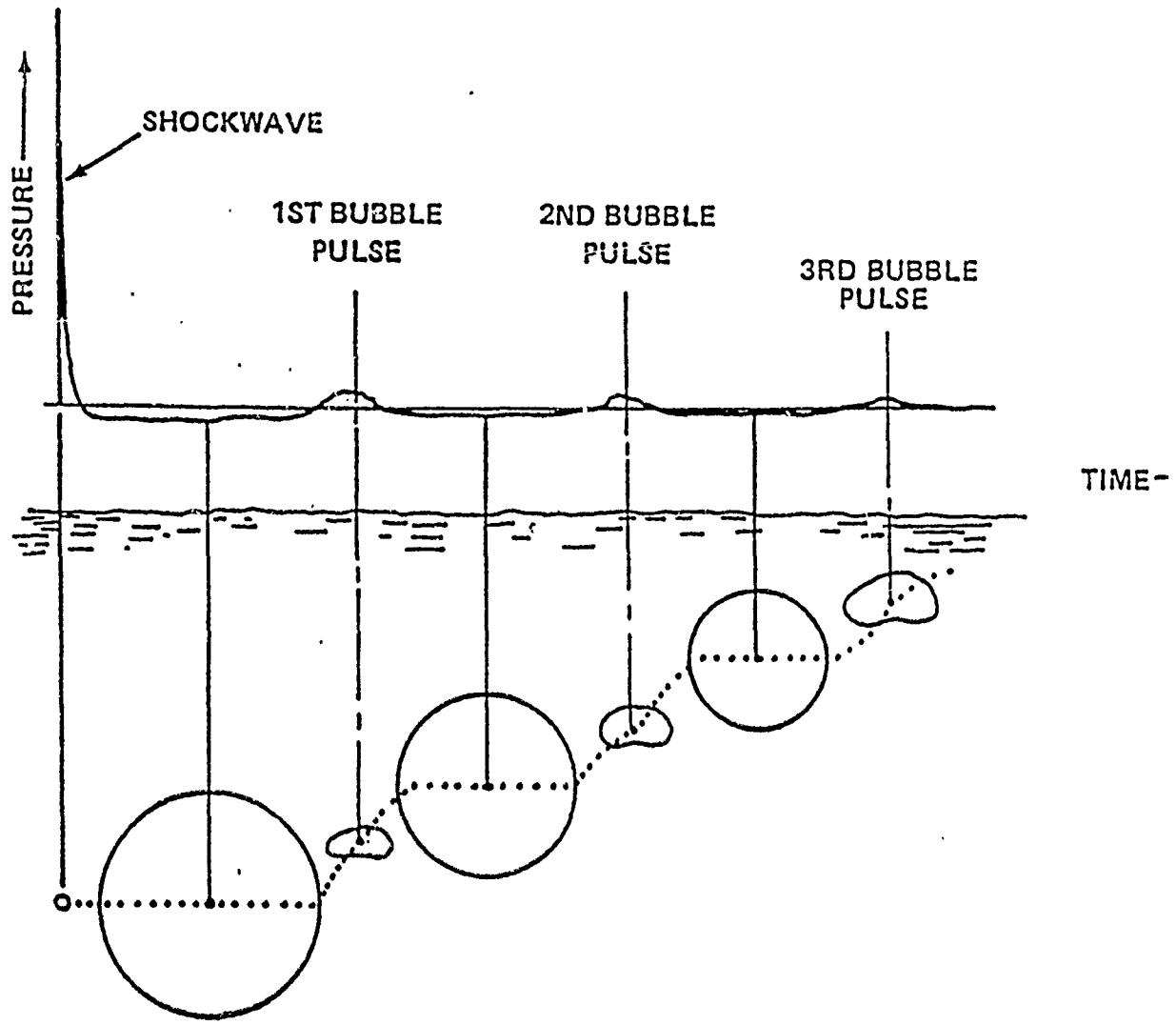

Figure 11. Pressure waves and bubble phenomena of underwater explosions. The upper part shows a pressure-time plot, the lowe the position and size of the bubble for specific moments which correspond to the curves above as indicated by the vertical line (From ref.4)

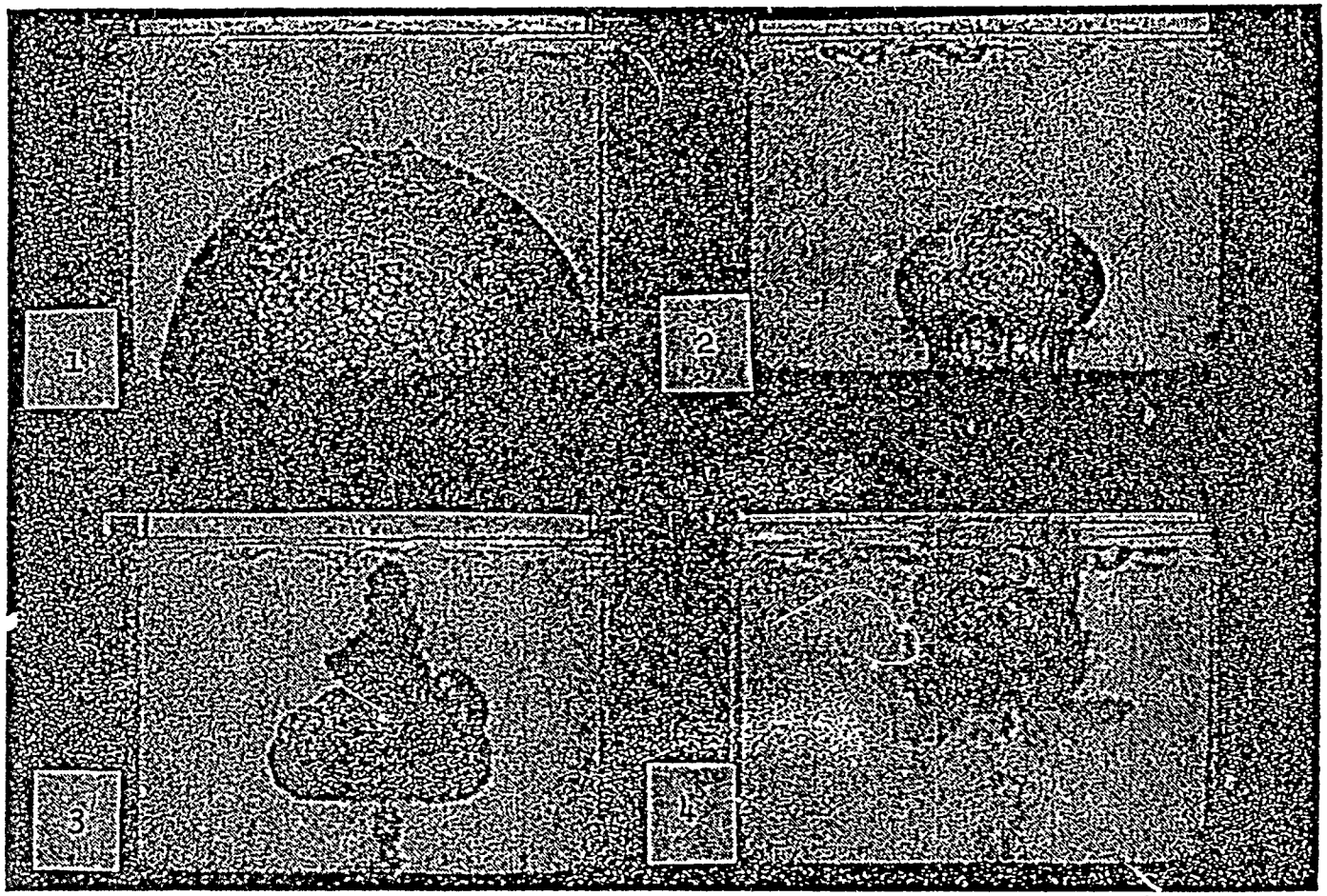

Figure 12. Bubble behavior of an explosion on a rigid surface. The charge was fired on a steel plate. (From ref.4)

The water surface is visible near the top of each frame.

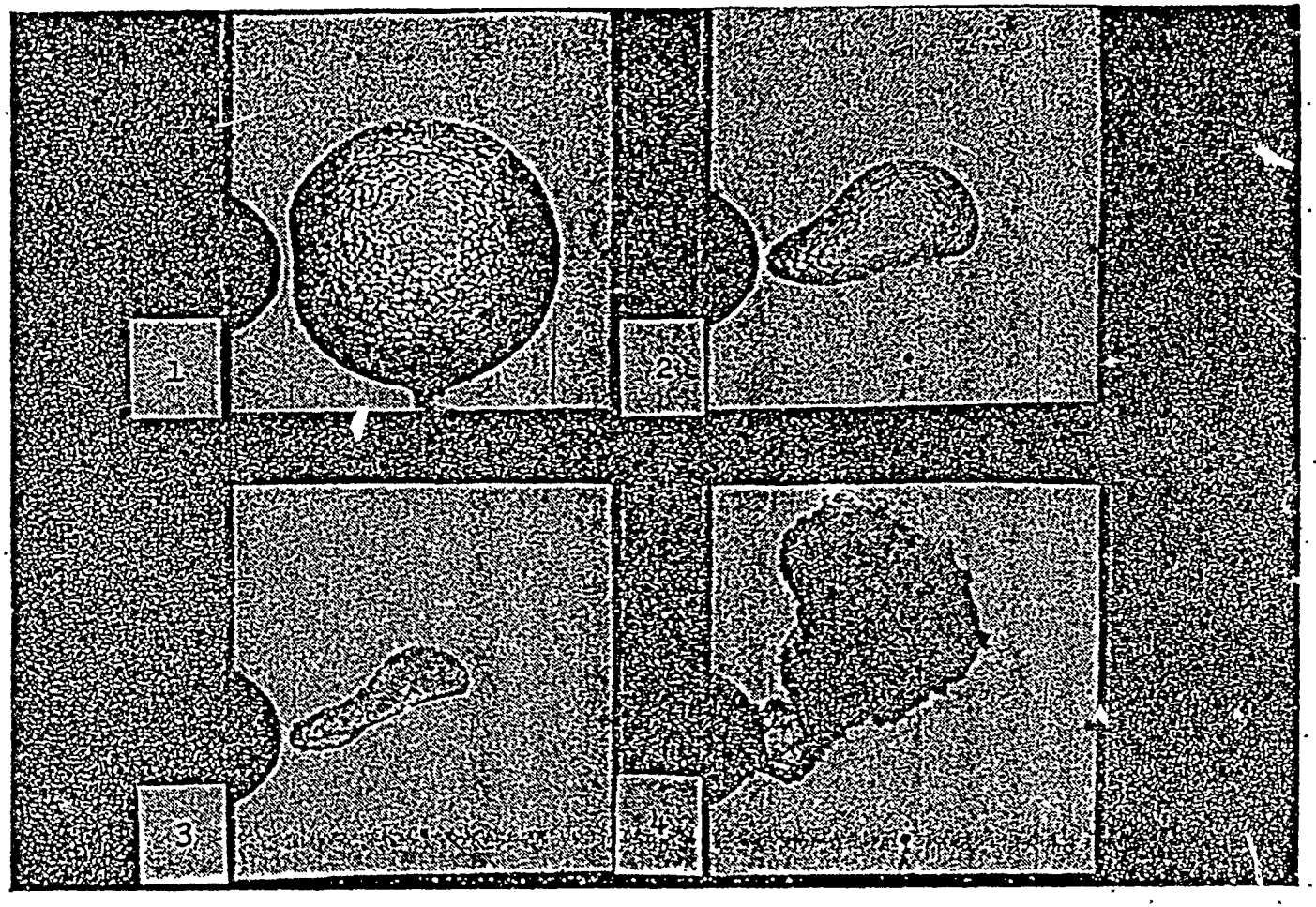

Figure 13. Bubble pulsation near a rigid cylinder. (From ref.4)

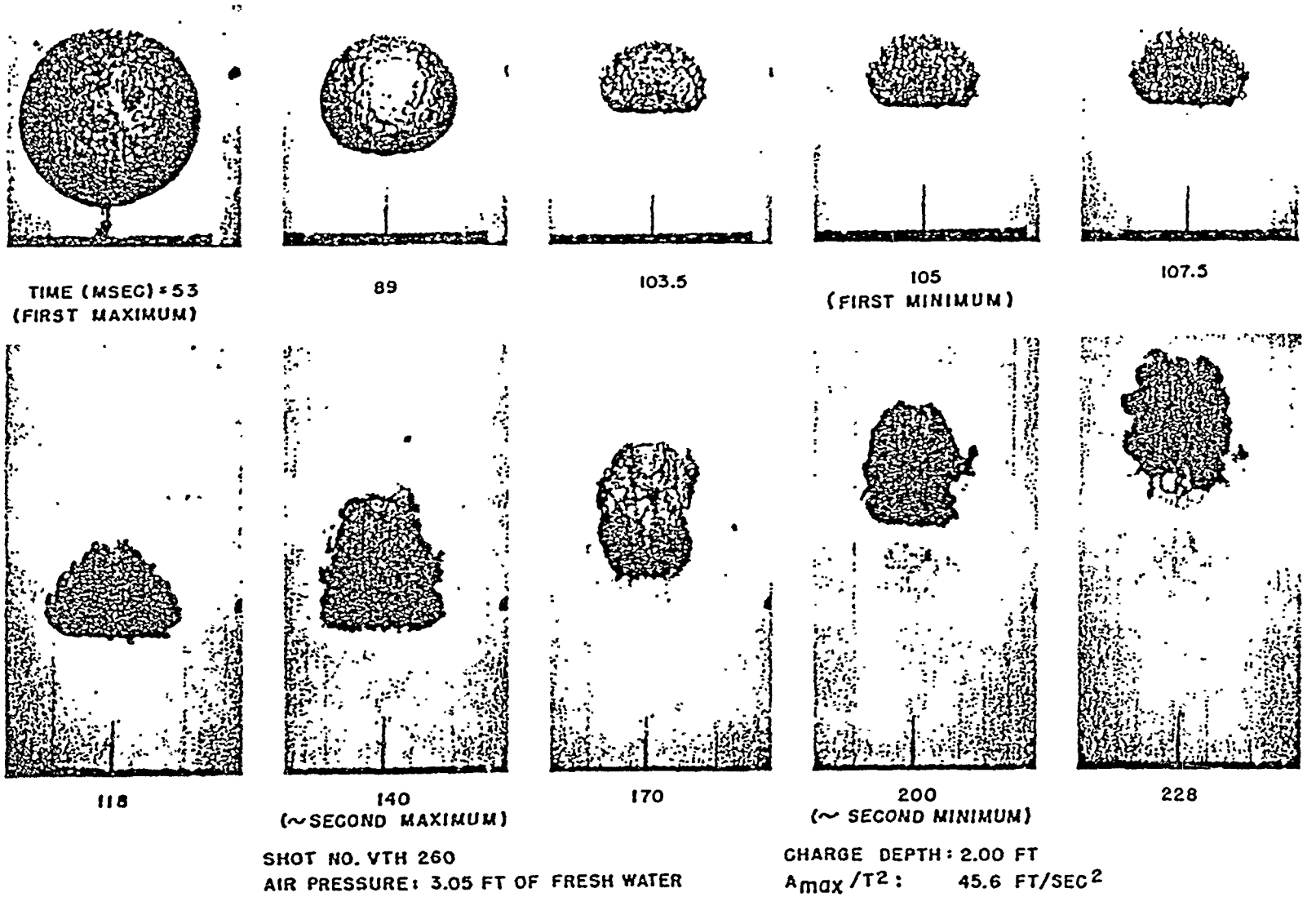

Figure 14. High speed photographs of shot at 100° F. (From ref.17)

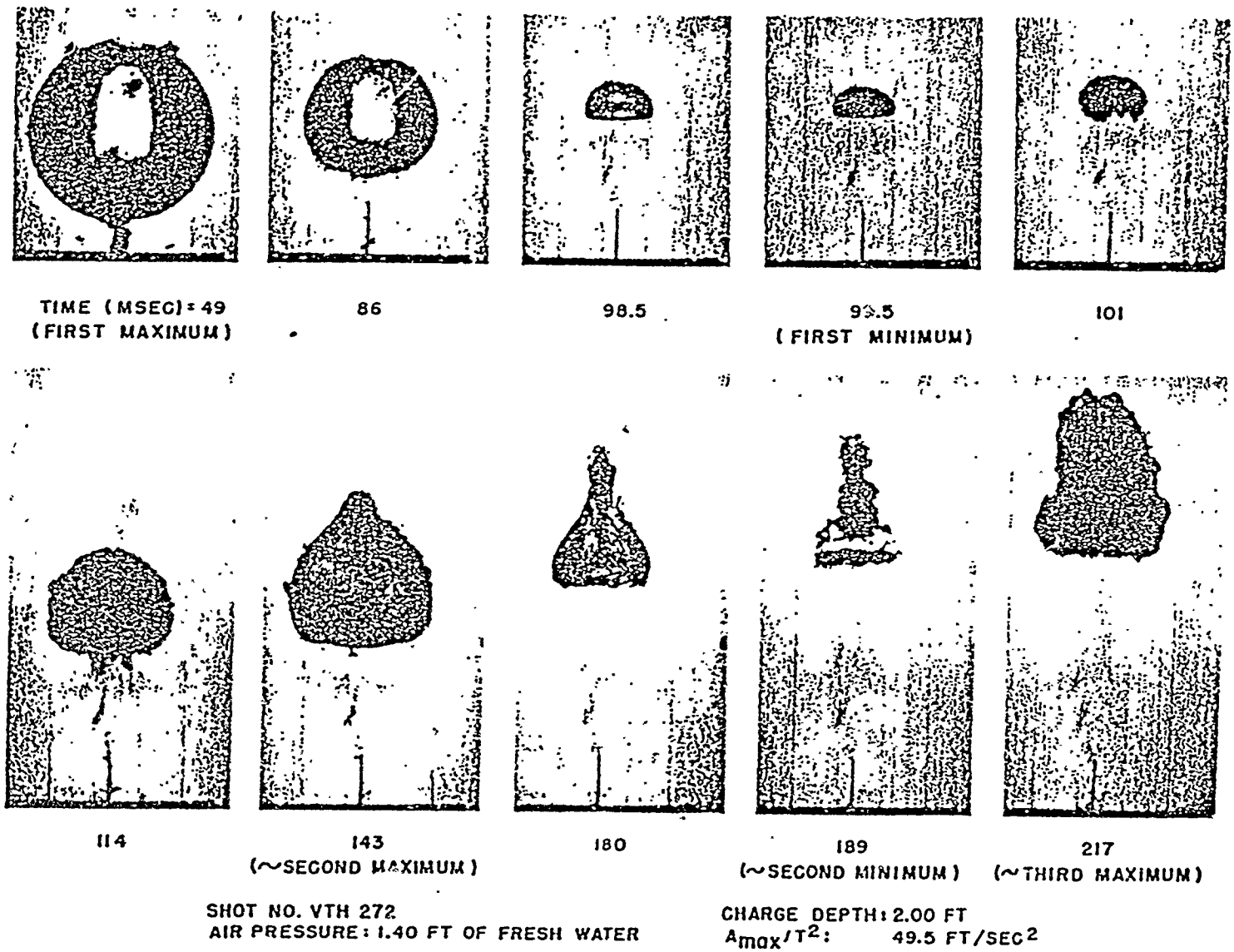

Figure 15. High speed photographs of shot at 36° F. (From ref.17)

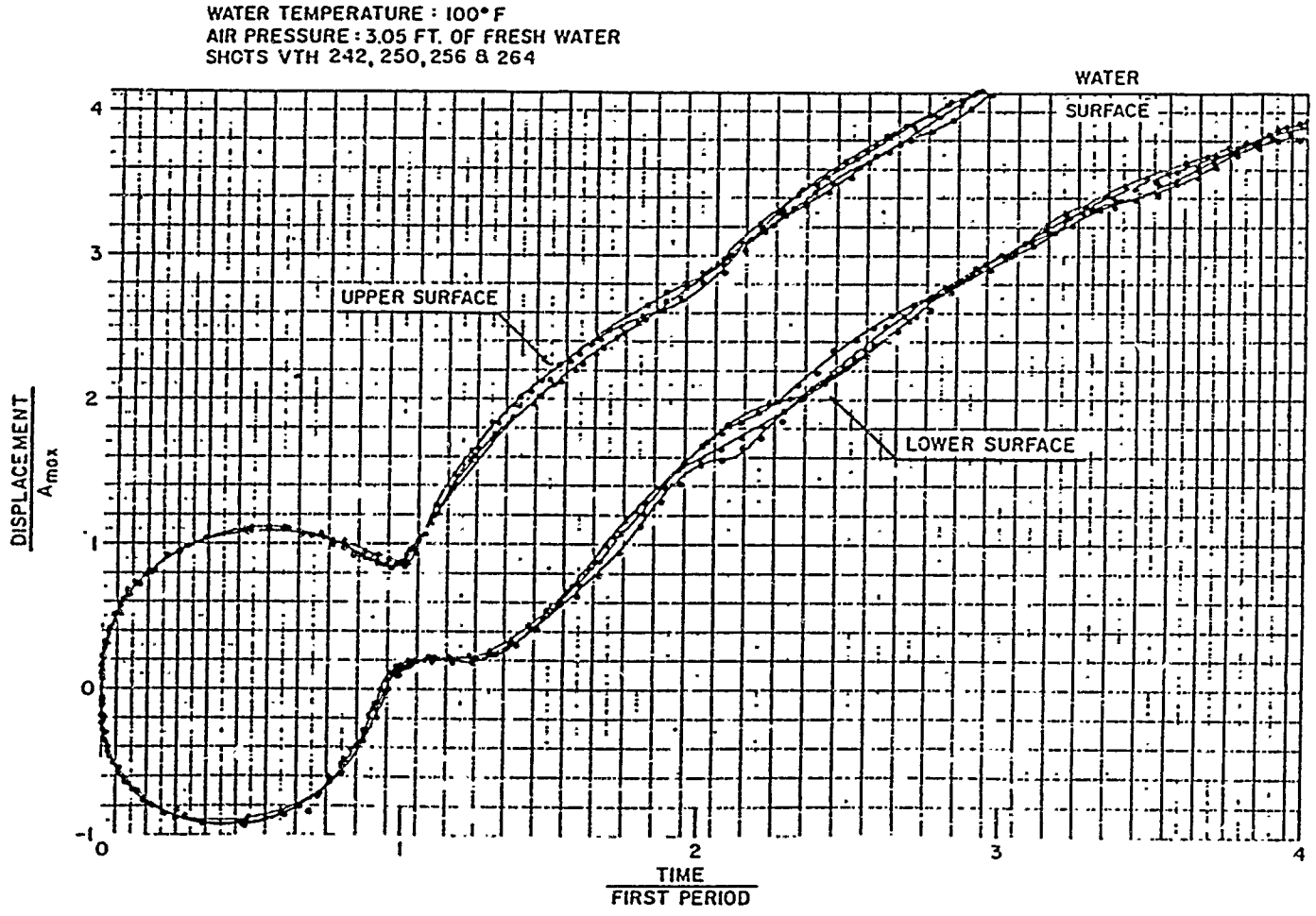

Figure 16. Bubble motion for conditions of Figure 4. (From ref.17)

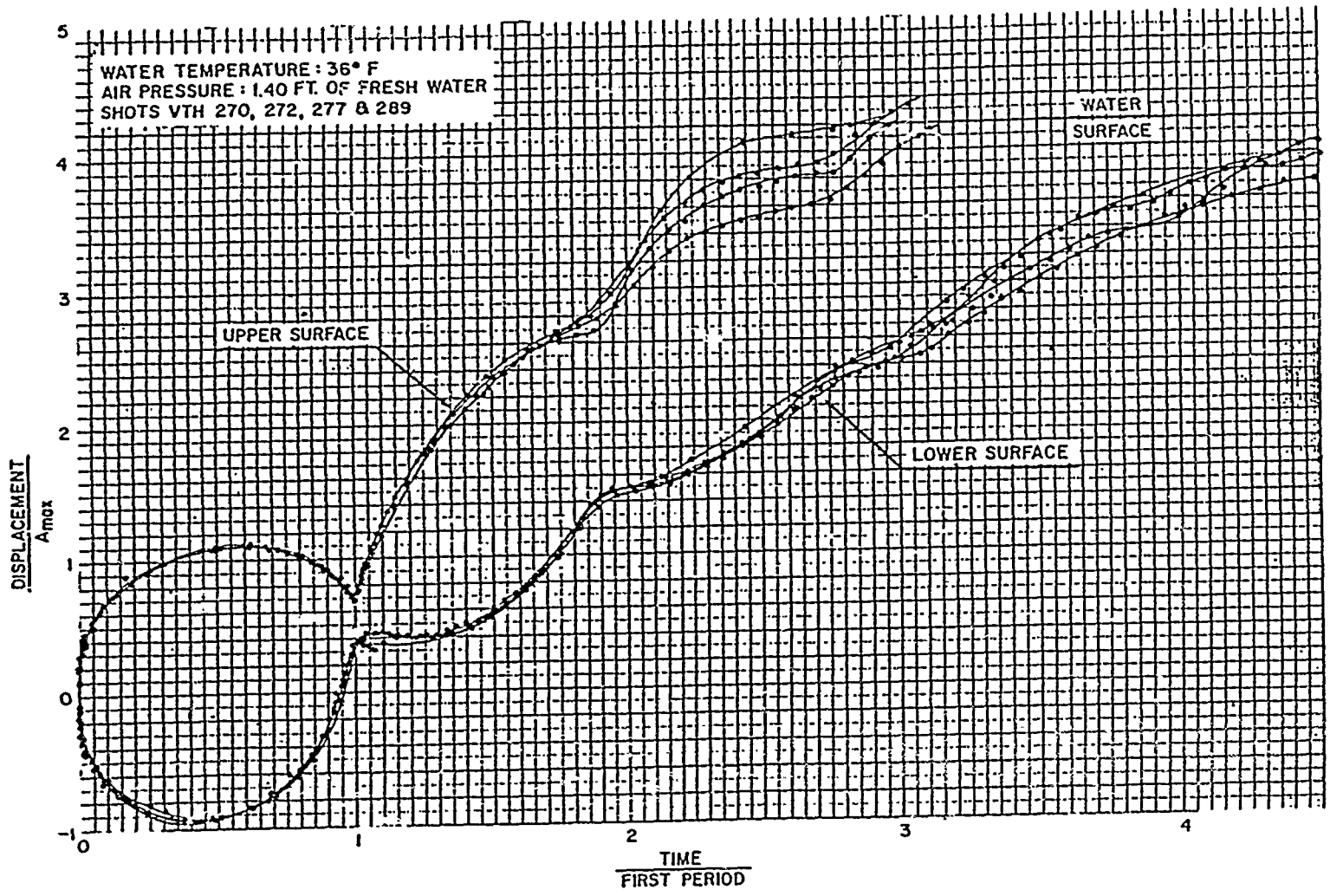

Figure 17. Bubble motion for conditions of Figure 5. (from ref.17)

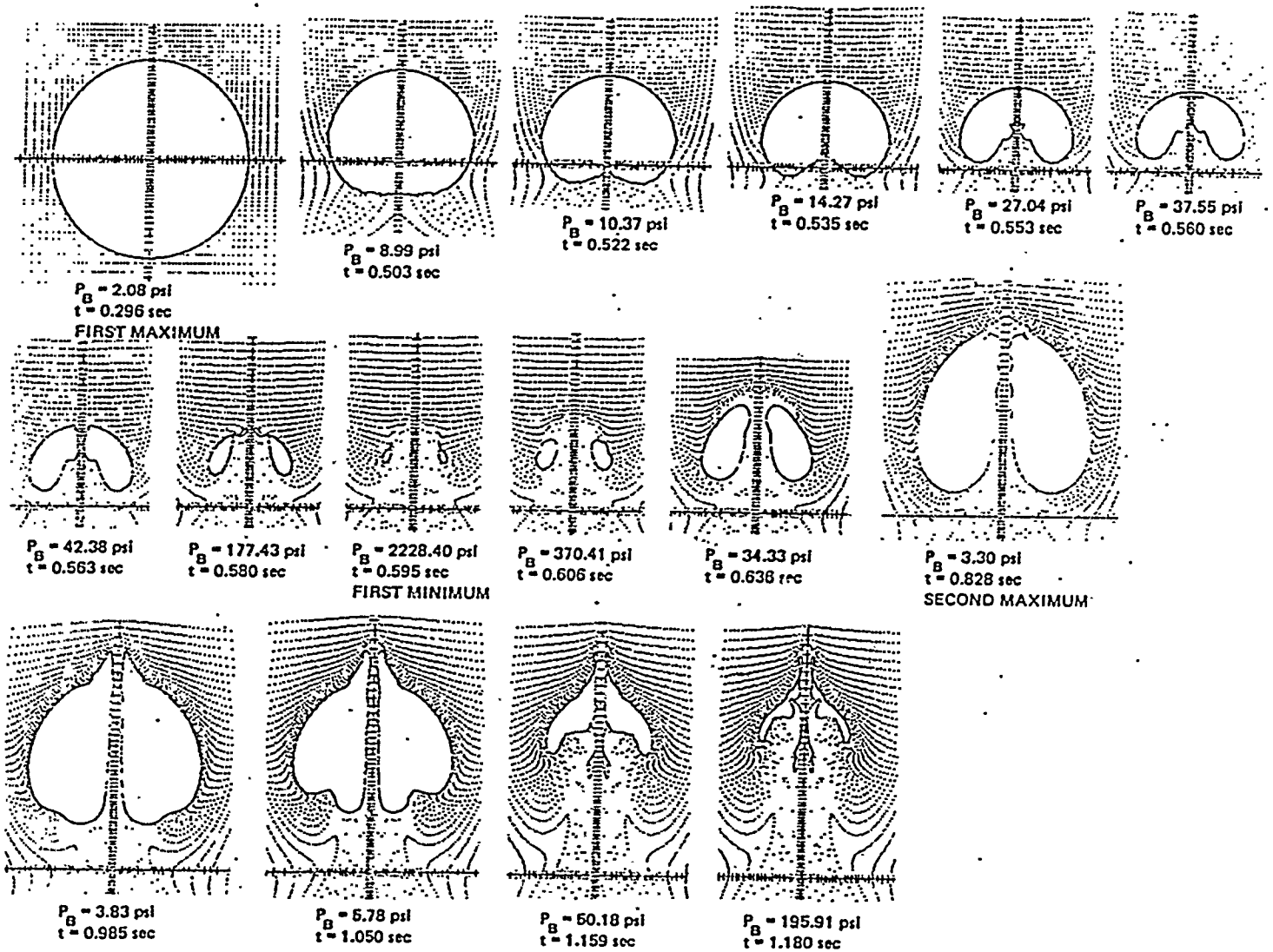

Figure 18. Explosion bubble resulting from detonation of a 354 lb. charge of TNT at a depth of 81 ft. (From ref.18)

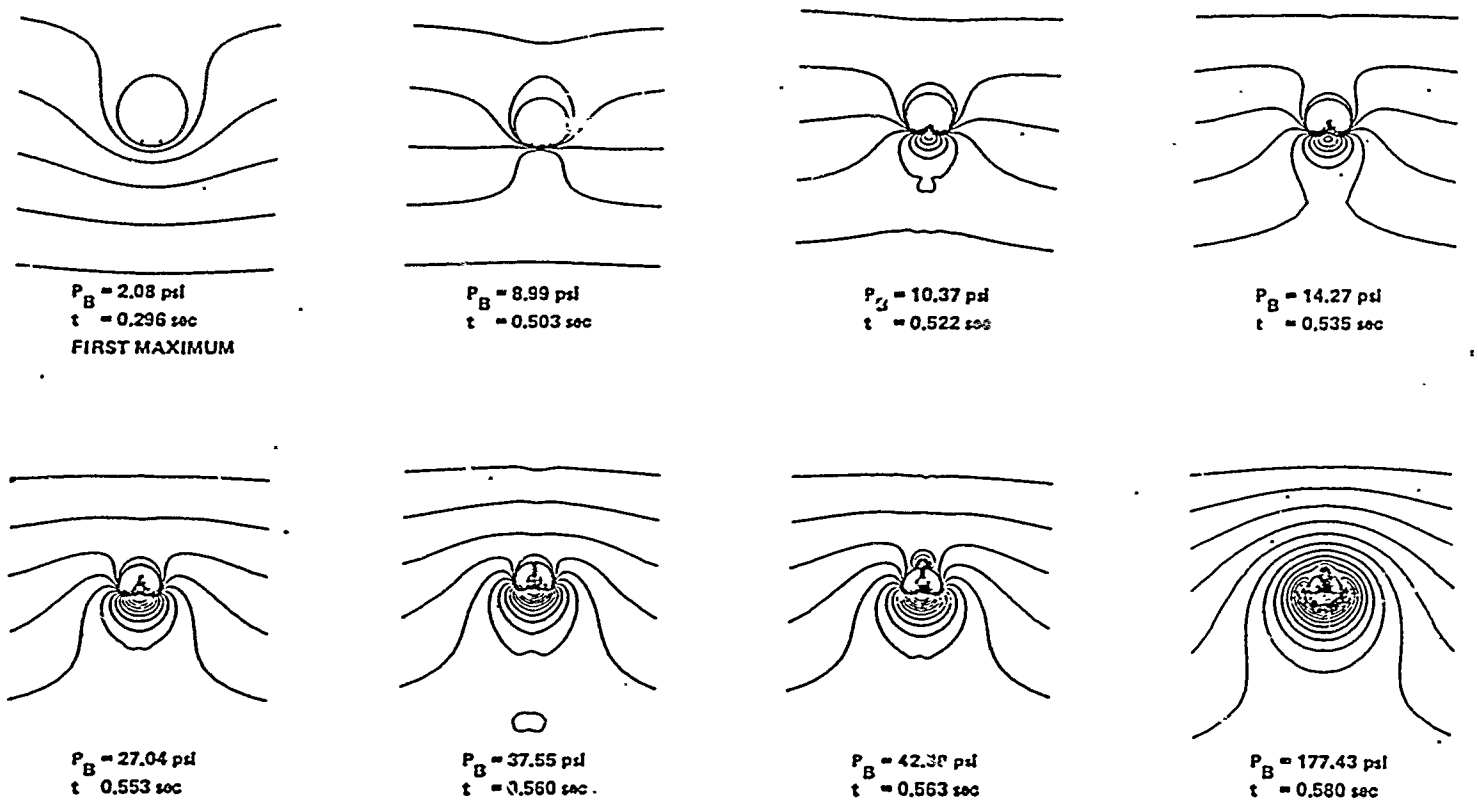

Figure 19. Isobars at 1 atm. intervals from detonation of 354 lb. TNT charge at a depth of 81 ft. (from ref.18)

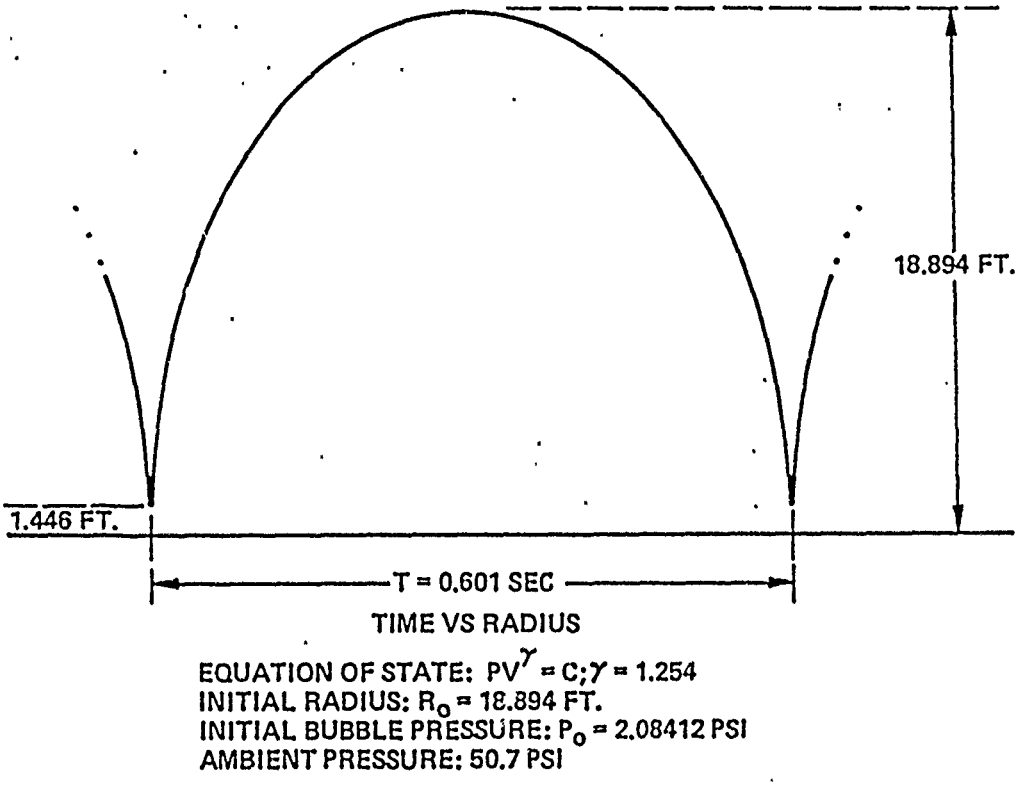

Figure 20. Periodic spherical non-migrating solution for a 354 lb. TNT charge at 81 feet. (From ref.18)

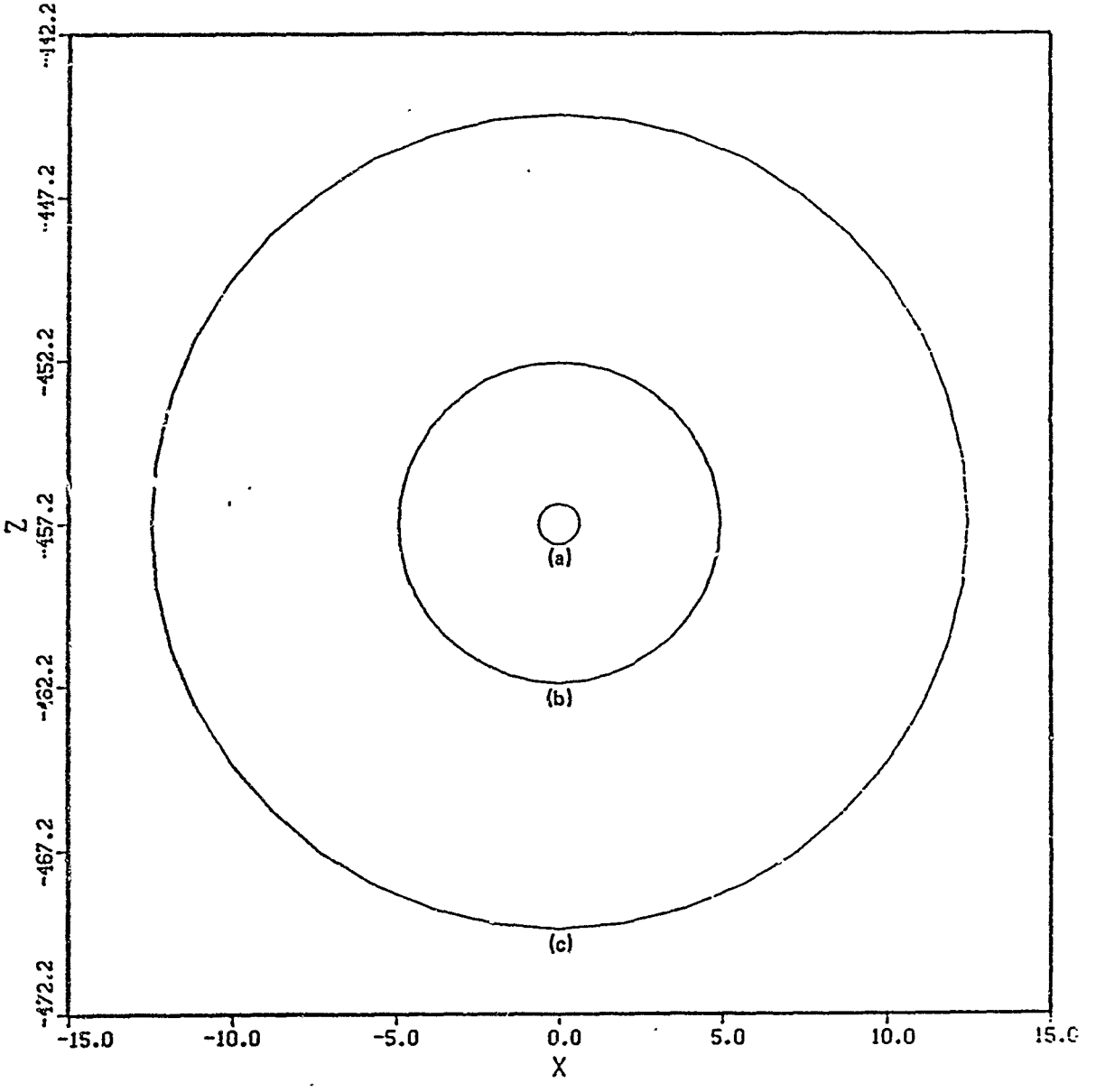

Figure 21. Explosion bubble of eqs. (7.1) and (7.2) at a depth of 457.2 cm with bottom at a depth of 1000 cm. expansion to first maximum. (a) cycle 1,t=0.0 ms; (b) cycle 41,t=0.567 ms; (c) cycle 59,t=9.797 ms. (From ref.22)

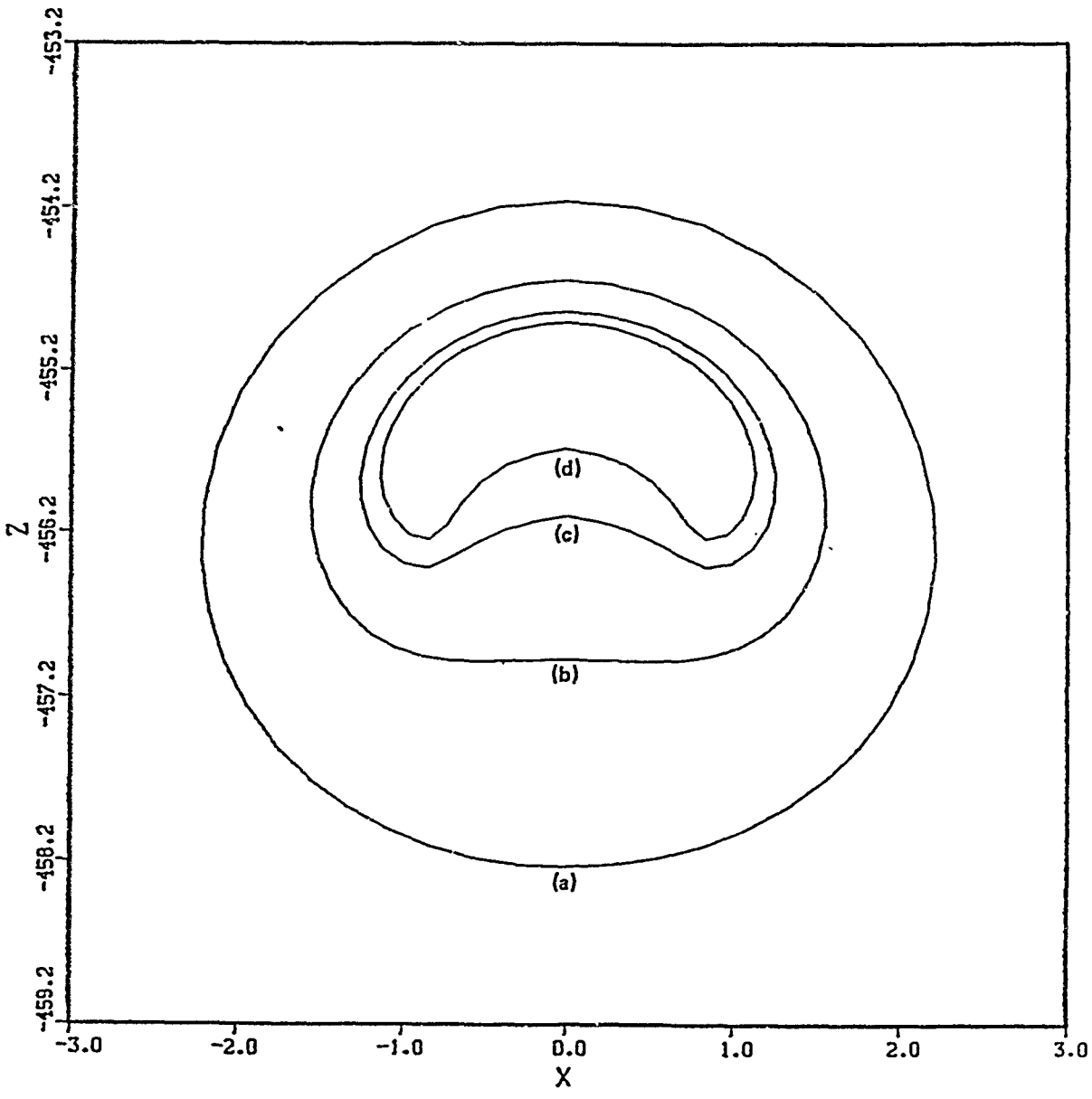

Figure 22. Explosion bubble of figure 21: formation of jet. (a) cycle 86,t=19.2433 ms; (b) cycle 93,t=19.2933 ms; (c) cycle

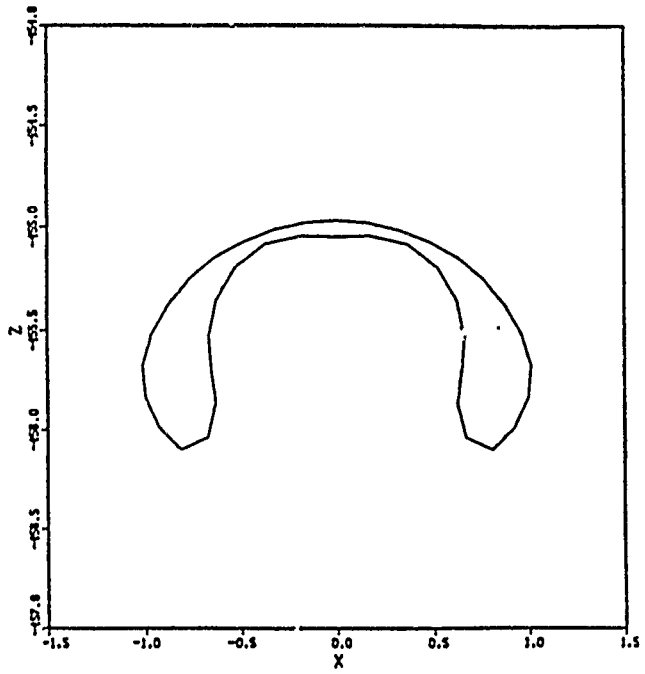

(a) CYCLE 130, t = 19.3299 MS

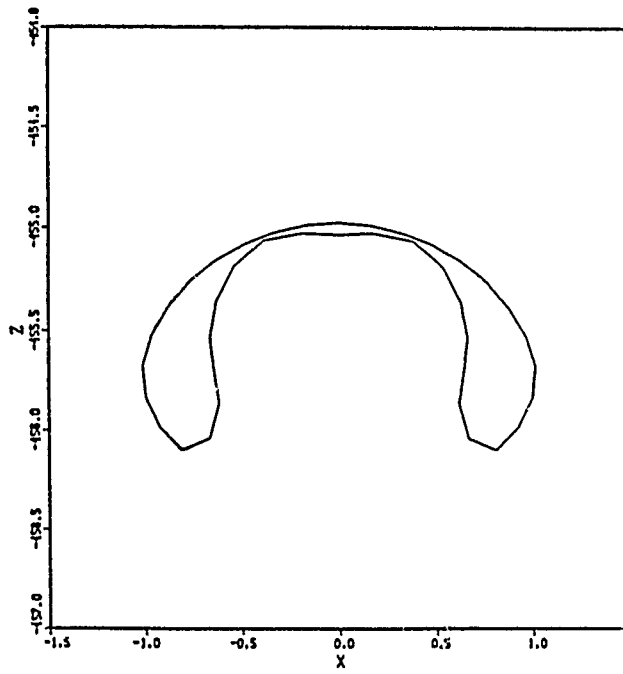

(b) CYCLE 140, t = 19.3301 MS

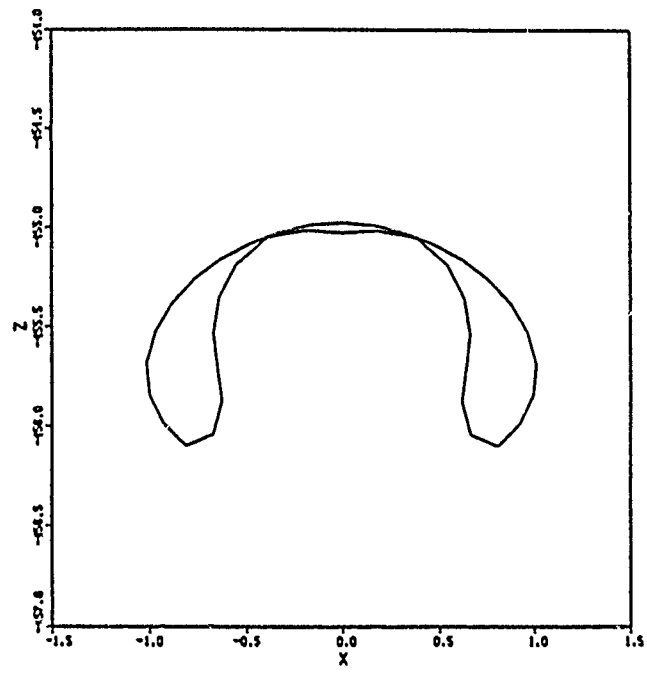

(c) CYCLE 149, t = 19.3302 MS

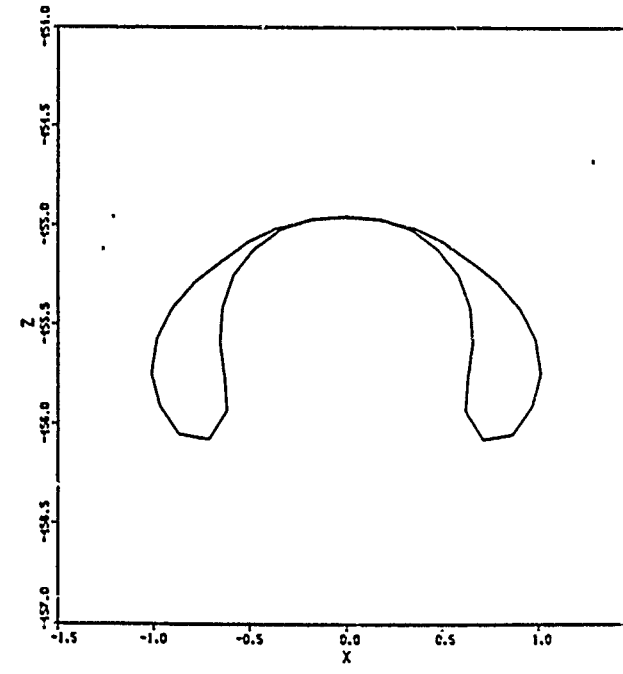

(d) CYCLE 190, t = 19.3304 MS

Figure 23. Explosion bubble of figure 21: contraction toward first minimum (From ref.22)

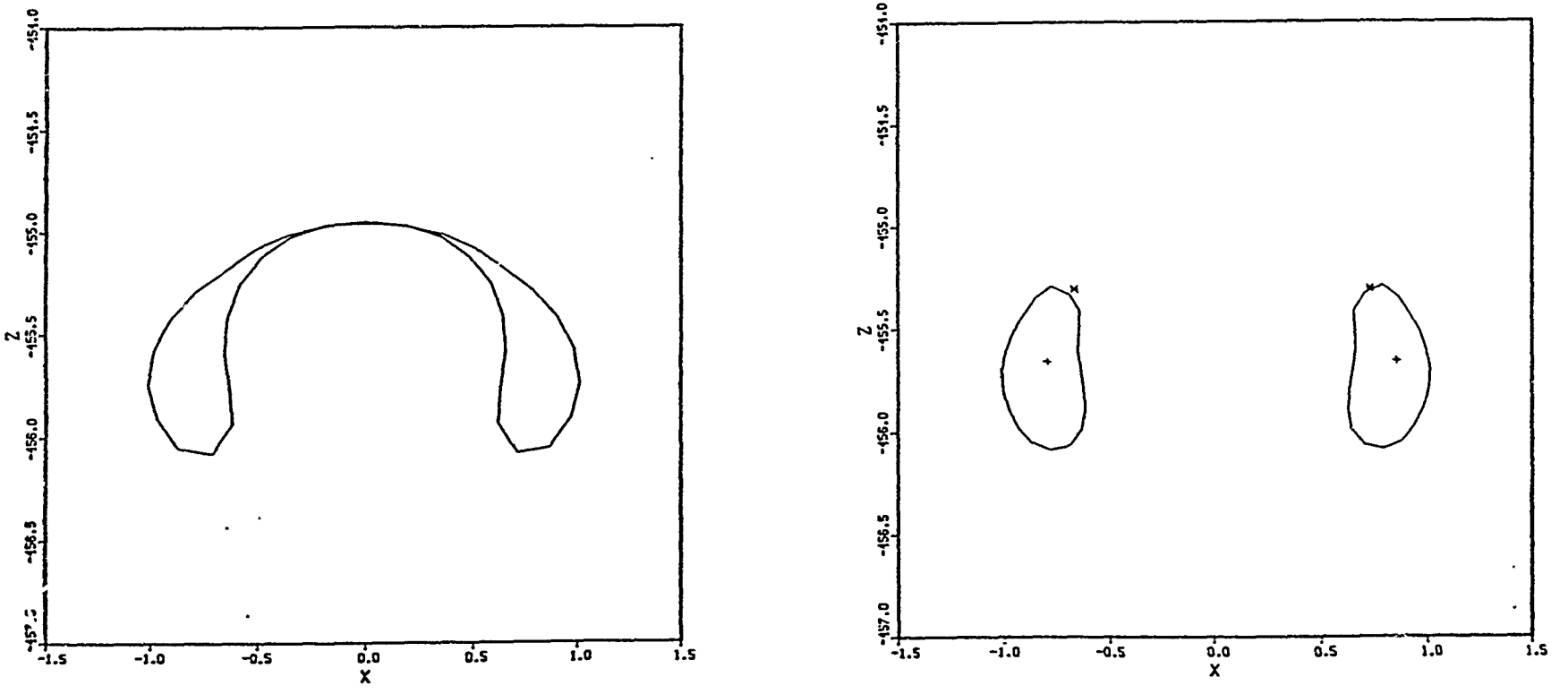

(a) BEFORE TORUS FORMATION

(b) TORUS

Figure 24. Explosion bubble of figure 21: torus formation. Cycle no. 190,t=19.3304 ms (From ref.22)

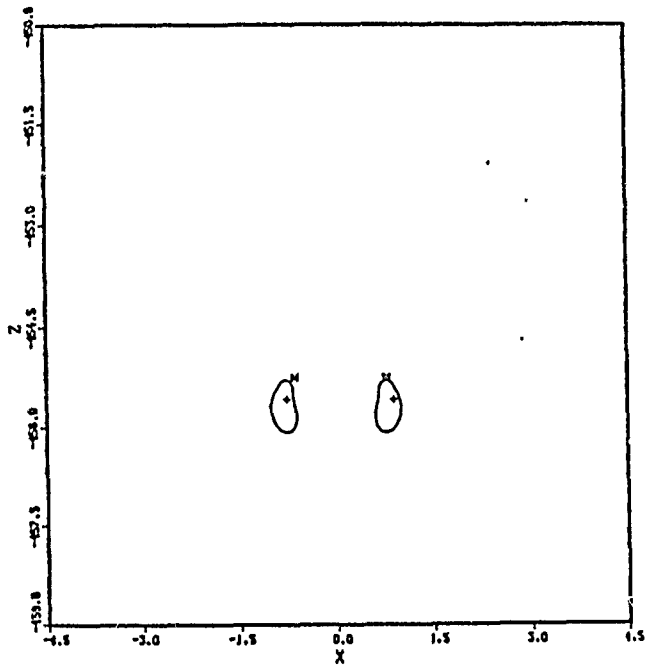

(a) CYCLE 194, t = 19.3311 MS (FIRST MINIMUM)

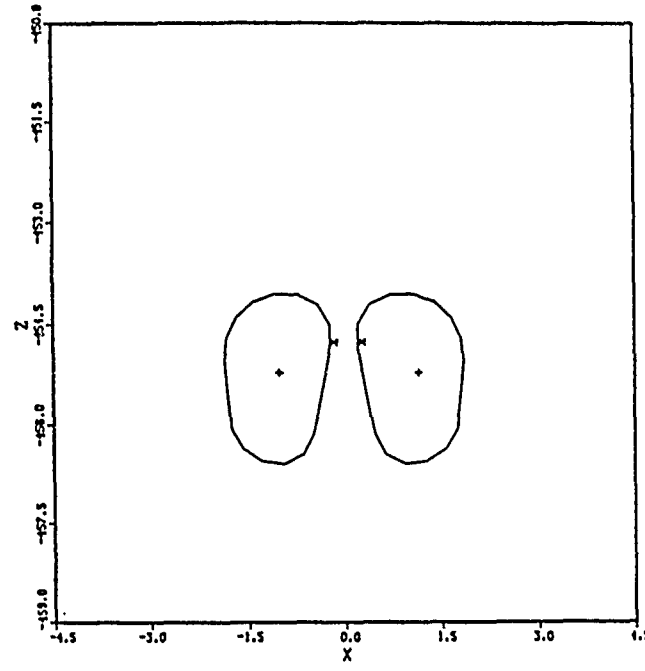

(b) CYCLE 270, t = 19.3852 MS

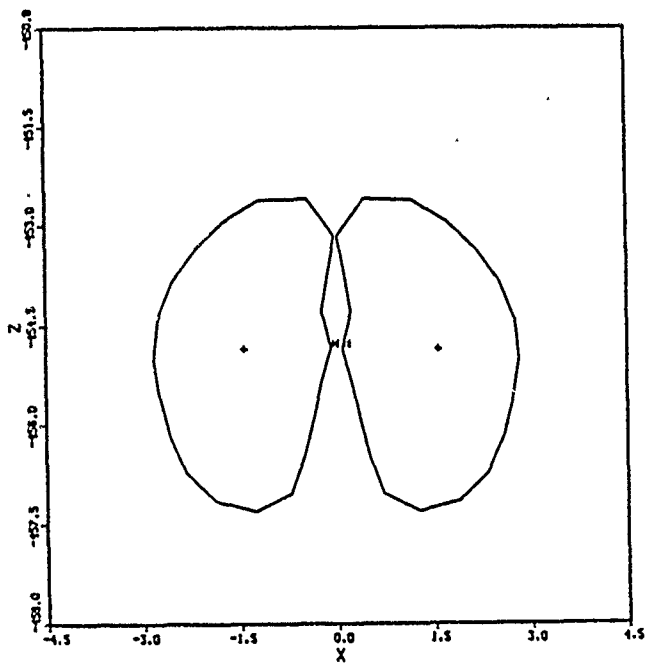

(c) CYCLE 290, t = 19.4772 MS

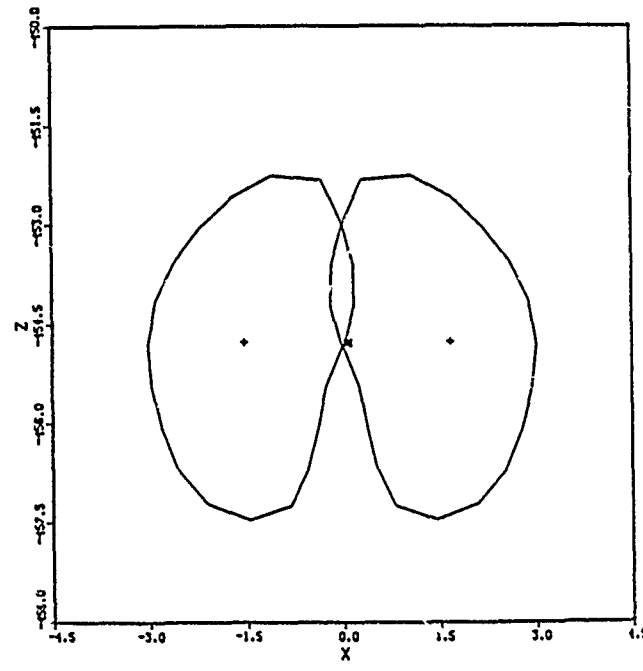

(d) CYCLE 300, t = 19.5027 MS

Figure 25. Explosion bubble of figure 21: expansion after first minimum (From ref.22)

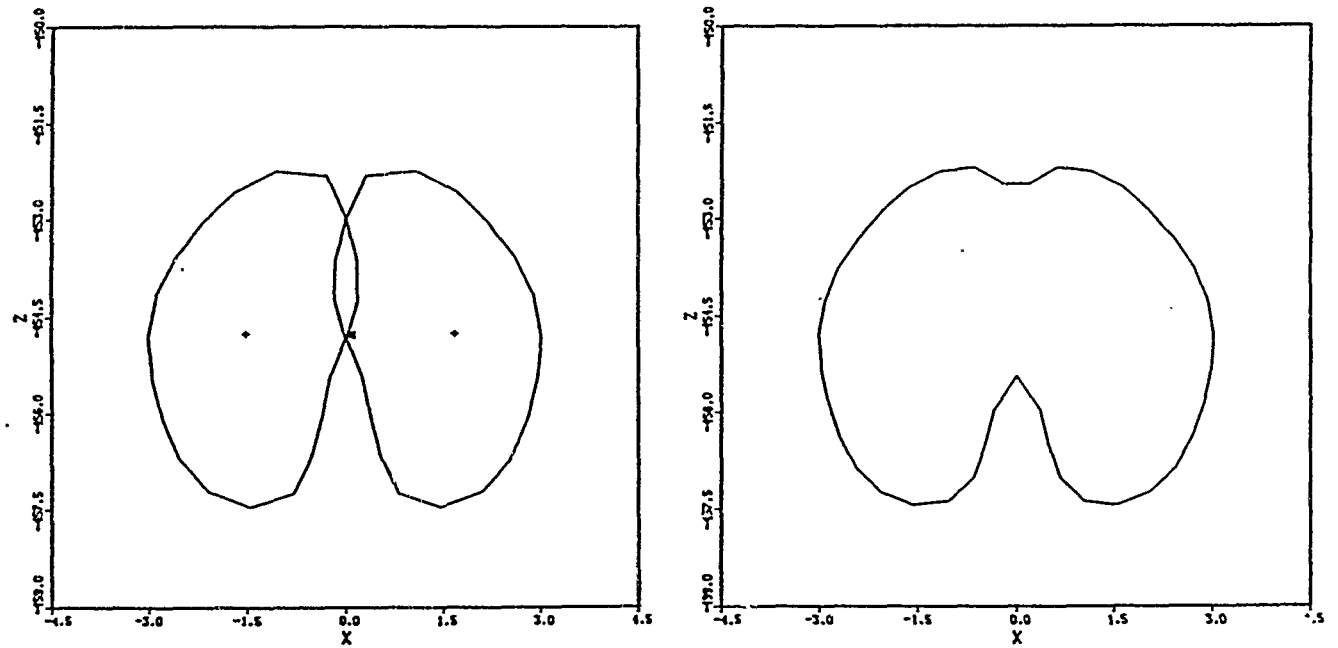

(a) BEFORE CLOSURE

(b) AFTER CLOSURE

Figure 26. Explosion bubble of figure 21: torus closure. cycle no. 300,t=19.5027 ms (From ref.22)

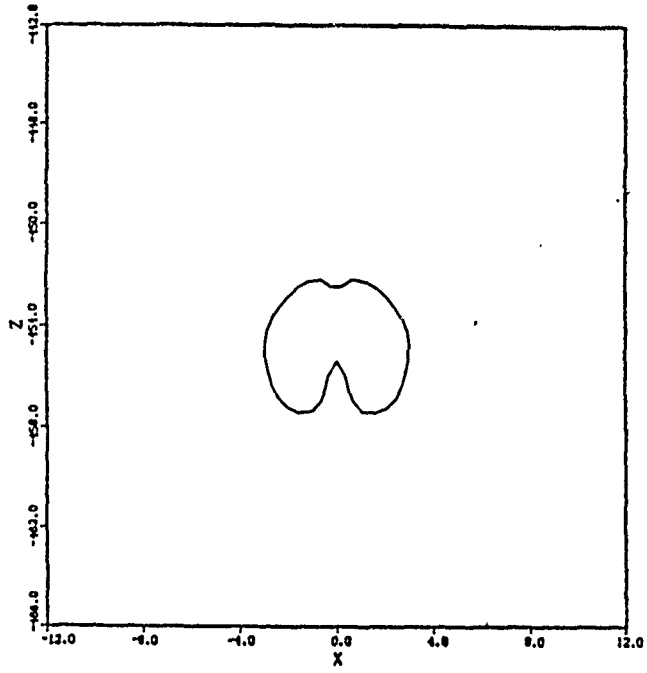

(a) CYCLE 300, t = 19.5027 MS

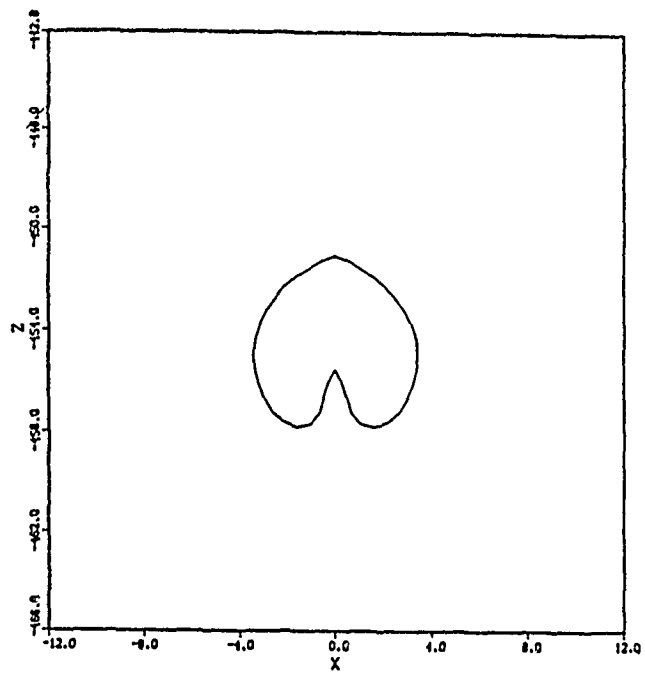

(b) CYCLE 310, t = 19.5648 MS

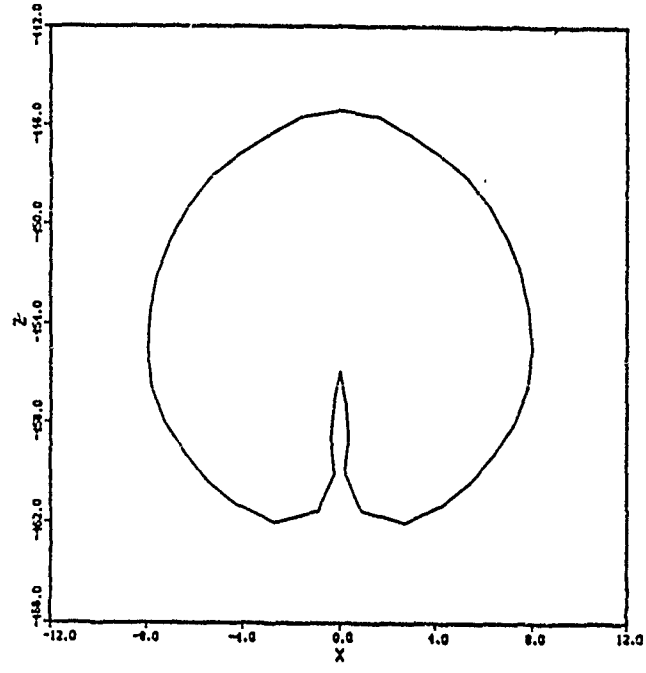

(c) CYCLE 340, t = 21.2258 MS

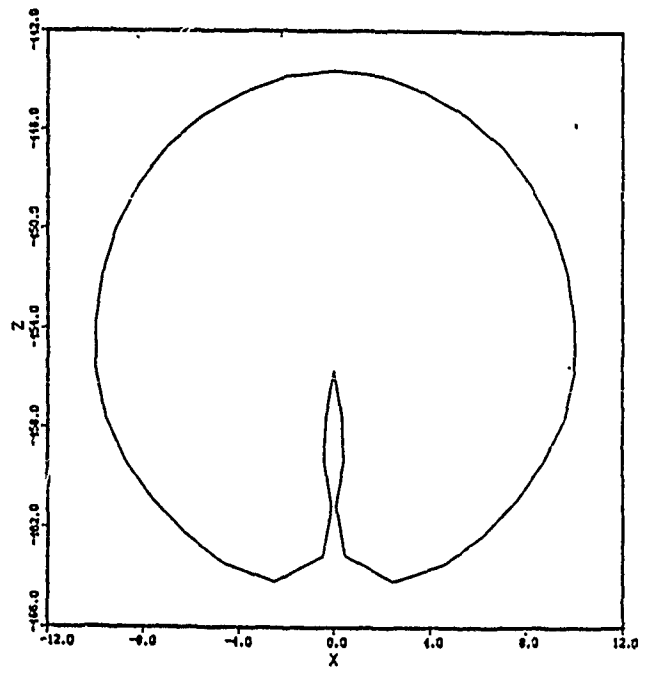

(d) CYCLE 350, t = 22.9283 MS

Figure 27. Explosion bubble of figure 21: expansion after torus closure (From ref.22)

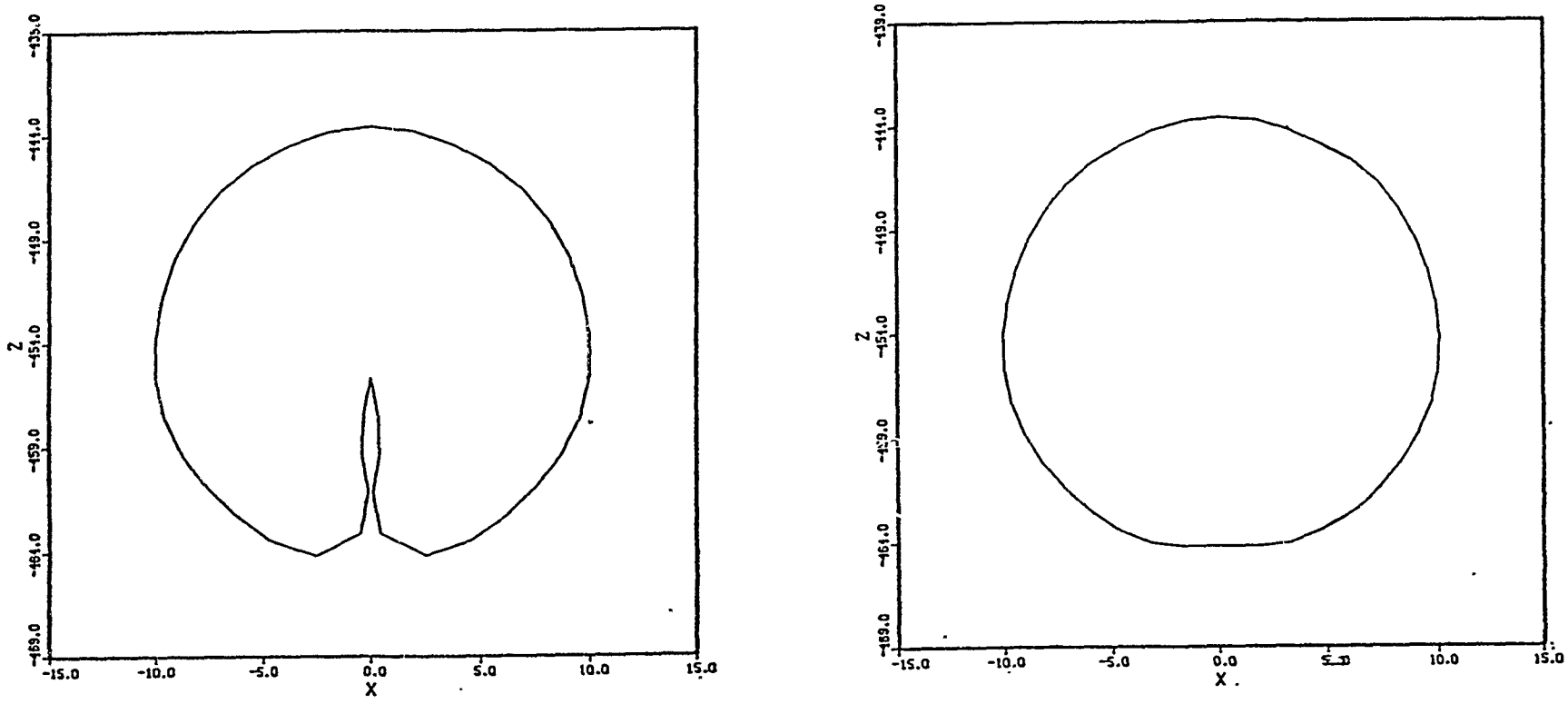

Figure 28. Explosion bubble of figure 21: second closure. cycle no. 350,t=22.9283 ms (From ref.22)

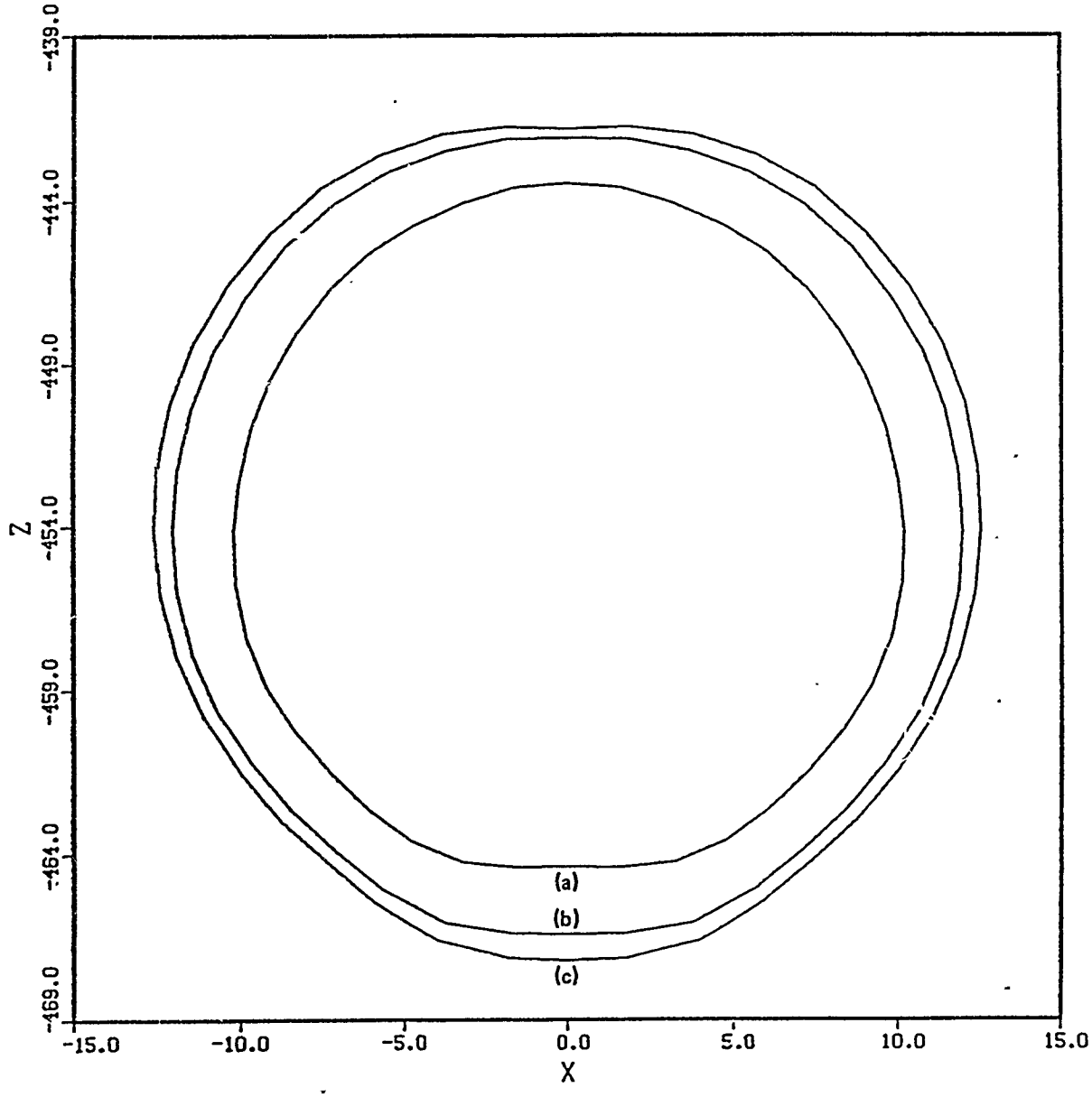

Figure 29. Explosion bubble of figure 21: expansion to second maximum after second closure. (a) cycle 351,t=23.1366 ms; (b)cycle 356,t=26.0828 ms; (c) cycle 361,t=29.2606 ms (second maximum) (From ref 22)

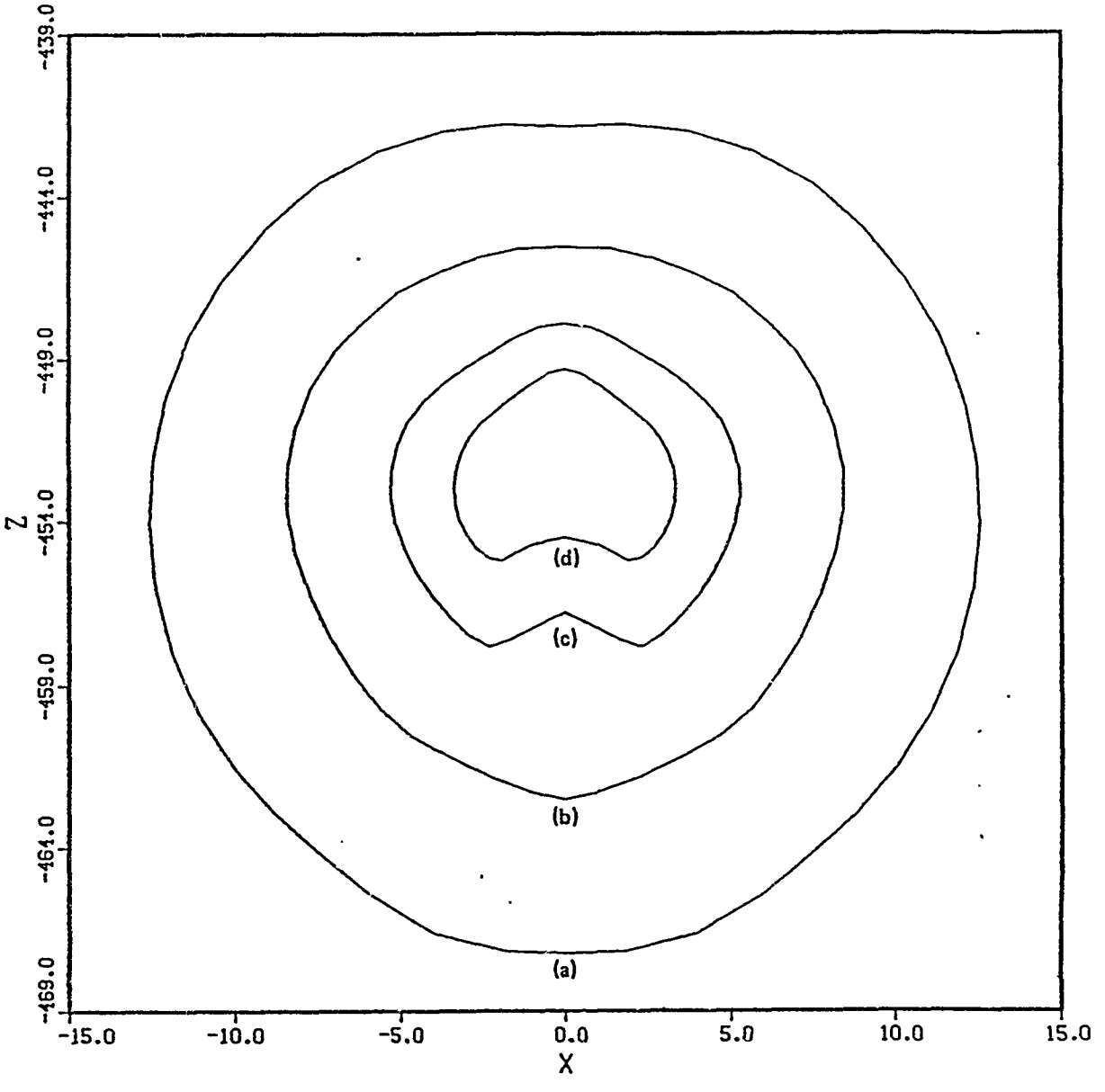

Figure 30. Explosion bubble of figure 21: contraction after second maximum. (a) cycle 361,t=29.2606 ms; (b) cycle 375, t=36.8694 ms; (c) cycle 389,t=38.3310 ms; (d) cycle 399,t=38.7416 ms (From ref.22)

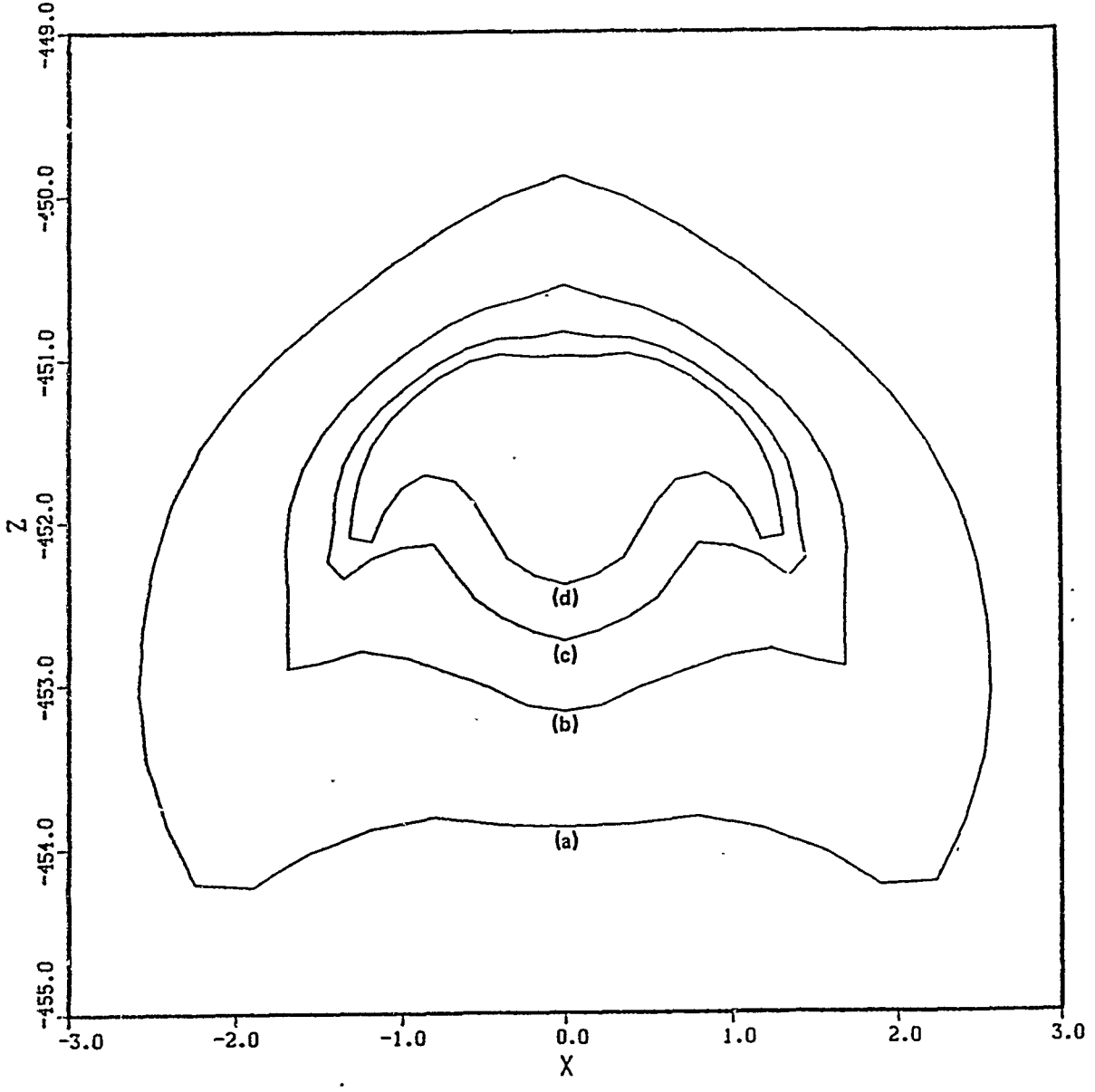

Figure 31. Explosion bubble of figure 21: contraction toward second minimum. (a) cycle 405,t=38.8233 ms; (b) cycle 425, t=38.9022 ms; (c) cycle 445,t=38.9216 ms; (d) cycle 459,t=38.9309 ms (From ref.22)

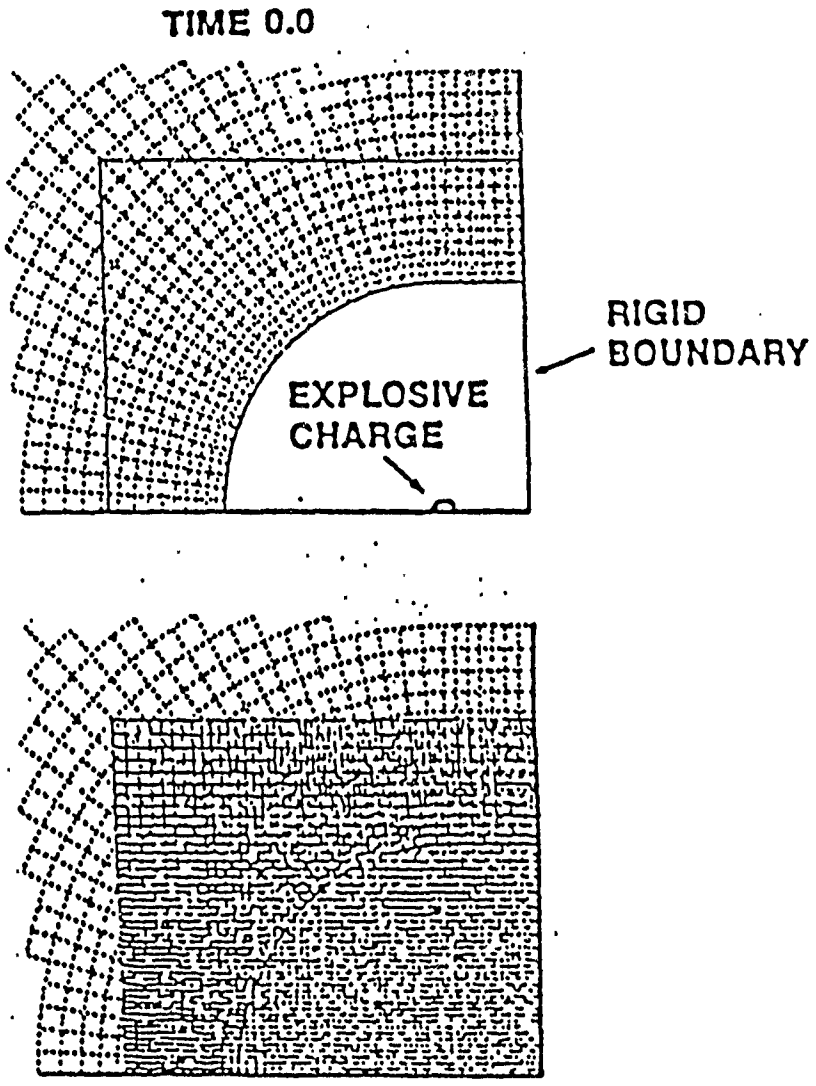

Figure 32. Coupled Euler-Lagrange grids for two dimensional calculation of underwater asymmetric explosion. (From ref.23)

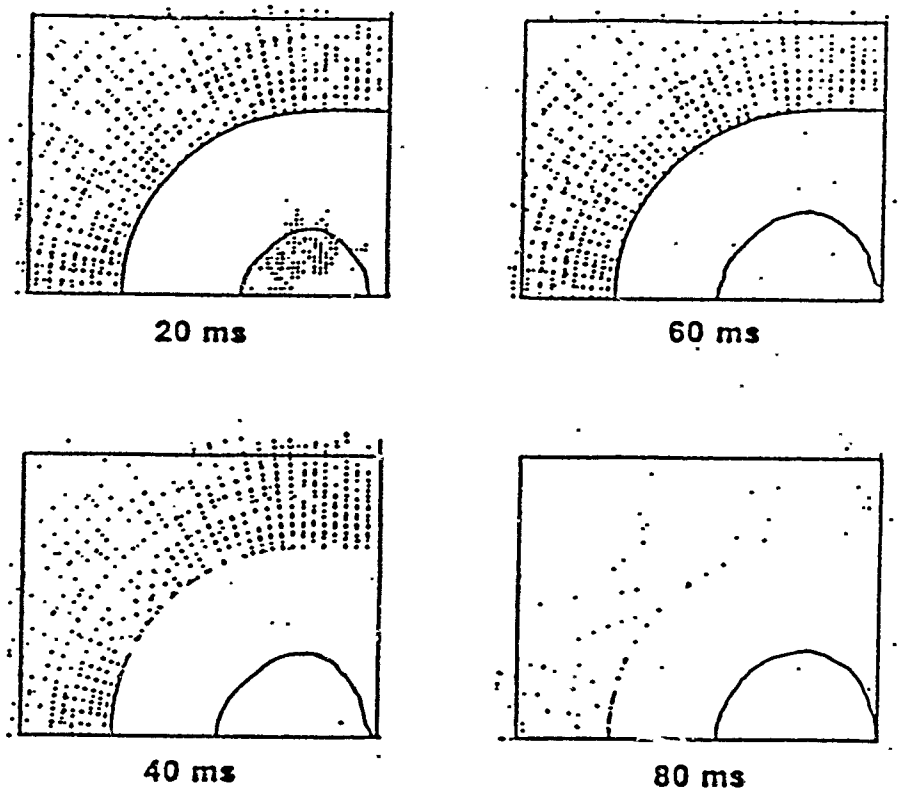

Figure 33. Growth of explosion bubble adjacent to rigid wall. (From ref.23)

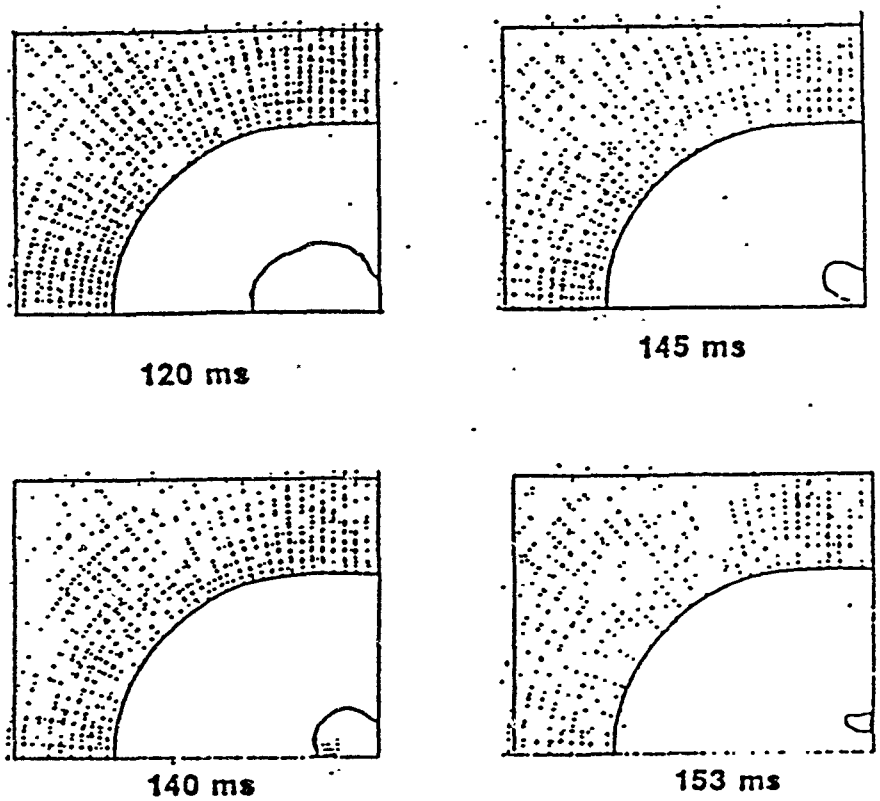

Figure 34. Collapse of explosion bubble adjacent to rigid wall. (From ref.23)

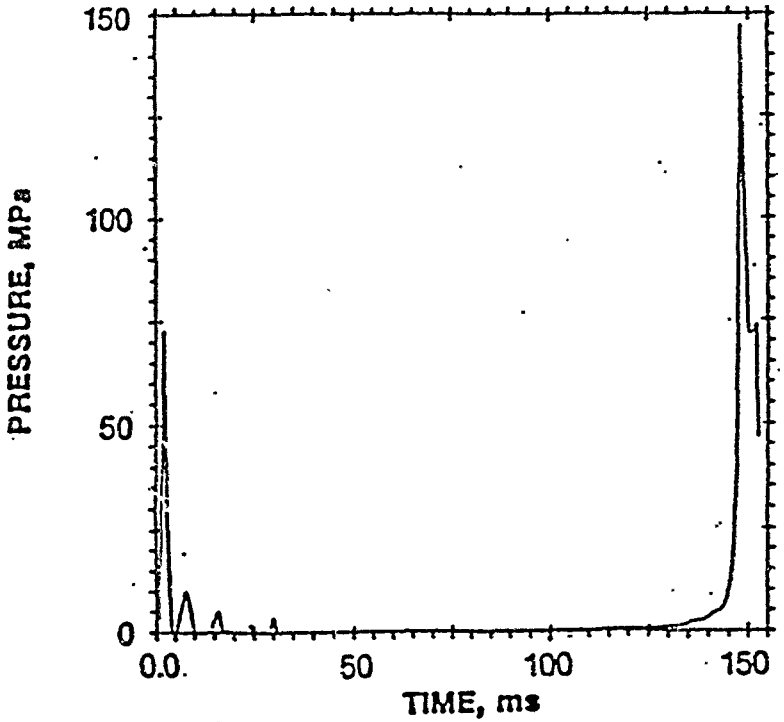

Figure 35. Pressure history at center of rigid wall. (From ref.23)

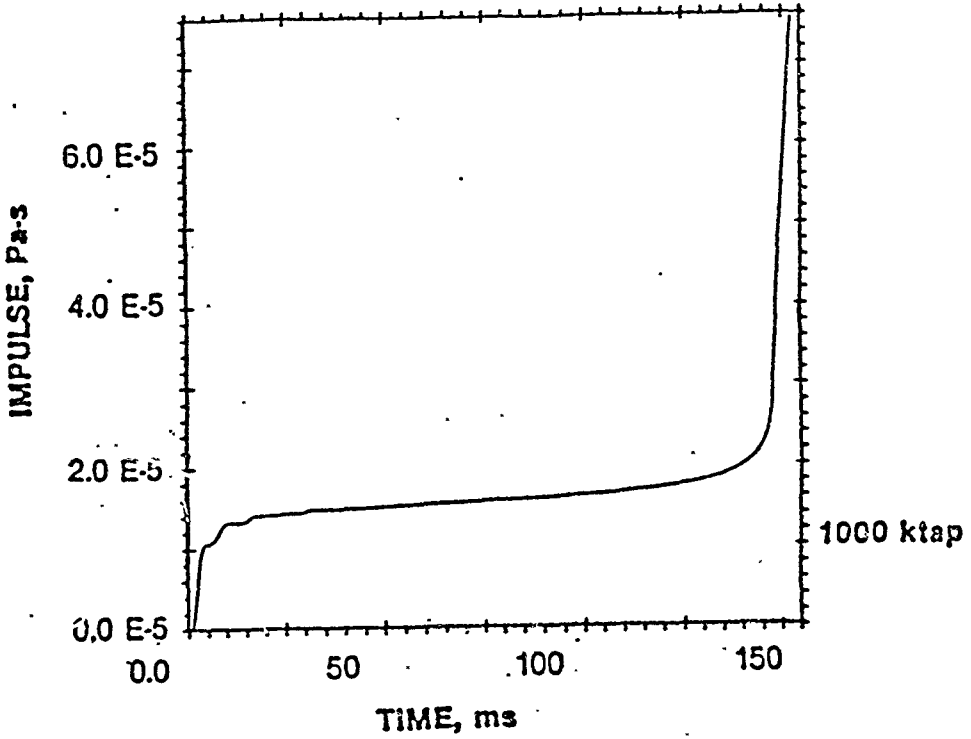

Figure 36. Impulse loading at center of rigid wall. (From ref.23)

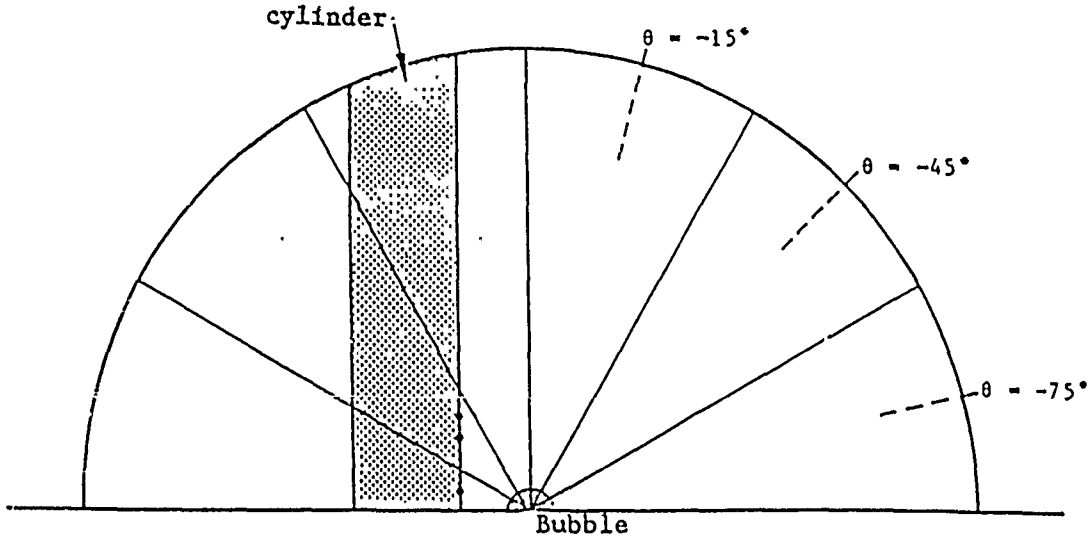

(a) Top view

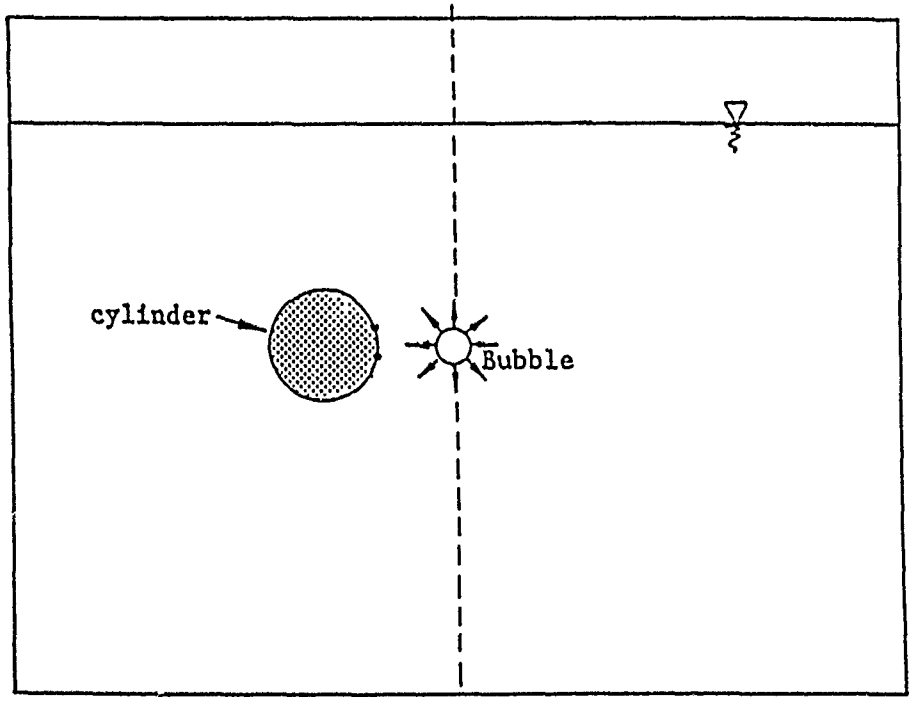

(b) Side view (vertical plane through center of bubble and perpendicular to the cylinder)

Figure 37. Location of cylinder. (From ref.24)

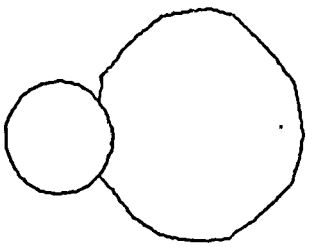

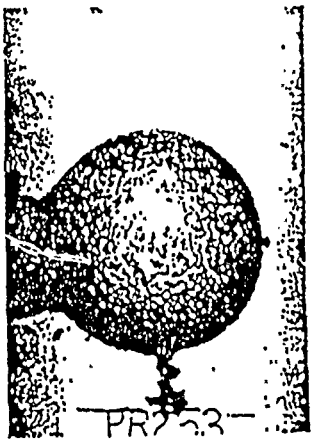

43
(FIRST MAXIMUM)

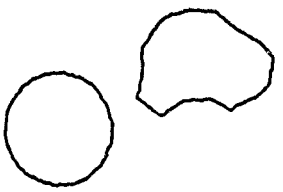

92
(FIRST MINIMUM)

Figure 38. Comparison of bubble shapes at the first maximum the first minimum (Shot n. 7) (From ref.24)

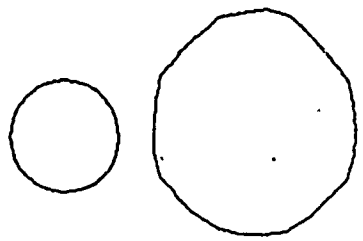

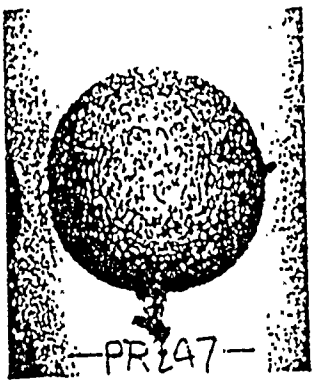

38.5
(FIRST MAXIMUM)

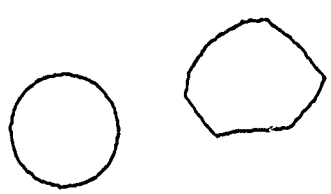

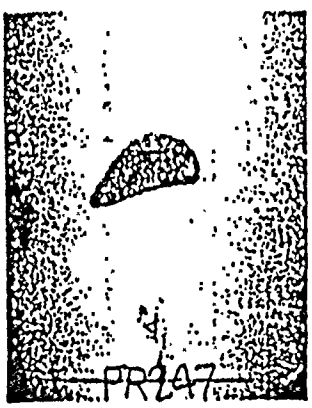

91
(FIRST MINIMUM)

Figure 39. Comparison of bubble shapes at the first maximum and the first minimum (Shot no. 8) (From ref.24)

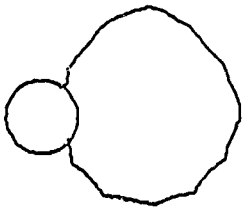

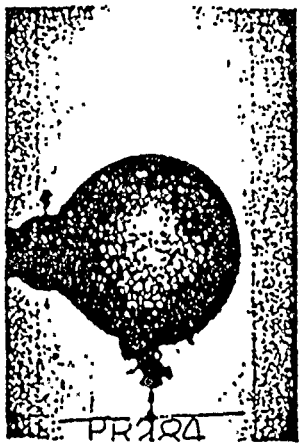

25
(FIRST MAXIMUM)

52
(FIRST MINIMUM)

Figure 40. Comparison of bubble shapes at the first maximum and the first minimum (Shot no. 9) (From ref.24)

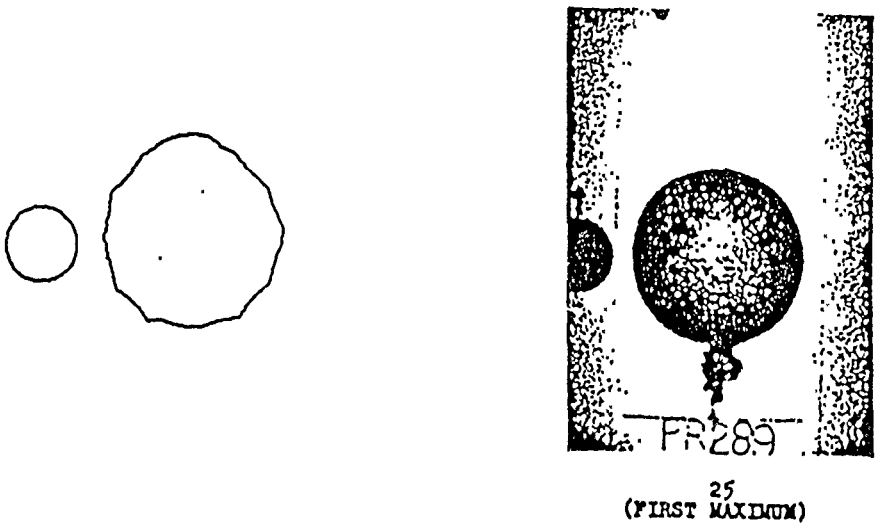

Figure 41. Comparison of bubble shapes at the first maximum and the first minimum (Shot no. 10) (From ref.24)

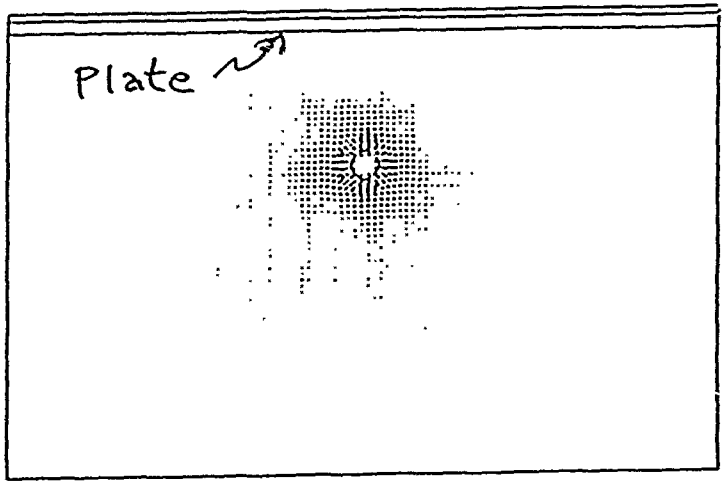

Time = 0.1 ms, ICYC = 10

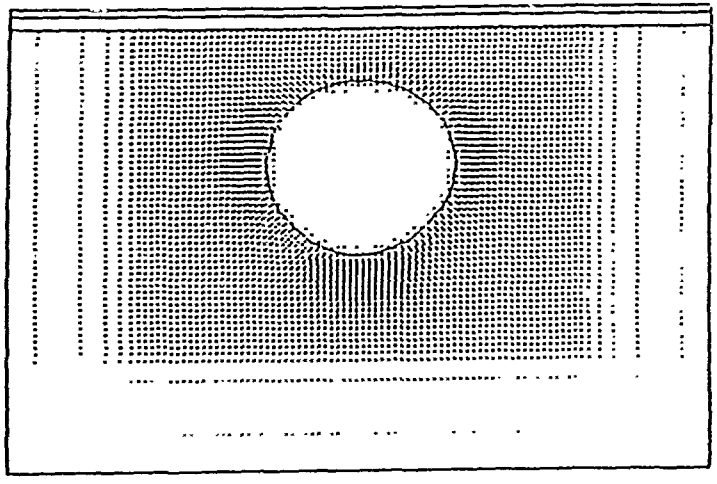

Time = 11.3 ms, ICYC = 45

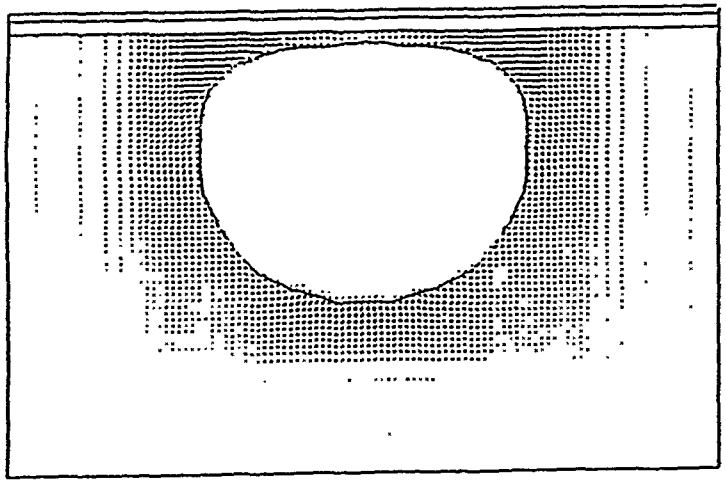

Time = 73.5 ms, ICYC = 80

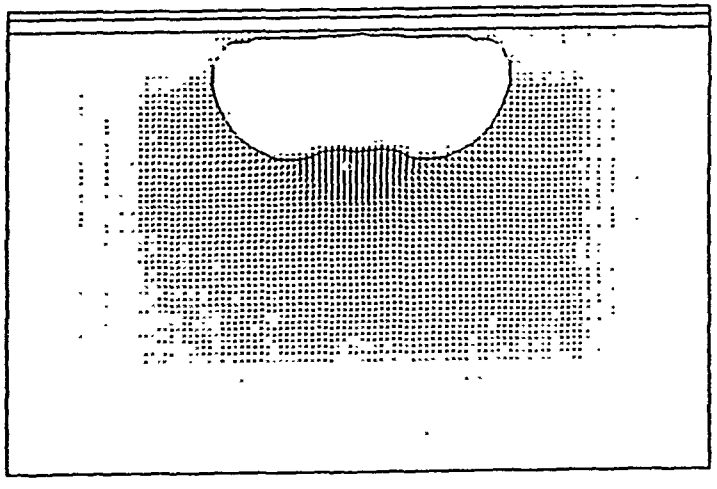

Time = 141.7 ms, ICYC = 120

Figure 42. Evolution of the bubble and the velocity field as a sequence of snapshots, Case A. (From ref.24)

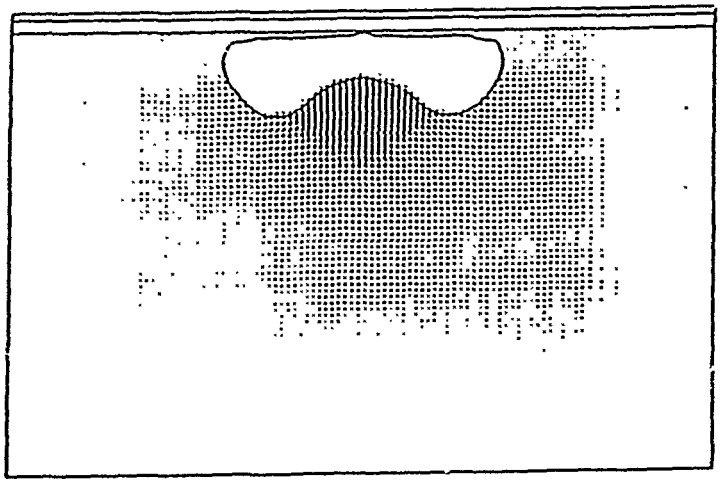

Time = 154.2 ms, ICYC = 135

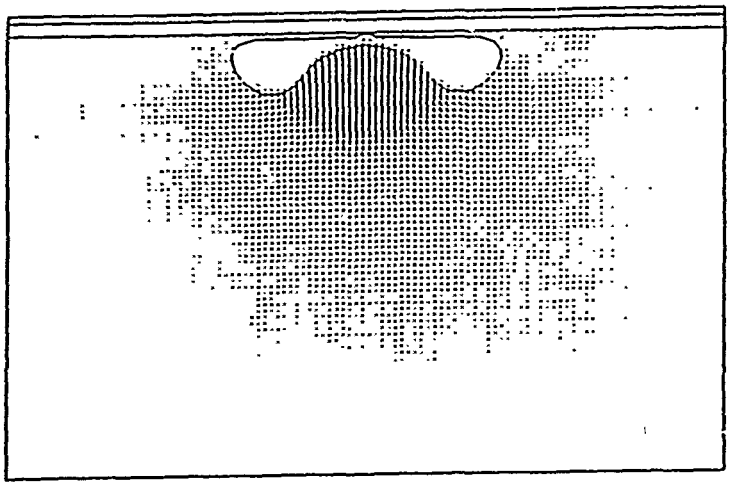

Time = 160.6 ms, ICYC = 145

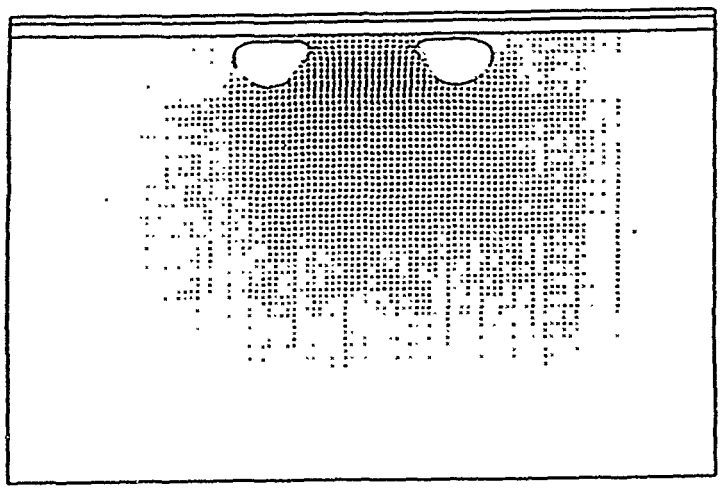

Time = 163.1 ms, ICYC = 150

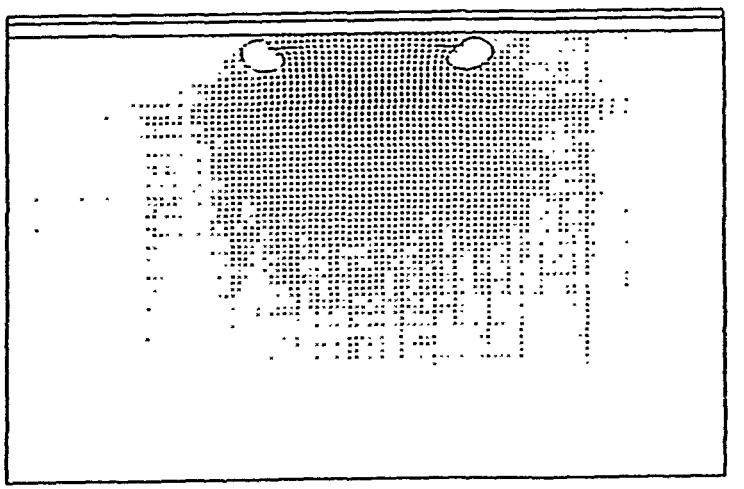

Time = 166.7 ms, ICYC = 160

Figure 42. (cont'd)

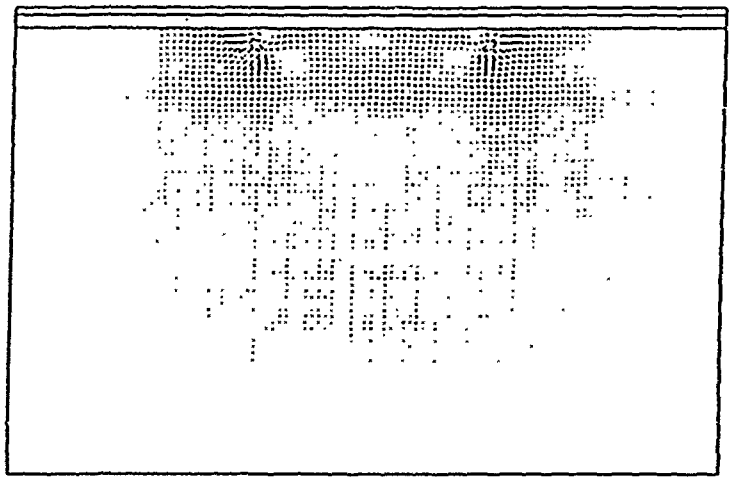

Time = 170.3 ms, ICYC = 190

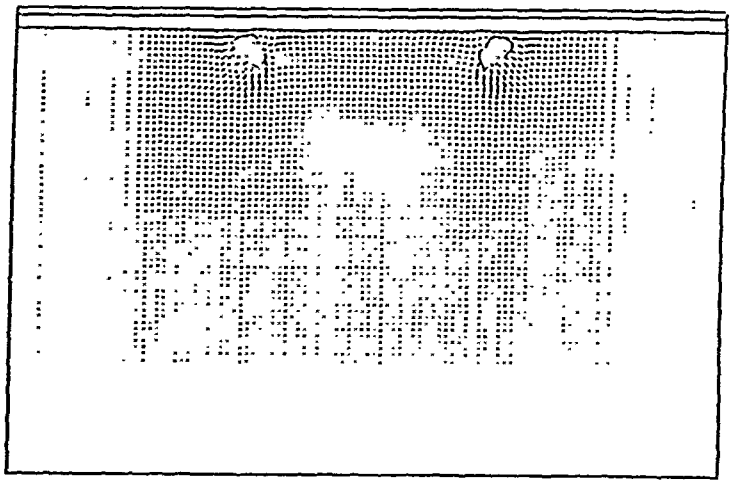

Time = 172.0 ms, ICYC = 200

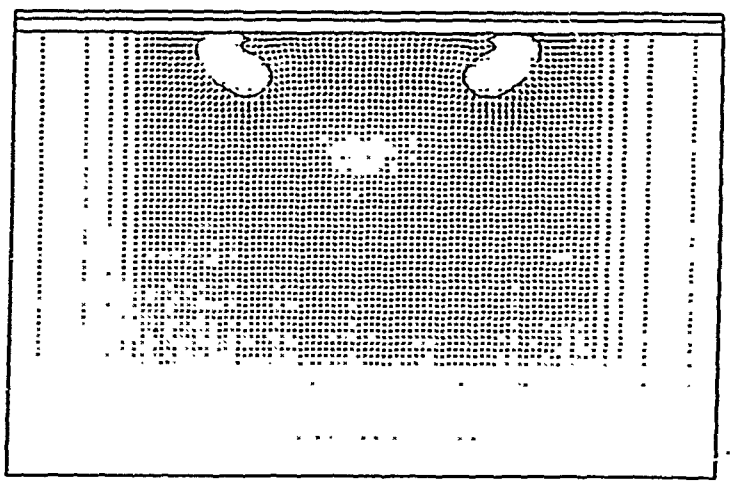

Time = 178.8 ms, ICYC = 210

Figure 42. (cont'd)

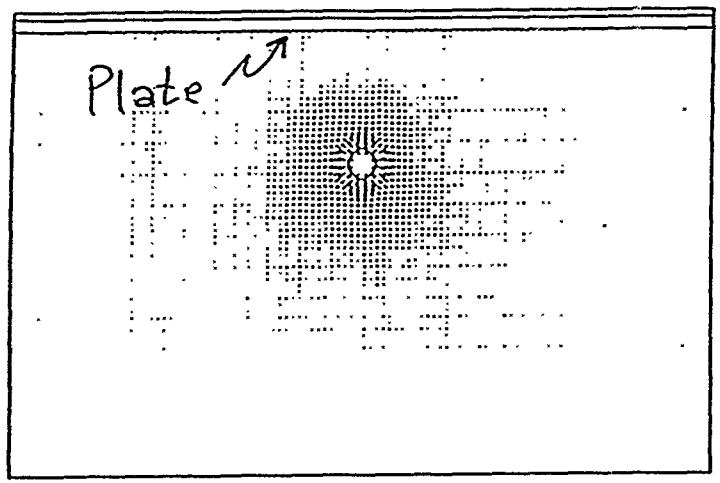

Time - 0.1 ms, ICYC - 10

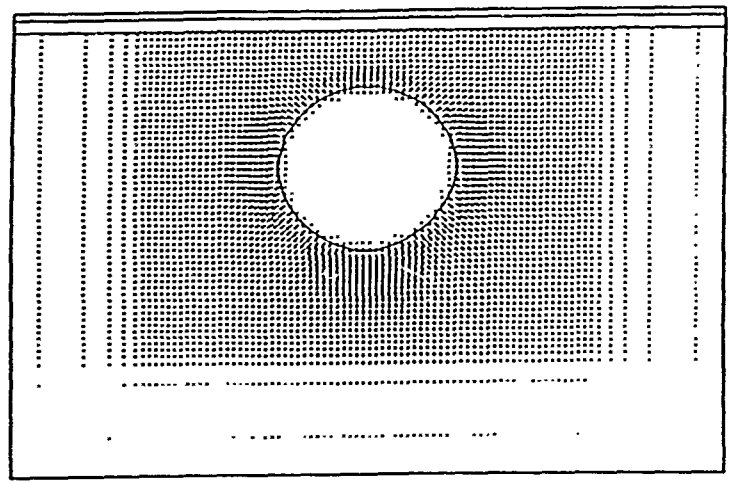

Time - 9.3 ms, ICYC - 44

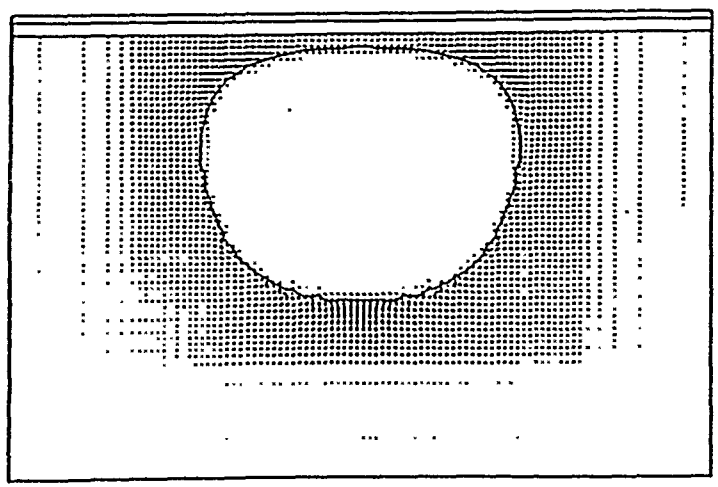

Time - 73.2 ms, ICYC - 87

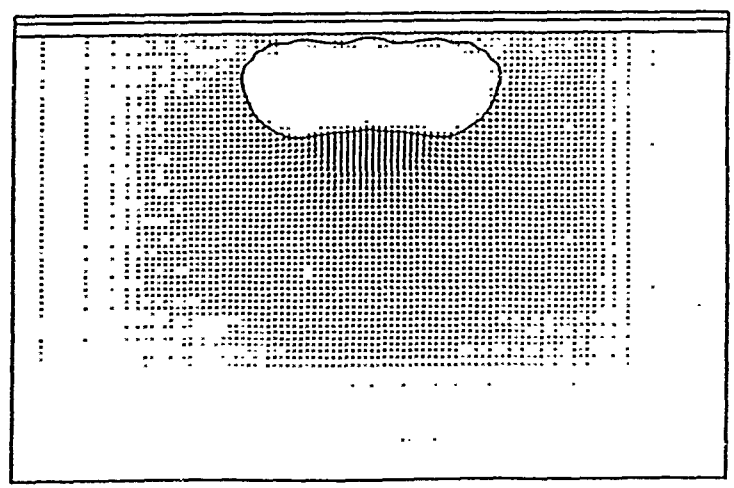

Time - 136.7 ms, ICYC - 130

Figure 43. Evolution of the bubble and the velocity field as a sequence of snapshots, Case B. (From ref.24)

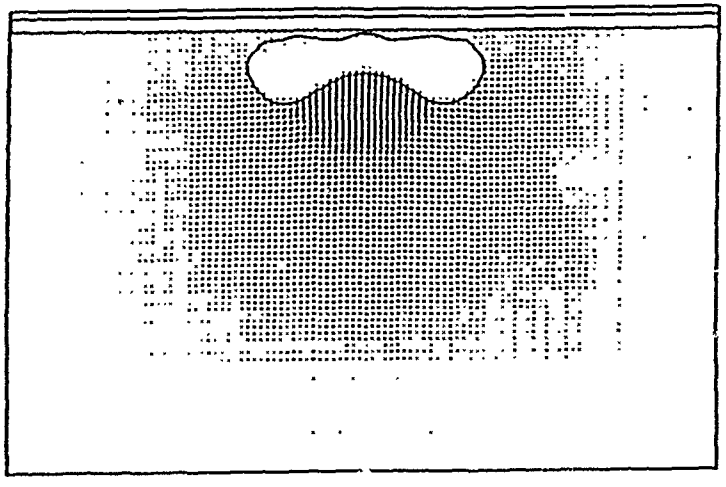

Time = 143.4 ms, ICYC = 141

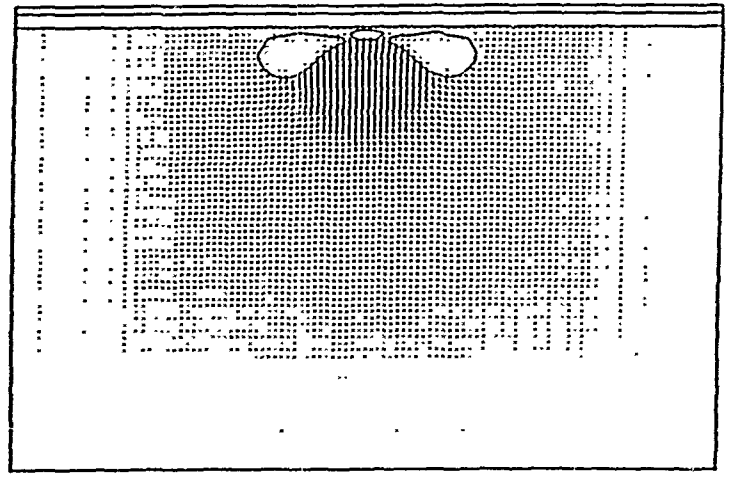

Time = 147.9 ms, ICYC = 151

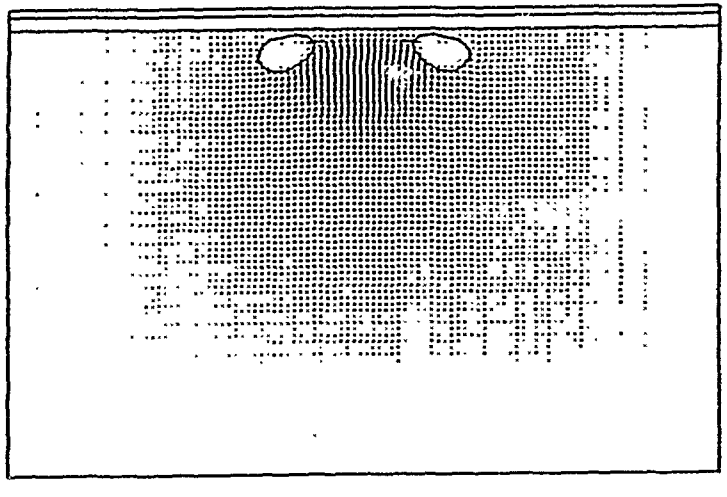

Time = 149.6 ms, ICYC = 240

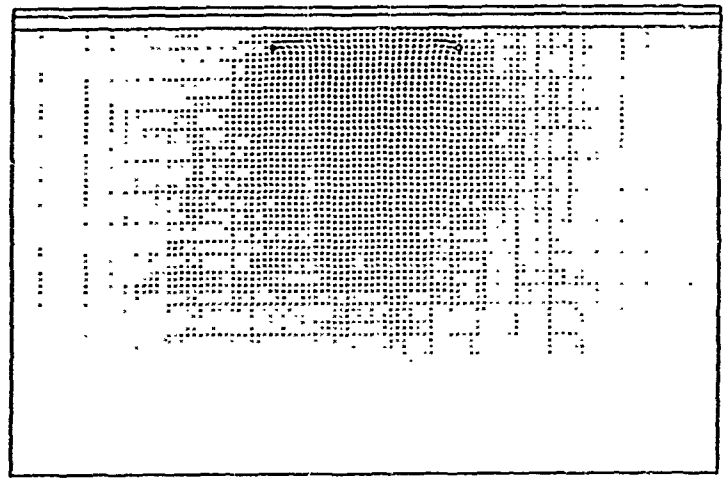

Time = 152.7 ms, ICYC = 270

Figure 43. (cont'd)

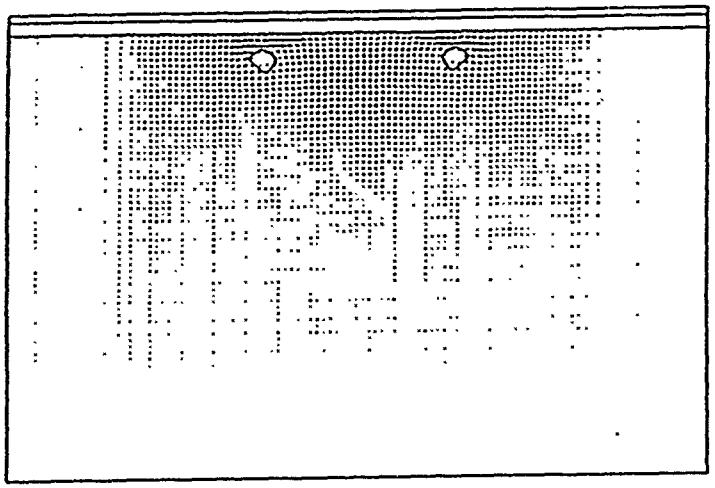

Time - 154.6 ms, ICYC - 300

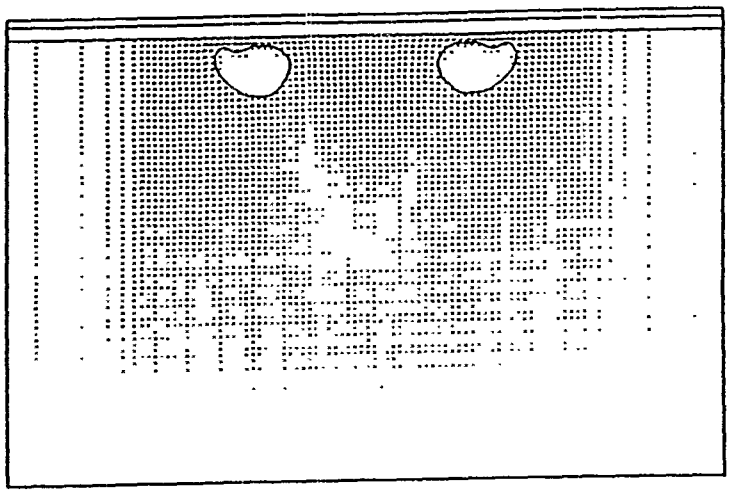

Time - 162.6 ms, ICYC - 315

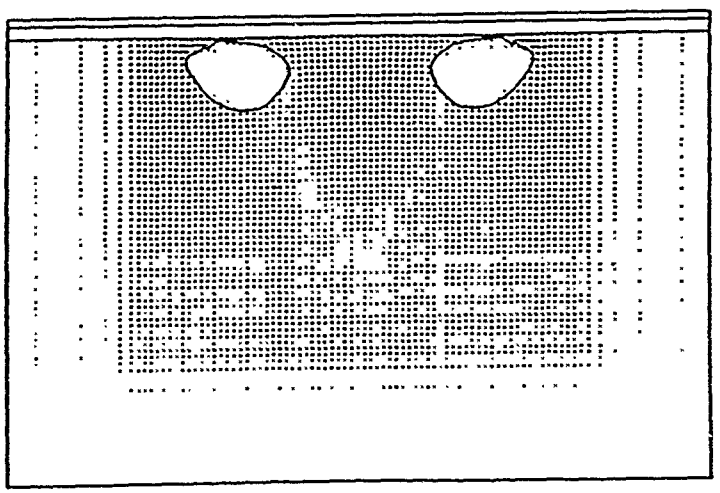

Time - 169.4 ms, ICYC - 325

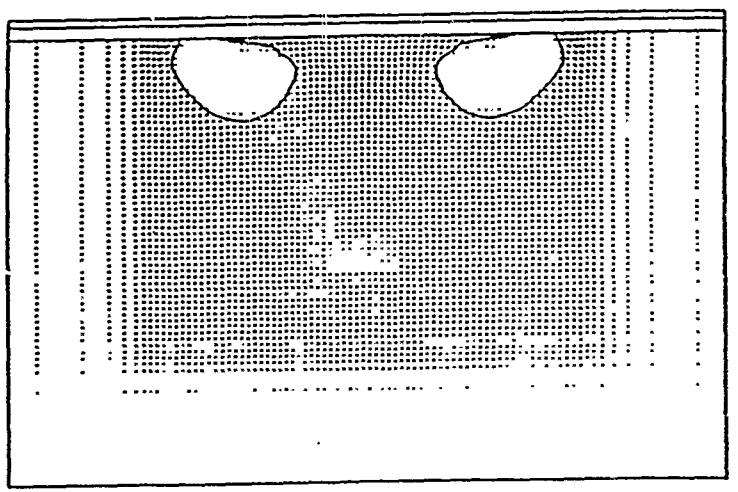

Time - 177.6 ms, ICYC - 335

Figure 43. (cont'd)

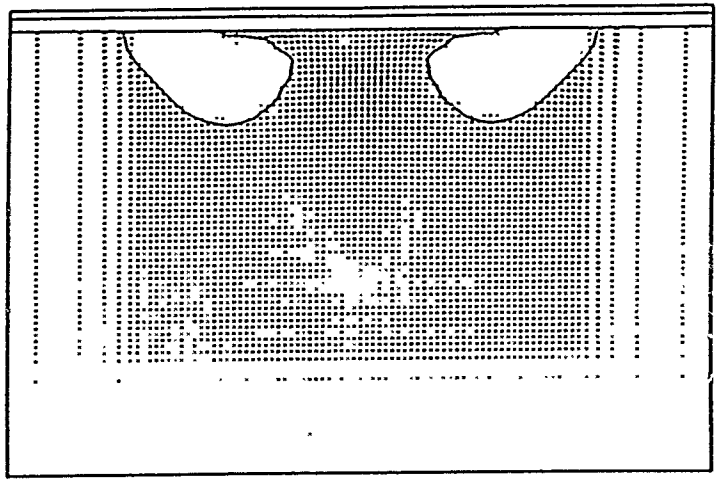

Time = 193.7 ms, ICYC = 350

Figure 43. (cont'd)

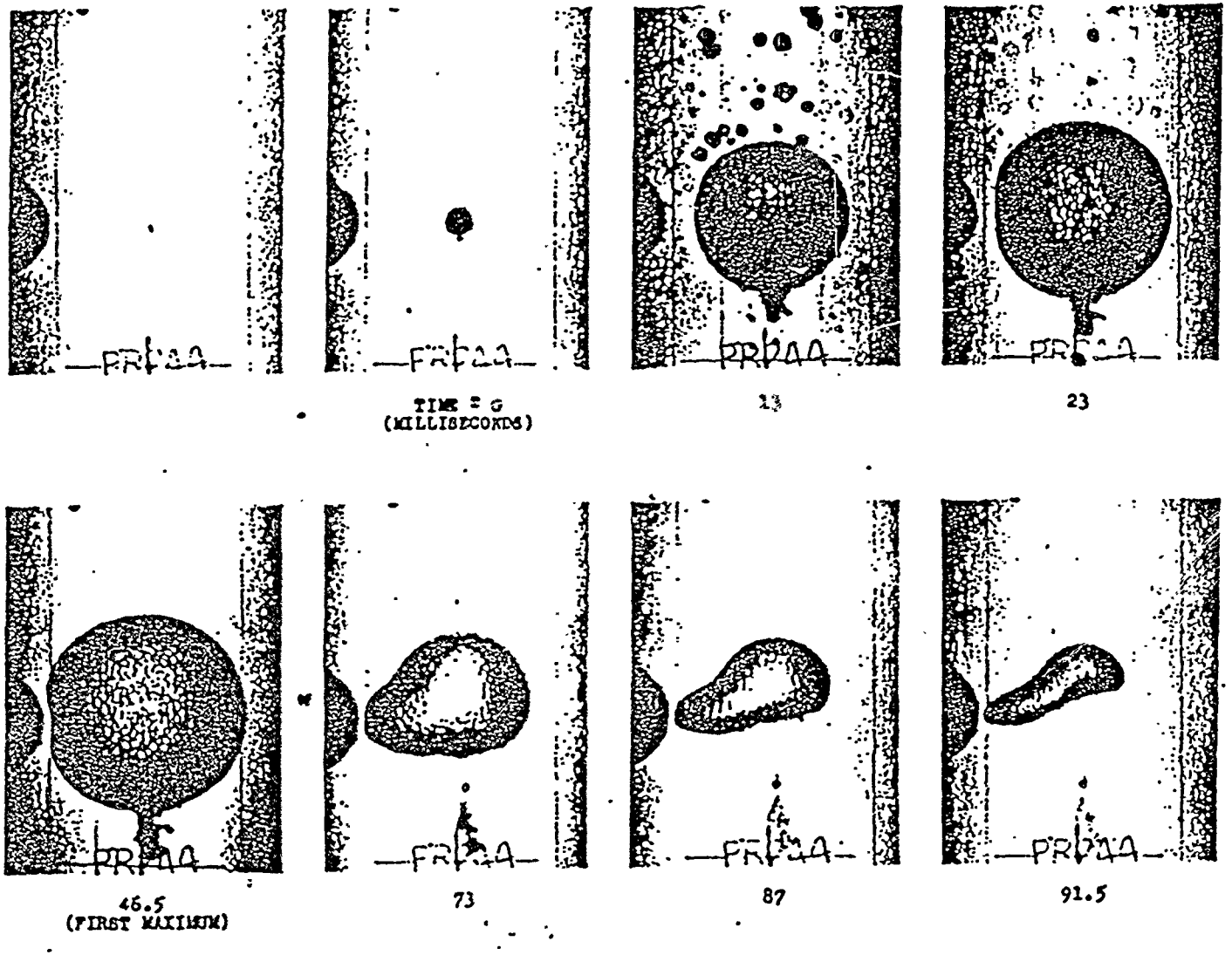

Figure 44. Bubble growth and collapse near cylinder, taken from NAVORD report 2280, 1952.

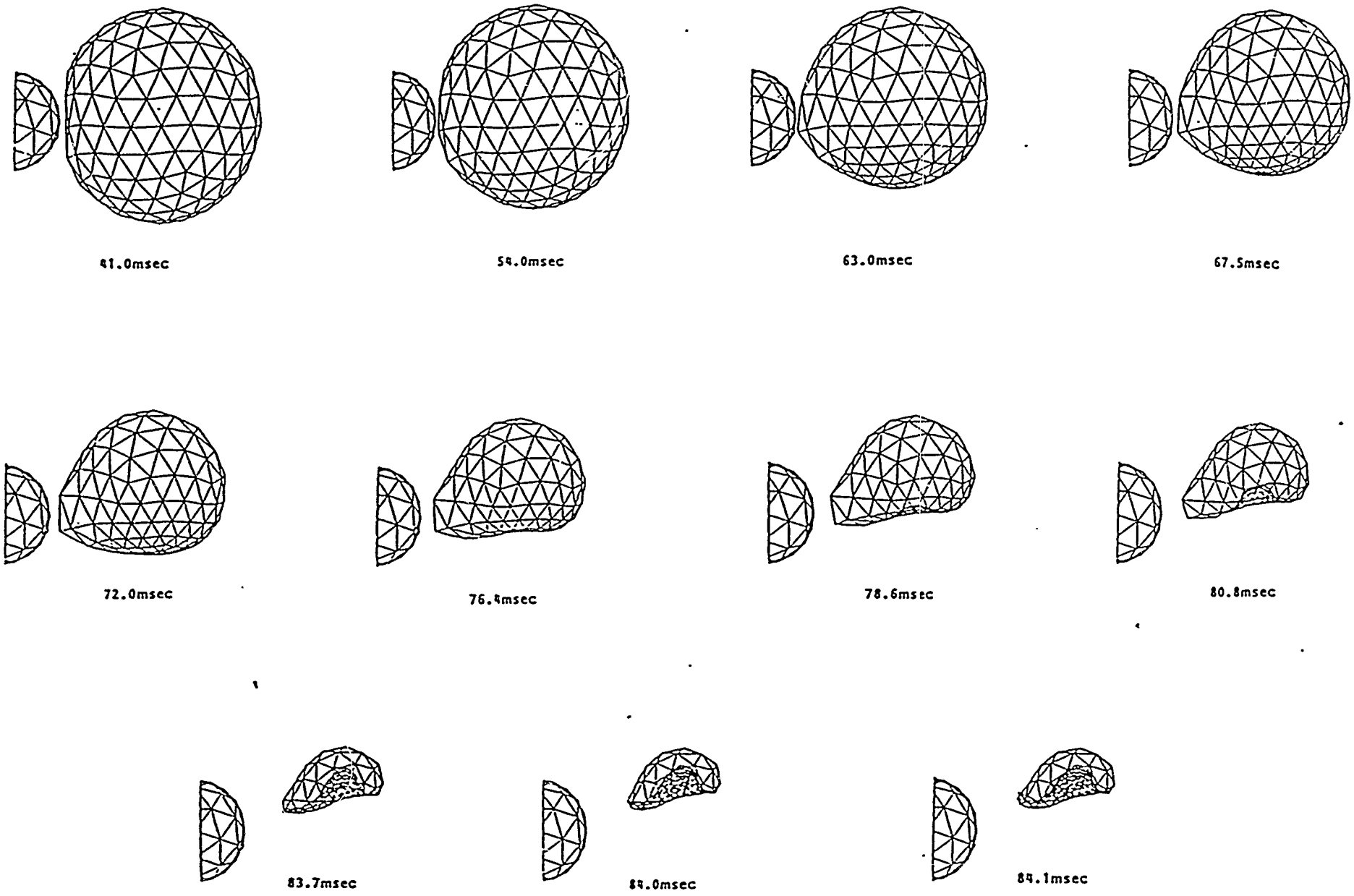

Figure 45. Bubble collapse near axisymmetric body (From ref.25)

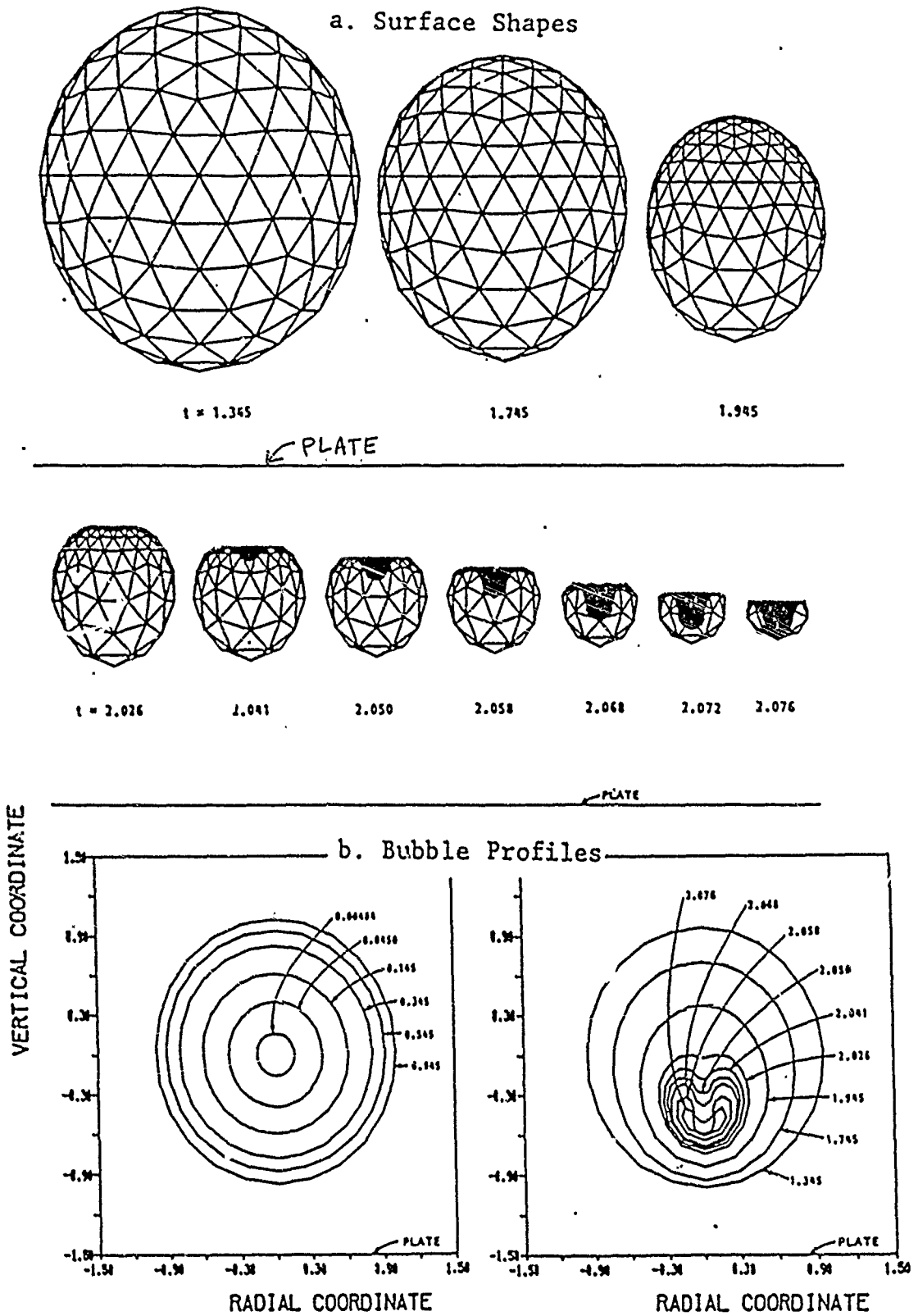

Figure 46. Axisymmetric bubble growth and collapse. L/R_{max}=1.50, R_{max}/R_o=17, P_{go}/P_a=150C, normalizing Rayleigh time=0.01453 sec. (From ref.25)

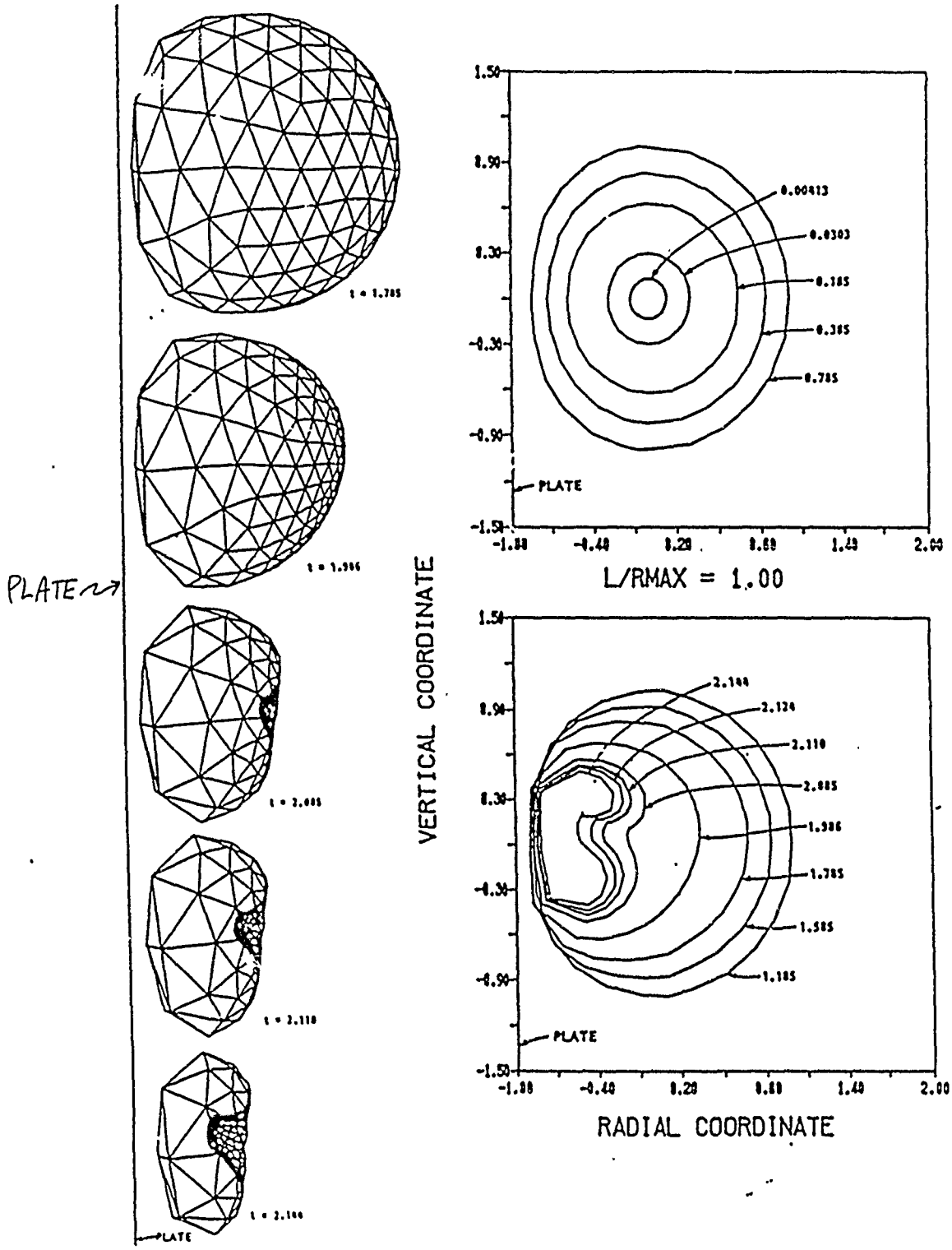

a. Surface Shapes b. Bubble Profiles

Figure 47 Three-dimensional bubble growth and collapse. L/R_{max}=1.00, R_{max}/R_o=17, P_{go}/P_a=1500, normalizing Rayleigh time=0.01453 sec. Vertical wall. (From ref.25)

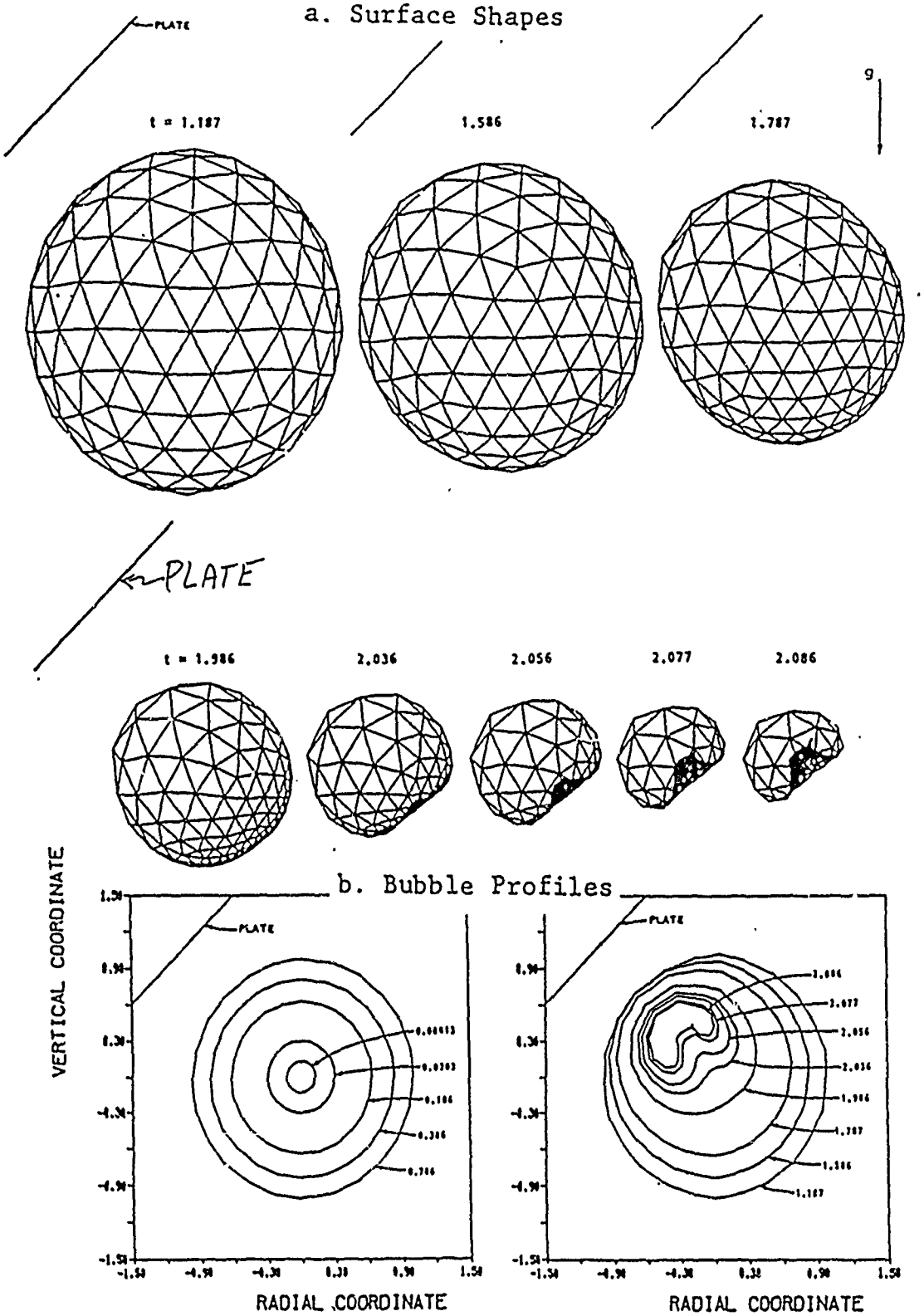

Figure 48. Three-dimensional bubble growth and collapse. L/R_{max}=1.50, R_{max}/R_o-17, P_{go}/P_a=1500, normalizing Rayleigh time=0.01453 sec. Wall at 135 degrees. (From ref.25)

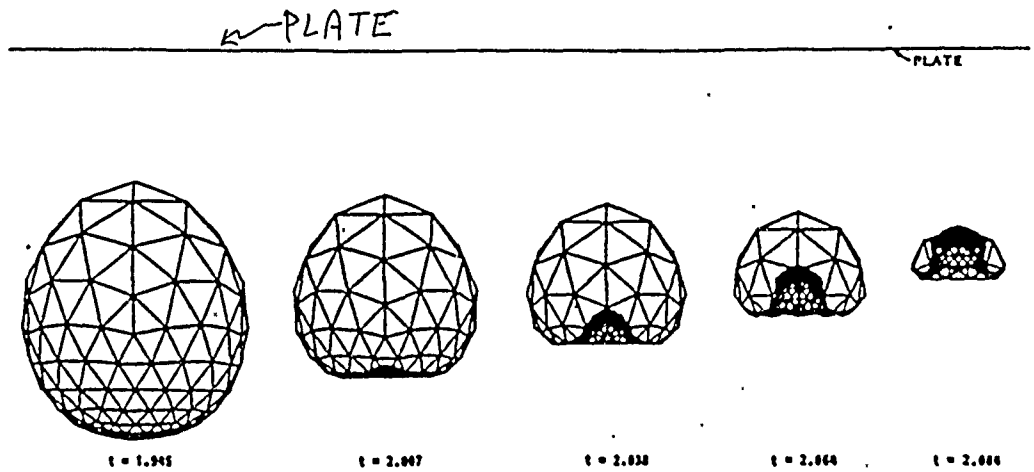

a. Surface Shapes

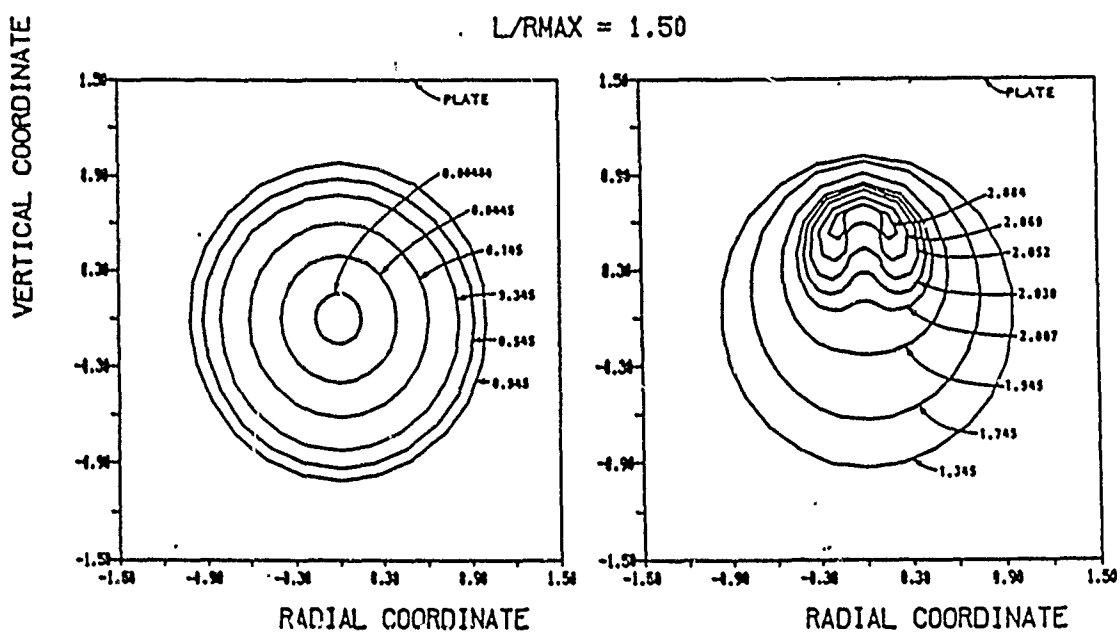

b. Bubble Profiles

Figure 49. Axisymmetric bubble growth and collapse. L/R_{max}=1.50, R_{max}/R_o=17, P_{go}/P_a=1500, normalizing Rayleigh time=0.01453 sec. (From ref.25)

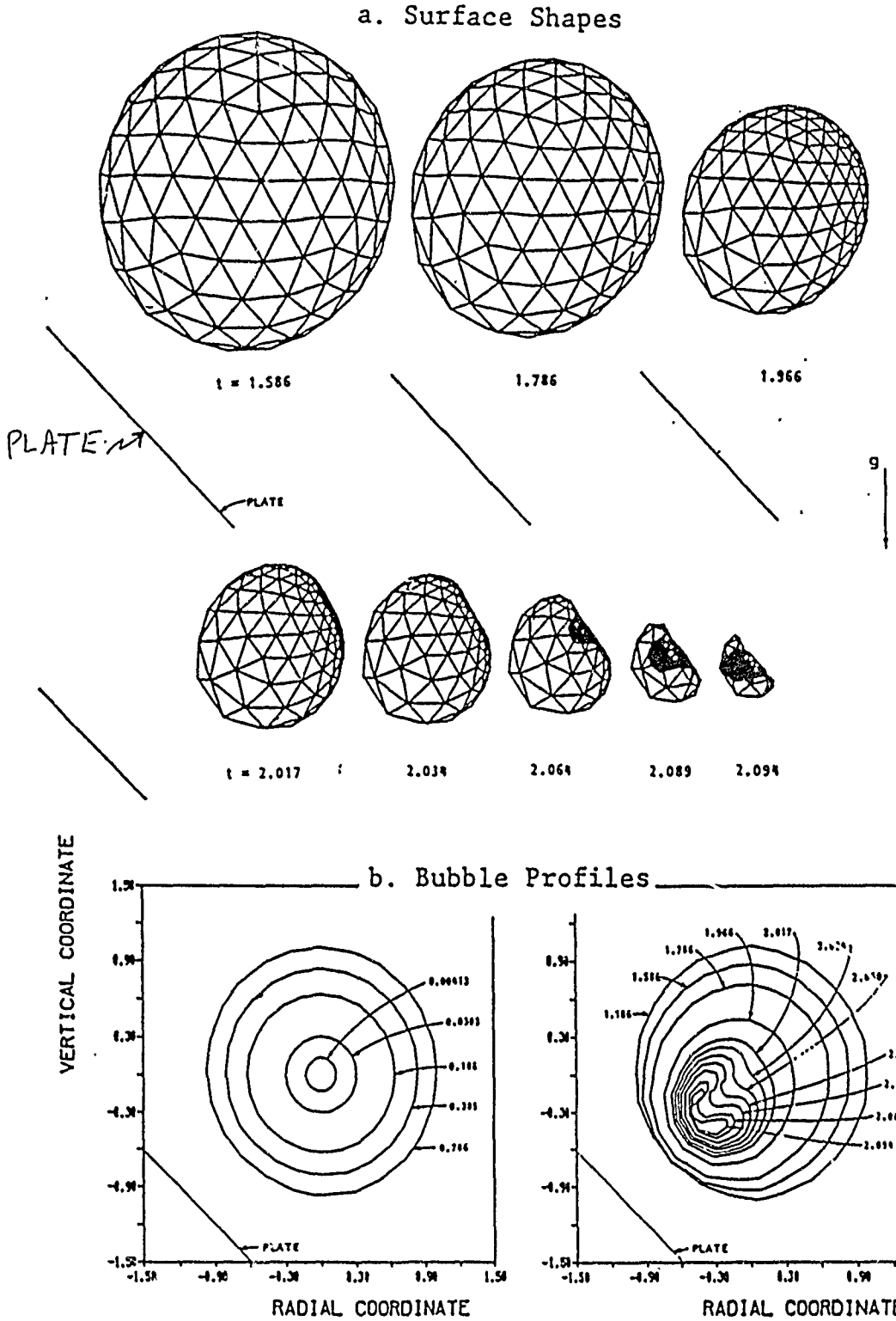

Figure 50. Three-dimensional bubble growth and collapse. $L/R_{max}=1.50$, $R_{max}/R_o=17$, $P_{go}/P_a=1500$, normalizing Rayleigh time=0.01453 sec. Wall at 45 degrees. (From ref.25)

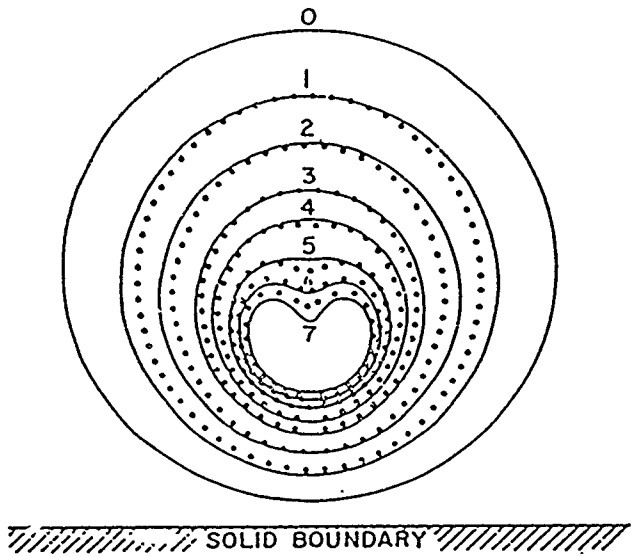

Figure 51. Comparison of the experimental results of Lauterborn & Bolle (ref.29, open circles) with the theoretical ones of Plesset & Chapman (ref.28) for the collapse of a aviation bubble in the vicinity of a rigid boundary (from Lauterborn & Bolle, ref.29). Bubble shapes corresponding to later values of time than those shown here are given by Plesset & Chapman (ref.28). (From ref.29)

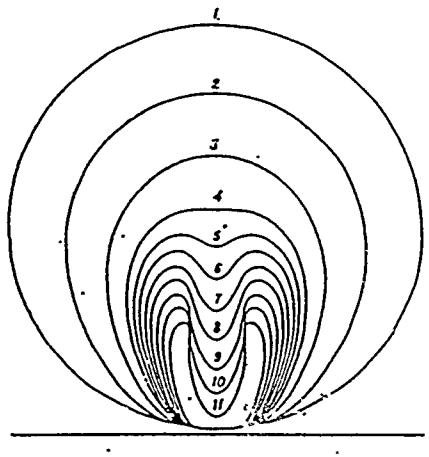

Figure 52. Collapse of a spherical cavity. (From ref.39)

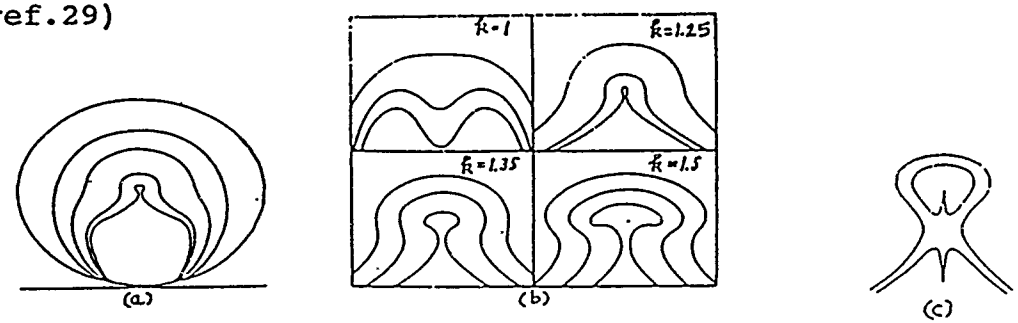

Figure 53. (From ref.38)

COMBUSTION OF THE METAL INGREDIENT IN UNDERWATER EXPLOSIVES

E. W. Price
Georgia Institute of Technology
Atlanta, Georgia 30332

INTRODUCTION

Underwater explosives are typically composed of a mixture of a granular oxidizer and a powdered metal fuel with a polymeric binder that serves also as a fuel, sometimes an explosive one. Powdered metals (usually aluminum) are used to add fuel content and density, thereby increasing explosive yield. The details of how the metal participates in the explosion are uncertain, as there is no way available to make direct observations. The net effects are determined by various measures of explosive yield such as shock wave strength or bubble energy and how they depend on metal concentration and particle size in the formulation. Because such measurements are very costly, contribution of the metal is often studied first by thermochemical calculations or detonation wave calculations. Since the details of combustion that determine reaction rate are unknown, such calculations must incorporate assumptions regarding the state of reaction, a procedure that provides results in which reaction assumptions are parameters. This means that optimization of formulation or rational tailoring to special performance needs remains a trial-and-error process involving very costly testing for every application. Evidently a better understanding of how metal powder ingredients participate in the explosion could not only reduce the cost of formulation optimization, but it might also yield means to substantially improve performance.

WHY METALS ARE USED

Heterogeneous explosives usually consist of ingredients that are themselves explosives, that decompose at moderate temperatures in a shock wave and supply energy to support that wave. In heterogeneous explosives, some of the explosive energy results from energy of reaction between vapor products of the individual ingredients, a process that can be rate-limited by mixing time. Metal powders are used because of the high reaction temperatures they produce. While the particular reaction products that contain the metal may be condensed phase (and in that sense less effective in the explosion), the

reaction reduces the molecular weight of the rest of the reaction products (primarily by reducing water and carbon dioxide) and raises their temperature. Further, this is done by a relatively small volume fraction of the explosive, because aluminum is used in a mass fraction that is about 20%, with a smaller volume fraction because of the relatively high density of the metal. Further, there are some indications that metal ingredients react to some extent with sea water in the bubble, an effect that offers the possibility of further exploitation in the future by utilization of the sea water as a reactant in the explosion.

WHY METALS POSE A UNIQUE PROBLEM

Metals do not decompose to vapors as do other ingredients. They vaporize endothermally, at relatively high temperatures. Thus mixing with oxidative species at the molecular level in the reaction wave is relatively slow. In addition, much of the reaction energy comes from formation of a condensed oxide product (e.g., Al_2O_3), a process that is limited by a "slow" condensation process consisting of heterogeneous reactions of lower oxides on liquid oxide nuclei. The rate of this reaction (with aluminum) is limited by the necessity of the nuclei to radiate energy to keep the droplets from dissoci ating. These features of metal combustion leave in doubt the question of where in the explosion process the metal reaction takes place, and how it could be controlled. While some investigators believe the metal combustion proceeds fast enough to support the detonation wave in the solid explosive, others argue that molecular scale mixing cannot be achieved in such a short (microsecond) time scale, and that metal combustion must contribute through support of bubble expansion. As noted earlier, there is some suspicion that metal reaction with sea water in the bubble also contributes to bubble expansion.

Combustion of metals has been studied in considerable detail in a variety of laboratory experiments that have been motivated mostly by fire and explosion hazards or by use of metals in rocket propellants. In such studies it is observed that metals are extraordinarily reactive, even in condensed phase, but that particles and droplets become coated with oxides that pose a barrier to contact of the metal with surrounding oxidizing species. The detailed behavior differs among the metals of interest depending on whether the oxide is soluble in the metal or not, and whether the oxide is resistant to melting and evaporation (oxides like Al_2O_3 are solid to 2000° C or so). In

many situations this determines where in a reaction wave the metal will burn. A good example is in detonation tube experiments where aluminum powder is dispersed in an explosive gas mixture that is subjected to a shock wave. A detonation wave develops in the gas, in which the metal does not appear to contribute. However the aluminum apparently melts and the droplets are disrupted into finer form by undetermined (shear?) forces. Reaction of this fog results in a second detonation front that moves with the first front. In this case original particles are heated very rapidly. The oxide inhibition of ignition which limits initial metal reaction is overwhelmed by either melting or mechanical disruption of the oxide film (on an already molten particle), and diffusion time is reduced by shear or explosive boiling dispersal of the droplet. In the detonation wave of a solid explosive (at much higher pressures and gas densities, similar processes may be at work, but there is no direct evidence, and no established basis for controlling such processes to maximum benefit.

Other laboratory experiments such as exploding wire and single particle burners have established important features about combustion of metals, as exemplified by the sketch of aluminum droplet combustion in Fig. 1. The findings of such studies are reflected in the comments made above, but one must recognize that conditions in explosion of an underwater explosive are so extreme (short time, high pressure, high temperature and high gradients) that new controlling processes such as droplet shattering may become dominant factors. Relatively little thought seems to have been given to questions such as heating histories or forces on particles under solid explosive detonation wave conditions, or to the whereabouts of unburned aluminum in the expanding bubble after detonation of the solid.

Clarification of the behavior of metals in the explosion would provide a relational basis for optimization of the choice and amount of metal and of the best placement of the metal in the explosive charge. There does not appear to exist sufficient knowledge of the metal behavior now to answer even such general questions as "where does the metal burn?". In this workshop we may hope to identify the most critical areas for research. In doing so, it seems we must address such general questions as the following

1. How should the effectiveness of a metal ingredient be measured?
2. Does the metal powder reaction
   - proceed fast enough to contribute to the detonation wave?
   - contribute to the shock wave in the water?
   - involve reaction with sea water?
   - do, or be made to do any or all of the above?
3. How well does our past research on metal ignition and combustion apply to the underwater detonation-explosion situation?
4. Would a combination of metals or an alloy be better?

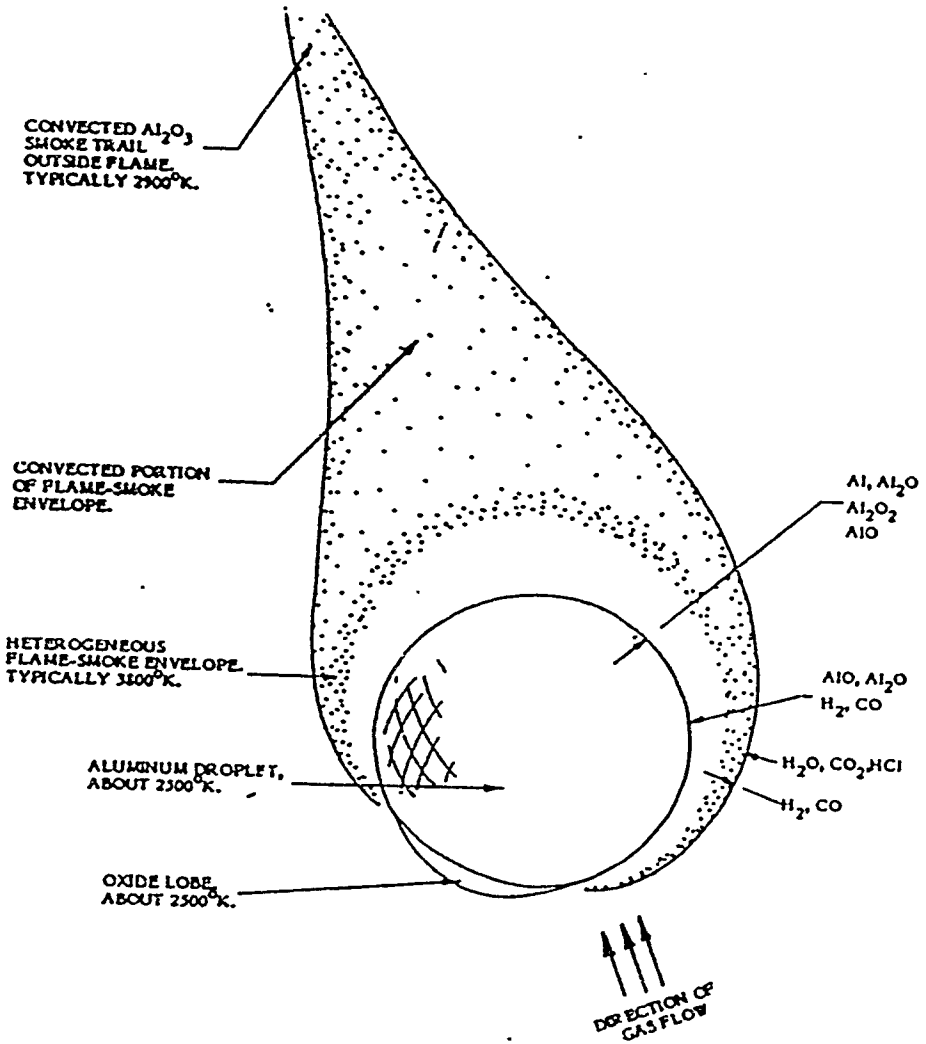

Fig. General nature of the combustion zone of an aluminum droplet burning in a mild convective flow.

DETONATIONS GROUP

Joseph Hershkowitz
Consultant
305 Passaio Ave.
West Caldwell, NJ 07006

INTRODUCTION

The Detonation Group consisted of eight scientists and engineers including the recorder as listed in Appendix A. The "Nominal Group Method" led to 23 topics proposed. The interdisciplinary composition of the group and the seminal role of the detonation characteristics to other designated areas of the workshop led to some overlap of proposed topics, particularly with respect to metal combustion. Voting led to a prioritized list corresponding to the rank order of the sum of the individual scores as shown in Appendix B. The group decided to present all the proposed topics in this report. These topics were listed within three headings according to general content. This approach is followed below, with the rank order and sum of individual scores given with each proposed topic. In addition some participants in this group are willing, on request, to provide additional details on particular proposed topics as indicated in Appendix A by associating the corresponding rank order numbers with their names. It was also unanimously agreed that improved diagnostics and modeling are required in all aspects of the subject; thus the proposed topic with Rank Order 8 should be regarded as a sub-topic of a general need.

MECHANISM AND DATA BASE FOR BEHAVIOR OF METALS IN DETONATION

Experiments for Action of Aluminum Particles in Detonation, Taylor Wave and Bubble Regimes [1, 132]

It was clear from presentations and discussions at the workshop that the action of the aluminum was critical at each stage but not adequately understood due to insufficient basic data and lack of quantitative models.

Data Base for Aluminum, Aluminum Sub-oxides, Aluminum Oxide providing Phase and Properties as a function of Temperature for High Pressures [2, 129]

The details of aluminum particle evolution in rocket propellants is well understood and most useful in optimization. The parallel data base for the high pressures of detonation and Taylor waves is very limited.

Appraise Value of Vaporific Explosions as an Underwater Mechanism [3, 115]

The interaction of hot metal with water phases including the p, V, T states created by precursor actions require evaluation from a fundamental viewpoint.

Metals Other than Aluminum in Explosives [6, 97]

Other metals, alloys, fuels may have advantages surpassing those of aluminum for underwater application. A comprehensive survey and screening experiments are needed.

Relation of Non-Ideality to Particle Size and Explosive Environment [10, 82]

The partition of the contribution of aluminum particles in advance of and behind the sonic flame is related to the particle size and shape distribution in the explosive and the evolution of those particles in the changing environment created when the explosive is detonated. Optimizing this partition is important for the underwater application requiring an experimental program leading to a quantitative model.

PROCESS OF TRANSFER OF EXPLOSIVE ENERGY TO WATER

Measure the Significant Parameters At and Near the Explosive Products - Water Interface [4, 103]

The details of the behavior at this interface underly the consequent bubble properties and action on the target.

The Equation of State of Explosive and Interaction Products from Large, Size-Dependent Charges that Correctly Describes Late-Time Energy Release [5, 100]

For the underwater application, equations of state derived from early metal acceleration experiments such as cylinder tests do not extrapolate adequately. Additional terms or a new form may be required. A model and a data base would be coordinated to achieve an appropriate equation of state.

Role of Casing on Explosive Charge on the Rate of Energy Transfer into the Water [12, 77] and Mechanism of Rate of Energy Transfer into Water from Explosives [9, 84]

The rate of energy transfer influences the fraction of the energy dissipated. To the extent a casing slows this rate it increase the fraction of the energy available to do mechanical work. It is proposed to quantify the relationship and delineate the role of various casings.

Geometric Effects for Optimum Underwater Performance [13, 74]

The configuration of one or more charges, the spacing and sequence of initiation may provide performance advantages. Such possibilities should be modeled by properly calibrated hydro-codes that contain all significant parameters.

Realistic Shock - Matching for Underwater Case [14, 69]

In other areas assuming that a shock or detonation zone may be treated as a simple discontinuity so that shock matching can be done by Hugoniot curves is adequate. The finite extent and structure of the interaction regions for the underwater application suggests that a treatment be generated which includes transport, chemistry, mixing, microstructure effects and turbulence at/in the vicinity of the interface.

Use of a Gas phase Analogue [19, 45]

Progress in understanding complex phenomena is often possible by initial study by a tractable analogue. It is proposed to experimental observe and then model facets of the action of a non-ideal explosive on a surrounding medium. Extrapolation to the underwater application would be pursued.

Two Phase Multi-Dimensional Mixture Theory [20, 35]

This theoretical area accompanied by numerical competence underlies the non-ideal explosive water interaction.

DETAILED DEFINITION OF REACTION ZONE

Mass Transport in Detonation Regime [7, 90]

To quantify the description of non-ideal explosives it is necessary to identify and measure the diffusion and turbulence parameters involved for the temperatures and pressures of the reaction zone. This realistic description would then permit optimizing non-ideal explosives for underwater applications.

Improve Diagnostics for Work in Explosives Field [8, 84]

Progress demands improved diagnostics as present techniques do not provide adequate information. Although this proposed topic was related to the detonation regime, there is a general need for enhanced capability.

Rate Dependent Processes for Detonations [11, 78]

Rate dependent physical and chemical processes have a strong effect on the structure of the detonation wave, the location of the sonic plane and the Taylor wave parameters. The rates involved are influenced by size, shape and confinement. Control of these rates is a direct path to tailoring an explosive for the application.

Multi-Phase Detonation Structure [15, 66]

It is proposed to follow the evolution of a multi-phase initial state to achievement of a detonation structure, or starting with an assumed but realistic detonation structure to follow subsequent behavior. This approach would identify the means to optimize partitions between phases of the energy and could reveal other possible states useful for the underwater application.

Decomposition Mechanisms for Detonation Parameters [16, 55]

Experimental work would be done at temperature and pressure ranges at or approaching those of detonation regimes to determine the reaction sequence, controlling reaction and rates of reaction for explosive components (e.g., perchlorates, nitrates).

Micromechanic Treatment of Explosive Detonation [17, 53]

An expanded macroscopic set of governing equations would be derived by including a larger set of elemental statistical ectivities as a basis for taking moments satisfying mass, momentum and energy constraints. This expanded set of equations would go beyond the Navier-Stokes equations, by including and defining parameters in addition to those of viscosity and diffusion. The predictions of these equations would be explored.

New Explosive Compositions for Underwater Application [18, 47]

Explosives for underwater application have historically been modifications of those available for other uses. It is proposed to describe the properties sought uniquely for the underwater application and seek candidates with those properties.

Temperature Dependent Rate Models [21, 34]

Reaction rates can be expressed in terms of pressure, temperature and species concentrations, (or equivalent parameters such as chemical potential, affinity, volume of activation, etc.). It is proposed to pursue a model for the rates that govern the evaluation of species in a detonation process that is dominated by temperature dependence.

Constitute Equation Related Directly to Processes Underway [22, 16]

Many constitutive equations involve an adopted form with arbitrary constants that are determined by fitting a data base. Such equations are limited to that data base and serious errors can result from improper extrapolation. A more fundamental approach is proposed.

Cellular Structure [23, 15]

Does cellular structure as seen in gaseous detonations exist in any aspect of explosives in underwater applications?

APPENDIX A - PARTICIPANTS IN DETONATIONS GROUP

The participants in the Detonations Group were as follows. The numbers that appear after several of the names correspond to the rank order of the topic(s) (see previous text) for which these individuals will provide additional information if called upon to do so.

Raymond R. McGuire, L324, Lawrence Livermore Nat'l Laboratory, Livermore, CA, 94550 (Group Leader)

Joseph Hershkowitz, 305 Passaie Ave, West Caldwell, NJ, 07006 (201) 575-0127 (Group Leader)

David Beck, Sandia Nat'l Laboratories, ORG 6427, Albuquerque, NM, 87115 (505) 846-7733
Rank Orders 1, 3

Michael J. Ginsberg, Los Alamos Nat'l Laboratory, MS-J960, Los Alamos, NM, 87545 (505) 667-3327
Rank Orders 1, 4, 5, 6, 8, 9, 10, 12, 13

Herman Krier, University of Illinois, M/IE Dept., 140 MEB, 1206 W. Green St., Urbana, IL, 61801
Rank Orders 7, 15

Martin Sichel, Dept. of Aerospace Engineering, The University of Michigan, Ann Arbor, MI, 48109
Rank Orders 13, 17, 19

Hyman M. Sternberg, Advanced Technology and Research, 14900 Sweitzer Lane, Laurel, MD, 20707

Rank Orders 5, 9, 12

Scott Stewart, Dept. of Theoretical and Applied Mechanics, University of Illinois, Urbana, IL, 61801 (217) 333-7947
Rank Orders 7, 14, 15, 17

APPENDIX B

There were 23 topics proposed. In voting, group members provided a 23 score to their first choice, a 22 score to their second, etc. until they provided a score of 12 to a topic. At this point each participant has ranked the twelve topics they considered most significant. The table that follows provides the scores achieved by each proposed topic. The latter are listed in the rank order achieved together with the corresponding sum of the scores. In the preceding text each proposed topic has the rank order and sum of scores listed with the title. As an example - Rank Order 11, had 78 as a sum of scores and is entitled - Rate Dependent Processes for Detonations.

DETONATION GROUP

RANK	SUM	SCORES							
1	132	22	21	19	18	18	18	16	
2	129	23	19	19	19	18	16	15	
3	115	20	19	18	16	15	14	13	
4	103	22	22	20	14	13	12		
5	100	23	20	17	14	14	12		
6	97	20	18	17	16	14	12		
7	90	23	21	20	13	13			
8	84	21	17	17	16	13			
9	84	23	21	21	19				
10	82	22	17	15	15	13			
11	78	22	17	14	13	12			
12	77	19	17	15	14	12			
13	74	22	19	18	15				
14	69	20	17	16	16				
15	66	23	22	21					
16	55	23	20	12					
17	53	21	18	14					
18	47	20	15	12					
19	45	23	22						
20	35	23	12						
21	34	21	13						
22	16	16							
23	15	15							

INTERFACE PHENOMENA

P. B. Butler
The University of Iowa

SUMMARY

Participants in the interfacial phenomena discussions included: D. Book, P. B. Butler, D. Ritzel, J. C. W. Rogers, J. E. Shepherd, and W. A. Sirignano. A number of potential research topics were suggested by group members, and each item was subsequently discussed in an open forum. During the group discussions, the suggested topics were consolidated into seven distinct areas. Following this, the members prioritized the seven areas. Three items received identical scores in the voting process, and are thus listed as priorities 4a, 4b, and 4c in the following list. In order of priority, the recommended research topics are:

1. A study of coupled heat/mass transfer at the bubble interface.

2. Nonlinear development of hydrodynamic instabilities.

3. Transport of evaporating water at interface and coupling with internal bubble flow.

4a. Extended multiphase interface.

4b. An understanding of the role of diffusive instabilities in underwater explosions.

4c. Development of advanced diagnostic techniques for spatial and temporal resolution of temperature, pressure, particle velocities, and species concentrations.

7. Dynamics of hot metal particles in water.

DISCUSSION OF TOPICS

1. Coupled heat/mass transfer at bubble interface.

Heat and mass transfer will be occurring in the boundary layers on each side of the bubble interface. Due to

vaporization or condensation, the interface will also be moving. The degree of heat and mass transfer at the bubble interface can be substantial in an underwater explosion. In particular, these transport processes control i) evaporation of sea water into the bubble interior, and ii) dissolution of product gases into the surrounding sea water. Thermal radiation from the explosion products can also augment conductive and convective heating.

Understanding the interface transport processes is a key step in determining bubble energy and mass changes following detonation. Analytical and numerical descriptions are needed before any realistic modeling and interpretation of experiments can be done. Models should be checked with subscale vaporization experiments which do not involve using high explosives. An idealized approach to this problem is the logical first step, followed by analyses of the more complex problems of the extended interface (see Item 4a), and convective transport within the bubble (see Item 3).

2. Nonlinear development of hydrodynamic instabilities

These interfacial phenomena (e.g., Rayleigh-Taylor and Kelvin-Helmholtz) play an important role in determining the temporal and spatial behavior of the interface. The long-term, nonlinear evolution of instabilities represent important mechanisms of energy loss and transfer. These instabilities will significantly influence the formation and collision of jets, and the amplification of bubble surface area that occurs near the minima of collapsing bubbles.

Kelvin-Helmholtz instabilities can become important when a tangential velocity difference occurs across the interface. The velocity difference can be the result of: asymmetric explosions; natural convection within the gas; distortion of the bubble shape; or interaction of the bubble with nearby solid boundaries.

More recent work has been done on the topic of hydrodynamic instabilities, particularly the Rayleigh-Taylor mechanisms, than in any other topic discussed here. As a consequence, the base of methods and technologies available for making further progress is the largest. Recent advances in computational resources such as pipeline and massively parallel computers, and new computational algorithms, promise rapid and substantial improvements in our understanding of these problems. All such instabilities can cause substantial changes in bubble shape and dynamics, and can increase entrainment and effective transport rates at the interface.

3. Transport of evaporating water

During the early stages of an underwater explosion a large amount of water could vaporize at the bubble interface; this would have a strong effect on the subsequent bubble dynamics. Internal circulation resulting from asymmetric explosions, natural convection, distortion of bubble shape, or

bubble/wall interactions can rapidly transport the vaporized water away from the interface and hot product gases towards the interface. If this convective transport does not occur, the vaporization rates will be diffusion-limited by the rate at which the relatively cool water vapor diffuses into the hot combustion products.

This topic requires special attention to multiphase flow and boundary conditions at the interface, and is a key element to understanding how water is transported into the bubble. It is important to determine if this can be a rate limiting step in underwater explosions.

4a. Extended multiphase interface.

This topic is subdivided into two categories: effects of supercritical conditions, and extended, multiphase interfaces resulting from the presence of casing fragments and other condensed phase materials. In the initial phases of an underwater explosions, very high pressures exist at the interface resulting in water states above the thermodynamic critical point. At such conditions, surface tension, latent heat of vaporization, and the density change across interface become very small. In addition, a large amount of gas can dissolve into the liquid across the interface. These nonideal effects can cause significant modifications to the phenomena discussed under Item #1.

Weapon systems and many experiments with high explosives have a metal casing, fragments of which will be dispersed throughout the interface following the explosion. The interface becomes an extended "mushy" zone (Much less defined than discussed in Item #1.) with multiple phases present. An extended interfacial zone can influence the development of nonlinear hydrodynamic instabilities. Analysis of this phenomenon requires detailed multi-phase flow modeling. This is a difficult, but important, problem in practical experimentation and weapons systems.

4b. Diffusive Instabilities

Evaporation rates at superheated conditions are determined by instabilities which generate large surface areas and produce evaporation rates that are 100-1000 times classical diffusion-limited rates. Diffusive instabilities can couple with hydrodynamic instabilities and cause significant augmentation to transport rates. It is important to determine these rates experimentally and understand through analyses, the conditions under which instability can occur.

4c. Diagnostic techniques

Improving our understanding of the interface phenomena will require a much more refined data base than presently exists. As the models become more sophisticated, more detailed measurements of pressure, temperature, particle velocity and

species concentrations are required. Particular attention should be paid to the difficult problem of measurements within the bubble, and in the water immediately adjacent to the bubble. Characterization of the interfacial area and geometry is also needed. This work will provide a detailed data base to test models and theories.

7. Dynamics of Hot Metal Particles in Water

It is anticipated that some underwater explosive systems will contain a significant percentage of metallic particles. Hot metal particles from combustion can be driven towards the bubble interface. These particles have a high density and significant kinematic inertia. Under certain conditions the particles can pierce the interface, and enter the surrounding water, especially during bubble collapse. This topic requires an analysis of particle trajectories and associated energy release rates. It is of interest to the development of "novel" explosives where metal reaction in water can be significant and also for understanding metal combustion in metal-loaded conventional explosives.

BUBBLE DYNAMICS

Professor Harland M. Glaz
Mathematics Department
University of Maryland
College Park, MD 20742

PROCEDURE AND RESULTS

Due to the substantial overlap and interrelation of the two fields, the Area 2 group meeting on Interface Phenomena and the Area 3 group meeting on Bubble Dynamics were initially combined on the first day. However, the number of people in attendance was far too large, so it was decided that the first order of business would be to break out into two distinct group, but avoid overlapping discussions to the extent possible. Consequently, the first hour or so was taken up by the two recorders obtaining, in round-robin fashion, a list of topics (and insisting that each item on the list be short) from the participants. It was then decided which topics were in the area of Interface Phenomena (denoted "I"), which were in the Bubble Dynamics (denoted "B") area, and which were in both areas. This list is reproduced in Appendix I.

Those of us remaining in the Bubble Dynamics area, focused our discussion into combining related topics, eliminating certain items from consideration, etc.; this was followed by a more technically intensive discussion of the status of the field and research priorities. Finally, eleven topics were selected for prioritization and it was decided to recommend seven of these, using the stipulated voting procedure.

At this point, seventeen voters were present. The final list of eleven topics and the details of the voting record are presented in Appendix II. A "Pareto chart" is presented in Appendix III.

At this point, each of the top seven topics were assigned to individuals or groups for further work overnight. Our session reconvened the following morning; short statements for each item were prepared and agreed upon. This constituted my presentation and the results are reproduced here in Appendix IV. I have included the statement preparers name when my memory was adequate to do so; my apologies to those omitted.

COMMENTARY

It was clear from the discussion that the limitations in our scientific understanding of the bubble dynamics arising from conventional underwater explosions are very severe, and that the community is in substantial consensus on this point.

My interpretation of the voting results are (1) in the short run, the most new knowledge can be obtained by the exercise of existing (or easily modified) hydrocodes which are relevant to the problem, and (2) in the long run, a first-rate research program must contain elements including improved flowfields diagnostics, improved numerical methods, more work on the EOS of the product gases, and the development of model problems at laboratory scale. In view of the great expense of full-scale field testing and the difficulties involved in obtaining reliable data from such tests, it is clear that numerical methods will play a leading role in future engineering design efforts in this area. Consequently, the research program should have at least one focus on the validation of hydrocodes, preferably on problems which are close to the real application but for which reliable and extensive flowfield data is available. Also, the numerical method development aspect of the program should be highly competitive once a set of validation cases are selected.

APPENDIX I. LIST OF TOPICS

1.	Prioritize physical issues / Evaluate numerical methods using computation	B
2.	Compute and measure jet after crossing (for validation)	B
3.	Development of quality suite of programs. Comparison and understanding theory and experiment	B
4.	Efficient 3D numerics	B
5.	Measure pressure loads (distribution on targets (code validation)	B
6.	Tradeoff between shock dissipation and bubble energy	B
7.	Reaction zone/interface coupling	I
8.	Improve exp. diagnostics	B, I
9.	R.-T. + 3-phase interface collapse	I
10.	Characterize gases/products in bubble	B, I
11.	Extensive computing using existing 3D codes	B
12.	Deformable surface loading	B
13.	Improved computational methods	B, I
14.	Analytic solutions to speed up calculations	B, I
15.	Realistic EOS product	B, I
16.	Highly diagnosed exp. large-scale	B, I
17.	Shock/Bubble/Water Jet Damage Mechanism	B
18.	Replace Cole's Book	
19.	Importance of radiation and heating at interface	I
20.	R.-T. instability nonlinear evolution	I
21.	Charge design for optimum partition of energy Shockwave and rest of waveform as function of charge symmetry and boundary impedance	B
22.	Exp. techniques to look through opaque products, e.g., x-rays	B, I
23.	Code validation	B, I
24.	Inclusion of heat transfer effects on bubble dynamics	B, I
25.	Energy/momentum consideration in bubble dynamics	B

26.	Math description of interface	I
27.	Interface debris considerations	I,B
28.	Include mass transfer in numerical models of bubble motion	I,B
29.	Total consideration of the influence of gravity	B
30.	Turbulence and boiling effects for codes	I,B
31.	Simplified loading for FE code impact	B
32.	Time scales of important physical phenomena	I,B
33.	JWL EOS for Navy (Al-ized) explosives	B
34.	More 2D code and validation experiments	B
35.	Natural convection and effects on transport @ interface	I
36.	Effect of geometry (of object) on jetting	B
37.	Effects on bubble dynamics of Al chemistry	B
38.	Full flowfield diagnostics	B
39.	Influence of moving and deforming boundaries on bubble dynamics	B
40.	Toroidal bubble dynamics/expansion	B
41.	Salinity, T, etc. effects	B,I
42.	Charge geometry, deformation effects on bubble interface	B,I
43.	Measure evaporation/condensation in super heated H_2O	I
44.	Compressibility effects on bubble formation	B
45.	Shock diffraction at fluid/solid interface	B
46.	Relation of shock strength and energy available for bubble	B
47.	All interfacial instabilities	I
48.	Metal partical trajectory through interface and H_2O	I
49.	Shock/bubble interaction	B
50.	Compressible/Incompressible 3D sequential joining	B
51.	Model problems	I,B
52.	Interpretation of exp. in restricted domains (validation)	B
53.	Measure H_2O concentration in bubble	B,I

APPENDIX II. FINAL TOPICS AND VOTING RESULT

A. Replace Cole's Book.

7	6	5	4	3	2	1	0
2	-	-	-	-	-	2	13

= 16

B. Develop New Flow Visualization Techniques
(e.g., x-rays, neutrons)

7	6	5	4	3	2	1	0
1	4	-	-	1	2	3	6

= 41

C. Characterize State of Condensible and Noncondensible Gases in Bubble EOS

7	6	5	4	3	2	1	0
1	1	2	-	2	4	1	6

= 38

D. Computation of Late-stage Bubble Dynamics Including Jet Impact With and Without Targets

7	6	5	4	3	2	1	0
6	5	3	1	-	1	-	1

= 93

E. Influence of boundary motion and Deformation

7	6	5	4	3	2	1	0
1	1	1	2	2	-	2	8

= 34

F. Single Component Condensible and Noncondensible Experiments for Validation

7	6	5	4	3	2	1	0
-	2	3	1	3	2	1	5

= 45

G. Inclusion of Heat and Mass Transfer on Bubble Dynamics

7	6	5	4	3	2	1	0
-	-	-	4	2	2	3	6

= 29

H. Improved Numerical Methods for Efficiency and Accuracy, + Adding New Capabilities

7	6	5	4	3	2	1	0
2	3	1	1	1	2	3	4

= 51

I. 3D Geometry Effects

7	6	5	4	3	2	1	0
1	-	4	1	1	1	-	9

= 36

J. Techniques for Measuring Jet Impact Loads

7	6	5	4	3	2	1	0
1	-	3	3	5	-	1	4

= 50

K. Effects of Late-time Combustion on Early Time Bubble Growth for Nonideal Explosives

7	6	5	4	3	2	1	0
2	1	1	3	-	4	1	5

= 46

APPENDIX III. PARETO CHART

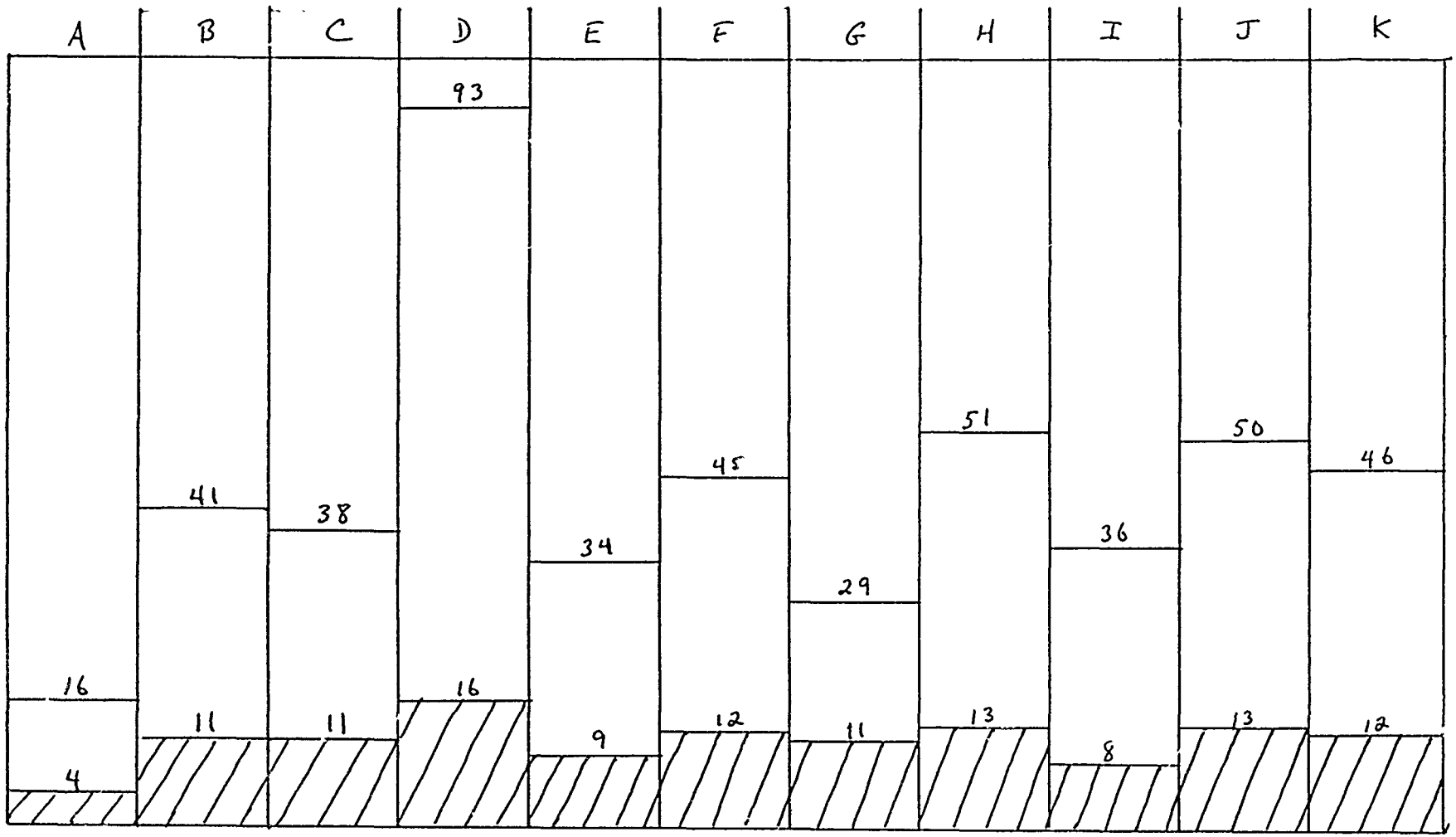

APPENDIX IV. DETAILED STATEMENTS

1. COMPUTATION OF LATE-STAGE BUBBLE DYNAMICS INCLUDING JET IMPACTS WITH AND WITHOUT TARGETS.

During the final stages of its contraction, an underwater bubble often develops a jet which passes through the interior and breaks through the opposite side. This phenomena and the subsequent expansion-contraction cycles after the jet breaks through represent a significant portion of the bubble's damage making potential. Existing computational methods are only capable of predicting the formation of jet up to the breakthrough.

The breakthrough represents a singularity in the classical continuum mechanics model where two distinct parts of a free-surface collide. The subsequent expansion after the breakthrough also exhibits this type of collision.

Modelling of the advancement of the jet in the fluid following the breakthrough is essential to later compute the loads on the nearby surface. Similarly, it is very important to model the bubble rebound after jet breakthrough including the formation of a vortex bubble ring and its subsequent motion, growth, and collapse.

Both in scaling experiments and in actual bubble explosions, the jet front is irregular and bubble entrapment on the target at impact modify the expected pressure impact values. Modelling of this "real fluid" effect is important to interpret and analyze experimental measurements and predict forces on target.

Prepared by Jay Solomon
and Georges Chahie.

2. IMPROVED NUMERICAL METHODS FOR EFFICIENCY, ACCURACY AND NEW CAPABILITIES

The underwater explosion bubble presents several extreme difficulties which are not sufficiently addressed by existing methods and codes.

The principle difficulties of the problem can be seen from the material contrast between the two fluids (gas and water), separated by an interface with complex and time dependent topology, which for meaningful problems must be run for late time through many time steps. Further complications arise from interface physics including mass transfer and phase transitions, which play a different role in scaled laboratory experiments than they do in the full scale problem.

The problem has a compressible aspect, as can be seen clearly from the lead shock caused by the explosion. Compressibility may play a role in the later time development of the bubble motion, but this question cannot be clearly resolved because compressible codes have not as yet been successfully run into this region. In any case, many features can be captured by an incompressible approximation. For this reason it is desirable to have both compressible and incompressible codes developed.

In order to deal with the explicit difficulties of the underwater explosion problem, we propose enhanced numerical methods. Among the possible lines of developerment which appear appropriate for this problem, we mention interface methods (boundary integral methods and front tracking), local mesh refinement, higher order Godunov mehtods, fixed domain mehtods, and adaption to parallel architecture.

Validation is an essential part of code development and should include comparison of code results to experiment, to other codes and to known solutions to benchmark problems. In addition, the code should demonstrate internal consistency and numerical accuracy (such as by convergence under mesh refinement) for sample problems of engineering interest.

Prepared by Ernest Battifarano
and James Glimm

3. DEVELOP TECHNIQUES FOR MEASURING JET IMPACT LOADS

The problem is to measure the pressue distribution on a target during jet impact and bubble collapse as a function of time for explosions at normal atmospheric air pressure.

(A1 present we can only measure this pressure distribution on HE explosives with reduced air pressure)

Two cases - deformable and rigid targets - are of interest.

Pressure transducers and amplifiers must survive the shock loading and be functional within milliseconds in order to record impact and bubble collapse pressures. This may require new or modified types of pressure transducers.

Prepared by John Goertner

4. THE EFFECT OF LATE-TIME COMBUSTION ON EARLY-TIME BUBBLE GROWTH FOR NONIDEAL EXPLOSIVES.

Early-time bubble growth is dependent on the rate of reaction in the detonation/combustion process. Rapid early bubble growth gives rise to fluid particle accelerations around the pulsating bubble, which are essential for inducing a type of target response known as hull whipping. The localized nature of the bubble loading along the length of the ship gives rise to large bending moments and flexural response of the entire ship hull. It is recognized that modern aluminized explosives are excellent explosives from a bubble energy standpoint, but the drive to produce explosives that give large bubbles may be sacrificing their whipping damage potential. Late-time combustion of Al certainly adds to the overall bubble energy, but some of its contribution is not available in the stages of early bubble growth.

It is essential that the detonation and late-time combustion process be understood, not only for aluminized explosives, but for other new and/or exotic explosive concepts or formulations.

Prepared by Greg Harris

5. SINGLE COMPONENT CONDENSIBLE AND NON-CONDENSIBLE EXPERIMENTS FOR CODE VALIDATION.

Although tests of conventional underwater explosions are prototypical, they can pose difficult problems for the experimenter attempting to provide high-quality data. The explosion bubble contains many gases, and frequently several phases (liquid, solid, gas). The initial and boundary conditions are difficult to both control and measure.

It is, however, possible to conduct experiments in which the initial conditions are well-characterized, and where the bubble contains a single phase composed of one or more gases, at the experimenter's discretion.

These experiments should provide data that are extremely valuable in validating computer codes, especially in terms of well-characterized initial conditions, simplified equations of state, and absence of opaque material obscuring the bubble behavior. Both two- and three-dimensional validation experiments could be conducted; the code developers could suggest initial conditions, confinement geometries, geometry and location of neighboring surfaces and other parameters useful for code assessment.

Prepared by Marshall Berman

6. DEVELOP NEW FLOW VISUALIZATION TECHNIQUES

It is clear that carefully controlled experimental measurements are needed in order to validate computational and analytic studies. It is to be hoped that such work can be performed at laboratory scale. Some of the objectives should be to produce a transparent bubble, a smooth interface (at least for a significant time interval) and a reliable EOS for the bubble gasses.

In reaching these objectives, some old techniques will need to be improved, new technologies brought into the picture, and some serious thought given to the experimental setup, explosives, etc.

7. CHARACTERIZE STATE OF CONDENSIBLE AND NON-CONDENSIBLE GASES IN THE BUBBLE AND DEVELOP EQUATIONS OF STATE

The explosion bubble gases move through the thermodynamic states that lie along the expansion isentrope through the CJ state to below 1 atm. Therefore, accurate equations of state that characterize the state of the permanent gases and any included steam are needed for the entire bubble motion history.

It is necessary to provide equations of state that are based on physical principles rather than curve-fitting equations of state with many adjustable parameters.

In order to do this, it is necessary to develop techniques for measuring explosion product components and the way, and in what amounts, steam appears in the explosion products as a result of water vaporization during bubble motion.

Prepared by Jules Enig

METAL COMBUSTION

Ruth M. Doherty
Naval Surface Warfare Center
Silver Spring, MD 20903-5000

INTRODUCTION

The group that discussed the area of metal combustion comprised ten members. The names of the members and their affiliations are listed in Table 1. In addition to these participants, several other workshop attendees contributed to portions of the discussions. The final result of the session was a list of seven research topics, ranked in order of decreasing importance, as perceived by the group.

Table 1. Members of the Metal Combustion Area Group

Member	Affiliation
Ed Price, Group Leader	Georgia Tech
Ruth Doherty, Group Recorder	Naval Surface Warfare Ctr
Andrew Baronavski	Naval Research Laboratory
M. Quinn Brewster	University of Illinois
Dorn Carlson	Naval Surface Warfare Ctr
Edward McHale	Atlantic Research Corp
Herb Nelson	Naval Research Laboratory
Lloyd Nelson	Sandia National Laboratories
Robert Peck	Arizona State University
William Tao	Lawrence Livermore Natl Lab

PROCEDURE FOR SELECTION AND ORDERING OF RESEARCH TOPICS

The procedure that was followed in arriving at the final ordered list of research areas was a modification of the Nominal Group Technique (NGT). The session began with a 15-minute brainstorming period, during which the participants silently listed the research

topics that they considered to be of importance in the area of metal combustion and its effect on underwater performance of explosives. At the end of this time, each group member was invited to read one of his choices. When each participant had presented one topic,the cycle was repeated, with each member listing another of his choices. During the presentation of the topics there was some discussion about overlap between topics and clarification of the statements. In this respect the group deviated from the prescribed NGT.

When all the topics of importance to all the members had been listed, there were twenty topics for consideration. Further discussion led to a consolidation of the list, reducing its size to 13 topics. The voting procedure employed by the Metal Combustion group was somewhat different from the method used in the NGT. Each member was asked to vote for the seven topics out of the 13 remaining after the consolidation step that he considered to be most important, without regard to rank. The votes were tallied by the recorder and the seven topics with the largest number of votes were carried on to the next step. Next the group members assigned to each of the seven selected topics a score ranging from seven (for the topic considered to be of highest importance) to one (for the least important topic).

RESULTS OF THE BRAINSTORMING PERIOD

General Remarks

During the listing of the research topics after the brainstorming period, it became clear that the topics covered a very wide range, from the very general (topic 1) to the highly specific (topic 15) to recommendations for the use of a particular experimental technique (topic 2). The subsequent culling of the list to produce a more or less nonredundant set of topics was made more difficult by this diversity in focus among the topics. The diversity persisted in the final list, but the ordering reflects the perceptions of the group that the more general topics are also the more important ones.

The original list of topics reflects the two approaches to explosive performance underwater. On the one hand, most of the work that has been done in the area of underwater explosives has dealt with composite explosives - mixtures which contain some high explosive component, a metal fuel and some oxidant source. The reactions of importance in the liberation of energy are those that involve the components of the original composition. On the other hand, the water surrounding an underwater explosive constitutes a source of oxidant for some fuel that might be

carried in the explosive charge. Since the energy that is available per unit charge weight from the oxidation of a metal such as aluminum by external water is very large compared with the energy from detonation of a high explosive such as RDX, optimizing the reaction of a fuel with ambient water might be an important route to improving underwater performance of an explosive charge.

These two approaches may involve different environments and time scales during which important reactions take place, so experimental techniques that provide information about one may not be relevant to an investigation of the other. In the final ordered list, the statement of the research topics was sufficiently broad that both approaches were included. It may be significant that topics that were specifically directed at one or the other of the two approaches, such as topics 11, 13, 17 and 19, did not make the final list of most important topics.

Another area of concern that emerged during the discussion was the weight that should be given to topics that might be extremely difficult to carry out at this time, given the state of the art in instrumentation and analytical techniques. The group agreed that no topic would be omitted if the need for the information sought under the topic was sufficiently great.

The Initial List of Twenty Topics

A summary of the discussion on each of the twenty initial topics will be presented here to put the subsequent culling and ranking in perspective. The statements of the topics are reproduced here as they were initially recorded during the session.

Topic 1. Where and how does metal react at high pressure? It was, perhaps, unfortunate that this was the first topic suggested, although the discussions in both the Metal Combustion Group and the other groups reinforced the impression that research in this area is critical to an understanding of the metalized compositions that are used as underwater explosives. The statement of the topic was so broad that it encompassed virtually all the questions about mechanism and timing of the metal combustion, leaving few topics that were not covered to some degree by the first. There was some discussion about the definition of high pressure, since the pressures in the expanding bubble are very much lower than the pressure at the Chapman-Jouguet state, but can still be high, compared to ambient, during the early stages of bubble expansion. It was agreed during the listing of topics that no exact definition of a pressure regime would be made. Many of the participants in the group repeated this topic in slightly different words as the listing of topics progressed, and it was

generally agreed that many of the more specific examples fell under this very general topic.

Topic 2. Pulse heating of metals in prototypical environments. This topic differed from most of the others in that it was a statement of the importance of an experimental technique (the exploding wire technique) that offers a very well-controlled means of probing the reactivity of metals in gaseous and liquid environments. The technique is currently being used at the Naval Surface Warfare Center (NSWC) and Lawrence Livermore National Laboratory (LLNL) to study the reactivity of metals and alloys in water, but it is very flexible and can be adapted to a wide range of conditions. There was some attempt to recast the topic in terms of what information can be gleaned from experiments that employ this method, but it was decided to leave it as presented for the first round of discussion. The reference to prototypical environments was included to reflect interest in the types of gaseous and aqueous surroundings that a metal is likely to see in an underwater explosion.

Topic 3. Real-time species, temperature and pressure determination in the bubble for metalized explosives. It was the consensus of the group that information on the concentrations as a function of time of various gases and solids in metalized systems would provide important clues about the role of metal combustion in explosive performance. It was also agreed that a temperature-time profile in the bubble would be very helpful in analyzing the reactivity of metals in the bubble, since reaction rates are temperature dependent. The main problem with the topic is the difficulty of making the prescribed measurements in such a hostile environment. Many optical techniques used in the study of combustion in propellants could not be used because of the water surrounding the explosion bubble and the turbulence in the bubble during growth and collapse. Nonetheless, this topic was considered to be of sufficiently great importance that research in the area is recommended despite the problems that are likely to be encountered.

Topic 4. Fuel particle dynamics and thermal response, including enhanced particle breakup. The importance of the behavior of the fuel (i.e., metal) particles in the performance of nonideal explosives is reflected in this topic. It also reflects the skepticism of the group concerning the completeness of reaction of the fuel particles in the detonation reaction zone and the general, intuitive belief that important reactions continue to take place beyond the Chapman-Jouguet state. The group recognized that such processes as melting, vaporization, loss of an oxide coating, and particle fracture are likely to be very important in determining the efficiency of a nonideal explosive. The concern with particle dynamics also reflects the interest in reaction of

fuel particles with external water. The behavior of any unreacted metal particles in the bubble, in particular their likelihood of coming into contact with ambient water by projection into the surrounding water, is relevant to the consideration of reaction with external water.

Topic 5. Temporal and spatial distribution of products in the bubble. Although closely related to topic 3, this was listed separately in the first pass since its focus included the spatial distribution of products, and therefore tied in more strongly than the former with the fuel-water concept. Another important facet of this topic was the possibility of learning something about the vaporization of water at the bubble water interface. It was agreed that the presence of water from the surroundings in the gas bubble might be very important in the combustion of metal in heavily metalized compositions.

Topic 6. Turbulence and mixing in the bubble. In reactions that involve the interaction of a fuel particle and some oxidant species, it is necessary for the fuel and oxidizer to come in contact with one another for reaction to take place. Turbulence in the bubble may offer a means of mixing fuel with oxidant, and is critical if the reaction is to be with external water. Turbulence at the interface may be especially important in getting efficient reaction between a fuel and external water.

Topic 7. The effect of metal loading on detonation temperature. TIGER calculations for metalized formulations indicate that the detonation temperature rises with increasing metal loading up to some point that depends on the composition of the matrix explosive into which the metal is loaded. It is the effect of the increased temperature on the efficiency of metal combustion (i.e., on the agreement between predicted and calculated performance) that is proposed to be investigated in this topic.

Topic 8. A comprehensive list of possible fuels and their products, and the enthalpies of formation thereof. The enthalpy of reaction for the combustion of any material depends on the product that is formed. Thermodynamic calculations that suggest whether one fuel is better than another on a weight or volume basis depend on what assumptions are made about the fate of the fuels. It was recommended that a comprehensive list of the possible products of oxidation of candidate fuels be compiled from which one could judge the relative merits of those fuels based on various assumptions about the products formed.

Topic 9. Particle combustion at high pressures. This topic was introduced because of the ambiguity of the pressure regime in Topic 1. It is directed more to the role of metals in the detonation wave, at pressures of the order of hundreds of

kilobars, rather than at the lower pressures found in the expanding gases.

Topic 10. The role of oxidant species in enhancing combustion. Although the enthalpy of reaction per unit weight of oxidant of a metal with fluorine is about the same as for reaction with oxygen, there are differences in the products (e.g., volatility and solubility in the molten metal) that might lead to different efficiencies of combustion of the metal, particularly in heavily metal-loaded systems. Questions suggested by this topic include whether the presence of fluorine affects the efficiency of combustion and, if so, the mechanism by which this occurs.

Topic 11. How to get optimal reaction with external water. This question focuses on the fuel-water or reactive case scenario, in which it is intended that a significant fraction of the energy of the explosive come from reaction of metal with external water. Thus, it assumes that reaction with external water can occur on a time scale that will be useful for contribution to performance (most likely bubble energy). This topic was considered by the group to be somewhat different in character from most of the other topics, since its goal is a clearly defined performance goal (as reflected by the "optimal" in the statement of the topic).

Topic 12. Modification of the oxide layer on the fuel. Since most of the experience with metalized explosives has been with aluminum, the nature of the oxide coating that forms on that metal is of prime importance. Aluminum oxide has a higher boiling point than the metal, and it is insoluble in molten aluminum. Therefore, formation of aluminum oxide on the surface of the aluminum particles may prevent complete combustion of the metal. If the integrity of the oxide coating on the aluminum could be disrupted (by alloying with another metal, for example) it might be possible to enhance the efficiency of metal combustion. For other metals this is not necessarily a consideration.

Topic 13. Explosion and bubble dynamics models of metalized explosives that incorporate reaction kinetics. The group recognized that the purpose of the experimental programs described in the foregoing topics is to provide a basis upon which estimates of reactivity or performance under a given set of conditions may be made. In order to make these estimates models must be available which take into account those factors which are demonstrably important in determining the output of the explosive, whether those factors are hydrodynamic or chemical in nature. Any model of explosive performance that assumes complete reaction between the von Neumann spike and the C-J state will not accurately predict measures of performance that depend on late-time reaction. The models that are currently in use do not treat reaction kinetics in a satisfactory manner.

Topic 14. Extent of surface reactions on the fuel particles. In nonideal explosives such as those used for underwater applications, the fuel particles must come into proximity with the oxidant species in order to react. However, it is not known at this time whether the oxidation reaction (or reactions) take place in the vapor phase surrounding the metal particles, on the surface of the metal particles or in the metal particles beneath the oxide layer, with the oxidant diffusing through an oxide coating to reach the unreacted metal. The relative importance of these pathways will affect the efficiency of combustion differently for different metals and under different conditions of temperature and pressure. It is important to understand the extent to which surface reactions contribute to the oxidation in order to determine whether the surface of the metal has a significant effect on the performance of an explosive.

Topic 15. Mechanism of oxide condensation. For elements such as boron and aluminum, a significant fraction of the heat of formation of the highest oxide comes from the condensation to the liquid phase and the crystal lattice energy of the solid. In order to get the most energy out of a metalized explosive it is important to understand the processes that lead to the liberation of this energy, and what factors can interfere with it. The group considered this to be a highly specialized topic, but worth attention on its own due to the significant amount of energy liberated by the formation of the condenses phases.

Topic 16. Other fuels than aluminum. Although aluminum has been the only metal to be used extensively in metalized explosives for underwater applications, due to the high heat of formation of its oxide, its density, its easy availability, and the low toxicity of its compounds, there are other elements that compare favorably with aluminum. In particular, recent advances in boronized propellants have shown that it can be made to react efficiently in solid fuel ram jet propellants. The group was reminded that, even though boron is not a metal, it has certain attractive features that may make it potentially competitive with aluminum, and the discussion of "metals" should not be taken to exclude boron.

Topic 17. Tailoring the spatial distribution of components. Although most explosive formulations are prepared so that the composition, on a macroscopic scale, is uniform throughout the charge, it is possible that some advantage could be realized if the components were separated from one another, perhaps in a way that might give rise to greater heating of the metal or other fuel and so increase its rate of reaction with the oxidizers present. If the fuel-water reaction is considered to be of importance, then geometrical considerations that would lead to

greater mixing of the fuel with external water would be of interest.

Topic 18. Modification of the mechanism and/or kinetics of oxidation by modification of the fuel or oxidant. This topic includes suggestions of many of the preceding topics, and is another of the more applied of the topics suggested. The discussion of this topic centered on the possibility of alloying the fuel (viz., aluminum) in such a way as to provide a pathway to a less protective oxide coating or different physical properties that might lead to more extensive particle breakup and consequently greater reactivity.

Topic 19. The effect of the matrix detonation temperature on the efficiency of metal combustion. This topic was suggested as the converse of Topic 7. Although calculations show higher detonation temperatures for explosive compositions as a whole when metal loading is increased, those calculations are generally based on the assumption of complete reaction of the metal. It may be equally important to ask how changes in the detonation properties of the explosive matrix affect the ignition of the imbedded metal particles.

Topic 20. Nonconventional metal sources. In the ordinary conception of a metalized explosive, the metal atoms are surrounded on an atomic scale by other metal atoms. Ideally, one would like to have the fuel atoms (as opposed to particles) surrounded by oxidant rather than other fuel. If one could construct a molecule with a metal atom in an oxidant molecule, one would expect very efficient oxidation. Some member of the group perceived this to be an extreme case of topic 18. Others did not.

Consolidation of the List

Subsequent discussion of the topics presented during the initial brainstorming period led to the consolidation of the list from 20 to 13 topics. It was felt that some topics overlapped and could be combined or eliminated. The discussion resulted in the following changes:

1. Topic 2 was combined with Topic 1, since it was considered to be a means of obtaining data rather than a research topic on its own;
2. Topic 5 was combined with Topic 3;
3. Topic 9 was combined with Topic 1, and the pressure regime specified was defined to cover both moderate pressures such as might be found in the bubble and high pressures characteristic of the reaction zone behind the detonation wave;

4. Topics 10 and 12 were combined with Topic 18, since they were considered to be special cases of that topic;
5. Topic 14 was combined with Topic 1, since it was felt that the question of where the reaction takes place included studies of surface reactions on the fuel particles; and
6. Topic 16 was eliminated, but it was agreed that, for purposes of this discussion, boron would be considered a metal and the topics would not be limited to aluminum.

The resulting list, with the topics modified to reflect the changes that had been made, was voted upon. The results of the vote are recorded in Table 2. No rank was implied by this first vote, only the judgement of the participants on whether the topics were in the more important or less important half of the list. Nonetheless, the results were very similar to those of the vote taken to rank the topics in order of decreasing priority.

Table 2. Total of votes for inclusion in top seven topics.

Topic No.	Total	Topic No.	Total
1	10	13	7
3	8	15	7
4	7	17	1
6	6	18	8
7	2	19	1
8	4	20	1
11	5		

The Final Ordered List

From the results of the first vote, Topics 1 (as modified), 3 (as modified), 4, 6, 13, 15 and 18 (as modified) were chosen for the final ordered list. The participants' next votes were on the order of importance of these topics. The ranking in the final list, given in Table 3, is based on the sum of the scores assigned by the ten voting members of the group. The individual votes that contributed to the score are also given to illustrate the agreement (or lack thereof) of the group about the topics in the list.

Table 3. Final score and rank in the ordered list of research topics

Topic No.	Score	Rank	Individual Votes									
1	70	1	7	7	7	7	7	7	7	7	7	7
3	48	2	5	5	5	5	5	6	6	1	5	5
4	43	3	6	4	4	6	2	3	1	5	6	6
6	20	7	1	1	1	1	1	4	4	4	2	1
13	35	4	3	2	3	3	6	2	3	6	4	3
15	30	6	4	3	2	2	3	5	2	2	3	4
18	34	5	2	6	6	4	4	1	5	2	1	2

As the individual votes show, there was unanimity about the importance of Topic 1. This was probably inevitable, given that it was very general and included three other topics that had been mentioned. Topic 3 was considered by nine of the ten voters to be of second or third importance, but one listed it as the least important. The high ranking of this topic by the majority of voters, to whom the difficulties of making the actual measurements had been pointed out, indicates the importance attached to developing a time-resolved picture of what is happening to the metal in metalized explosives. Its close connections with the universally approved Topic 1 are also reflected in its score.

Topic 4 was ranked second in importance by more voters than was Topic 3, but it was also ranked lower by more voters. Topics 13 and 18 each received two votes as the second most important topic, but were ranked somewhere in the middle by most. Topic 6 was clearly the lowest rated of the seven topics, although it had three supporters who believed it to be of middling importance.

RATIONALE FOR SELECTION AND RANKING OF THE IMPORTANT RESEARCH TOPICS

After the ranking had been done, the group undertook to provide a rationale for the selection and ranking of the topics that appear in the final list. The topics were restated to reflect the discussions and combinations of topics that had taken place. These reformulated topics are presented below in order of decreasing score, and a rationale for the importance of each is given.

Kinetics, Mechanisms and Spatial Distribution of Reactions at Both Moderate and High Pressures.

Any interpretation or modeling of the role of metals in explosions must be based on a qualitatively valid understanding of this subject, which we do not now have. In the absence of experimental data, predictions of performance of new explosives, or of old explosives under other than standard conditions, must rely on models with admitted deficiencies. New techniques are available now that permit us to make measurements that have not been possible in the past. Recommended efforts would include four strategies:

1. Inference from global explosion measurements;
2. Inference from direct measurement in the explosion using new methods;
3. Inference from laboratory experiments, such as those employing exploding wires; and
4. Inference from analytical models of particle-droplet combustion.

Real-time Species, Temperature and Pressure Determination in the Bubble for Metalized Explosives.

Information gathered on this topic will help to answer the basic question of whether metal combustion occurs in the bubble, which was included in Topic 1. It is necessary if models of underwater explosions are to be validated. Information of this type will help answer the questions of what oxidants are preferred (related to Topic 18) and may give some clues to the conditions under which metal oxide condensation occurs (Topic 15). It may be possible to use such information to determine the extent to which evaporation of ambient water is important in the composition of the bubble, which is relevant to the questions of interface phenomena and their impact on underwater performance.

Fuel Particle Dynamics and Thermal Response.

Since metalized explosives are in general nonideal, the behavior of the metal (fuel) particles themselves is very important to our understanding of their interactions with oxidants. Such topics as melting and vaporization under detonation conditions, break-up of particles, stripping away of any oxide coating and the motion of particles under the influence of the expanding product gases in a detonating explosive will all have an effect on the timing and efficiency of the combustion reactions. The generation and

dispersal of metal particles into water in a fuel-water reaction (as would occur in a reactive case arrangement) will also be very important to the usefulness of fuel water reactions in underwater explosions.

Models for Metalized Explosion and Bubble Dynamics That Specifically Incorporate Chemical Kinetics

Current models of detonation usually assume that all interesting chemistry occurs between the detonation front and the Chapman-Jouguet plane, by mechanisms unknown and largely irrelevant to the accuracy of the model. Bubble hydrodynamics codes assume a given pressure, volume and temperature at zero time, which controls all subsequent behavior. Since there is evidence that some chemical reactions that lead to higher observed measures of shockwave and bubble performance occur too late to contribute to the propagation of the detonation wave, it is important to include these in models that purport to model adequately the performance of nonideal explosives.

Modification of the Mechanism and Kinetics of Metal Combustion by Modification of Fuel or Oxidant

Once information is available on the rates and mechanisms of some important chemical reactions involved in metal combustion (Topics 1, 3, 4 and 15) steps can be taken to probe the relative importance of these steps in improving performance. Some examples of the types of tasks included in this topic are the use of alloys to change such physical properties of the fuel as surface tension or melting point, which might affect dispersal of the metal and possibly the integrity and strength of an oxide coating, use of other oxidant species such as fluorine containing oxidants, which might give gaseous products rather than a solid oxide, addition of catalysts (such as burn-rate modifiers used in propellants), or surface coating of metal particles (e.g., Ni on Al) to increase the temperature of the metal.

Mechanism of Oxide Condensation

Most calculations show the higher energy output of metalized explosives as being due to the large, negative heats of formation of the metal oxide. Because a substantial fraction of the enthalpy of reaction is released during the product condensation phase, it is imperative to understand the underlying rates and mechanisms governing this process. A prerequisite is knowledge of the rate of formation and distribution of gas-phase products (related to Topic 3). Basic information on the condensation

kinetics of these species is needed for conditions encountered in underwater explosions. The condensation mechanism, including steps for homogeneous/heterogeneous nucleation and particle growth/agglomeration needs to be determined. A comprehensive explosion model must include an accurate description of oxide condensation.

Effects of Turbulence and Mixing in the Gas Bubble

Turbulence can be a very effective means of mixing fuel and oxidizer, or mixing the gas in the bubble with the surrounding water in the interfacial region. In either case, these effects must be quantified. In the former case, turbulence may contribute to more efficient reaction since most of the reactions at the pressures encountered are probably diffusion controlled. Turbulence at the interfacial boundary may indicate that vaporization of water at the interface is taking place, modifying the expected composition of the product gas bubble. Another consequence of turbulence is in the application of any optical diagnostic probes. Turbulence causes index of refraction gradients, leading to problems in the interpretation of data. The extent of these problems must be addressed in order to use spectroscopic probes for species.

REMARKS ON THE NOMINAL GROUP TECHNIQUE

For the metal combustion group, the Nominal Group Technique was a useful method of approaching the task of generation of an ordered list of research topics. Although the directions for the use of this technique were not followed exactly, it was generally agreed by the group members that the result was a good indicator of the research areas that should be emphasized.

One deviation from the NGT directions occurred during the listing of the topics after the brainstorming session. Rather than just listing the topics when they were suggested without further comment, the group discussed overlap between topics and requested clarification from the author as each topic came up. This led to a partially-selected list at the time when discussion should have been started, but it probably had little effect on the final result.

The other major difference between our implementation of the NGT and the prescribed procedure was in the voting. We split the voting into two parts - one to limit the number of topics and one to rank the remaining topics. A comparison of the scores from Tables 2 and 3 shows that the results are very similar, with

Topic 1 being on everyone's list and Topic 6 being the least often recommended of the top seven. It appears that the ranks of only Topics 8 and 11 were likely to have been affected.

The major drawback of the NGT as used by this group was the lack of direction regarding the breadth of subjects to be covered by any single topic. This led to some confusion among the members of the group and to the variation from very general to very specific in the topics that made the initial list. It was felt that, if some ground rules had been laid down at the outset, the later agonizing over how to rate broad topics compared with specific ones would have been minimized.

One objection that was expressed about the NGT was that it imposed an arbitrary limit on the number of topics that could be given a nonzero score. In our particular group, that is unlikely to have had a major impact on the results, given the close agreement between the two votes and the agreement between voters about the relative importance of the topics in the final list.

DISTRIBUTION LIST

ATTENDEES

1. Roger Arndt
   Saint Anthony Falls Hyd. Lab
   University of Minnesota
   Minneapolis, MN 55414 (612) 627-4012

2. Andrew Baronavski
   Chemistry Div., Code 6110
   Naval Research Lab.
   Washington, DC 20375 (202) 767-3124

3. Ernest Battifarano
   New Jersey Institute
   Mathematics Dept. (212) 691-1379
   Newark, NJ 07102 (201) 596-3481

4. David Beck
   Sandia National Labs.
   ORG. 6427
   Albuquerque, NM 87185 (505) 846-7733

5. Marshall Berman
   Sandia National Labs.
   Div. 6427
   Albuquerque, NM 87185 (505) 844-1545

6. John Blake
   Dept. of Mathematics
   Univ. of Wollongong
   Wollongong, NSW, 2500
   Australia

7. David Book
   US Naval Research Lab.
   Washington, DC 20375 (202) 767-2078

8. Barry Bowman
   Lawrence Livermore Nat'l Lab.
   P. O. Box 808
   Livermore, CA 94550 (415) 422-0325

9. M. Quinn Brewster
   Dept. of Mech & Ind Engineering
   Univ. of Illinois
   Urbana, IL 61801 (217) 244-1628

10. P. Barry Butler
    Univ. of Iowa
    Summer Faculty
    Sandia National Labs (319) 335-5672
    Albuquerque, NM 87185 (505) 846-0157 (Summer)

11. Dorn Carlson
NSWC Code R11
Silver Spring, MD 20903 (202) 394-2715

12. Georges Chahine
Tracor Hydronautics
7210 Pindell School Rd.
Laurel, MD 20707 (301) 604-4325

13. Bob Chan
JAYCOR (619) 535-3112

14. William R. Conley
David Taylor Research Center
Code 175.2
Bethesda, MD 20084-5000 (202) 227-1824

15. Charles Dickinson
Naval Surface Warfare Center
Code R04
White Oak, MD 20903-5000 (202) 394-1259

16. Ruth M. Doherty
Naval Surface Warfare Center
Code R11
Silver Spring, MD 20903-5000 (202) 394-2745

17. Jules Enig
Enig Associates, Inc.
13230 Ingleside Dr.
Beltsville, MD 20705-1034 (301) 572-4421

18. David Epstein
Suny Maritime College
Ft. Schuyler
Bronx, NY 10465 (212) 409-7376

19. Michael T. Ginsberg
Los Alamos National Lab.
MS J 960
Los Alamos, NM 87545 (505) 667-3327

20. Harland Glaz
Univ. of Maryland
Mathematics Dept.
College Park, MD 20742 (301) 454-7058

21. James Glimm
Courant Institute, NYU
251 Mercer St.
New York, NY 10012 (212) 998-3282

22. John Goertner
NSWC
White Oak, ND 20903-5000 (202) 394-2583

23. Greg Harris
Naval Surface Warfare Center
Code R14
10901 New Hampshire Ave.
Silver Spring, MD 20903-5000 (202) 394-2888

24. Joseph Hershkowitz
305 Passaio Ave.
West Caldwell, NJ 07006

25. J. I. Jagoda
Aerospace Engineering
Georgia Tech.
Atlanta, GA 30332 (404) 894-3060

26. Herman Krier
Dept. of Mech and Ind Engineering
140 MEB; 1206 W. Green
Univ. of Illinois
Urbana, IL 61801 (217) 356-4478

27. Dick Lau
Office of Naval Research
Ballston Tower #1
800 North Quincy St.
Arlington, VA 22217 (202) 696-4316

28. Spyrdon Lekoudis
Office of Naval Research
Ballston Tower #1
800 North Quincy St.
Arlington, VA 22217 (202) 696-4405

29. Raymond R. McGuire
Lawrence Livermore Nat'l Labs
L-324
Livermore, CA 94550 (415) 422-7791

30. Edward T. McHale
Atlantic Research Corp.
5390 Cherokee Ave.
Alexandria, VA 22312 (703) 642-4088

31. Michael J. Miksis
Dept. of Eng Science and
Applied Math.
Northwestern Univ.
Evanston, IL 60208 (312) 491-5585

32. R. S. Miller
Office of Naval Research
Code 1132P
Arlington, VA 22217 (202) 696-4403

33. Michael J. Murphy
Lawrence Livermore Nat'l Labs
Box 808
Livermore, CA 94550 (415) 447-2320

34. Herb Nelson
Code 6110
Naval Research Lab.
Washington, DC 20375 (202) 767-3686

35. Lloyd S. Nelson
Sandia National Labs
ORG. 6427
Albuquerque, NM 87185 (505) 844-6258

36. Robert E. Peck
Arizona State University
Dept. of Mechanical and
Aerospace Engineering
Tempe, AZ 85287-6106 (602) 965-6676

37. E. W. Price
Aerospace Engineering
Georgia Tech.
Atlanta, GA 30332 (404) 894-3063

38. David Ritzel
Defense Research Establishment
Suffield
Ralston, Alberta
Canada (403) 549-3701 Ext. 4787

39. Joel C. W. Rogers
Dept. of Mathematics
Polytechnic University
333 Jay Street
Brooklyn, NY 11201 (718) 260-3501

40. Gabriel Roy
Office of Naval Research
Power Program Office
Ballston Tower #1
800 North Quincy St.
Arlington, VA 22217 (202) 696-4403

41. L. N. Sankar
Aerospace Engineering
Georgia Tech.
Atlanta, GA 30332 (404) 894-3014

42. Martin Sichel
Univ. of Michigan
Dept. of Aerospace Engineering
Ann Arbor, MI 48109 (313) 764-3388

43. Robert K. Sigman
Aerospace Engineering
Georgia Tech.
Atlanta, GA 30332 (404) 894-3041

44. W. A. Sirignano
School of Engineering
Univ. of California Irvine
Irvine, CA 92717 (714) 856-6002

45. Joseph E. Shepherd
RPI
Dept. of Mechanical Engineering
Troy, NY 12180-3590 (518) 276-6192

46. Jay M. Solomon
NSWC
White Oak, MD 20903-5000 (202) 394-2062

47. Hyman Sternberg
Advanced Technology & Research
14900 Sweitzer Lane
Laurel, MD 20707 (301) 498-8200

48. D. Scott Stewart
Theoretical and Applied
Mathematics
Univ. of Illinois
Urbana, IL 61801

49. Warren C. Strahle
Aerospace Engineering
Georgia Tech.
Atlanta, GA 30332 (404) 894-3032

50. William C. Tao
Lawrence Livermore Lab.
High Explosives Tech.
7000 East Ave., L-324
Livermore, CA 94550 (415) 423-0499

51. Ron Walterick
Aerospace Engineering
Georgia Tech.
Atlanta, GA 30332 (404) 894-3050

52. Stephen Wilkenson
NSWC
Silver Spring, MD 20903-5000 (301) 394-3971

53. Ben T. Zinn
Aerospace Engineering
Georgia Tech.
Atlanta, GA 30332 (404) 894-3033

ADDITIONAL DISTRIBUTION

Mr. Russ Ogle
Honeywell MN 48-3700
7225 Northland Dr.
Brooklyn Park, MN 55428

Dr. Alan Roberts
Code 123
Power Program Office
Ballston Tower #1
800 North Quincy St.
Arlington, VA 22217

Defense Technical Information Center
Building 5, Cameron Station
Alexandria, VA 22314

Office of Naval Research
Resident Representative
Georgia Institute of Technology
206 O'Keefe Bldg.
Atlanta, GA 30332-0490